

Universität Stuttgart
Institut für Energiewirtschaft und
Rationelle Energieanwendung

**On the Process Integration of
Organic Rankine Cycles
and Absorption Chillers into Heat
Exchanger Networks**

Forschungsbericht

Luis Carlos
Chamorro Romero

Band 153

On the Process Integration of Organic Rankine Cycles and Absorption Chillers into Heat Exchanger Networks

Von der Fakultät Energie-, Verfahrens- und Biotechnik der Universität Stuttgart zur
Erlangung der Würde eines Doktor-Ingenieurs (Dr.-Ing.) genehmigte Abhandlung

Vorgelegt von

Luis Carlos Chamorro Romero

geboren in Sincelejo, Kolumbien

Hauptberichter:

Prof. Dr.-Ing. Peter Radgen

Mitberichter:

Prof. Dr. Konstantinos Stergiaropoulos

Tag der Einreichung:

07.02.2022

Tag der mündlichen Prüfung:

30.01.2023

Institut für Energiewirtschaft und Rationelle Energieanwendung, Stuttgart

Prof. Dr.-Ing. Kai Hufendiek

Abteilung Effiziente Energienutzung (EE)

Prof Dr.-Ing. Peter Radgen

2023

ISSN 0938-1228

D93 (Dissertation der Universität Stuttgart)

Acknowledgements

This dissertation was written during my time at the Institute for Energy Economics and Rational Energy Use (IER) of the University of Stuttgart, with the financial support of the Graduate and Research School for Energy Efficiency Stuttgart (GREES).

I would like to use this opportunity to thank Professor Peter Radger for his academic supervision, enriching feedback and personal support during these last 5 years. A big thank you also goes to my ex-colleagues and friends at IER for their support and interesting discussions, as well as the joyous times and laughs shared during these challenging but rewarding times. Big shout-out to Natalia, Helene, Nils, Ulf, Manuel, Paula, Dirk, Sebastian, Matthias and Hanna and the many occasions our time together brought joy to my journey at IER on a professional and personal level.

To my friends and loved ones outside the university, Yuqing, Angel, Jose, David, Hamza, Sergio, Giancarlo, Melissa, Angyela, Ricardo and my peers at the “Colombia Candela Tanz- und Kulturverein” thank you for the wonderful times and personal support during these years.

Finally, I would like to thank my family in Colombia for the love and support as well as the inspiration and guidance that helped me to navigate through adversity in order to achieve my professional and personal goals. To my sister Karina, thank you for always being there for me, and to my parents Jaime and Tarcila, who are waiting for me in eternity:

Gracias Papa, Gracias Mama, los amo y hasta que nos volvamos a encontrar...

Table of Content

List of Figures	I
List of Tables.....	V
List of Symbols	IX
Nomenclature.....	XVIII
Abstract	XX
Kurzfassung	XXI
1 Introduction.....	1
1.1 Motivation and Background.....	2
1.2 Problem Description and Objectives	4
1.3 Scope of the Research	6
1.4 Outline of the Work.....	14
2 Fundamentals	16
2.1 Waste Heat: Definition	16
2.2 Industrial Waste Heat Potential	17
2.3 Waste Heat Recovery Technologies.....	20
2.3.1 Heat Exchangers.....	21
2.3.2 Heat Distribution	21
2.3.3 Heat Storage	23
2.3.4 Waste Heat to Cooling	27
2.3.4.1 Absorption Chillers	27
2.3.4.2 Adsorption Chillers	31
2.3.5 Waste Heat to Power	32
2.3.5.1 Organic Rankine Cycle (ORC)	32
2.3.5.2 Kalina Cycle.....	38
2.3.6 Waste Heat to Heating (Heat Pumps)	39
2.4 Process Integration	39
2.4.1 Pinch Analysis.....	40

Table of Content

2.4.2	Mathematical Programming.....	41
2.5	Process Integration in Discontinuous Processes	43
3	State-of-the-Art	48
3.1	Process Integration of Organic Rankine Cycles into Heat Exchanger Networks	48
3.2	Process Integration of Absorption Chillers into Heat Exchanger Networks.....	53
3.3	Process Integration of Organic Rankine Cycles and Absorption Chillers into Heat Exchanger Networks (Combined Models)	55
3.4	Summary of the State-of-the-Art and Overview of Mathematical Framework	55
4	Mathematical Framework	59
4.1	Methodology and General Assumptions	59
4.2	Model Formulations	60
4.2.1	Continuous Processes.....	64
4.2.1.1	Organic Rankine Cycles (HEN-ORC)	64
4.2.1.2	Absorption Chillers (HEN-ABC).....	71
4.2.1.3	Combined Model (HEN-WHR).....	77
4.2.2	Multi-Period Processes without Heat Storage (Semi-Continuous Processes).....	85
4.2.2.1	Organic Rankine Cycles (MP-ORC).....	85
4.2.2.2	Absorption Chillers (MP-ABC).....	89
4.2.2.3	Combined Model (MP-WHR)	92
4.2.3	Multi-Period Processes with Heat Storage (Batch Processes)	95
4.2.3.1	Storage Equations	96
4.2.3.2	Organic Rankine Cycles (MP-ST-ORC).....	100
4.2.3.3	Absorption Chillers (MP-ST-ABC).....	104
4.2.3.4	Combined Model (MP-ST-WHR)	107
4.3	Mathematical Considerations and Models Limitations.....	111
5	Applications of the Framework	115

Table of Content

5.1	Case Study 1 (Continuous Process).....	116
5.1.1	Process Integration of Organic Rankine Cycle	119
5.1.2	Process Integration of Absorption Chillers	123
5.1.3	Process Integration of Waste Heat Recovery Technologies (Combined Model)	124
5.2	Case Study 2 (Semi-Continuous Process).....	127
5.2.1	Process Integration of Organic Rankine Cycle	130
5.2.2	Process Integration of Absorption Chillers	132
5.2.3	Process Integration of Waste Heat Recovery Technologies (Combined Model)	133
5.3	Case Study 3 (Batch Process).....	136
5.3.1	Process Integration of Organic Rankine Cycle	141
5.3.2	Process Integration of Absorption Chillers	143
5.3.3	Process Integration of Waste Heat Recovery Technologies (Combined Model)	144
5.4	Sensitivity Analysis.....	147
5.4.1	Economical parameters	148
5.4.2	Key temperatures in the subsystems ORC and ABC	149
5.4.3	Minimum approach temperatures	153
5.4.4	General comments on the sensitivity analysis	154
5.5	Critical Discussion	158
6	Conclusions and Future Work.....	163
6.1	Conclusions	163
6.2	Future Work	164
6.3	Final Remarks.....	166
7	Bibliography	167
Appendix A	Modeling of Single-Effect Absorption Chiller	195
Appendix B	Thermophysical properties of ORC Working Fluids	203

Table of Content

Appendix C	Explicit presentation of Mathematical Models.....	209
Appendix D	Additional results from Case Studies	248
Appendix E	Extended State-of-the-Art	261
Appendix F	Estimations of theoretical industrial waste heat potentials (Ext.) ..	264

List of Figures

Figure 1-1.	Global Green House Gas (GHG) emissions in percentage of CO ₂ eq per sector in 2016.....	2
Figure 1-2.	"Onion Diagram" for process design.....	3
Figure 1-3.	General and specific objectives of the dissertation.	6
Figure 1-4.	Structure of the dissertation.....	15
Figure 2-1.	Classification of industrial waste heat recovery technologies.....	21
Figure 2-2.	Classification of Thermal Energy Storages (TES) according to the underlying storage processes.	24
Figure 2-3.	Schematic representation of a single-effect absorption chiller.....	27
Figure 2-4.	Schematic representation of double-effect absorption chiller.	30
Figure 2-5.	Basic ORC cycle.....	35
Figure 2-6.	Types of working fluids according to their T-s diagram.....	36
Figure 3-1.	Appropriate placement of ORCs driven by waste heat according to pinch analysis.	49
Figure 3-2.	Appropriate placement of ABCs driven by waste heat according to pinch analysis.	54
Figure 4-1.	Overview of the superstructures developed in this dissertation.	60
Figure 4-2.	Schematic representation of the Superstructure for the Process Integration of Organic Rankine Cycles into Continuous Processes (HEN-ORC).	66
Figure 4-3.	Schematic representation of the Superstructure for the Process Integration of Absorption Chillers into Continuous Processes (HEN-ABC).....	74
Figure 4-4.	Schematic representation of the Superstructure for the Process Integration of Organic Rankine Cycles and Absorption Chillers into Continuous Processes (HEN-WHR).....	78
Figure 4-5.	Schematic representation of the Superstructure for the Process Integration of Organic Rankine Cycles into Multi-Period Processes without Heat Storage (MP-ORC).....	86

Figure 4-6.	Schematic representation of the Superstructure for the Process Integration of Absorption Chillers into Multi-Period Processes without Heat Storage (MP-ABC)	91
Figure 4-7.	Schematic representation of the Superstructure for the Process Integration of Organic Rankine Cycles and Absorption Chillers into Multi-Period Processes without Heat Storage (MP-ABC).....	94
Figure 4-8.	Schematic representation of the Superstructure for the Synthesis of Heat Exchanger Networks in Multi-Period Process with Fixed Temperature Variable Mass (FTVM) Heat Storage Tanks.....	98
Figure 4-9.	Schematic representation of the Superstructure for the Process Integration of Organic Rankine Cycles into Multi-Period Processes with FTVM Heat Storage Tanks (MP-ST-ORC)	101
Figure 4-10.	Schematic representation of the Superstructure for the Process Integration of Absorption Chillers into Multi-Period Processes with FTVM Heat Storage Tanks (MP-ST-ABC)	105
Figure 4-11.	Schematic representation of the Superstructure for the Process Integration of Organic Rankine Cycles and Absorption Chillers into Multi-Period Processes with FTVM Heat Storage Tanks (MP-ST-WHR).....	108
Figure 4-12.	Approximations to the logarithmic mean temperature difference.....	113
Figure 5-1.	Pinch analysis for Case Study 1	117
Figure 5-2.	Prescreening algorithm for the selection of the ORC working fluid and operating temperatures	120
Figure 5-3.	Grid diagram of HEN-WHR for Case Study 1	125
Figure 5-4.	Event diagram of Case Study 2	128
Figure 5-5.	Grand Composite Curves for the different periods of operation in Case Study 2.....	128
Figure 5-6.	Grid diagram MP-WHR for Case Study 2.....	135
Figure 5-7.	Event diagram Case Study 3.....	138
Figure 5-8.	Grand Composite Curves for the different periods of operation in Case Study 3.....	139

Figure 5-9.	Pinch analysis of the time-averaged process streams in Case Study 3.....	140
Figure 5-10.	Grid diagram MP-ST-WHR for Case Study 3.....	146
Figure 5-11.	Sensitivity analysis of the Total Annualized Cost (TAC) of the system generated using HEN-WHR for Case Study 1 (Economical Parameters).....	149
Figure 5-12.	Sensitivity analysis of multiple design variables of the system as generated using HEN-WHR for Case Study 1 (Economical Parameters).	150
Figure 5-13.	Sensitivity analysis of the Total Annualized Cost (TAC) of the system generated using HEN-WHR for Case Study 1 (Key temperatures in the subsystems ORC and ABC).	151
Figure 5-14.	Sensitivity Analysis of multiple design variables of the system as generated using HEN-WHR for Case Study 1 (Key temperatures in the subsystems ORC and ABC).	152
Figure 5-15.	Sensitivity Analysis of the Total Annualized Cost (TAC) of the system generated using HEN-WHR for Case Study 1 (Minimum approach temperatures between different stream types).	154
Figure 5-16.	Sensitivity Analysis of multiple design variables of the system as generated using HEN-WHR for Case Study 1 (Minimum approach temperatures between different stream types).	155
Figure 5-17.	Sensitivity Analysis of the Total Annualized Cost (TAC) of the system generated using HEN-WHR for Case Study 1 (Number of intraprocess stages in the superstructure).	156
Figure 5-18.	Sensitivity Analysis of multiple design variables of the system as generated using HEN-WHR for Case Study 1 (Number of intraprocess stages in the superstructure).	157
Figure A-1.	Schematic representation of a single-effect absorption chiller.....	196
Figure A-2.	Results for the data fitting procedures for the case studies.	202
Figure B-1.	Basic ORC cycle.....	206
Figure D-1.	Grid diagram HEN1 for Case Study 1.....	248
Figure D-2.	Grid diagram HEN2 for Case Study 1.....	249

Figure D-3.	Grid diagram HEN-ORC for Case Study 1	250
Figure D-4.	Grid diagram HEN-ABC for Case Study 1	251
Figure D-5.	Grid diagram HEN1 for Case Study 2.....	252
Figure D-6.	Grid diagram HEN2 for Case Study 2.....	253
Figure D-7.	Grid diagram MP-ORC for Case Study 2.....	254
Figure D-8.	Grid diagram MP-ABC for Case Study 2.....	256
Figure D-9.	Grid diagram HEN1 for Case Study 3.....	257
Figure D-10.	Grid diagram HEN2 for Case Study 3.....	258
Figure D-11.	Grid diagram MP-ST-ORC for Case Study 3.....	259
Figure D-12.	Grid diagram MP-ST-ABC for Case Study 3.....	260
Figure F-1.	Sankey diagram for the estimated energy flows and waste heat potential in the industrial sector worldwide for 2012.....	265

List of Tables

Table 2-1.	Estimations of theoretical industrial waste heat potentials in different geographical areas.	18
Table 2-2.	Estimations of theoretical industrial waste heat potentials in Germany.....	19
Table 2-3.	Overview of characteristic parameters for typical Thermal Energy Storage technologies.	25
Table 2-4.	Change of enthalpy during charge/discharge for different storage types.	25
Table 2-5.	Comparison LiBr/H ₂ O and H ₂ O/NH ₃ working pairs for absorption refrigeration	28
Table 3-1.	Selection of relevant studies on the Process Integration of Organic Rankine Cycles and Absorption Chillers into Heat Exchanger Networks.	56
Table 4-1.	Generic depiction of common equations for all superstructures for the Process Integration of Waste Heat Recovery Technologies.....	61
Table 4-2.	Generic depiction of specific equations for the Process Integration of Waste Heat Recovery Technologies depending on the technologies considered.....	62
Table 4-3.	Generic depiction of "Maximum Size" equations for the Process Integration of Waste Heat Recovery Technologies into Multi-Period Processes.....	63
Table 4-4.	Generic depiction of equations for the Process Integration of Fixed Temperature Variable Mass (FTVM) Storage Systems	64
Table 4-5.	Heat exchanger duties, binary variables and approach temperatures for all the possible heat exchangers in the Superstructures for the Process Integration of Waste Heat Recovery Technologies into Heat Exchanger Networks in Continuous Processes.....	84
Table 4-6.	Equivalences between variables and parameters between continuous and multi-period models.....	88
Table 5-1.	Stream data Case Study 1. 8H5C.....	116
Table 5-2.	Design parameters for Case Study 1 and 2.....	116

Table 5-3.	Results of stand-alone Heat Exchanger Network for Case Study 1	119
Table 5-4.	Results of working fluids prescreening for Case Study 1	121
Table 5-5.	Results of HEN-ORC for Case Study 1.....	122
Table 5-6.	Results of HEN-ABC for Case Study 1.....	123
Table 5-7.	Results of HEN-WHR for Case Study 1	124
Table 5-8.	Heat exchanger information for HEN-WHR in Case Study 1.....	126
Table 5-9.	Stream data Case Study 2. 8H5C Discontinuous	127
Table 5-10.	Energy targets Case Study 2 according to TSM.....	129
Table 5-11.	Results of stand-alone Heat Exchanger Network for Case Study 2	129
Table 5-12.	Results of working fluids prescreening for Case Study 2	130
Table 5-13.	Results of MP-ORC for Case Study 2.....	131
Table 5-14.	Results of MP-ABC for Case Study 2.....	132
Table 5-15.	Results of MP-WHR for Case Study 2.....	134
Table 5-16.	Heat exchanger information for MP-WHR in Case Study 2.....	136
Table 5-17.	Turbine and pump information for MP-WHR in Case Study 2	136
Table 5-18.	Stream data Case Study 3. 3H2C.....	137
Table 5-19.	Design parameters for Case Study 3.....	137
Table 5-20.	Energy targets Case Study 3 according to TAM and TSM	138
Table 5-21.	Results of stand-alone Heat Exchanger Network with Heat Storage for Case Study 3	141
Table 5-22.	Results of working fluids prescreening for Case Study 3	141
Table 5-23.	Results of MP-ST-ORC for Case Study 3	142
Table 5-24.	Results of MP-ST-ABC for Case Study 3	143
Table 5-25.	Results of MP-ST-WHR for Case Study 3.....	145
Table 5-26.	Heat exchanger information for MP-ST-WHR in Case Study 3	147
Table 5-27.	Turbine and pump information for MP-ST-WHR in Case Study 3	147
Table 5-28.	Economical parameters for the sensitivity analysis of model HEN-WHR. ...	148

Table 5-29.	Key temperatures used for the sensitivity analysis of model HEN-WHR.	150
Table 5-30.	Minimum approach temperatures used for the sensitivity analysis of model HEN-WHR.	153
Table 5-31.	CO ₂ -Savings of the integrated designs in comparison with the stand-alone HENs	160
Table 5-32.	Economical, technical and environmental evaluation of the results of the case studies.	162
Table A-1.	Coefficients for the calculation of the saturation pressure of H ₂ O.....	198
Table A-2.	Coefficients for the calculation of the saturation temperature of H ₂ O.....	198
Table A-3.	Coefficients for the calculation of the specific enthalpy at saturation of H ₂ O (Part 1).....	199
Table A-4.	Coefficients for the calculation of the specific enthalpy at saturation of H ₂ O (Part 2).....	199
Table A-5.	Coefficients for the calculation of the specific enthalpy of superheated H ₂ O.....	200
Table A-6.	Coefficients for the calculation of dew temperature of LiBr/H ₂ O solution. ..	200
Table A-7.	Coefficients for the calculation of specific enthalpy of LiBr/H ₂ O solution. 200	200
Table A-8.	Coefficients for the calculation of density of LiBr/H ₂ O solution.....	201
Table A-9.	Coefficients for the fitting functions generated for the case studies.	201
Table B-1.	Parameters for the calculation of thermophysical properties of selected working fluids.....	205
Table D-1.	Heat exchanger information for HEN1 in Case Study 1	248
Table D-2.	Heat exchanger information for HEN2 in Case Study 1	249
Table D-3.	Heat exchanger information for HEN-ORC in Case Study 1.....	250
Table D-4.	Heat exchanger information for HEN-ABC in Case Study 1.....	252
Table D-5.	Heat exchanger information for HEN1 in Case Study 2	253
Table D-6.	Heat exchanger information for HEN2 in Case Study 2	254

Table D-7.	Heat exchanger information for MP-ORC in Case Study 2	255
Table D-8.	Turbine and pump information for MP-ORC in Case Study 2.....	255
Table D-9.	Heat exchanger information for MP-ABC in Case Study 2	256
Table D-10.	Heat exchanger information for HEN1 in Case Study 3	257
Table D-11.	Heat exchanger information for HEN2 in Case Study 3	258
Table D-12.	Heat exchanger information for MP-ST-ORC in Case Study 3	259
Table D-13.	Turbine and pump information for MP-ST-ORC in Case Study 3.....	260
Table D-14.	Heat exchanger information for MP-ST-ABC in Case Study 3	260
Table E-1.	Extended State-of-the-Art for the Process Integration of Organic Rankine Cycles and Absorption Chillers into Heat Exchanger Networks	261
Table F-1.	Estimations of theoretical industrial waste heat potentials (Extended).....	264

List of Symbols

Parameters

Symbol		Units	Meaning
Continuous	Multi-period		
AF	-	generic	Annualization Factor
C_1 to C_{11}	-	generic	Fitting parameters for the fit functions for COP, C2G, t_{gen}^{in} and t_{abs}^{in} at the ABC cycle
c_{cost}	-	generic	Capital cost of a component
c_{cu}	-	€/kWh	Unitary cost of cold utility
c_{fix}	-	generic	Fixed cost coefficient for a component
c_{fix}^{HEN}	-	generic	Fixed cost coefficient for the heat exchangers
c_{fix}^{pump}	-	generic	Fixed cost coefficient for the ORC-Pump
c_{fix}^{turb}	-	generic	Fixed cost coefficient for the ORC-Turbine
c_{hu}	-	€/kWh	Unitary cost of hot utility
c_{var}	-	generic	Variable cost coefficient for a component
c_{var}^{HEN}	-	generic	Variable cost coefficient for the heat exchangers
c_{var}^{pump}	-	generic	Variable cost coefficient for the ORC-Pump
c_{var}^{turb}	-	generic	Variable cost coefficient for the ORC-Turbine
$cp_{w(g)}$	-	kJ/kg °C	Average specific heat capacity of working fluid as a gas
$cp_{w(l)}$	-	kJ/kg °C	Average specific heat capacity of working fluid as a liquid
E	-	generic	Equipment cost attribute for a component
e_{cost}	-	€/kWh	Cost of electricity required by the ORC
e_{price}	-	€/kWh	Price of the electricity generated by the ORC
F_i	$F_{i,p}$	kW/°C	Heat capacity flow rate of hot stream $i \in HP$ (during period $p \in P$)
F_j	$F_{j,p}$	kW/°C	Heat capacity flow rate of cold stream $j \in CP$ (during period $p \in P$)
h	-	kW/m ² °C	Heat transfer coefficient /Film coefficient of a stream
H_y	-	h	Operating hours per year
N_{Hot}	-	-	Number of hot streams
N_{Cold}	-	-	Number of cold streams
N_{Stages}	-	-	Number of superstructure stages
N_{Limit}	-	-	Limit to the number of heat exchanger units
NOK	-	-	Number of intra-process stages
P_{cond}	-	kPa	Condensation pressure for working fluid in ORC-Evaporator
P_{evap}	-	kPa	Evaporation pressure for working fluid in ORC-Evaporator
R^2	-	-	Coefficient of determination (“R-Squared”)

T_{abs}	-	°C	Outlet temperature of the refrigerant solution from the ABC-Absorber
T_{cond}	-	°C	Outlet temperature of the refrigerant from the ABC-Condenser
T_{cond}^{in}	-	°C	Inlet temperature of the working fluid to the ORC-Condenser
T_{cond}^{out}	-	°C	Outlet temperature of the working fluid from the ORC-Condenser
T_{cu}^{in}	-	°C	Inlet temperature cold utility
T_{cu}^{out}	-	°C	Outlet temperature cold utility
T_{evap}^{in}	-	°C	Inlet temperature of the working fluid to the ORC-Evaporator
T_{evap}^{out}	-	°C	Outlet temperature of the working fluid from the ORC-Evaporator
T_{gen}^{out}	-	°C	Outlet temperature of the refrigerant from the ABC-Generator
T_{hu}^{in}	-	°C	Inlet temperature hot utility
T_{hu}^{out}	-	°C	Outlet temperature hot utility
T_i^{in}	$T_{i,p}^{in}$	°C	Inlet temperature of hot stream $i \in HP$ (during period $p \in P$)
T_i^{out}	$T_{i,p}^{out}$	°C	Outlet temperature of hot stream $i \in HP$ (during period $p \in P$)
T_j^{in}	$T_{j,p}^{in}$	°C	Inlet temperature of cold stream $j \in CP$ (during period $p \in P$)
T_j^{out}	$T_{j,p}^{out}$	°C	Outlet temperature of cold stream $j \in CP$ (during period $p \in P$)
T_{ref}	-	°C	Temperature of the refrigerant at the ABC-Evaporator
U_{abca}	U_p^{abca}	kW/m ² °C	Overall heat transfer coefficient of ABC-Absorber (during period $p \in P$)
U_{abcc}	U_p^{abcc}	kW/m ² °C	Overall heat transfer coefficient of ABC-Condenser (during period $p \in P$)
U_{acu}	U_p^{acu}	kW/m ² °C	Overall heat transfer coefficient of ORC-Condenser located in cold utility (during period $p \in P$)
$U_{i,j,k}$	$U_{i,j,k,p}$	kW/m ² °C	Overall heat transfer coefficient of heat exchanger between hot stream $i \in HP$ and cold stream $j \in CP$ at stage $k \in ST$ (during period $p \in P$)
U_i^{abce}	$U_{i,p}^{abce}$	kW/m ² °C	Overall heat transfer coefficient of ABC-Evaporator located in hot stream $i \in HP$ (during period $p \in P$)
U_i^{abcg}	$U_{i,p}^{abcg}$	kW/m ² °C	Overall heat transfer coefficient of ABC-Generator located in hot stream $i \in HP$ (during period $p \in P$)
U_i^{cu}	$U_{i,p}^{cu}$	kW/m ² °C	Overall heat transfer coefficient of heat exchanger between hot stream $i \in HP$ and cold utility (during period $p \in P$)
U_i^{evap}	$U_{i,p}^{evap}$	kW/m ² °C	Overall heat transfer coefficient of ORC-Evaporator located in hot stream $i \in HP$ (during period $p \in P$)
U_j^{cond}	$U_{j,p}^{cond}$	kW/m ² °C	Overall heat transfer coefficient of ORC-Condenser located in cold stream $j \in CP$ (during period $p \in P$)
U_j^{hu}	$U_{j,p}^{hu}$	kW/m ² °C	Overall heat transfer coefficient of heat exchanger between cold stream $j \in CP$ and hot utility (during period $p \in P$)
w_{pump}	-	kJ/kg	Specific work required by the pump at the ORC cycle
w_{turb}	-	kJ/kg	Specific work generated by the turbine at the ORC cycle
β	-	generic	Cost exponent for a component
β^{HEN}	-	generic	Cost exponent for the heat exchangers
β^{pump}	-	generic	Cost exponent for the ORC-Turbine

β^{turb}	-	generic	Cost exponent for the ORC-Pump
Γ	-	°C	Upper limit for the approach temperatures at the heat exchangers
ΔT_{min}	-	°C	Minimum approach temperature permissible at a heat exchanger
ΔT_{min}^{ABC}	-	°C	Minimum approach temperature permissible between ABC working pair and process streams
ΔT_{min}^{HEN}	-	°C	Minimum approach temperature permissible between process streams
ΔT_{min}^{ORC}	-	°C	Minimum approach temperature permissible between ORC working fluid and process streams
ε_{SHEX}	-	-	Effectiveness of the refrigerant solution heat exchanger
λ_{cond}	-	kJ/kg	Latent heat of condensation of working fluid at the condenser pressure
λ_{evap}	-	kJ/kg	Latent heat of evaporation of working fluid at the evaporator pressure
Ω	-	kW	Upper limit for the Logarithmic mean temperature difference of the heat exchangers
-	c_{fix}^{sto}	generic	Fixed cost coefficient for the storage tanks
-	c_{var}^{sto}	generic	Variable cost coefficient for the storage tanks
-	cp_{st}	kJ/kg °C	Average specific heat capacity of the storage fluid
-	DOP_p	h	Duration of period in hours
-	h_{pc}	kJ/kg	Specific enthalpy of phase change
-	M^{st}	kg	Storage mass
-	$NOLV$	-	Number of storage levels
-	NOP	-	Number of periods of operation
-	T^{st}	°C	Storage temperature
-	$U_{i,p,lv}^{stoc}$	kW/m ² °C	Overall heat transfer coefficient of heat exchanger between hot stream $i \in HP$ and Cold Storage Stream at level $lv \in LV$ during period $p \in P$
-	$U_{j,p,lv}^{stoh}$	kW/m ² °C	Overall heat transfer coefficient of heat exchanger between hot stream $j \in CP$ and Hot Storage Stream at level $lv \in LV$ during period $p \in P$
-	β^{sto}	generic	Cost exponent for the storage tanks
-	ΔH^{st}	kJ	Change of enthalpy of storage during charge or discharge
-	ρ_{st}	kg/m ³	Density of storage fluid
-	Ψ	kW	Upper limit to the energy rate transferred to the Storage Tanks in a period

Variables

Symbol		Units	Meaning
Continuous	Multi-period		
$C2G$	-	-	Ratio between heat exchanger duties of ABC-Condenser and ABC-Generator
$CAPEX$	-	€/a	Capital expenditure

COP	-	-	Coefficient of Performance of ABC. Ratio between total heat exchanger duties of ABC-Evaporators and ABC-Generators
COP_{el}	-	-	Electrical coefficient of performance. Ratio between the cooling output at the evaporator and the electrical requirement of the solution pump
COP_{VCR}	-	-	Coefficient of Performance of VCR. Ratio between the cooling output at the evaporator and the electrical requirement of the compressor
$dt1^{abca}$	$dt1_p^{abca}$	$^{\circ}C$	Approach temperature at the hot end of ABC-Absorber (during period $p \in P$)
$dt1^{abcc}$	$dt1_p^{abcc}$	$^{\circ}C$	Approach temperature at the hot end of ABC-Condenser (during period $p \in P$)
$dt1^{acu}$	$dt1_p^{acu}$	$^{\circ}C$	Approach temperature at the hot end of ORC-Condenser located in cold utility (during period $p \in P$)
$dt1_{i,j,k}$	$dt1_{i,j,k,p}$	$^{\circ}C$	Approach temperature at the hot end of heat exchanger located between hot stream $i \in HP$ and cold stream $j \in CP$ at stage $k \in ST$ (during period $p \in P$)
$dt1_i^{abce}$	$dt1_{i,p}^{abce}$	$^{\circ}C$	Approach temperature at the hot end of ABC-Evaporator located in hot stream $i \in HP$ (during period $p \in P$)
$dt1_i^{abcg}$	$dt1_{i,p}^{abcg}$	$^{\circ}C$	Approach temperature at the hot end of ABC-Generator located in hot stream $i \in HP$ (during period $p \in P$)
$dt1_i^{cu}$	$dt1_{i,p}^{cu}$	$^{\circ}C$	Approach temperature at the hot end of heat exchanger located between hot stream $i \in HP$ and cold utility (during period $p \in P$)
$dt1_i^{evap}$	$dt1_{i,p}^{evap}$	$^{\circ}C$	Approach temperature at the hot end of ORC-Evaporator located in hot stream $i \in HP$ (during period $p \in P$)
$dt1_j^{cond}$	$dt1_{j,p}^{cond}$	$^{\circ}C$	Approach temperature at the hot end of ORC-Condenser located in cold stream $j \in CP$ (during period $p \in P$)
$dt1_j^{hu}$	$dt1_{j,p}^{hu}$	$^{\circ}C$	Approach temperature at the hot end of heat exchanger located between cold stream $j \in CP$ and hot utility (during period $p \in P$)
$dt2^{abca}$	$dt2_p^{abca}$	$^{\circ}C$	Approach temperature at the cold end of ABC-Absorber (during period $p \in P$)
$dt2^{abcc}$	$dt2_p^{abcc}$	$^{\circ}C$	Approach temperature at the cold end of ABC-Condenser (during period $p \in P$)
$dt2^{acu}$	$dt2_p^{acu}$	$^{\circ}C$	Approach temperature at the cold end of ORC-Condenser located in cold utility (during period $p \in P$)
$dt2_{i,j,k}$	$dt2_{i,j,k,p}$	$^{\circ}C$	Approach temperature at the cold end of heat exchanger located between hot stream $i \in HP$ and cold stream $j \in CP$ at stage $k \in ST$ (during period $p \in P$)
$dt2_i^{abce}$	$dt2_{i,p}^{abce}$	$^{\circ}C$	Approach temperature at the cold end of ABC-Evaporator located in hot stream $i \in HP$ (during period $p \in P$)
$dt2_i^{abcg}$	$dt2_{i,p}^{abcg}$	$^{\circ}C$	Approach temperature at the cold end of ABC-Generator located in hot stream $i \in HP$ (during period $p \in P$)
$dt2_i^{cu}$	$dt2_{i,p}^{cu}$	$^{\circ}C$	Approach temperature at the cold end of heat exchanger located between hot stream $i \in HP$ and cold utility (during period $p \in P$)
$dt2_i^{evap}$	$dt2_{i,p}^{evap}$	$^{\circ}C$	Approach temperature at the cold end of ORC-Evaporator located in hot stream $i \in HP$ (during period $p \in P$)

$dt2_j^{cond}$	$dt2_{j,p}^{cond}$	°C	Approach temperature at the cold end of ORC-Condenser located in cold stream $j \in CP$ (during period $p \in P$)
$dt2_j^{hu}$	$dt2_{j,p}^{hu}$	°C	Approach temperature at the cold end of heat exchanger located between cold stream $j \in CP$ and hot utility (during period $p \in P$)
$dt3_i^{evap}$	$dt3_{i,p}^{evap}$	°C	Approach temperature inside of ORC-Evaporator located in hot stream $i \in HP$ (during period $p \in P$)
$dt3_j^{cond}$	$dt3_{j,p}^{cond}$	°C	Approach temperature inside of ORC-Condenser located in cold stream $j \in CP$ (during period $p \in P$)
$LMTD^{abca}$	$LMTD_p^{abca}$	°C	Logarithmic mean temperature difference of ABC-Absorber (during period $p \in P$)
$LMTD^{abcc}$	$LMTD_p^{abcc}$	°C	Logarithmic mean temperature difference of ABC-Condenser (during period $p \in P$)
$LMTD^{acu}$	$LMTD_p^{acu}$	°C	Logarithmic mean temperature difference of ORC-Condenser located in cold utility (during period $p \in P$)
$LMTD_{i,j,k}$	$LMTD_{i,j,k,p}$	°C	Logarithmic mean temperature difference of heat exchanger located between hot stream $i \in HP$ and cold stream $j \in CP$ at stage $k \in ST$ (during period $p \in P$)
$LMTD_i^{abce}$	$LMTD_{i,p}^{abce}$	°C	Logarithmic mean temperature difference of ABC-Evaporator located in hot stream $i \in HP$ (during period $p \in P$)
$LMTD_i^{abcg}$	$LMTD_{i,p}^{abcg}$	°C	Logarithmic mean temperature difference of ABC-Generator located in hot stream $i \in HP$ (during period $p \in P$)
$LMTD_i^{cu}$	$LMTD_{i,p}^{cu}$	°C	Logarithmic mean temperature difference of heat exchanger located between hot stream $i \in HP$ and cold utility (during period $p \in P$)
$LMTD_i^{evap}$	$LMTD_{i,p}^{evap}$	°C	Logarithmic mean temperature difference of ORC-Evaporator located in hot stream $i \in HP$ (during period $p \in P$)
$LMTD_j^{cond}$	$LMTD_{j,p}^{cond}$	°C	Logarithmic mean temperature difference of ORC-Condenser located in cold stream $j \in CP$ (during period $p \in P$)
$LMTD_j^{hu}$	$LMTD_{j,p}^{hu}$	°C	Logarithmic mean temperature difference of heat exchanger located between cold stream $j \in CP$ and hot utility (during period $p \in P$)
\dot{m}_w	$\dot{m}_{w,p}$	kg/s	Mass flow rate of working fluid inside the ORC cycle (during period $p \in P$)
$OPEX$	-	€/a	Operational expenditure
q^{abca}	q_p^{abca}	kW	Heat transfer duty of ABC-Absorber (during period $p \in P$)
q^{abcc}	q_p^{abcc}	kW	Heat transfer duty of ABC-Condenser (during period $p \in P$)
q^{abce}	-	kW	Heat transfer duty of ABC-Evaporator
q^{abcg}	-	kW	Heat transfer duty of ABC-Generator
q^{acu}	q_p^{acu}	kW	Heat transfer duty of ORC-Condenser located in cold utility (during period $p \in P$)
$q_{i,j,k}$	$q_{i,j,k,p}$	kW	Heat transfer duty of heat exchanger located between hot stream $i \in HP$ and cold stream $j \in CP$ at stage $k \in ST$ (during period $p \in P$)
q_i^{abce}	$q_{i,p}^{abce}$	kW	Heat transfer duty of ABC-Evaporator located in hot stream $i \in HP$ (during period $p \in P$)
q_i^{abcg}	$q_{i,p}^{abcg}$	kW	Heat transfer duty of ABC-Generator located in hot stream $i \in HP$ (during period $p \in P$)

q_i^{cu}	$q_{i,p}^{cu}$	kW	Heat transfer duty of heat exchanger located between hot stream $i \in HP$ and cold utility (during period $p \in P$)
q_i^{evap}	$q_{i,p}^{evap}$	kW	Heat transfer duty of ORC-Evaporator located in hot stream $i \in HP$ (during period $p \in P$)
q_j^{cond}	$q_{j,p}^{cond}$	kW	Heat transfer duty of ORC-Condenser located in cold stream $j \in CP$ (during period $p \in P$)
q_j^{hu}	$q_{j,p}^{hu}$	kW	Heat transfer duty of heat exchanger located between cold stream $j \in CP$ and hot utility (during period $p \in P$)
r_{w_i}	$r_{w_{i,p}}$	-	Split fraction of working fluid that circulates through ORC-Evaporator located in hot stream $i \in HP$ (during period $p \in P$)
r_{w_j}	$r_{w_{j,p}}$	-	Split fraction of working fluid that circulates through ORC-Condenser located in cold stream $j \in CP$ (during period $p \in P$)
$t_{i,k}$	$t_{i,k,p}$	°C	Temperature of hot stream $i \in HP$ at the start of stage $k \in ST$ (during period $p \in P$)
$t_{i,NOK+1}$	$t_{i,NOK+1,p}$	°C	Temperature of hot stream $i \in HP$ at the end of the last intra-process stage (during period $p \in P$)
$t_{j,k}$	$t_{j,k,p}$	°C	Temperature of cold stream $j \in CP$ at the start of stage $k \in ST$ (during period $p \in P$)
$t_{j,k,NOK+1}$	$t_{j,NOK+1,p}$	°C	Temperature of cold stream $j \in CP$ at the end of the last intra-process stage (during period $p \in P$)
t_{abs}^{in}	-	°C	Inlet temperature of the refrigerant solution to the ABC-Absorber
t_{gen}	-	°C	Outlet temperature of the refrigerant solution from the ABC-Generator
t_{gen}^{in}	-	°C	Inlet temperature of the refrigerant solution to the ABC-Generator
t_i^{abce}	$t_{i,p}^{abce}$	°C	Temperature of hot stream $i \in HP$ at the start of ABC-Evaporator stage (during period $p \in P$)
t_i^{abcg}	$t_{i,p}^{abcg}$	°C	Temperature of hot stream $i \in HP$ at the end of ABC-Generator stage (during period $p \in P$)
t_i^{orc}	$t_{i,p}^{orc}$	°C	Temperature of hot stream $i \in HP$ at the end of ORC stage (during period $p \in P$)
TAC	-	€/a	Total annualized cost
W_{net}	$W_{net,p}$	kW	Net work generated by ORC (during period $p \in P$)
W_{pump}	$W_{pump,p}$	kW	Work required by the ORC-Pump (during period $p \in P$)
W_{pump}^{abc}	-	kW	Work required by the ABC-Pump
W_{turb}	$W_{turb,p}$	kW	Work generated by the ORC-Turbine (during period $p \in P$)
$\Delta T_{Cold-End}$	-	°C	Temperature differences at the cold end of a heat exchanger
$\Delta T_{Hot-End}$	-	°C	Temperature differences at the hot end of a heat exchanger
η_{orc}	-	-	Cycle efficiency of ORC
-	A^{abca}	m ²	Effective area of ABC-Absorber
-	A^{abcc}	m ²	Effective area of ABC-Condenser
-	A^{acu}	m ²	Effective area of ORC-Condenser located in cold utility
-	$A_{i,j,k}$	m ²	Effective area of heat exchanger located between hot stream $i \in HP$ and cold stream $j \in CP$ at stage $k \in ST$

-	$A_{i,k,lv}^{stoc}$	m^2	Effective area of heat exchanger located between hot stream $i \in HP$ and Cold Storage Stream at stage $k \in ST$ and level $lv \in LV$
-	$A_{j,k,lv}^{stoh}$	m^2	Effective area of heat exchanger located between cold stream $j \in CP$ and Hot Storage Stream at stage $k \in ST$ and level $lv \in LV$
-	A_i^{abce}	m^2	Effective area of ABC-Evaporator located in hot stream $i \in HP$
-	A_i^{abcg}	m^2	Effective area of ABC-Generator located in hot stream $i \in HP$
-	A_i^{cu}	m^2	Effective area of heat exchanger located between hot stream $i \in HP$ and cold utility
-	A_i^{evap}	m^2	Effective area of ORC-Evaporator located in hot stream $i \in HP$
-	A_j^{cond}	m^2	Effective area of ORC-Condenser located in cold stream $j \in CP$
-	A_j^{hu}	m^2	Effective area of heat exchanger located between cold stream $j \in CP$ and hot utility
-	$dt1_{i,k,p,lv}^{stoc}$	$^{\circ}C$	Approach temperature at the hot end of heat exchanger located between hot stream $i \in HP$ and Cold Storage Stream at stage $k \in ST$ and level $lv \in LV$ during period $p \in P$
-	$dt1_{j,k,p,lv}^{stoh}$	$^{\circ}C$	Approach temperature at the hot end of heat exchanger located between cold stream $j \in CP$ and Hot Storage Stream at stage $k \in ST$ and level $lv \in LV$ during period $p \in P$
-	$dt2_{i,k,p,lv}^{stoc}$	$^{\circ}C$	Approach temperature at the cold end of heat exchanger located between hot stream $i \in HP$ and Cold Storage Stream at stage $k \in ST$ and level $lv \in LV$ during period $p \in P$
-	$dt2_{j,k,p,lv}^{stoh}$	$^{\circ}C$	Approach temperature at the cold end of heat exchanger located between cold stream $j \in CP$ and Hot Storage Stream at stage $k \in ST$ and level $lv \in LV$ during period $p \in P$
-	$LMTD_{i,k,p,lv}^{stoc}$	$^{\circ}C$	Logarithmic mean temperature difference of heat exchanger located between hot stream $i \in HP$ and Cold Storage Stream at stage $k \in ST$ and level $lv \in LV$ during period $p \in P$
-	$LMTD_{j,k,p,lv}^{stoh}$	$^{\circ}C$	Logarithmic mean temperature difference of heat exchanger located between cold stream $j \in CP$ and Hot Storage Stream at stage $k \in ST$ and level $lv \in LV$ during period $p \in P$
-	M_{lv}^{stoc}	kg	Minimum storage mass required for Cold Storage Tank in level $lv \in LV$
-	M_{lv}^{stoh}	kg	Minimum storage mass required for Hot Storage Tank in level $lv \in LV$
-	$q_{i,k,p,lv}^{stoc}$	kW	Heat transfer duty of heat exchanger located between hot stream $i \in HP$ and Cold Storage Stream at stage $k \in ST$ and level $lv \in LV$ during period $p \in P$
-	$q_{j,k,p,lv}^{stoh}$	kW	Heat transfer duty of heat exchanger located between cold stream $j \in CP$ and Hot Storage Stream at stage $k \in ST$ and level $lv \in LV$ during period $p \in P$
-	$Q_{p,lv}^c$	kWh	Cumulated thermal energy stored in Cold Storage Tank located in level $lv \in LV$ at the start of the Process Cycle at the end of period $p \in P$
-	$q_{p,lv}^{charc}$	kW	Energy rate of charging of Cold Storage Tank located in level $lv \in LV$ during period $p \in P$
-	$q_{p,lv}^{charh}$	kW	Energy rate of charging of Hot Storage Tank located in level $lv \in LV$ during period $p \in P$

-	$q_{p,lv}^{discharc}$	kW	Energy rate of discharging of Cold Storage Tank located in level $lv \in LV$ during period $p \in P$
-	$q_{p,lv}^{discharh}$	kW	Energy rate of discharging of Hot Storage Tank located in level $lv \in LV$ during period $p \in P$
-	$Q_{p,lv}^h$	kWh	Cumulated thermal energy stored in Hot Storage Tank located in level $lv \in LV$ at the end of period $p \in P$
-	$Q_{lv\,start}^c$	kWh	Cumulated thermal energy stored in Cold Storage Tank located in level $lv \in LV$ at the start of the Process Cycle
-	$Q_{lv\,start}^h$	kWh	Cumulated thermal energy stored in Hot Storage Tank located in level $lv \in LV$ at the start of the Process Cycle
-	$t_{k,lv}^{stoc}$	°C	Temperature of Cold Storage Stream in level $lv \in LV$ at the start of stage $k \in ST$
-	$t_{k,lv}^{stoh}$	°C	Temperature of Hot Storage Stream in level $lv \in LV$ at the start of stage $k \in ST$
-	$t_{NOK+1,lv}^{stoc}$	°C	Temperature of Cold Storage Stream in level $lv \in LV$ end of the last intra-process stage
-	$t_{NOK+1,lv}^{stoh}$	°C	Temperature of Hot Storage Stream in level $lv \in LV$ at the end of the last intra-process stage
-	t_{lv}^{stoc}	°C	Temperature of Cold Storage Tank in level $lv \in LV$
-	t_{lv}^{stoh}	°C	Temperature of Hot Storage Tank in level $lv \in LV$
-	V_{lv}^{stoc}	m ³	Minimum storage volume required for Cold Storage Tank in level $lv \in LV$
-	V_{lv}^{stoh}	m ³	Minimum storage volume required for Hot Storage Tank in level $lv \in LV$
-	W_{pump}^{max}	kW	Effective size of ORC-Pump for cost calculations
-	W_{turb}^{max}	kW	Effective size of ORC-Turbine for cost calculations

Binary Variables

Symbol		Meaning
Continuous	Multi-period	
	-	Existence of ORC-Condenser located in cold utility
	-	Existence of heat exchanger located between hot stream $i \in HP$ and cold stream $j \in CP$ at stage $k \in ST$
	-	Existence of AR-Evaporator located in hot stream $i \in HP$
	-	Existence of AR-Generator located in hot stream $i \in HP$
	-	Existence of heat exchanger located between hot stream $i \in HP$ and cold utility
	-	Existence of ORC-Evaporator located in hot stream $i \in HP$
	-	Existence of ORC-Condenser located in cold stream $j \in CP$
	-	Existence of heat exchanger located between cold stream $j \in CP$ and hot utility
-	$y_{p,lv}^{charge}$	Charge (1) or discharge (0) of Hot Storage Tank Located in level $lv \in LV$ during period $p \in P$

-	$z_{i,k,lv}^{stoc}$	Existence of heat exchanger located between hot stream $i \in HP$ and Cold Storage Stream at stage $k \in ST$ and level $lv \in LV$
-	$z_{j,k,lv}^{stoh}$	Existence of heat exchanger located between cold stream $j \in CP$ and Hot Storage Stream at stage $k \in ST$ and level $lv \in LV$

Sets

Set	Meaning
CP	Set of cold process streams j
HP	Set of hot process streams i
LV	Set of storage levels lv
P	Set of periods of operation p
ST	Set of intra-process stages k

Nomenclature

Abbreviation	Meaning
ABC	Absorption Chiller
BARON	Branch-And-Reduce Optimization Navigator
CC	Composite Curve
CHP	Combined Heat and Power
COP	Coefficient of Performance
COP 21	21st Conference of the Parties
DH	District Heating
FTVM	Fixed Temperature Variable Mass
GA	Genetic Algorithm
GAMS	General Algebraic Modeling System
GAX	Generator-Absorber Heat Exchanger
GCC	Grand Composite Curves
GHG	Greenhouse Gases
GMST	Global Mean Surface Temperature
GWP	Global Warming Potential
HEN	Heat Exchanger Network
HRL	Heat Recovery Loop
HTF	Heat Transfer Fluid
HVAC	Heat, Ventilation and Air Conditioning
IEA	International Energy Agency
IPCC	Intergovernmental Panel on Climate Change
IWH	Industrial Waste Heat
LIES	Locally Integrated Energy Sectors
LP	Linear Programming
MILP	Mixed Integer Linear Programming
MINLP	Mixed Integer Non-Linear Programming
MP	Mathematical Programming
NLP	Non-Linear Programming
ORC	Organic Rankine Cycle
PA	Pinch Analysis
PCM	Phase Change Materials
PI	Process Integration
PR-EOS	Peng Robinson Equations of State
PTA	Problem Table Algorithm
REFPROP	Reference Fluid Thermodynamic and Transport Properties Database
RHEX	Refrigerant Heat Exchanger
SHEX	Solution Heat Exchanger
SYNHEAT	Stage-wise superstructure for the Synthesis of Heat Exchanger Networks
TAC	Total Annualized Cost
TAM	Time Average Model
TES	Thermal Energy Storage
TSA	Total Site Analysis
TSHI	Total Site Heat Integration
TSM	Time Slice Model
UN	United Nations
UNFCCC	United Nations Framework Convention on Climate Change

VCR	Vapor Compression Refrigeration
VTFM	Variable Temperature Fixed Mass
WHR	Waste Heat Recovery

Abstract

The industrial sector accounts for almost a third of the global GHG emissions, from which around 80% correspond to energy-related emissions. The decrease of energy consumption in the industrial sectors has therefore a direct impact in the reduction of the global GHG emission as required by the Paris Agreement, in order to limit the increase of the global average temperature below 2°C above pre-industrial levels. Around 30% of the energy input into the industrial sector worldwide is released unused to the environment as waste heat. The internal and external recovery of waste heat represents in consequence, an attractive strategy for the reduction of the industrial energy consumption. Typically, the internal waste heat recovery and the external waste heat recovery are treated as separated problems in the hierarchical sequential approach for the design of industrial processes. Although a practical and successful design strategy, this sequential approach neglects possible synergies generated by considering simultaneously the internal and external waste heat recovery options during the process design.

In this work, a mathematical framework considering simultaneously internal (represented by the synthesis of the heat exchanger network for the system) and external (represented by the use of waste heat transformation technologies) waste heat recovery options is presented. The mathematical framework focuses on two of the most mature waste heat transformation technologies, Organic Rankine Cycles (ORCs) and Absorption Chillers (ABCs), and integrates them into Heat Exchanger Networks (HENs) in continuous and multi-period process with and without Fixed Temperature Variable Mass (FTVM) heat storage. The generated system designs have the potential to be economically, technically and environmentally more attractive than systems solely factoring heat exchanger networks.

The work is organized in six chapters. First, an introduction to the research problem, motivation and objectives, is provided. Next, fundamental concepts of waste heat recovery and process integration, as well as the State-of-the-Art of the process integration of ORCs, ABCs or both into HENs, are presented. The mathematic framework developed in this work is then introduced and its application is illustrated using three case studies from the literature. Finally, conclusions and future work are outlined.

The main conclusion from this dissertation is, that combined design methodologies, considering the process integration of ORCs, ABCs or both, into HENs in continuous and multi-period processes with and without FTVM heat storage, can generate economically, technically or environmentally attractive system designs.

Kurzfassung

Rund 30 % des Energieeinsatzes im industriellen Sektor weltweit wird als Abwärme ungenutzt an die Umwelt abgegeben. Die interne und externe Rückgewinnung von Abwärme stellt folglich eine attraktive Strategie zur Reduzierung des industriellen Energieverbrauchs dar. Typischerweise werden die interne und die externe Rückgewinnung (bzw. Wärmerückgewinnung und Abwärmenutzung) als getrennte Probleme im hierarchisch-sequenziellen Ansatz für das Design von industriellen Prozessen behandelt. Obwohl dies eine praktische und erfolgreiche Designstrategie ist, vernachlässigt dieser sequentielle Ansatz mögliche Synergien, die durch die gleichzeitige Berücksichtigung der internen und externen Rückgewinnungsoptionen während des Prozessdesigns entstehen.

In dieser Arbeit wird ein mathematisches Rahmenwerk entwickelt, das gleichzeitig interne (Auslegung des Wärmeübertragernetzwerks für das System) und externe (Einsatz von Abwärme-Umwandlungstechnologien) Rückgewinnungsoptionen berücksichtigt. Das mathematische Rahmenwerk konzentriert sich auf zwei der etabliertesten Abwärme-Umwandlungstechnologien, Organic Rankine Cycles (ORCs) und Absorptionskältemaschinen (engl. ABCs), und integriert sie in Wärmeübertragernetzwerken (engl. HENs) in kontinuierlichen und mehrperiodigen Prozessen mit und ohne FTVM-Wärmespeicher (engl. Fixed Temperature Variable Mass Heat Storage). Die generierten Systemdesigns haben das Potenzial, wirtschaftlich, technisch und ökologisch attraktiver zu sein als Systeme, die nur Wärmeübertragernetzwerke berücksichtigen.

Die Arbeit ist in sechs Kapitel gegliedert. Zunächst wird eine Einführung in die Forschungsfrage, die Motivation und die Ziele gegeben. Anschließend werden grundlegende Konzepte der Abwärmenutzung und Prozessintegration sowie der Stand der Technik der Prozessintegration von ORCs, ABCs und deren Kombination in HENs vorgestellt. Im nächsten Schritt wird das in dieser Arbeit entwickelte mathematische Rahmenwerk vorgestellt und seine Umsetzung wird durch drei Fallstudien aus der Literatur erläutert. Abschließend werden Schlussfolgerungen und Ansätze für zukünftige Forschungsarbeiten skizziert.

Die wichtigste Schlussfolgerung aus dieser Arbeit ist, dass kombinierte Auslegungsmethoden, die die Prozessintegration von ORCs, ABCs und deren Kombination in HENs in kontinuierlichen und mehrperiodigen Prozessen mit und ohne FTVM-Wärmespeicher berücksichtigen, wirtschaftlich, technisch und ökologisch attraktive Systemauslegungen generieren können.

1 Introduction

On the 12th of December 2015, the legally binding Paris Agreement was adopted by 195 countries (plus the European Union as a legal entity) during the 2015 United Nations Climate Change Conference, also known as the 21st United Nations Framework Convention on Climate Change (UNFCCC) Conference of the Parties (COP 21). The main objective of the agreement is to “...strengthen the global response to the threat of climate change...” by “... holding the global average temperature¹ to well below 2°C above pre-industrial levels² and pursue efforts to limit the temperature increase to 1.5°C above pre-industrial levels...” (UNFCCC 2015). The agreement, which entered into force on the 4th of November 2016 presents a legal framework for the global fight against climate change. More recently, on the special report “Global Warming of 1.5°C” (IPCC 2018) the Intergovernmental Panel on Climate Change (IPCC) of the United Nations (UN) warned about the long-term consequences that a temperature increase of more than 1.5°C above pre-industrial levels will have on natural and human systems and encourage policy makers to support the implementation of ambitious actions to limit the global warming to the 1.5°C target. The expected consequences in comparison with the 2°C scenario include but are not limited to increases in the mean temperatures of most land and ocean regions, increases in extreme weather conditions (i.e. hot extremes, heavy precipitation, droughts, etc.) in several regions, increases on sea level rising, increases on species loss and extinction (6% of insects, 8% of plants and 4% of vertebrates in 1.5°C scenario in comparison with 18% of insects, 16% of plants and 8% of vertebrates in 2°C scenario) and increases on climate-related risks to health, food and human security, water supply and economic growth, etc.

According to data from the World Resources Institute, in 2016 the industrial sector accounted for 29.4% of the global greenhouse gases (GHG) emissions, with 82.3% of this share (24.2% of the global GHG emissions) as energy-related emissions and 17.7% (5.2% of the global GHG emissions) generated as byproduct of industrial processes, mainly in cement, chemical and petrochemical manufacturing (Ritchie, et-al 2020). As presented in Figure 1-1, energy-related GHG emissions in the industrial sector have the largest contribution to the GHG emissions of

¹ Global average temperature is defined by the Intergovernmental Panel on Climate Change of the United Nations (IPCC) as the Global Mean Surface Temperature (GMST) and is calculated as a weighted average of the Near-Surface Air Temperature (SAT) and the Sea Surface Temperature (SST).

² Pre-Industrial levels are defined by the IPCC as the “...multi-century period prior to the onset of large-scale industrial activity around 1750...” IPCC 2018. The GMST calculations for pre-industrial levels are based on the reference period 1850-1900.

any anthropogenic activity with a 24.2% of the global GHG emissions and therefore the decarbonization and the decrease of the energy consumption in the industrial sector have a direct impact on the global efforts against climate change. In numbers, the global GHG emissions in 2016 were roughly 49.4 GtCO₂eq³ from which 12.0 GtCO₂eq were energy-related emissions from the industrial sector (Ritchie, et-al 2020).

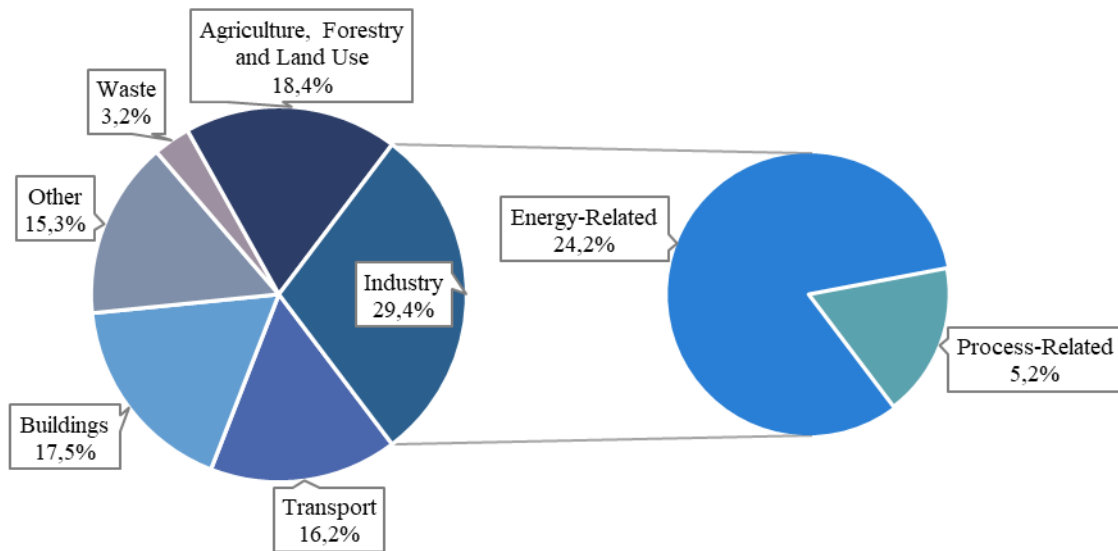


Figure 1-1. Global Green House Gas (GHG) emissions in percentage of CO₂eq per sector in 2016.

Source: Own diagram based on Ritchie, et-al (2020).

1.1 Motivation and Background

In the only study estimating the total global waste heat potential, Forman et al. (2016) calculated that around 30% of the energy input into the industrial sector, is released unused to the environment through a heat carrier as industrial waste heat. Increasing environmental standards and the dissemination of better technological practices worldwide can be expected to decrease the proportion of industrial waste heat.

Even then, for physical, technological and economic reasons, some level of industrial waste heat is unavoidable and new methodologies and technologies need to be implemented in order to design systems that minimize the waste heat generated by a given process (reuse or internal recovery) or that transform it into other useful energy forms or transport it to other external

³ Non-SI standard unit for GHG emissions. Calculated using global warming potentials (GWPs) over a 100-year period. For non-CO₂ gases, CO₂ equivalent is calculated as the amount of CO₂ which generate the same GWP.

locations where it can be used (external recovery or utilization). Although in English, both concepts are usually referred to with the term “Waste Heat Recovery” (WHR), in the German language a clearer separation between the internal (“Wärmerückgewinnung”) and external (“Abwärmenutzung”) recovery of waste heat exists (Gabathuler 1994).

In most publications in the literature, as well as in practice, internal and external heat recovery in industrial processes are treated as independent and separated problems. The internal heat recovery is studied as part of the design of a heat recovery system, which mainly refers to the synthesis of a cost-optimal heat exchanger network (HEN) for the process, and it constitutes the main research problem of a family of methodologies known as “Process Integration” (PI). On the other hand, the external waste heat recovery, and more specifically the use of energy conversion technologies, is treated sometimes as an independent problem or sometimes as part of the design of the utility system. An overview of this hierarchal approach is represented in the famous “onion diagram” for process design as shown in Figure 1-2.

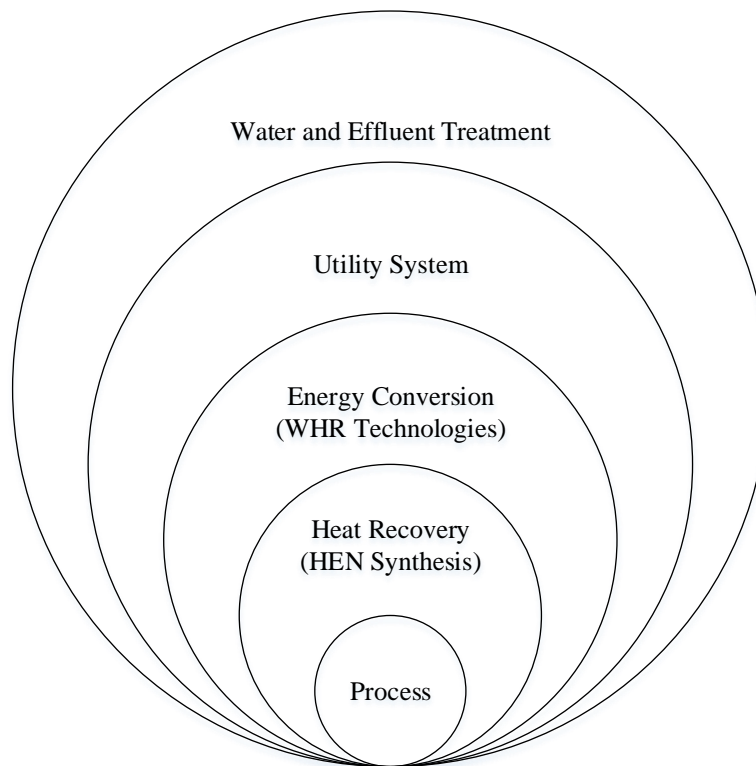


Figure 1-2. "Onion Diagram" for process design.

Source: Own diagram based on Peesel et al. (2016) and Smith (2005)

The typical onion diagram for process design represents a sequential approach for the design of industrial processes which is a successful and practical strategy for the synthesis of industrial systems. Even then, the sequential nature of the method, although often iterative, neglects the possible synergies that can be generated by considering simultaneously two or more levels in

the process design hierarchy. In this research, two of those process design levels are considered simultaneously: the design of the heat exchanger network (including heat storage) and the integration of waste heat recovery technologies into the background processes. By considering the integration of waste heat recovery technologies and the synthesis of the heat exchanger network simultaneously, new possibilities and synergies can be generated which could contribute to design energy systems that are economically, technically and/or environmentally attractive for industrial implementation.

1.2 Problem Description and Objectives

Given the number of waste heat recovery technologies available, considering the integration of all of them into heat exchanger networks is a considerable task. For time and resources limitations, only a few selected technologies are considered in this work. Two of the most mature technologies for WHR are the “Organic Rankine Cycles” (ORC) and the “Absorption Chillers” (ABC). While a few studies have been presented considering the integration of these WHR technologies into HENs, they typically only considered one technology at a time, do not consider the thermophysical properties for the working fluids/pairs and/or are limited to continuous processes (see State-of-the-Art in Chapter 3). This research is an effort to expand the literature in this area of research and study the process integration of ORCs, ABCs or both into HENs in continuous and multi-period processes with or without heat storage.

From the heat storage technologies available in the market for industrial applications, only “Fixed Temperature Variable Mass” (FTVM) heat storages are considered in this research. The main reason for this selection is the maturity level of this technology for industrial applications. FTVM storages includes two-tank, multi-tank and stratified tanks systems, and their use is a common and accepted practice in industrial processes worldwide (see discussion on heat storage technologies in Section 2.3.3).

The overarching research question for this dissertation can be formulated as:

“Can a combined design methodology considering simultaneously the synthesis of heat exchanger networks and the process integration of organic Rankine cycles, absorption chillers or both into the background processes in continuous and multi-period operation with and without FTVM heat storage, generate system designs that are economically, technically and/or environmentally more attractive than systems solely factoring heat exchanger networks?”

In order to answer this overarching research question, a mathematical framework is developed for the process integration of organic Rankine cycles, absorption chillers or both into heat exchanger networks in continuous and multi-period processes with and without FTVM heat storage.

The novelty of the research resides in two key aspects: first, the modification of existing mathematical models for the integration of ORCs and ABCs into HENs in continuous processes in order to include both technologies simultaneously while considering the working fluid/pair properties and second, the expansion of the modified models to include multi-period processes with and without FTVM heat storage.

The research question can also be formulated as a synthesis problem (problem statement). The use of problem statement is a common practice in studies related to the synthesis of heat exchanger networks. For this dissertation, the synthesis problem, can be formulated as:

“Given are a continuous or a multi-period industrial process with a set of streams to be cooled $i \in HP$ (hot streams) and a set of streams to be heated $j \in CP$ (cold streams) with known inlet and outlet temperatures as well as known heat capacity flow rates and heat transfer coefficients. Moreover, hot and cold utilities of known temperatures and heat transfer coefficients are available to supply or to accept thermal energy to or from the system, respectively. Additionally in the case of multi-period processes, a set of periods of operation $p \in P$, each of them of known duration is given. Design a heat exchanger network (including heat storage) integrating organic Rankine cycles, absorption chillers or both into the background processes, that optimizes the total annualized cost (TAC) of the system”.

An overview of the general and specific objectives of this dissertation is presented in Figure 1-3. The main objective of the dissertation is to generate the aforementioned mathematical framework for the integration of organic Rankine cycles, absorption chillers or both, into heat exchanger networks in continuous and multi-period processes with and without FTVM heat storage. This objective is accomplished through the generation of nine superstructures (three for continuous processes, three for multi-period processes without heat storage and three for multi-period processes with FTVM storage) with their respective mathematical models, that can be used to explore integration opportunities of ORCs, ABCs or both, into HENs, while simultaneously designing the HEN, integrating FTVM heat storage if necessary and calculating the TAC of the system.

The main objective is subdivided into three different specific objectives, one for each type of process considered in this dissertation, as presented in Figure 1-3. For continuous processes, the acronyms HEN-ORC, HEN-ABC and HEN-WHR indicate the superstructures for the process integration of organic Rankine cycles, absorption chillers and both technologies simultaneously into HENs, respectively. Similar acronyms are used to represent the superstructures developed for multi-period processes without heat storage (MP-ORC, MP-ABC and MP-WHR) and also to represent the superstructures developed for multi-period processes with FTVM heat storage (MP-ST-ORC, MP-ST-ABC and MP-ST-WHR).

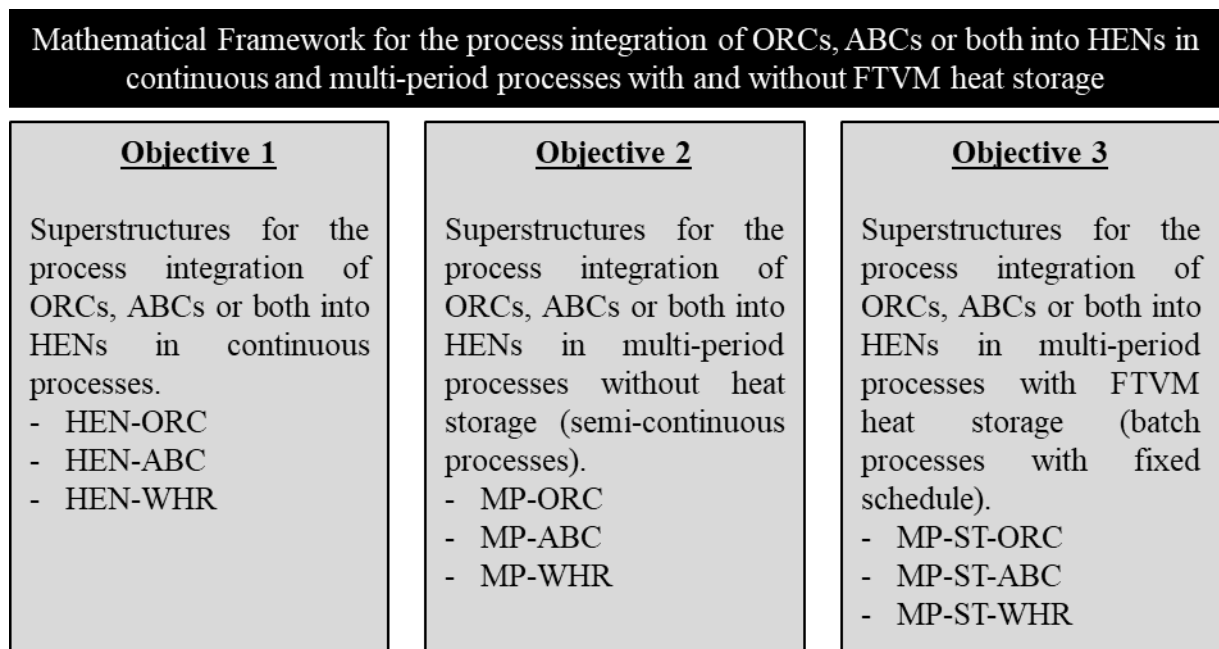


Figure 1-3. General and specific objectives of the dissertation.

Source: Own diagram

1.3 Scope of the Research

As all mathematical models, the mathematical framework developed in this dissertation has certain limitations due to the assumptions made during its generation. Some of these limitations are related to the system arrangements possible in the superstructures, as certain system configurations are not considered. Other limitations are related to assumptions made to simplify the number of variables and computational complexity of the mathematical models.

This dissertation attempts to provide viable designs for the synthesis problem within the following assumptions:

1) General assumptions:

- The method is a mathematical programming approach for the simultaneous synthesis of HEN and the integration of ORC, ABC or both into the background processes. Pinch analysis (PA) is used only to establish upper limits to the hot and cold utility consumption in the system (i.e., hot and cold utility targets) and as visual aid (i.e., “Grand Composite Curves” or GCC) for the understanding of the case studies presented in Chapter 4. The synthesis results (i.e., system designs) are generated exclusively from mathematical optimization techniques. In contrast to sequential methods for the synthesis of HEN and the integration of ORC, ABC or both into the background processes, the methodology developed in this work considers simultaneously trade-offs and interactions between the different components and subsystems of the design.
- ORC and ABC will operate only with “waste heat”, that is only with energy already supplied to the HEN which it would be otherwise rejected to the cold utility if not “recovered”. In this work, only waste heat attached to fluid heat carriers is considered (no diffuse waste heat or waste heat attached to solid carriers) and it is defined as “*the unused or residual heat from an industrial process, after the maximum internal heat recovery through heat exchange according to the pinch analysis is achieved*” (Oluleye 2015) . Numerically, the waste heat available in the system is equal to the cold utility target as calculated with pinch analysis. Please see Section 2.1 for an extended discussion on the multiple definitions of waste heat in the scientific literature.
- The superstructures are based on the “stage-wise” superstructure for the synthesis of HENs also known as SYNHEAT model by Yee and Grossmann (1990). From current mathematical programming methods for the design of HENs in continuous processes, SYNHEAT offers the best combined performance in terms of quality of the solutions and computational effort (Escobar and Trierweiler 2013). Additionally, SYNHEAT has already been successfully extended and applied for the design of multi-period HENs (Aaltola 2003).
- As with any superstructure-based methodology, only certain system configurations are considered. The detailed description of the configurations developed in this work is presented in Chapter 4. Some of the system designs that are not considered include:
 - Systems with multiple ORCs and ABCs. The developed models only include one ORC and one ABC.

- Systems where the ORC and ABC exchange energy directly with each other, or with the storage system. In the developed models the ORC and the ABC only interact with the process streams or the utilities.
 - Systems with ORC configurations other than the basic cycle.
 - Systems with ABC configuration other than the single-effect ABC.
-
- Only one ORC can be integrated to a given HEN. Multiple evaporators and condensers in parallel can be installed in each of the hot and cold process streams, respectively, but the ORC system operates only with one working fluid, one pump and one turbine.
 - Similar to the ORC, only one ABC can be integrated to a given HEN. Multiple generators and evaporators in parallel can be installed in each of the hot process streams, but the ABC operates with only one refrigerant couple, one absorber, one condenser, one pump and one solution heat exchanger (SHEX).
 - ORC and ABC integration can only occur in certain places in the superstructure (dedicated stages). This assumption reduces the number of binary variables significantly, as the number of binary variables describing the existence (or not) of ORCs and ABCs is only proportional to the number of hot and cold streams and not the number of stages in the superstructure. Successful applications of this approach were first presented by Hipólito-Valencia et al. (2013).
 - The locations of the dedicated stages for the ORC and ABC integration in the different models developed are fixed and they take place at the cold end of the process streams. The schematic representations for the nine superstructures developed in this work are presented in Chapter 4 and provide a detailed description of the stage locations for the different superstructures. With the exception of the “ABC-Evaporator Stage” located directly after the “Cold Utility Stage”, the fixed locations for the dedicated stages are not thermodynamically optimal (that would be directly after the pinch point for the “ORC Stage” and the “ABC-Generator” Stage). Even then, by fixing the location of the dedicated stages, the computational complexity and model size of the different superstructures is reduced significantly. Additionally, the fixed locations allow to generate systems without expert knowledge of the internal flow of energy between the process streams, that is without the need of a detailed pinch analysis.
 - The main objective of all the models developed in this work is the minimization of “Total Annualized Cost” (TAC) of the systems (Objective Function). Different than methodologies based on the “Pinch Design Method” (Linnhoff and Hindmarsh 1983),

where the economical optimum is not the objective function, and instead “near optimal” designs optimizing related variables (e.g., the hot and utility consumptions, the number of units, total heat transfer area, power generated by ORC, etc.) are sequentially generated, the mathematical approach used in this work allows to search directly for the economic optimum of the system.

- Heat capacities and heat transfer coefficients of all fluids involved are constant.
- If streams splits are required in the HEN, mixing takes place isothermally. This limitation is inherited from the original formulation of the SYNHEAT model and it allows to reduce the size of the model formulation, as it eliminates the need for non-linear mixing equations (mass and heat balances) at each stage of the superstructure (Yee and Grossmann 1990).
- All the components in the systems are adiabatic (no thermal losses).
- Dynamic and transient or partial-load effects in the multi-period processes are not considered. This limitation simplifies the mathematical optimization problem but can have a significant impact on the performance of real-life systems. Additional research in this area is suggested for future works (see Section 6.2).
- The capital cost for each heat exchanger, turbine, pump and storage tank in the system is described by a formula of the type:

$$c_{cost} = c_{fix} + c_{var} E^{\beta} \quad (1-1)$$

Where c_{cost} represents the capital cost of the component, c_{fix} the fixed cost of a unit of the component, c_{var} the variable cost coefficient for the given component, E the equipment cost attribute, that is the equipment parameter which is used to correlate capital costs (heat transfer area for heat exchangers, power generated or required for turbines and pumps and storage volume for storage tanks), and β the capital cost exponent. The superstructures developed on this work can be applied with any arbitrary set of cost coefficients. For each case study presented in Chapter 5, a new set of cost coefficients is used.

- For multi-period processes, the capital cost for each component in the system is calculated using the “Maximum Size Approach” . This methodology, first presented by by Verheyen and Zhang (2006) for the synthesis of multi-period HENs, defines the effective heat transfer area of a heat exchanger to be used in TAC calculations as the biggest of the heat transfer areas required (i.e, maximum size) by the given heat exchanger, if each period of operation were considered independently. In this work, the

“Maximum Size Approach” is extended to other unit types (turbines, pumps and storage tanks) using the maximum value of their equipment cost attributes (power generated, power required and storage volume, respectively). The “Maximum Size Approach” allows the generated designs to operate under all the possible conditions in the system, and the minimization of the TAC as objective function forces the optimization algorithm to generate the “cheapest” (i.e., smallest) system which is able to operate under all conditions in all the period of operation.

2) For system involving ORCs:

- Only the basic ORC configuration is considered, due to its simplicity and good thermoeconomic performance (Imran et al. 2014; Branchini et al. 2013).
- Working fluid is set in advance. Only pure substances that are dry working fluids are allowed. Dry and isentropic fluids are preferred for most ORC applications, as no liquid droplets are generated during the expansion and therefore no superheating is required to preserve the turbine blades (Liu et al. 2004).
- ORC evaporation and condensation temperatures/pressures are set in advance. Models including the ORC evaporation and condensation temperatures as optimization variables have already been presented in the literature for continuous processes (Yu et al. 2017a), but this approach increases substantially the complexity of the model formulations, as it requires the inclusion of highly non-linear equations of state in the optimization models. More recently, approaches using fit functions instead of equations of state for the working fluid properties have been used with promising results and could be explored for future works (Dong et al. 2020).
- Specific thermophysical properties (per unit of mass) of the working fluid at the entrance/exit of each ORC component are calculated in advance independently of the optimization model. At least two independent intensive thermophysical properties of the working fluid are known in advance at the entrance/exit of each component of the ORC cycle, and therefore its thermodynamical state in these locations is completely defined (the so called “State Principle”). Although properties databases can be used, for the case studies presented in Chapter 5, the properties are calculated using the Peng-Robinson equations of state. See Appendix B for a detailed description of the property calculations and the ORC cycle simulation.
- Related to the point above, working fluids leave the evaporators and condensers at a saturated state (vapor/liquid respectively).

-
- Isentropic efficiencies of turbines and pumps are known in advance.
 - If required, stream splits of the working fluid mix isothermally after evaporators and condensers. Similar to the streams splits of process streams in the HEN, the isothermal mixing assumption reduces the size and complexity of the model formulation.
 - The capital cost of the ORC is equal to the sum of the capital costs of its constituent heat exchangers (evaporators and condensers) and the costs of the turbine and pump.
- 3) For system involving ABCs
- Refrigerant couple is set as LiBr/H₂O, as is the preferred refrigerant couple used in applications with refrigeration temperatures above 0°C (Papadopoulos et al. 2020). For a detail explanation of the properties of this refrigerant couple, please see Section 2.3.4.1.
 - Only single-effect absorption chillers are considered. This assumption decreases the size and complexity of the model formulation in comparison with multi-effect systems, while providing a good thermodynamical performance.
 - For given refrigeration (T_{ref}) and condensation temperatures (T_{cond}), and a given effectiveness of the “Solution Heat Exchanger” (ϵ_{SHEX}), a unique set of fit functions describing the physical behavior of the ABC is generated. All the fit functions obtained have $R^2 \geq 0.95$. The objective of these fit functions is to integrate the physical behaviour of the ABC into the optimization model. For more details on the ABC simulation and the properties of refrigerant and refrigerant couple, please refer to Appendix A.
 - The fit functions are generated based on a detailed simulation of the ABC behavior (see Appendix A). The refrigerant and refrigerant solution properties used to perform this detailed simulation are taken from experimental correlations. For the LiBr/H₂O solution properties are taken from the correlations by Sun (1997). Properties for pure H₂O inside the absorption cycle are obtained from Irvine and Liley (1984). The use of fit functions simplifies the modeling of the ABC and it replaces the use of the highly complex experimental correlations for the properties of the refrigerant and refrigerant couple (plus the additional mass and energy balances for every component of the ABC) in the optimization model.
 - At least three independent intensive properties of the refrigerant solution, and two independent intensive properties of the pure refrigerant are known at the entrance/exit of each ABC component.

- Temperatures of the refrigerant at the exit of the condenser (T_{cond}) and the refrigerant couple at the exit absorber (T_{abs}) are set in advance. They are considered the same and equal to the sum of the temperature of the available cold utility and the minimum approach temperature allowed between the ABC componets and the process streams. This assumption implies that the refrigerant and refrigerant couple at the condenser and absorber, respectively, are cooled down to the minimum achievable temperature by the cold utility.
- Evaporator (refrigeration) temperature (T_{ref}) is set in advance.
- Mixing of streams after the generators and evaporators takes place isothermally. Similar to the streams splits of process streams in the HEN, and working fluid in the ORC, the isothermal mixing assumption reduces the size and complexity of the model formulation.
- Concentration of LiBr in solution remains always between 0.4 and 0.7 in mass, to avoid crystallization. This concentration range is typically used for the design of absoption machines (Kaita 2001). In reality, the concentration at which a LiBr solution crystallize is a function of its temperature (Gilani and Ahmed 2015). A further exploration of the crystallization effect in the design of the system is proposed as an area of future work.
- Refrigerant (H_2O) leaves condenser and evaporators at a saturated state as liquid and vapor respectively (Wonchala et al. 2014).
- H_2O leaves the generator as a superheated steam at the generator pressure and at the equilibrium temperature of the LiBr/ H_2O solution (Wonchala et al. 2014).
- Refrigerant solution (LiBr/ H_2O) leaves absorber and the generators at a saturated state as liquid and vapor respectively (Wonchala et al. 2014).
- Efficiency of “Solution Heat Exchanger” (ϵ_{SHEX}) is set in advance .
The costs of the SHEX, the solution pump and the pumping costs of the ABC are neglected in the cost calculations as they are small in comparison to the capital costs of the generators, condensers, evaporators and absorbers (Mussati et al. 2016).
- The capital cost of the ABC is equal to the sum of the capital costs of its constituent heat exchangers (except the SHEX as pointed in the previous point).
- In order to simplify the cost calculations for the ABC Absorber and the ABC Condenser, and as they do not interact directly with the process streams (the are not part of the HEN), no related binary variables have been defined and their fixed costs (C_{fix} in Equation (1-1)) are set to zero ($C_{fix} = 0$).

4) For system involving storage:

- Only two-tank and multi-tank “Fixed Temperature Variable Mass” (FTVM) storage systems are considered. Although numerous technologies for “Thermal Energy Storage” (TES) are available in the market, sensible storages such as the FTVM storage tanks remain the most popular alternative for industrial processes (Sarbu and Sebarchievici 2018).
- The number of tanks is defined in advance. Stratified tanks can be considered as two-tank systems.
- The temperatures at each storage tank remain fixed during the whole cycle and are calculated during the optimization process.
- Tanks operate cyclically. Tank level at the start of the cycle is equal to the level at the end of the cycle. The amount of energy stored/accumulated in a given storage tank at the beginning and end of the process duration (cycle) is the same.
- Storage fluid is set in advance.
- Thermophysical properties of the storage fluid are known and constant.
- Utilities do not supply/extract energy to/from the storage systems. Only the process streams exchange heat with the storage system.
- The FTVM storage tanks are fed by hot and cold storage streams that exchange energy exclusively with the process streams. For a schematic representation of the storage system, as well as a detail explanation of its operation, please see Section 4.2.3.1.
- The tanks are organized in energy levels. In each energy level, two tanks exist, one acting like a hot storage and one as a cold storage. A tank acting as a cold storage in one energy level, is considered a hot storage in the next one. The temperatures of the tanks decrease with each increasing energy level.
- In each energy level, one hot storage stream flows from the hot storage tank to the cold storage tank, exchanging energy exclusively with the cold process streams. Similarly, in each energy level, one cold storage stream flows from the cold storage tank to the hot storage tank, exchanging energy exclusively with the hot process streams along the way. For each period of operation and at a given energy level, only one of the storage streams, either the hot storage stream or the cold storage stream, is active.
- The costs of the storage fluid, the capital cost of the required pumps and the pumping cost of the storage system are not considered, as they are assumed small in comparison to the cost of the storage tanks. The capital cost of the storage system is equal to the sum of the capital costs of its constituent storage tanks.

1.4 Outline of the Work

The structure of the dissertation is presented in Figure 1-4. Chapter 2 presents fundamental concepts of waste heat recovery and process integration. These fundamentals include a working definition for waste heat to be used in the rest of this work; estimations for industrial waste heat (IWH) potentials around the world, in Europe and in Germany; an overview of different WHR technologies with emphasis on ORC and ABC, and an introduction to key concepts of process integration in continuous and discontinuous process. Chapter 3 provides a State-of-the-Art on the process integration of ORCs, ABCs and both, into HENs and Chapter 4 presents the mathematical framework developed in this research for the integration of ORC, ABC or both into HENs in continuous and multi-period processes with and without FTVM heat storage. In total nine different superstructures involving the integration of the individual and combined WHR technologies in to HENs are presented. At the end of Chapter 4, the mathematical considerations and limitations for the nine superstructures are discussed. The use of the superstructures developed in Chapter 4 is illustrated with help of three case studies from the literature in Chapter 5, corresponding to continuous, semi-continuous and batch processes. After an exemplary sensitivity analysis of one the developed models and the critical discussion of the results of the case studies and the performance of the developed superstructures, conclusions and possible future work are outlined in Chapter 6.

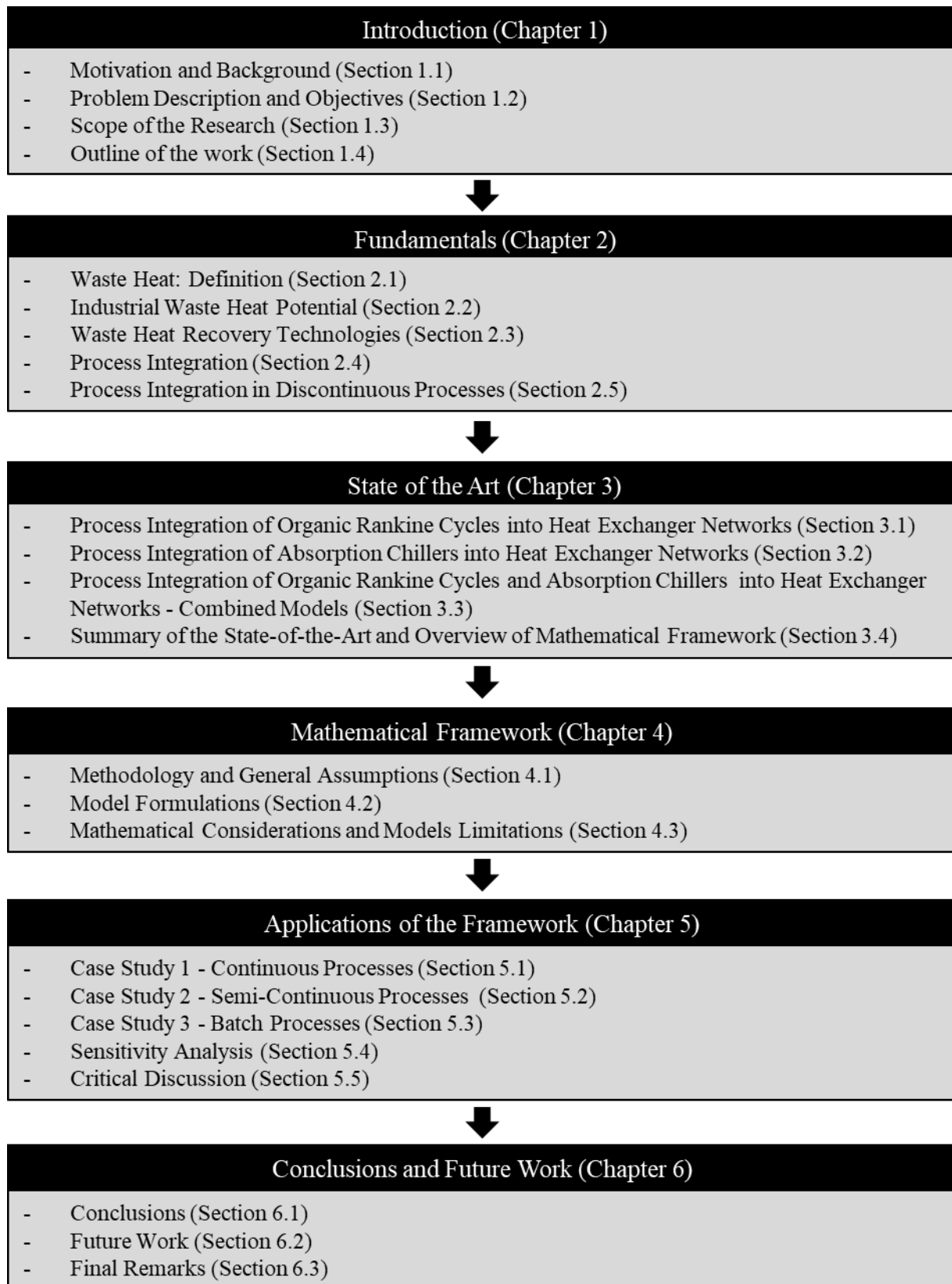


Figure 1-4. Structure of the dissertation

Source: Own diagram

2 Fundamentals

This chapter presents an overview about key concepts of “Waste Heat Recovery” (WHR) from industrial processes and “Process Integration” (PI). Section 2.1 provides a number of definitions for waste heat and establishes the definition of waste heat to be used in the context of this research; Section 2.2 presents estimations for the theoretical potential for WHR from industrial sites in Germany, Europe and the world; Section 2.3 presents an overview of the technologies available for WHR; section 2.4 offers an introduction to PI, describing key concepts of Pinch Analysis (PA) and Mathematical Programming (MP) and section 2.5 definitions for key concepts for PI in discontinuous processes.

2.1 Waste Heat: Definition

In the most general sense, “Industrial Waste Heat” (IWH) can be defined as “...*the energy that is generated in industrial processes which is not put into any practical use and is lost, wasted and dumped into the environment...*” (Jouhara et al. 2018). Similar definitions are offered by Brückner et al. (2015), Broberg Viklund and Johansson (2014), Ludwig (2012) and Johnson et al. (2008).

Ludwig (2012) categorizes waste heat as either “diffuse” or “concentrated”. Diffuse waste heat, is energy lost or dissipated directly to the environment without the use of a heat carrier. Energy lost through radiation and convection from hot surfaces, generated by friction between moving surfaces or by dissipation due to electrical resistances are examples of diffuse waste heat (Forman et al. 2016). This waste heat is difficult to reuse in industrial processes but can be partially recovered in industrial facilities through “Heat, Ventilation and, Air Conditioning” (HVAC) systems to be used for space heating, or minimized by means of better insulation of pipes and hot surfaces and better lubrication between moving surfaces. Concentrated waste heat, is defined as the portion of the unused energy from industrial processes that is released to the environment attached to heat carriers, typically fluids. Although solid heat carriers exist, they are difficult to handle and heat recovery from them, tends to be expensive and technically challenging (Papapetrou et al. 2018).

From a practical point of view, only waste heat attached to a fluid heat carrier can be technically and economically recovered to be reused in industrial processes or transformed in other useful energy forms, i.e. higher-grade heat, cooling and electricity (Papapetrou et al. 2018), and it is this share of the unused energy from industrial process that it is commonly referred as waste

heat or “industrial excess heat” (Berntsson and Åsblad 2015) in most of the studies about waste heat and waste heat potentials.

More technically-driven definitions for waste heat, focus on the fact, that some unavoidable heat losses are part of all physical processes and in contrast, some of the heat from industrial processes can be internally or externally recovered using different technologies and methods. Oluleye (2015) defines waste heat as “...*the residual heat rejected to cooling water and air when a single process or a site has reached its limit for heat recovery...*”. This limit for heat recovery is established using PA (Linnhoff and Flower 1978a). Berntsson and Åsblad (2015) call “true waste heat” or “non-usable excess heat” to the “...*remaining part of the excess heat, when all internally and externally usable parts have been deducted...*”. Bendig et al. (2013) define waste heat as the “...*the sum of the exergy that is available in a process after pinch analysis, heat recovery, process integration and energy conversion (utility) integration with the help of exergy analysis...*”, that is all the exergy that is available after all possible internal and external energy recovery is exhausted. Ammar et al. (2012) refer to waste heat or “low-grade heat” to the heat that “...*is not viable to recover within the process and is rejected to the environment...*”. As for “viable” recovery, Ammar et al. (2012) consider not only the physical feasibility but the economic aspects of the heat recovery.

In this work, IWH is defined similar to Oluleye (2015), as:

“The unused or residual heat from an industrial process, after the maximum internal heat recovery through heat exchange according to the pinch analysis is achieved. Under the absence of any other heat recovery options, i.e. heat transformation technologies, this heat would be rejected to the environment through a fluid heat carrier”.

This definition only includes waste heat attached to fluid heat carriers and ignores diffuse waste heat and waste heat contained in solid heat carriers (see Section 1.3).

2.2 Industrial Waste Heat Potential

Multiple studies estimating the industrial waste heat potential in different geographical zones have been published in the last years. For all of the studies, the calculated IWH potential refers only to the waste heat contained in fluid heat carriers. A review by Brückner et al. (2014) categorizes methods for the estimation of IWH potential depending on the scale of the study (single company, industrial park, neighborhood, town, region, country or the world), the data acquisition method (survey/measurement, estimation or combined) and the approach used for

the calculation of the waste heat potential (bottom-up, top-down or combined), the latter being the most popular method for the classification of waste heat potential studies (Pehnt et al. 2010). In this classification, bottom-up approach refers to the aggregation of information from single companies or studies into a general result and top-down approach refers to the use of general parameters, like efficiency factors from machines, processes or industrial sectors, in order to calculate an estimate of the waste heat potential for a given system (process, industrial sector or geographical region). Other authors like Blesl et al. (2008) also categorize the waste heat potential studies according to the accuracy of the estimation into rough, medium or high accuracy methods, with increasing requirements in the level and accuracy of the information required for the estimation.

Additionally, Brückner et al. (2014) distinguish between different types of waste heat potential: theoretical or physical potential which accounts for the recoverable heat according to the laws of physics; technical potential which considers technological and practical limitations to the possible heat recovery and the economic potential which refers to the feasible energy recovery when considering economic and financial parameters. Most of the studies in the literature only refer to the theoretical potential. Table 2-1 offers an overview of studies estimating theoretical industrial waste heat potentials published in the last decade. Only studies for Germany, the European Union or the world as a whole are considered. Studies for regions, cities or individual countries (except Germany) are not presented in the table. Also, studies focusing on selected industrial sectors (e.g., non-metallic, food, energy intensive industries) are not included.

Table 2-1. *Estimations of theoretical industrial waste heat potentials in different geographical areas.*

Source	Area	Approach	Reference Temp. (°C)	Estimation (PJ/a)	Reference Year
Papapetrou et al. (2018)	EU	Top-Down	N.A.	1 091.7	2015
Brückner et al. (2017)	Germany	Bottom-Up	>35.0	223.0	2008
Forman et al. (2016)	World	Top-Down	N.A.	31 902.0	2012
I-ThERM Consortium (2016)	EU	Top-Down	N.A.	1 225.5	2010
Persson et al. (2014)	EU	Top-Down	>90.0	2 924.0	2010
Pehnt et al. (2010)	Germany	Top-Down	>60.0	476.0	2007

Source: *Own table based on Papapetrou et al. (2018), Brückner et al. (2017), Forman et al. (2016), I-ThERM Consortium (2016), Persson et al. (2014) and Pehnt et al. (2010).*

From the studies in Table 2-1, only Forman et al. (2016) estimates the global IWH available. Additionally, the study presents estimated theoretical waste heat potentials for the transportation, commerce, residential and energy generation sectors. The global IWH potential is estimated as 31 902.0 PJ/a, which corresponds to almost 7% of the global energy input and 30% of the energy consumed in the industrial sector. As for European studies, the values provided by the I-ThERM Consortium (2016) and Papapetrou et al. (2018) are similar, with

estimated theoretical IWH potentials of 1 225.5 PJ/ and 1 094.9 PJ/a respectively. In contrast, the value provided by Persson et al. (2014) of 2 924.0 PJ/a is approximately 2.5 times higher than the other values, and it is considered in their study as an upper limit for the IWH recovery potential in Europe. The conservative value estimated by Papapetrou et al. (2018) corresponds to 9.5% of the total energy consumption in the industrial sector in Europe.

Table 2-2. *Estimations of theoretical industrial waste heat potentials in Germany*

Source	Approach	Reference Temp (°C)	Estimation (PJ/a)	Reference Year
Papapetrou et al. (2018)	Top-Down	N.A.	269.5	2015
Brückner et al. (2017)	Bottom-Up	>35.0	223.0	2008
I-ThERM Consortium (2016)	Top-Down	N.A.	321.1	2010
Persson et al. (2014)	Top-Down	>90.0	566.0	2010
Pehnt et al. (2010)	Top-Down	>60.0	476.0	2007

Source: *Own table based on Papapetrou et al. (2018), Brückner et al. (2017), I-ThERM Consortium (2016), Persson et al. (2014) and Pehnt et al. (2010).*

As for Germany, the two dedicated studies by Brückner et al. (2017) and Pehnt et al. (2010) presented in Table 2-1, reported dissimilar values. Using a bottom-up approach and waste streams emission data from 81 000 data points in Germany, Brückner et al. (2017) calculated an IWH potential of 223.0 PJ/a which corresponded to 5.7% of the total industrial energy consumption in Germany in the reference year 2008, according to the Statistisches Bundesamt (2019). In contrast, Pehnt et al. (2010) estimated an IWH potential of 476.0 PJ/a, that is more than 2 times the value from Brückner et al. (2017). This is to be expected as Brückner et al. (2017) considered their value to be a lower limit for the German IWH potential. Other values for the German IWH potential (See Table 2-2) as reported by Papapetrou et al. (2018), I-ThERM Consortium (2016) and Persson et al. (2014) in their European studies, are 269.5 PJ/a, 321.1 PJ/a and 566.0 PJ/a, respectively. Although different, these values are in the same order of magnitude as the values from the dedicated (Germany-only) studies. The differences between the estimations can be explained by the different methodologies used in the studies and the various efficiency factors and data sets used for the estimations. An extended breakdown of the studies, in Table 2-1 is presented in Appendix F, including their methodologies, data sources and a Sankey diagram for the waste heat potential of the industrial sector worldwide based on Forman et al. (2016) .

As a conclusion from the reviewed studies, at least 223.0 PJ/a of IWH are available in Germany, 1 095.0 PJ/a in Europe and 31 902.0 PJ/a worldwide, which correspond to 5.7%, 9.5% and 30% of their total industrial energy consumption, respectively. The ratios of IWH to the total industrial energy consumption, illustrate the high efficiency of the energy use in the German

and European industrial sector in comparison with the rest of the world and the potential for improvements in the design of industrial processes around the world.

2.3 Waste Heat Recovery Technologies

Brückner et al. (2015) and later Chowdhury et al. (2018) categorize the WHR technologies into “active” and “passive” technologies. For Brückner et al. (2015), passive WHR technologies use the waste heat directly at the same, or at a lower temperature level, than the heat source temperature, while active WHR technologies use the heat at a higher temperature level than the heat source or transform the waste heat to another form of energy through the use of thermodynamic cycles. Chowdhury et al. (2018) modify the definitions to include innovative WHR technologies like thermoelectric generators and thermophotovoltaic devices. For Chowdhury et al. (2018) passive WHR technologies are those which require no significant energy input (mechanical, thermal or electrical) to operate, as on them, the heat moves spontaneously from a state of high temperature to a lower temperature level according to the Clausius’s formulation of the Second Law of Thermodynamics (Clausius 1854). On the other hand, active WHR technologies require a significant energy input to operate and typically are based on thermodynamic cycles. More recently, Xu et al. (2019) categorize WHR technologies into “direct use” technologies and “heat conversion” technologies, depending on the use of the heat. This classification roughly corresponds to the passive and active technologies as described by Brückner et al. (2015).

Figure 2-1 presents a classification of industrial WHR technologies. This classification is based on the definitions of active and passive technologies according to Brückner et al. (2015). Chowdhury et al. (2018) and Oluleye (2015) also mention unconventional heat recovery technologies such as thermoelectric generators, supercritical CO₂ cycles or trilateral cycles, in their classifications, but these technologies are only in development phase and have not been used in large scale industrial applications. These unconventional technologies are not considered in this dissertation. In the following sections, an overview of different industrial WHR technologies is presented. Special emphasis is placed on organic Rankine cycles, absorption chillers and heat storages, as they are the technologies to be integrated into heat exchanger networks with the use of the mathematical framework developed in Chapter 4. Steam cycles are not considered, as their investment costs are too high to be considered for most waste heat recovery applications and for temperatures lower than 300°C (at which most of the waste heat is available) ORCs efficiencies outperform those from steam cycles (Vanslambrouck et al. 2012).

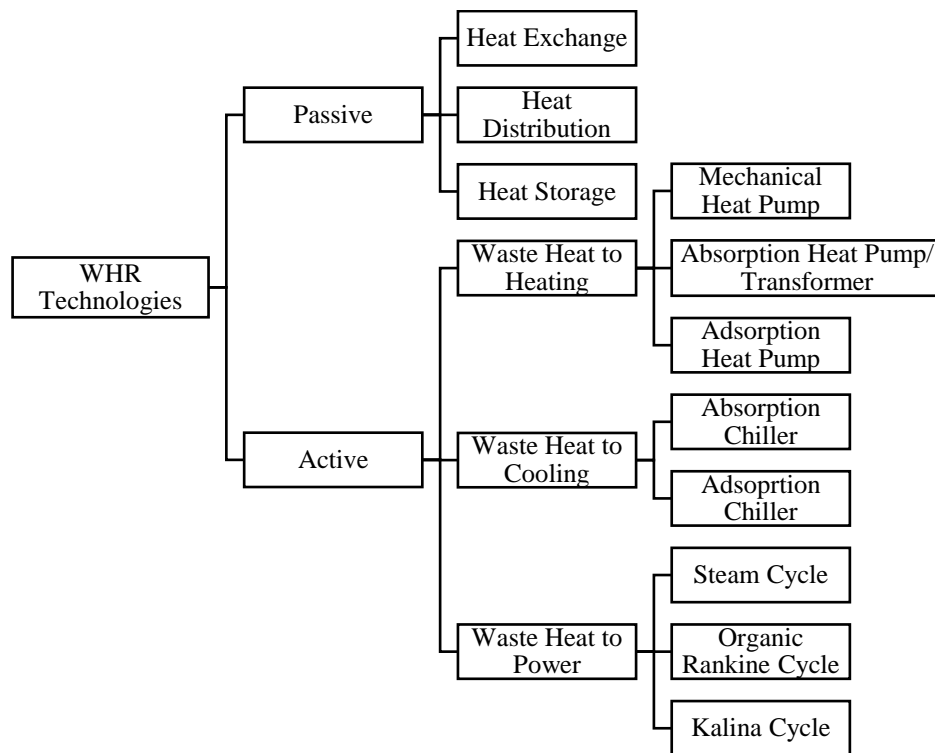


Figure 2-1. Classification of industrial waste heat recovery technologies.

Source: Own diagram based on Brückner et al. (2015).

2.3.1 Heat Exchangers

Heat exchangers are devices used to transfer thermal energy between substances, typically fluids (Abou Elmaaty et al. 2017). Although heat exchangers have been used in an extensive number of applications and sectors for a long time, even today, the thermal, economical, hydraulic and mechanical enhancement on the performance of heat exchangers is an active area of research. The basic principles for the design and operation of heat exchangers are covered in most process and chemical engineering textbooks. The reader is referred to Smith (2005) for more information about the basics of heat exchangers. In this work, the detailed design and selection of the optimal type of heat exchanger for a given process is not performed. Instead, the heat exchangers are assumed to be perfect countercurrent heat exchangers and are characterized by their heat transfer areas and heat transfer duties.

2.3.2 Heat Distribution

“One man’s trash is another man’s treasure” and IWH from an industrial plant can certainly be of value to other industries or neighboring buildings and communities. For centuries, industries, businesses and communities located in a close proximity have developed synergies through the

exchange of byproducts (materials, energy or resources). The networks generated by these interactions are now known as “Eco-Industrial Parks” or “Industrial Symbiosis” (Desrochers 2001). Although the concept itself is centuries old, the modern use of the terms “Industrial Symbiosis” and “Eco-Industrial Parks”, emphasizes the environmental benefits of such synergies, and it can be traced to the studies published in the early 1990s about the industrial region of Kalundborg in Denmark, which since the 1960s developed a network of interrelationships for the exchange of byproducts between local companies in which also participates the municipality of Kalundborg (Chertow 2004). Recent reviews by Lawal et al. (2021) and Butturi et al. (2019) offer an overview of the recent developments and tools used in industrial symbiosis.

For the exchange of IWH between neighboring plants, or between neighboring processes at an industrial site, Dhole and Linnhoff (1993) developed the concept of “Total Site Analysis” (TSA) also known as “Total Site Heat Integration” (TSHI). They extended concepts and tools of “Pinch Analysis” (PA) in order to optimize the internal energy recovery in total sites, which they defined as “...*factories incorporating several processes, serviced by and linked through a central utility system...*”. The concept was later extended to include renewable energy sources as well as different heat sinks, such as large complex buildings, offices and residential areas, in what is also known as “Locally Integrated Energy Sectors” (LIES) (Perry et al. 2008). A recent review by Liew et al. (2017) presents the recent advances in this area of research.

Industrial waste heat can also be used to generate hot water or low pressure steam to satisfy space heating and domestic hot water needs from different consumers by using a heat distribution network of insulated pipes. This is part of the more general concept of “District Heating” (DH) which includes other heat sources such as “Combined Heat and Power Plants” (CHP), biomass, solar thermal heat, geothermal, conventional boilers driven by fossil fuels or renewable energies, etc. (Mazhar et al. 2018). Although the use of district heating can be already found in the Middle Ages and some authors even suggest that it was used in Roman times (Wiltshire 2016), the modern concept of district heating can be traced to the steam distribution systems installed in New York and other US Cities in the 1870s and 1880s, many of which are still in use today (Werner 2017). Since then, the use of DH has expanded around the world and, by 2015, it provided 12% of all the heating and cooling requirements in the EU28 (Fraunhofer ISI et al. 2017). As for technological developments, the trend has been the replacement of steam with liquid water as heat carrier, the decrease of the transmission temperatures, the addition of district cooling networks, the use of prefabricated materials for the distribution pipes, and the

integration of heat pumps at the generation (Lund et al. 2014) and distribution levels (Buffa et al. 2019).

The use of IWH for DH has particular challenges. IWH is often available at low temperatures unsuitable for the use in DH networks. Most of the DH networks operating currently have supply temperatures of at least 90°C, which means that the waste heat source has to be at a higher temperature. This discards a significant portion of the available IWH. According to Fang et al. (2015), there are three key issues for the use of IWH for DH: 1) the integration of IWH with different heat sources at different temperature levels, 2) the distance between the industrial sites and the heat consumers, and 3) the regulations and controls for the DH system due to the variable temporal availability of the IWH.

The heterogeneous sources of IWH are a technical challenge for the optimal integration of the heat sources into the DH system, and, in most cases, only a single waste heat source or multiple waste heat sources in parallel are considered. This combination of multiple heat sources in parallel is simple but tends to be thermodynamically inefficient. The distance between the industrial sites and the heat consumers has also a significant influence on the feasibility of DH networks. Heat losses in heat distribution networks in Europe are between 5% and 20% of the heat fed to the system (Mathiesen et al. 2019) and increase with the distance between source and consumer. Considering economics, distances between industrial sites and heat consumers up to 30 km are recommended, but the maximum distance should be calculated in a case-by-case basis, depending on the local conditions (Fang et al. 2013). Finally, the discrepancy between the temporal availability of the IWH and the heat demand at the district heating means that IWH can never be the only source of heat for a district heating network, but it can be used as base load source to cover the heating demand (Fang et al. 2015).

In this work, neither Total Site Heat Integration nor District Heating are considered. The objective of the work is to optimize the waste heat recovery in industrial processes by the exclusive use of heat exchanger networks with or without heat storage and organic Rankine cycles or absorption chillers.

2.3.3 Heat Storage

Ausfelder et al. (2015) define storage systems as systems which: 1) collect energy in a controlled way (charge), 2) retain it during a certain time attached to a storage material (storage), and 3) after a given time, release the energy back also in a controlled manner (discharge). If the energy collected is thermal energy, the system is referred to as “Thermal

Energy Storage” (TES). The stored heat is used to match temporally or geographically the heat sources with the heat sinks (Miró et al. 2016). TES can be classified depending on the method for the storage of the thermal energy into physical and thermochemical processes (Jouhara et al. 2020). Thermal energy can be stored through physical processes by heating or cooling of a storage medium (sensible energy storage) or by inducing a phase change in the storage material (latent energy storage). On the other hand, thermochemical processes use thermally driven reversible chemical reactions or sorption processes to store thermal energy. Figure 2-2 presents this classification for TES.

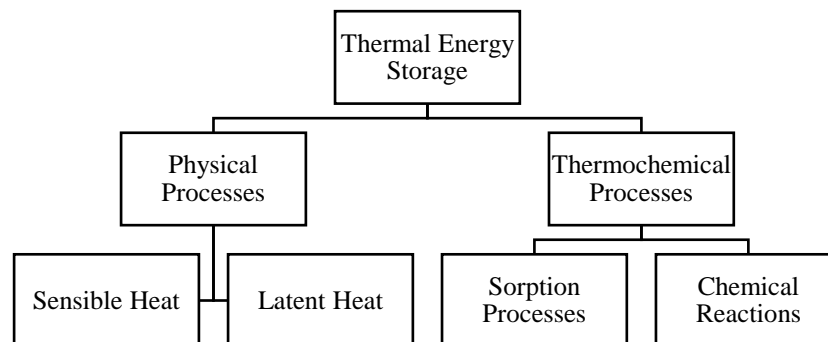


Figure 2-2. Classification of Thermal Energy Storages (TES) according to the underlying storage processes. Source: Own diagram based on Jouhara et al. (2020).

Sensible storage is by far the most used storage technology (Mewes et al. 2008), due to its maturity level (Nguyen et al. 2017), simplicity and low cost (Sarbu and Sebarchievici 2018). Water is the most common storage material and it is used extensively in low temperature applications (<100 °C), in residential and industrial sectors (International Renewable Energy Agency 2013). Thermal oils, molten salts and solid material such as sand-rocks minerals, concrete, etc. are also commonly used in certain applications (Dinker et al. 2017). The main disadvantages of the use of sensible storage are the low energy densities and variable heat transfer rates due to the variable heat transfer temperatures.

Latent heat storage improves on these issues, as it takes place isothermally and the latent heat storage materials, also known as “Phase Change Materials” (PCM), have higher energy densities than the sensible storage materials, which leads to smaller space requirements for the storage (Jouhara et al. 2020). Higher costs and low thermal conductivities with the associated low heat transfer rates (Hofmann et al. 2019), are a barrier for the industrial implementation of latent heat storage and currently it is only used in niche industrial applications (e.g., ice storage), and research and pilot projects (Pieper 2019). For both the sensible and latent storage systems, some thermal losses during the storage time are unavoidable and limit the period of time that

heat can be stored. These heat losses are the product of imperfect insulation and can be minimized but not eradicated (Jarimi et al. 2019).

Finally, thermochemical processes are characterized by high energy densities and low energy losses, as the heat is stored as chemical potential energy in the reactants instead of thermal energy (Bauer et al. 2012), but the systems are rather complex and expensive and they are currently in an early stage of development (Airò Farulla et al. 2020). Table 2-3 presents an overview of the different thermal energy storage technologies available.

Table 2-3. Overview of characteristic parameters for typical Thermal Energy Storage technologies.

	Sensible	Latent	Thermochemical
Capacity (kWh/t)	10-50	50-150	120-250
Power (MW)	0.001-10	0.001-1	0.01-1
Efficiency (%)	50-90	75-90	75-100
Storage period	Days to Years	Hours to Weeks	Hours to Days
Cost (€/kWh)	0.1-10	10-50	8-100

Source: Own table based on International Renewable Energy Agency (2013)

TES based on physical processes can be also classified by its behavior during operation. Stoltze et al. (1995) categorize TES into “Fixed Temperature Variable Mass” (FTVM) storage, “Variable Temperature Fixed Mass” (VTFM) storage and “Fixed Temperature Fixed Mass” (FTFM) storage which are equivalent to latent heat storages. This classification has the advantage that the mathematical modeling of the heat content of storages of the same type is similar, that is, the change of enthalpy during charge or discharge for a given storage type can be described by similar equations. Table 2-4 presents generic descriptions of the change of enthalpy during charge or discharge for FTVM, VTFM and latent heat storages respectively.

Table 2-4. Change of enthalpy during charge/discharge for different storage types.

Type of Storage	Enthalpy Change during Charge/Discharge	Equation Number
FTVM	$\Delta H^{st} = T^{st} \Delta M^{st} cp_{st}$	(2-1)
VTFM	$\Delta H^{st} = M^{st} \Delta T^{st} cp_{st}$	(2-2)
FTFM (Latent)	$\Delta H^{st} = M^{st} h_{pc}$	(2-3)

Source: Own table based on Stoltze et al. (1995)

In these expressions ΔH^{st} represents the change of enthalpy of the storage during charge or discharge, T^{st} the temperature of the storage material, M^{st} the mass of the storage, cp_{st} the specific heat capacity of the storage material and h_{pc} the enthalpy of phase change (enthalpy of fusion/solidification or enthalpy of vaporization/condensation for solid/liquid and liquid/gas phase changes respectively).

In this work and for the mathematical framework developed in Chapter 4, only FTVM storage is considered. This type of storage includes two-tank and multi-tank systems, stratified tanks

and packed bed storages. Two-tank and multi-tank systems, as their name suggested, are composed by two or more separated and insulated tanks, which are connected by a network of pipes and auxiliaries, typically pumps and valves to control the flow between the tanks (Roos and Haselbacher 2021). The storage material, typically a liquid, acts also as heat transfer fluid and it flows between the tanks releasing or absorbing sensible heat in a controlled way through heat exchangers located in the pipe network. During operation, the temperature of the storage fluid in the tanks remains constant and only the mass stored in each tanks changes.

Stratified tanks work similarly to two-tank storage with two clear regions of hot and cold fluid, but instead of a solid physical separation, the regions are separated by a mixed temperature zone known as thermocline, which acts a barrier for the heat exchange between hot and cold fluids. Regions are generated due to the difference in density between the hot and cold fluids, with the cold zone at the bottom of the tank and the hot zone at the top (Koçak et al. 2020). For a given tank size, the size of thermocline negatively impacts the storage capacity of the tank and therefore measures are taken to minimize it (Fertahi et al. 2018). Some of this measures includes the addition of baffle plates, diffusors, the modification of the geometry of the tank and control of the operating conditions such as the velocity of charge or discharge of the storage fluid, etc. (Chandra and Matuska 2019).

Packed bed storages are made of a tank or several tanks filled with a packing solid material which acts as storage medium, and a heat transfer fluid that flows though the tanks to charge or discharge the storage (Almendros-Ibáñez et al. 2019). The main advantages of these type of systems is that they can reach higher storage temperatures than liquid based storages due to the chemical stability of the solid materials and the improved thermal stratification in the case of single tank systems (Gautam and Saini 2020).

The methodology developed in this work and the case studies provided in Chapter 5 are focused only on two-tank and multi-tank systems, as they facilitate the graphical representation of the storage system. For the purpose of this work, two-tank systems can be replaced by stratified tanks without loss of generality, but the objective functions should be adjusted to illustrate the differences in cost and storage volume between the technologies.

2.3.4 Waste Heat to Cooling

2.3.4.1 Absorption Chillers

Absorption refrigeration systems are thermally driven systems that generate a cooling effect through the use of low-grade temperature sources. Figure 2-3 presents a schematic representation of a typical single-effect “Absorption Chiller” (ABC) in a P-T diagram, in order to illustrate the relative position of pressures and temperatures in the system. The refrigeration cycle starts at the outlet from the absorber where a weak refrigerant solution (weak in solvent concentration) is pumped to the generator, where the refrigerant is separated from the solution in an endothermic desorption process. The refrigerant leaves the generator as a vapor and it flows to the condenser where it releases heat and exits as a liquid. The refrigerant is then expanded at the throttling valve decreasing its temperature and pressure and flows to the evaporator where it evaporates by absorbing heat from the environment (or fluid to be cooled), providing the cooling effect. The refrigerant leaves the evaporator as vapor and flows to the absorber where it is mixed with the strong refrigerant solution (strong in solvent concentration) returning from the generator and it is absorbed by the solution through an exothermic process. The newly generated weak refrigerant solution rejects the heat of absorption and it is cooled down before restarting the cycle again. An additional heat exchanger (SHEX) is used to recover heat from the strong solution returning to the absorber and preheat the weak solution flowing to the generator.

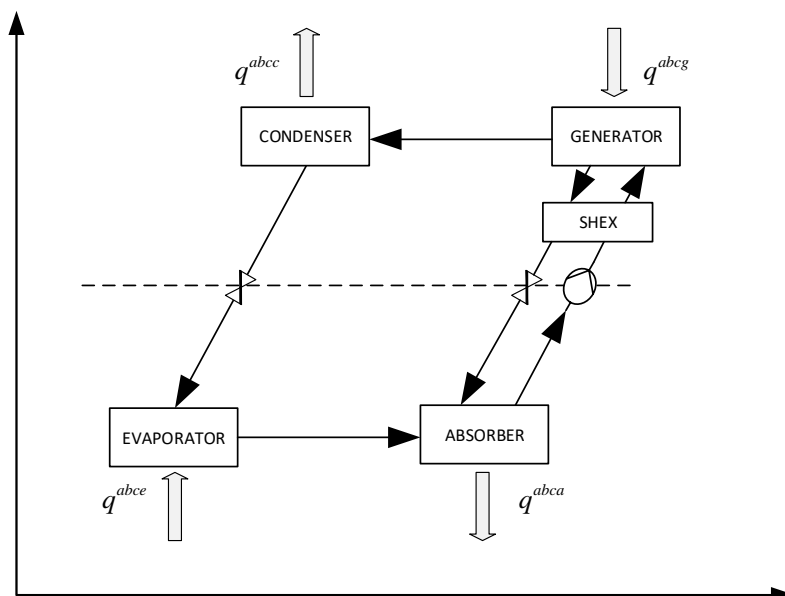


Figure 2-3. Schematic representation of a single-effect absorption chiller (not in scale).

Source: Own diagram based on Nikbakhti et al. (2020)

Historically, the refrigeration effect of the absorption process has been known since the 1700s (Reif-Acherman 2012), but it was only in the late 1850s that the first commercial absorption refrigerator, using $\text{H}_2\text{O}/\text{NH}_3$ as working pair, was available, patented by French inventor Ferdinand Carré (Carré 1860). Although many pairs of refrigerant and absorbent have since then been suggested, most commercially available systems today use $\text{LiBr}/\text{H}_2\text{O}$ or $\text{H}_2\text{O}/\text{NH}_3$ as working pairs (Papadopoulos et al. 2020).

In the case of $\text{LiBr}/\text{H}_2\text{O}$ as working pair, H_2O acts as the refrigerant and LiBr as the solvent, which limits the minimum cooling temperature achievable in the system to 0°C (Freezing point of pure water for pressures ranging from its triple point 611.7 Pa up to ca. 20 MPa (Glasser 2004)). For most industrial and space cooling applications, this temperature is low enough. For applications in which cooling to sub-zero temperatures is required, the $\text{H}_2\text{O}/\text{NH}_3$ pair is used, with NH_3 acting as refrigerant and H_2O as the solvent. In this case, a minimum cooling temperature of -77°C is possible. Recent reviews by Papadopoulos et al. (2019) and Sun et al. (2012) present a survey from other possible working pairs, including organic working pair mixtures, alcohols, inorganic salts and ionic liquids, etc., but most of them are only used in research and at lab-scale. Table 2-5 presents a comparison between the $\text{LiBr}/\text{H}_2\text{O}$ and $\text{H}_2\text{O}/\text{NH}_3$ working pairs.

Table 2-5. Comparison $\text{LiBr}/\text{H}_2\text{O}$ and $\text{H}_2\text{O}/\text{NH}_3$ working pairs for absorption refrigeration

$\text{LiBr}/\text{H}_2\text{O}$	$\text{H}_2\text{O}/\text{NH}_3$
Refrigerant H_2O and solvent LiBr	Refrigerant NH_3 and solvent H_2O
Minimum refrigeration temperature 0°C (Freezing point of H_2O)	Minimum refrigeration temperature -77°C (Freezing point of NH_3)
LiBr forms solid crystals at high concentrations in the solution depending on the solution temperature (crystallization)	No crystallization problems
LiBr is non-volatile and therefore no rectifier is required	Due to water volatility, it requires rectifier after generator to separate water vapor from NH_3 , in order to guaranty high purity of NH_3 flowing to the condenser ($>99.8\%$)
H_2O is non-toxic and has zero ozone depletion potential. LiBr can be corrosive to certain materials (e.g., Copper)	NH_3 is toxic and corrosive at high concentrations
Cycle operates below the atmospheric pressure (vacuum conditions)	Cycle operates at relatively high pressures
Under similar operating conditions better performance than $\text{H}_2\text{O}/\text{NH}_3$ (COP = ~ 0.8 for single-effect)	Under similar operating conditions worst performance than $\text{LiBr}/\text{H}_2\text{O}$ (COP = ~ 0.5 for single-effect)

Source: Own table based on Sun et al. (2012)

The performance of the absorption chiller is described through the “Coefficient of Performance” (COP), which is described as the ratio between the cooling output at the evaporator (q^{abce}) and the heating input required at the generator (q^{abcg}) as presented in equation (2-4). Some authors also define an electrical coefficient of performance (COP_{el}) which represents the ratio between the cooling output at the evaporator and the electrical requirement of the solution pump (equation (2-5)), which typically is negligible in comparison with the thermal input required in the generator (Wonchala et al. 2014).

$$COP = \frac{q^{abce}}{q^{abcg}} \quad (2-4)$$

$$COP_{el} = \frac{q^{abce}}{W_{pump}^{abc}} \quad (2-5)$$

In order to improve the COP of the system, many modifications have been proposed to the single-effect ABC presented in Figure 2-3, including multi-effect cycles, GAX cycles and the addition of additional components such as refrigerant heat exchangers, ejectors, etc. (Nikbakhti et al. 2020). Multi-effect cycles combine single-effect absorption cycles in cascade, where the energy rejected at the condenser in a high temperature and pressure level serves as heat input to the generator of an absorption cycle at a lower level. Each additional level can operate to a higher temperature and take advantage of higher-grade energy sources. The simplest of the multi-effect cycles is the double-effect system as presented in Figure 2-4. In double-effect systems, the heat released in the condensation at the high temperature condenser is used to power the low temperature generator. Depending on the type of hydraulic connection between the generators, the systems can be classified as parallel, series or reverse (series) cycles. In the case of parallel cycles, the weak solution coming from the absorber is fed to the low temperature and high temperature simultaneously, while in the series configuration the weak solution flows first to the high temperature and then to the low temperature generator (vice versa in reverse cycles). For LiBr/H₂O chillers, parallel cycles have the best thermal performance (Yang et al. 2017). Double-effect ABCs have been commercially available since the 1950s but first efforts to improve their performance were only made during the oil crisis of the mid 1970s, with its corresponding high energy prices (Vliet et al. 1980). Typically, double-effect refrigeration cycles have higher COPs compared with the single-effect cycles (almost double) and slightly higher exergetic efficiencies (Gomri 2009). Similarly, triple-effect and other multi-effect cycles have been also studied since the 1980s (Alefeld 1983, 1982) with different configurations proposed and are characterized by decreasing improvements in COP and exergetic efficiencies with each additional stage (Gomri 2010).

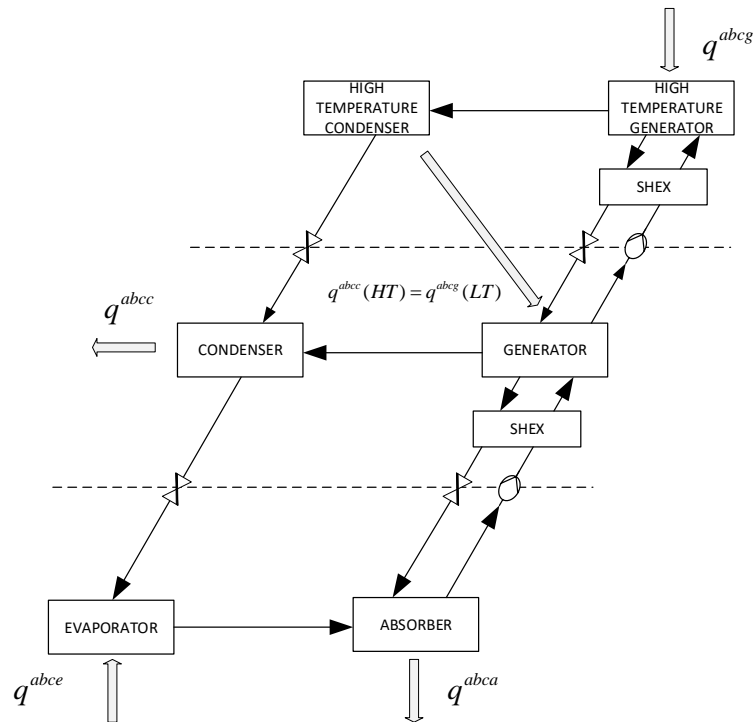


Figure 2-4. Schematic representation of double-effect absorption chiller. In diagram reverse cycle.

Source: Own diagram based on Nikbakhti et al. (2020)

In the case of $\text{H}_2\text{O}/\text{NH}_3$ absorption chillers, an overlap between the generation and absorption temperatures allows the integration of direct heat exchangers between the generator and the absorber (GAX Cycles) to take advantage of the heat released at the absorber (Jawahar and Saravanan 2010). This cycle optimizes the internal heat recovery inside of the absorption cycle and it has been proved to be thermodynamically optimal according to the pinch method (Chen et al. 2017). Additional components for the single-effect cycle have also been proposed. Sözen (2001) studied the addition of a refrigerant heat exchanger (RHEX) between the refrigerant flowing to the condenser and flowing to the absorber, but found almost no improvements in the performance of the cycle. Chen (1988) and Sun et al. (1996) proposed the addition of ejectors at the entrance to the absorber and at the entrance to the condenser, respectively and found that the systems are equivalent to multi-stage cycles, but with less components. A recent work by Nikbakhti et al. (2020) presents a comprehensive review of different techniques for the improvement of the energy performance of absorption cycles.

In this work only single-effect ABCs with $\text{LiBr}/\text{H}_2\text{O}$ as working pair are considered. The selection is based on their suitability for most process applications with temperatures above 0°C , the higher COPs in comparison with the $\text{H}_2\text{O}/\text{NH}_3$ chillers and the simplicity of the design (no rectifier).

As mentioned in Table 2-5, crystallization is the main operational problem of the LiBr/H₂O working pair, as it decreases the performance of the system and could cause a blockade of the circulation of the solution due to the solidification of the LiBr. The critical component for the crystallization is the absorber, as the strong solution returning from the generator is expanded before entering it. This creates a situation where a high concentration of LiBr and low temperatures in the solution, due to throttling, take place simultaneously and therefore the LiBr in the solution is susceptible to crystallize. According to Liao and Radermacher (2007) the six major causes for crystallization in LiBr/H₂O systems are: 1) high absorber and condenser temperatures, 2) low absorber and condenser temperatures combined with full load operation, 3) air leakages or non-absorbable gases generated due to corrosion in the pipes, 4) high temperatures in the generator, 5) failed dilution after shutdown when the machine cools down to ambient temperature, and 6) too low evaporation temperatures for given condensation and absorption temperatures. In general, a strict control of the operating temperatures and concentrations of LiBr in the solution is required to avoid crystallization. In this work, such control is not considered and as a simplified approach the mass concentration of LiBr in the solution is kept between 40% and 70% at all times, which corresponds to the usual operating concentrations in absorption machines (Kaita 2001).

A detailed simulation of the single-effect LiBr/H₂O ABC is presented in Appendix A. Fit functions are generated from the results of the simulation in order to simplify the mathematical modeling of the ABC. These fit functions are used in the models developed in Chapter 4 for the integration of ABCs into HENs.

2.3.4.2 Adsorption Chillers

Similar to ABCs, adsorption chillers take advantage of the thermally activated adsorption process to drive the refrigeration cycle (Sarbu and Sebarchievici 2015). In the adsorption process, an adsorption bed filled with solid adsorbent releases or adsorbs refrigerant vapor depending on the temperature of the bed. If a heat source is used to heat the bed, the adsorbent increases its internal pressure and temperature and then releases the vapor refrigerant after enough thermal energy is provided. The vapor refrigerant at high pressure is then condensed and expanded similar to the vapor compression and absorption processes, generating the cooling effect. In the other hand, if heat is extracted from the bed through a cooling medium, the adsorbent decreases its internal pressure and temperature and adsorbs the vapor refrigerant to restart the cycle (Fernandes et al. 2014). As the adsorption and desorption processes cannot

take place simultaneously in the same adsorbent bed, a minimum of two beds is required to guarantee the continuous operation of the cycle.

Adsorption chillers are characterized by low COPs in comparison to absorption or vapor compression cycles ($COP = \sim 0.15$) but their construction is simple, and the lack of crystallization problems or moving part makes them attractive for certain applications. Recent reviews by Shmroukh et al. (2015) and Ojha et al. (2020) provide information about possible working pairs (solid adsorbent/fluid refrigerant) and recent advancements in the research, respectively. Additionally, Choudhury et al. (2010) presents a historical review of adsorption refrigeration technologies from the 1920s (air conditioning using silica gel) until 2010, including the influential work by Tchernev (1978) and its pioneer work in the use of zeolite-water working pairs.

2.3.5 Waste Heat to Power

2.3.5.1 Organic Rankine Cycle (ORC)

“Organic Rankine Cycles” or ORCs are closed power generation cycles based on the traditional Rankine cycle (or steam cycle), that use organic fluids instead of steam as working fluid. The idea of using organic fluids instead of water to drive traditional power cycles dates back to the beginning of the 19th century, where it was suggested the use of “ether”⁴ or “alcohol”⁵ to replace steam in steam reciprocating engines due to their lower boiling points and low latent heat of evaporation at atmospheric pressure. By 1830, it had been already suggested that the low specific volumes of the vapors generated by the evaporation of alcohol and ether offset any gain from the low boiling temperatures and low latent heat of evaporation, and therefore water was more suitable for the steam cycle (Ainger 1830). On the other hand, Ainger (1830) also proposed the use of cascading steam cycles using working fluids with different evaporation temperatures, so that the energy rejected at the condenser of one cycle could drive the evaporation of another working fluid at a lower temperature, but technical limitations at that time made that kind of cascade system unattractive.

The first commercial application of organic fluids in engines on record is the Du Trembley Combined Vapor Engine (Fulton 1851) fabricated at the Novelty Iron Works of Stillman, Allen & Co. in New York. The maritime reciprocating engine combined 2 cylinders with pistons, one

⁴ Referred to the compound known today as Diethyl ether ($C_2H_5-O-C_2H_5$).

⁵ Referred to Ethanol (C_2H_5-OH)

cylinder operating with water and the other with “perchloride”⁶. The energy rejected by the condensation of water in one cylinder was used to drive the evaporation of the perchloride in the other one in a cascading cycle. Other working fluids tested were “ether”, “chloroform” and “sulphur of carbon”⁷. Similar systems were developed for niche applications in maritime and solar thermal projects in the late 1800s and early 1900s but advances in the design of high pressure reciprocating engines and the development of steam turbines, as well as accidents due to the use of flammable and explosive fluids, diminished the interest in the use of organic fluids in power generation applications (Bronicki 2017).

The modern study of ORCs dates from the late 1950s and early 1960s driven by the study of solar thermal engines at the National Physical Laboratory of Israel in Jerusalem. There, Tabor, Bronicki (1961) studied the use of basic and recuperative ORCs using small turbines for the harnessing of solar energy. Later, the same authors developed scientific criteria for the selection of working fluids for power cycles at low to medium temperatures (below 200°C) and established that the systems should operate turbines instead of reciprocating engines, due to their low maintenance, high reliability, easy control and lubrication and large volumetric expansion (Tabor and Bronicki 1965). The developments at the laboratory lead to the creation of ORMAT in 1964, the first company specialized in the design, developing and operation of turbines and general ORCs equipment, currently the market leader and operating predominantly in the fields of geothermal generation and waste heat recovery (Ormat Technologies Inc. 2020).

Currently, at least a dozen companies commercialize ORC systems for different applications (mainly biomass, geothermal, solar and WHR) with at least 2700 MW of total installed capacity worldwide (by 2017). Although still a niche market, and heavily dependent on fossil fuel prices for its economic viability, the increasing interest in renewable energies and sustainability, makes ORCs a commercially attractive technology for current and future power generation applications (Tartière and Astolfi 2017). Recent works by Bronicki (2017) and Tartière and Astolfi (2017) offer a historical perspective of the development of ORC technologies and insights in their current market size and futures perspectives.

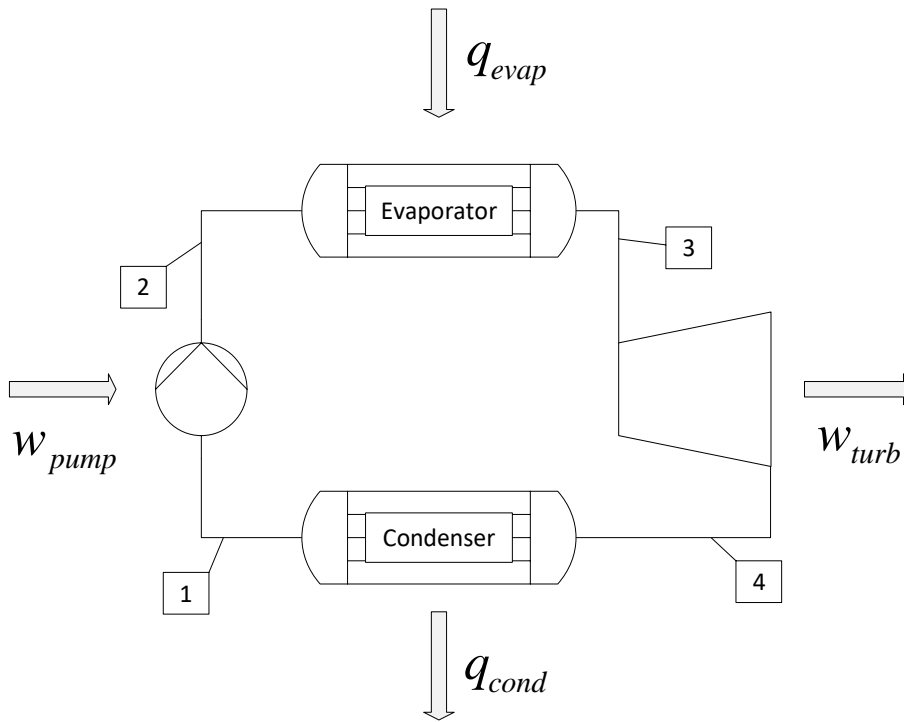
From a technical perspective, the ORCs are similar to traditional Rankine cycles used in most power plants around the world. A schematic representation and a T-s diagram illustrating the cycle for a pure working fluid are presented in Figure 2-5. The cycle starts in point (1), where

⁶ Probably referred to perchlorate ion (ClO_4^-)

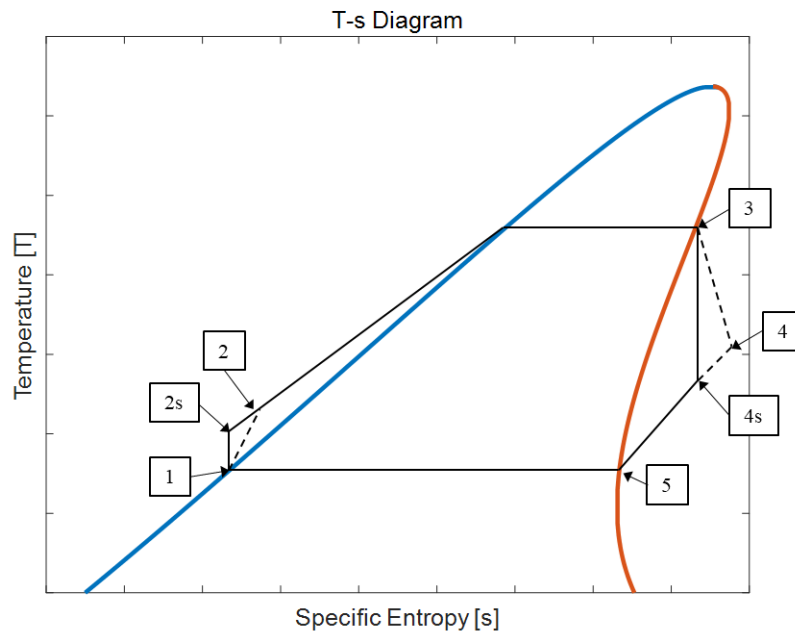
⁷ Currently known as carbon disulfide (CS_2)

the working fluid enters the pump as a saturated liquid and its pressure is elevated until the evaporation pressure. Ideally, the process is isentropic (2s) but in real operation irreversibilities in the pump are unavoidable (2). The working fluid at the evaporation pressure is then heated and evaporated in the evaporator, leaving it as a saturated vapor (3). The saturated vapor is expanded in the expander (typically a turbine) leaving it as a superheated vapor at the condensation pressure. Again, the ideal process is isentropic (4s) but irreversibilities in the turbine are also unavoidable in real operation (4). Finally, the superheated vapor is cooled in the condenser where it rejects its excess heat, leaving the condenser as a saturated liquid to restart the cycle (1). Other configurations aside from the basic ORC presented in Figure 2-5 have also been proposed. Preheating the working fluid entering the evaporator with heat from the fluid at the exit from the expander (referred as recuperative cycle) is a common configuration also used in commercial applications. Other more complex configurations based on the traditional Rankine cycle (with turbine bleeding also known as regenerative cycle, superheating, multiple expansions, reheating etc.) have also been studied but the increased capital costs, increased complexity and generally small improvements in the efficiency of the cycle made these configurations unattractive for many practical applications (Shu et al. 2014; Braimakis and Karellas 2018). In this work, only the basic ORC configuration are considered in the methodology developed in Chapter 4, due to its simplicity and good thermoeconomic performance (Imran et al. 2014; Branchini et al. 2013). The integration of complex ORC configurations in the methodology is proposed as a future work. Recent reviews by Mahmoudi et al. (2018) and Lecompte et al. (2015) present comprehensive descriptions of the different ORC configurations used in waste heat recovery applications.

One of the main factors influencing the performance of the ORC cycle is the working fluid. Depending on the shape of their T-s diagram, fluids can be characterized as ‘dry’, ‘isentropic’ or ‘wet’ working fluids. Dry working fluids have mainly a positive slope ($\frac{dT}{ds} > 0$) in the saturated vapor part of their curve (red in Figure 2-6). That means that an isentropic expansion of the saturated vapor entering the turbine produces a superheated vapor and therefore no liquid droplets interfere with the operation of the expander (Hung 2001). As for isentropic ($\frac{dT}{ds} = 0$) and wet fluids ($\frac{dT}{ds} < 0$), an isentropic expansion of the saturated vapor entering the turbine produces saturated vapor or a liquid-vapor mix, respectively. Dry and isentropic fluids are preferred for most ORC applications, as no liquid droplets are generated during the expansion (Liu et al. 2004).



a) Schematic representation of a basic ORC Cycle



b) T-s Diagram of a basic ORC cycle

Figure 2-5. Basic ORC cycle

Source: Own diagrams based on Hung (2001).

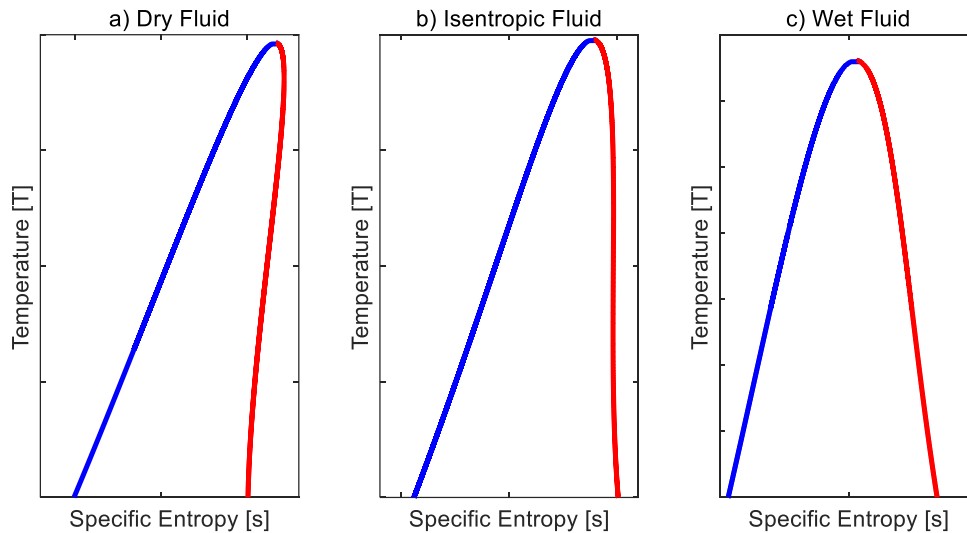


Figure 2-6. Types of working fluids according to their T-s diagram

Source: Own diagram based on Mikielewicz and Mikielewicz (2010)

Combinations of pure working fluids with different evaporation temperatures at the same pressure, known as zeotropic mixtures, have also been studied. Their main difference with pure working fluids is that the evaporation and condensation processes do not take place isothermally. By manipulating the composition of the mixture, it is also possible to generate working fluids with the desirable thermophysical, environmental and safety properties for a given application (Chys et al. 2012). Additionally, the variable temperature at the evaporation and condensation stages allows the cycle to follow closer the temperature profile of the heat sources. This feature decreases the irreversibilities in the cycle during heat transfer (exergy destruction) increasing its second law efficiency (Lecompte et al. 2014).

The optimal selection of a working fluid for a given application is a complex task. The optimal working fluid should have not only a good thermophysical behavior and chemical and thermal stability but also fulfill ever increasing environmental and safety requirements. Multiple studies have been performed studying the selection of working fluids under different conditions, and using different criteria. Thurairaja et al. (2019) studied 82 different working fluids and compared their thermal efficiency in a basic ORC cycle at different evaporation temperatures (between 30°C to 320°C) and generated recommendations for the selection of working fluids according to the evaporation temperature. Kermani et al. (2018) developed an interactive tool to visualize the properties of 84 working fluids for waste heat recovery applications. Darvish et al. (2015) analyzed 9 working fluids for a regenerative ORC cycle using energy and exergy efficiencies at fixed operating conditions and found that R134a and iso-butane have the best energy and exergy efficiencies at a evaporation temperature of 120°C. Feng et al. (2015)

performed a thermoeconomic comparison between the pure working fluids and zeotropic mixtures of R227ea and R245fa in basic ORC cycles and found that mixtures with an optimal mass fraction in composition have a better thermoeconomic performance than pure fluids. Vivian et al. (2015) studied the thermal efficiency of 27 pure working fluids at 3 different ORC configurations with heat sources at different temperatures and concluded that the performance of the cycle depends on the difference between the starting temperature of the heat source and the critical temperature of the working fluid, with the best results for temperature differences between 35°C and 55°C for basic ORC cycles.

Lecompte et al. (2014) studied 8 pure fluid and 8 zeotropic mixtures in basic and regenerative cycles at fixed conditions and determined that mixtures have better exergy efficiencies. They also established that for each mixture an optimal composition exists that maximizes the exergy efficiency. Similar studies and results for zeotropic mixtures with different fluids and compositions are presented by Chys et al. (2012) and Heberle et al. (2012). Stijepovic et al. (2012) concluded that mainly 5 thermophysical properties affect the thermal efficiency of a working fluid : the expansion ratio in the turbine, the heat capacity of ideal gas, the molar mass, the compressibility factor and the density of the saturated liquid. Rayegan and Tao (2011) studied 34 working fluids for solar thermal applications and classify them according to energy and exergy efficiencies, as well as net power generated and vapor expansion ration in the turbines. Similar studies for solar thermal applications have been presented by Hung et al. (2010) and Tchanche et al. (2009). For ORC applications in WHR from internal combustion engines in vehicles, a study was presented by Wang et al. (2011).

As evident from the mentioned studies, no single working fluid or evaluation criteria has been established for the optimal selection of organic working fluids. Depending on the operating conditions and environmental and safety factors, the best working fluid for a given application has to be determined. For the case studies in Chapter 5, only a selected number of working fluids is considered. This selection does not represent all the possible working fluids that could be used for the case studies. As long as their thermophysical properties are available, the methodology developed in Chapter 4 can be applied to any pure dry working fluid. Additionally, no rigorous optimization of the operating parameters in the ORC cycle is performed. Appendix B presents a list of the working fluids considered in the case studies in Chapter 5, with some of their thermophysical properties.

Another relevant factor for the design of ORC systems is the selection of the expander. In general, the design of the expander influences the isentropic efficiency of the expansion, the

cost and size of the system and the operating parameters of the cycle. Different expander technologies have been proposed, but they can be classified in two main groups: turbo expanders, also known as velocity type (e.g., axial and radial flow turbines) and volumetric expanders also referred to as positive displacement type (e.g., scroll expanders, screw expanders, rotary vane expanders, piston expanders) (Quoilin 2011). Turbo expanders are similar to steam turbines and are characterized by high rotational speeds, compact and simple structure, and high efficiencies. They are preferred for applications with power outputs higher than 50 kW_{el}, but for lower power outputs their performance decreases rapidly (Qiu et al. 2011). For small-scale applications, volumetric expanders are preferred. They are characterized by lower flow rates, higher pressure ratios and lower rotational speeds than turbo expanders. Additionally, some volumetric expanders (e.g., Screw and scroll expanders) can operate with wet working fluids (Kolasiński 2020). Bao and Zhao (2013) present a review of expander technologies for ORC. In this work, the expander technology is not considered and the performance of the expander is described only by their isentropic efficiency.

2.3.5.2 Kalina Cycle

Kalina cycle (Kalina 1984) is a power generation cycle based on the use of a zeotropic mixture of ammonia-water (NH₃/H₂O). Similar to zeotropic mixtures of organic fluids in ORC, the main advantage of the Kalina cycle is the variable temperature at the evaporation and condensation stages, with the associated increases in second law efficiencies. The cycle is similar to the ORC cycle with compression, evaporation, expansion and condensation stages, but also includes additional stages due to the handling and manipulation of the NH₃/H₂O mixture. The additional stages include mixing, separation, and preheating stages. The exact configuration of the cycle is flexible and depends on the application, the main common feature is the use of the NH₃/H₂O mixture as working fluid. The composition of the NH₃/H₂O mixture varies during the cycle with higher NH₃ concentration in the evaporation stage and lower concentrations during condensation.

In general, Kalina cycles tend to have slightly better thermal performances than ORC cycles but their complex design and operation, high operating pressures and the requirement of non-corrosive material due to the NH₃, limit their use in practical applications (Zhang et al. 2012; Modi and Haglind 2017).

2.3.6 Waste Heat to Heating (Heat Pumps)

From a historical and technological perspective, heat pumps share the same origins and fundamental principles than refrigeration technologies, but they operate in a reverse cycle. Up until the oil crisis in 1973 and due to low energy prices and the large availability of fossil fuels, almost all heating requirements in residential, commercial and industrial applications worldwide were supplied by other technologies, mainly steam networks and typical coal, biomass and gas driven boilers. The oil crisis had a deep impact on the worldwide views on energy and energy efficiency, alternative energies sources and energy security became part of the public and political priorities of governments worldwide and there was a boom on the research and installation of heat pumps on residential, commercial and industrial applications (Zogg 2008). The use and integration of heat pumps in industrial processes is an active field of research. An analysis of heat pump technologies, their industrial applications and their economic and technical potentials it is out of the scope of this work. The reader is referred to a recent work by Wolf (2017) for an in-depth study of the integration of heat pumps in industrial systems.

2.4 Process Integration

The Handbook of Process Integration defines “Process Integration” (PI) as a “...*family of methodologies for combining operations within a process or several processes to reduce consumption of resources and/or harmful emissions...*” (Varbanov 2013). Similarly, the IEA defines PI as the “...*systematic and general methods for designing integrated production systems, ranging from individual processes to total sites, with special emphasis on the efficient use of energy and reducing environmental effects...*” (Gundersen 2002). From these definitions it is clear that PI is a group of methodologies for the combination and integration of processes in order to reduce their resource intensity and emissions. Although initially developed for the synthesis of heat exchanger networks (HENs), that is, for the optimization of thermal energy flows in single processes (Heat Integration) (Linnhoff and Flower 1978a, 1978b; Linnhoff 1979) and then the combined heat and power (CHP) in total sites (Dhole and Linnhoff 1993), the current scope includes other resources and processes such as mass flow (Mass Integration) (El-Halwagi and Manousiouthakis 1989), hydrogen (Alves and Towler 2002), oxygen (Zhelev and Ntlhakana 1999), supply chain flows (Singhvi and Shenoy 2002), material reuse (Foo et al. 2006), carbon footprint (Tan and Foo 2007), etc. A recent review by Klemeš et al. (2018) presents the current developments on 15 different fields of application of Pinch Analysis (PA),

which is the main tool of Process Integration and sometimes is used as a synonym. In this work, the term “Process Integration” is used as stated by the IEA and refers to “... *systematic and general methods for designing integrated production systems...*”. The design of systems integrating ORCs and ABCs into HENs is then considered as part of the field of study of “Process Integration”.

2.4.1 Pinch Analysis

Gundersen (2002) defines “Pinch Analysis” (PA) as a tool that provides information about the flow of a quantity in a process. The quantity or amount (e.g., heat or mass) is characterized by a quality (e.g., temperature, concentration, etc.). Three main elements are basic for PA: (1) “Composite Curves” (CC) that are used to represent graphically the quantity flows in the system and provide an overview of the state of the process; (2) “Performance Targets” based on physical insights obtained through analysis of the Composite Curves or algorithmic methods like the “Problem Table Algorithm” (PTA) and (3) a “Pinch Decomposition”, that separates the system at the pinch point in “excess” or “deficit” regions with respect to the quality considered. In the case of “Heat Integration”, the quantity and quality are heat or more precisely, enthalpy and temperature, respectively, and the objective of PA is to generate or “synthesize” optimal heat exchanger networks. An optimal HEN is a reliable and safe HEN design with a minimum “Total Annualized Cost” (TAC). As the direct optimization of TAC using only PA is not possible, this objective is substituted by “near optimal” HEN designs with minimum utility targets, minimum number of units or matches, and minimum heat transfer areas, which are related calculations that are attainable with PA tools. The set of rules and heuristics procedures used to generate system designs using the principles of PA is known as “Pinch Design Method” (Linnhoff and Hindmarsh 1983).

The “Composite Curves” and “Performances Targets” were first presented by Hohmann (1971) in its PhD Thesis at the University of Southern California but it wasn’t until two articles published by Linnhoff and Flower (1978a, 1978b) and then the PhD thesis by Linnhoff (1979) that the pinch point decomposition was identified and the practical potential of PA for the synthesis of HEN was recognized (Linnhoff and Hindmarsh 1983). Pinch point(s) or simply “pinch”, is defined in the Handbook of Process Integration (Varbanov 2013) as “...*the location(s) in the problem where the process driving force is equal to the minimum allowed...*”. For thermal systems, the driving force is the temperature difference between the hot and cold process streams. The fundamentals of PA and its utilization have been covered extensively in many publications and are not presented in detail in this work. For more information about PA

please refer to reference books and manuals such as Kemp (2007), Klemes (2013) and Brunner et al. (2015).

2.4.2 Mathematical Programming

Parallel to the development of PA techniques, a mathematical approach based on mathematical optimization techniques also known as “Mathematical Programming” (MP) was developed for the synthesis of HEN. The main advantage of MP is the optimality, feasibility and integrality of the solutions (Klemeš et al. 2013). The optimality can be related to one or multiple objective functions and trade-offs and complex interactions between the different components and subsystems can be studied and evaluated in a direct and flexible way. The main drawbacks of MP are the lack of global optimization techniques for complex models, the relative difficulty for the formulation of the mathematical problem and the difficult interpretation and analysis of the results. While PA is intuitive and presents a clear graphical indication of the state of the system, the interpretation and analysis of the MP results requires relatively advance knowledge of the mathematical model and the optimization technique and strategies used, which limits its application in industrial scale problems (Klemeš and Kravanja 2013). Klemeš and Kravanja (2013) presented a comparison between PA and MP and concluded that a combination of both techniques for real life applications could lead to improved industrial designs, as PA is already a standard practice in many industries and its results can be refined and improved with the use of MP techniques.

MP approaches for the synthesis of HEN can be classified as sequential or simultaneous methods. Sequential methods divide the HEN synthesis problem in subproblems, which are solved sequentially, with the results of one subproblems serving as input information for the next one. Typically, the subproblems are three: (1) the minimization of the utility consumption; (2) the minimum number of units or matches and (3) the minimum heat transfer area or investment cost. In the case of simultaneous models, the objective function is typically the minimum “Total Annualized Cost” (TAC) and the models consider simultaneously all the trade-offs and interactions between the different components in the system.

The three subproblems for sequential methods resemble the targets calculations in Pinch Analysis. Each of the subproblems is solved independently using different mathematical formulations. Mathematical models for the minimum utility consumption problem were proposed independently by Papoulias and Grossmann (1983) and Cerda et al. (1983) based on the transshipment and transportation problems of operational research, respectively. In both

models, the resulting problem is a “Linear Programming” (LP) problem, of which the transshipment model is the most known formulation. Similarly, mathematical formulations for the problem of the minimum number of matches were also proposed by Papoulias and Grossmann (1983) and Cerda and Westerburg (1983) again based on the transshipment and transportation problems. The resulting formulations are “Mixed Integer Linear Programming” (MILP) problems. Finally, for the third problem, the minimum investment cost is typically solved using the formulation by Floudas et al. (1986), which results in an “Non Linear Programming” (NLP) problem. Similarly, the models generated in the simultaneous approach also have different mathematical formulations, the most known being the “Hyperstructure” (Ciric and Floudas 1991) and the “stage-wise superstructure” more commonly referred as “SYNHEAT” model (Yee and Grossmann 1990). In both cases, the resulting problems are “Mixed Integer Non Linear Programming” (MINLP) problems. Both MINLP formulations for HEN synthesis as well as the MILP formulation for the minimum number of matches in the sequential methods have been proved NP-Hard problems in the strong sense, which means that no known algorithm provides exact solutions in a computationally efficient way (polynomial time⁸) (Furman and Sahinidis 2001).

In general, sequential methods tend to be faster and easier to implement but, similarly to PA, they generate sub-optimal solutions and do not take into consideration the tradeoffs in the system. Simultaneous methods, on the other hand, tend to generate better results but they are computationally demanding and global optimization techniques tend to get trapped in local optima. A comparative study by Escobar and Trierweiler (2013) concluded that from all MP methods available, SYNHEAT tends to provide the best results even with the isothermal mixing assumption, and with appropriated initialization procedures, the flexibility and robustness of the model allows to generate good local optima relatively fast.

In this work a purely MP approach is used for the design of systems integrating HEN, ORCs and ABCs for continuous and discontinuous processes with and without FTVM heat storage. MP is the best option in this case, due to the high number of subsystems and complex interaction between them. PA tools such as “Performance Targets”, “Composite Curves” and “Grand Composite Curves” (GCC) are used to facilitate the understanding of the case studies presented in Chapter 5, but the results are based on purely mathematical considerations.

⁸ Furman and Sahinidis 2001 define polynomial time algorithms as “...algorithms whose run time is polynomially bounded in the size of input and the logarithm of the size of the input values...” .

2.5 Process Integration in Discontinuous Processes

The methods and approaches discussed in section 2.4 were all developed originally for continuous processes but they have been extended to analyze systems with discontinuous operation. As the name suggested, discontinuous processes are characterized by intervals or periods of operation where the operating conditions, the streams involved and/or the processing units, change. The terms “batch” and “multi-period” processes have been used to describe processes with discontinuous operation. Becker (2012) differentiates between batch and multi-period processes, indicating that although the distinction is not always evident, multi-period processes refer to processes with different scenarios, periods of operation, or operating states. In this case, no time dependence is considered and each scenario is independent of the others. Processes with clear periods of operation and with their own specific operating conditions are multi-period. Seasonal and monthly variations, workday/weekend operations or shift work are typical examples of multi-period processes and are also known as “semi-continuous” processes. Batch processes are also characterized by periods or intervals of operation, but there is a time dependency between them. Some processes cannot start until other are finished and in most cases processes share operating units. Time limitations have to be considered at the design and operation of batch processes and they are characterized by short periods of operation, and a sequence of predetermined discrete tasks (recipe) that have to be followed to transform raw materials into products (Barker et al. 2005). Typical examples of batch processes are those in the pharmaceutical industry, the production of specialty chemicals and processes in food and beverage industry like breweries and dairies. In this work, batch processes with fixed schedules are treated as multi-period processes, as in that case the time dependency between the intervals or periods of operation can be ignored.

The two main tools for PA in discontinuous processes are the “Time Average Model” (TAM) and the “Time Slice Model” (TSM) developed by Linnhoff March Ltd. in the late 80s (Clayton 1986; Linnhoff et al. 1988). In the TAM, the heat flows are averaged over a cycle of operation and the system is treated as a continuous process with process streams with the same initial and target temperatures as in the batch process and heat flows capacities equal to the weighted time averages of the heat flows capacities during the cycle. On the other hand, TSM treats each period of operation, also referred as time intervals, independently of each other and the energy targets and pinch temperatures are calculated for each time interval also independently with cycle targets equal to the sum of the energy targets in each interval. The TAM targets represent an upper limit to the heat recovery in the process (best case) and are only attainable with

sufficient heat storage and no time/scheduling constraints in the system. The TSM targets represent the best attainable energy recovery only using direct heat integration (no storage and no rescheduling).

A popular extension of the TSM model is the “Cascade Analysis” proposed by Kemp (1990). The cascade analysis takes advantage of the different pinch temperatures in each of the time intervals according to the TSM and evaluates the possibility of heat transfer from below the pinch temperature in an interval to above the pinch on another interval. In this case, energy from below the pinch in an interval can be stored to be later released and used above the pinch in another time interval with a lower pinch temperature, so that the effective heat transfer takes place always above the pinch. Cascade analysis can be used to evaluate fixed-temperature storage options and rescheduling opportunities and its results match those of TAM if the number of storages is big enough and the same minimum approach temperature is used between process streams and between process streams and heat storages.

Other pinch-based techniques have been proposed in order to facilitate the design of the required heat storages for a given discontinuous processes. Stoltze et al. (1995) found that a low number of heat storages is sufficient to reach the TAM targets in many industrial cases (between 2 and 6 storages for the cases evaluated) and proposed a combinatorial method for the synthesis of HEN integrating streams and heat storages. This method, later referred as “Permutation Method”, assumes initially that two FTVM storages are available and generates the corresponding HEN, then the number of storages units is increased by one, and again a HEN is generated. The process continues until the design is able to achieve the TAM targets or all the possible combinations/permutations are evaluated. The maximum number of storages to be evaluated is equal to twice the number of process streams, but as mentioned before, a low number of storages is sufficient to reach the TAM targets. As for storage temperatures, all the possible combinations between the initial and end temperature of the process streams (corrected by ΔT_{min}) can be used. Krummenacher and Favrat (2001) presented a graphical method based on modified CCs to calculate the minimum number of storage units required to achieve the TAM targets or a given level of energy recovery. Krummenacher (1999) also proposed a metaheuristic method based on “Genetic Algorithms” (GA) for the synthesis of batch HENs with or without heat storage. Atkins et al. (2010) extended the use of pinch-based techniques to total sites and used it to integrate multi-period (semi-continuous) processes in a milk powder plant using stratified storage tanks and “Heat Recovery Loops” (HRL). Later, the same research group extended the methodology to account for dynamic effects in the HRL (Atkins et al. 2012), the optimization of the heat transfer areas in the HEN (Walmsley et al. 2013b) and the

integration of solar energy and variable temperature storages (Walmsley et al. 2014). A comprehensive explanation of the methodology is available in the Handbook of Process Integration (Walmsley et al. 2013a). Recent works by Olsen et al. (2017) and Abdelouadoud et al. (2019) extended the graphical tools developed by Kruppenacher and Favrat (2001) to facilitate the design and evaluation of heat storages including economic and practical considerations and Stampfli et al. (2020) presented a LP model that complemented the graphical approach in order to evaluate heat storage when there are volume constraints.

Parallel to pinch-based techniques, mathematical programming approaches for the design of discontinuous HENs have been also developed. In most cases, MP approaches treat batch and multi-period HEN methods separately. In the case of batch HEN synthesis, Vaselenak et al. (1986) presented a heuristic and a MILP algorithm to match processing units (tanks) requiring heating and cooling in batch processes. The work can be considered as a pioneer work in direct heat integration in batch processes using MP. Corominas et al. (1993, 1994) presented a methodology combining heuristics and an MILP formulation for the design of batch HENs in multiproduct/multipurpose, maximizing energy recovery using direct heat integration and rescheduling. The heuristics are used to evaluate rescheduling opportunities and the MILP for the calculation of the optimal matches between process streams. Papageorgiou et al. (1994) combines the scheduling and heat integration problems using a MINLP formulation for direct and indirect heat integration. The formulation is an extension of the MILP developed by Kondili et al. (1993) for the optimal short-term scheduling of batch processes, known as discrete-time formulation. Another mathematical formulation developed originally for the optimal scheduling of batch processes, known as continuous-time formulation (Majozi and Zhu 2001), was also modified to include the direct heat integration problem in multipurpose/multiproduct batch processes (Majozi 2006). The same research group later extended the formulation to include indirect heat integration (Majozi 2009; Stamp and Majozi 2011), modifications to the scheduling formulation to reduce the number of variables (Seid and Majozi 2012, 2014a), water minimization (Seid and Majozi 2014b), consideration of heat integration with batch streams while they are moving from one unit of operation to another one (material transfer) (Lee et al. 2015, 2016), long-term scheduling (Stamp and Majozi 2017) and multiple storage vessels (Sebelebele and Majozi 2017).

Other MP formulations for the synthesis of batch HENs without considering rescheduling were developed by Chen and Ciou (2008, 2009) for the design of batch HENs with only indirect heat integration using fixed and variable temperature storages. Hellwig (1998) also developed independently an optimization algorithm for the selection of a set of possible matches between

hot and cold streams in continuous and discontinuous processes (direct integration only) which maximizes energy recovery (OMNIUM Method). The method is based on the Hungarian algorithm, a classical algorithm to solve linear assignment problems in operations research (Kuhn 2012). Uhlenbruck et al. (2000) compared the results of OMNIUM and the TSM targets and found that OMNIUM does not reach the pinch targets and tends to generate complex networks. They proposed the repeated/recursive application of OMNIUM to improve the results and generated designs that reached in average up to 95% of the pinch targets. More recently Heyden (2016) extended the OMNIUM method to include cost and technical calculations, as well as heat storage options, and used it to evaluate waste heat recovery opportunities in an industrial laundry and in the German laundry sector as a whole, using representative laundries for “small” and “big” facilities.

Studies focused on multi-period processes have their origin in the problem of design of flexible HENs. Verheyen and Zhang (2006) define flexible HEN as those that can operate even if there are variations of certain parameters around a nominal value due to uncertainties (resilient HENs) or that can operate even if there are planned periodical changes in their operating conditions (multi-period HENs). In the case of multi-period HENs, some of the first influential studies were published by Floudas and Grossmann (1986, 1987). They presented an automated sequential method for the design of multi-period HENs. Their work is an extension of the transshipment model developed by Papoulias and Grossmann (1983) and Floudas et al. (1986) for the design of continuous HENs. Later Aaltola (2003) in his dissertation presented a multi-period extension to the SYNHEAT model (Yee and Grossmann 1990) for the simultaneous synthesis of continuous HENs. He used an “average area approach” in which the effective area for a given match to be used for TAC calculations is equal to the arithmetic average of the areas required for the heat exchanger in the match at each period of operation. This formulation results in an underestimation of the required heat transfer areas and the TAC, but avoids the introduction of non-linearities in the constraints or the objective function. Chen and Hung (2004) proposed then an “maximum area approach” through the use of a discontinuous maximum function in their objective function, but the resulting computational times were discouraging. Then Verheyen and Zhang (2006) reformulated the “maximum area approach” by the use of area inequalities in the constraints instead of discontinuous functions in the objective. This formulation is one of the bases of the framework presented in section 4.2.2 for the integration of ORCs and ABC into multi-period HENs without heat storage. In the three formulations by Aaltola (2003), Chen and Hung (2004) and Verheyen and Zhang (2006), only processes with periods of equal duration are considered. Isafiade and Fraser (2010) modified

the objective function by Verheyen and Zhang (2006) to improve the results in processes with periods of unequal duration. Other recent improvements to the superstructure of Verheyen and Zhang (2006) include the integration of multiple utilities (Isafiade et al. 2015), the consideration of detail heat exchanger design (Short et al. 2016a, 2016b), better initialization techniques for the MINLP and lower overdesign of the heat exchangers (Isafiade and Short 2016; Isafiade 2017) and the integration of heat storages options for fixed (Beck and Hofmann 2018b) and variable temperature fixed mass storages (Beck and Hofmann 2019). The formulation by Beck and Hofmann (2018b) is used as base for the methodology presented in section 4.2.3 for the integration of ORC and ABC into HEN in multi-period processes with FTVM storage. As for extensions to the sequential method by Floudas and Grossmann (1987), Mian et al. (2015) integrated multiple utilities, that could be located in any position in the superstructure. The problem is solved using a metaheuristic algorithm developed by the same research group and named PGS-COM (Martelli and Amaldi 2014). The same research group later included heat storage options to the formulation (Mian et al. 2016).

Another interesting development in the multi-period HEN research is the “timesharing mechanism” (Sadeli and Chang 2012), that is, the reuse of heat exchangers in different matches each period of operation, depending on the characteristics of the process. Heuristics (Jiang and Chang 2013) and algorithmic (Jiang and Chang 2015) approaches to the timesharing mechanism have been developed with encouraging results, as it tends to decrease the capital cost of the HEN, and heat exchangers can be reused in different matches in a way that minimized their overdesign. Possible disadvantages of this method include but are not limited to the need of cleaning procedures for the heat exchangers with their associated additional costs. Recent studies also include non-isothermal mixing (Miranda et al. 2016) and metaheuristic methods for the MINLP solution (Pavão et al. 2018) combined with the timesharing mechanism. In this work, the timesharing mechanism is not considered for the mathematical framework developed in Chapter 4, but research in this area is encouraged for future works.

3 State-of-the-Art

In this chapter, a State-of-the-Art of the process integration of ORCs and ABCs into HENs is presented. The process integration of other WHR technologies, including heat pumps and alternative “waste heat to heating” and “waste heat to cooling” technologies, are not considered but their study and integration to the framework developed in Chapter 4 are recommended for future works. The chapter is divided in three subsections covering the process integration of ORCs, ABCs and the combined technologies independently. Most of the works on the integration of WHR technologies into HENs have been focused on continuous processes and only study the integration of one WHR technology at a time. The few works combining different WHR technologies tend to oversimplify the mathematical modeling and behavior of the WHR technologies, i.e. assuming fixed ORC and ABC efficiencies ignoring the working fluid and working pairs properties and the physical behavior of the ORC and refrigeration cycles. This dissertation is an effort to bridge these research gaps and proposes a mathematical framework and superstructure for the integration of multiple WHR technologies (ORCs and ABCs) into HEN in continuous and multi-period processes, with or without FTVM storage, while considering in detail, the physical behavior of the working fluids in the ORC and working pairs in the ABC.

3.1 Process Integration of Organic Rankine Cycles into Heat Exchanger Networks

The basic pinch rules for the integration of heat engines (ORCs included) and heat pumps (ABCs included) into HEN were presented by Townsend and Linnhoff (1983b, 1983a) already in the first years of pinch analysis. The “Appropriate Placement” rules (Townsend and Linnhoff 1983a) state that heat engines should be located entirely above or entirely below the pinch in order to avoid cross-pinch transfer and generate mechanical work with a theoretical 100% efficiency in the heat to work conversion (Figure 3-1). For a system with hot utility consumption fixed to its pinch targets, that 100% heat to work conversion efficiency means that a heat engine located entirely below the pinch will generate mechanical work from waste heat, that would be otherwise rejected to the cooling utility. On the other hand, a heat engine located entirely above the pinch will generate mechanical work from energy already supplied to the system by the hot utility, with 100% efficiency and without increasing the utility consumption of the system. Townsend and Linnhoff (1983b) already considered the possibility of integration ORCs below the pinch in order to generate mechanical work from waste heat and suggested selecting

working fluids with critical temperatures near to the pinch temperature as they increased the temperatures at the top of the cycle, increasing its efficiency. They also recognized the tradeoff between the temperature at the ORC-Evaporator and the amount of energy that the ORC is able to extract from the hot process streams below the pinch. Moreover, in the same work Townsend and Linnhoff (1983b) considered technical limitations and shapes of the heat profiles generated by working fluids in Rankine and Bryton (Gas Turbines) cycles and how they should be considered when exploring the integration of heat engines into industrial processes. Due to the relatively low temperatures, low efficiencies and high costs of heat engines below the pinch, the study of the process integration of ORCs into HENs fell in relative obscurity during the following decades until a study by Desai and Bandyopadhyay (2009) and increased energy prices and sensibilities about energy efficiency and environmental protection, reactivated this field of research. However, the integration of heat engines above the pinch was further developed and studied as part of the design of utility systems, which includes the Total Site Analysis (Dhole and Linnhoff 1993) mentioned in section 2.3.2. The utility system design comprises among other objectives, the selection of temperature and pressure levels for the hot utilities and the identification of the optimal turbine configuration between the hot utility (usually steam) mains that maximizes the cogeneration (heat and power) potential of the system (Mavromatis and Kokossis 1998).

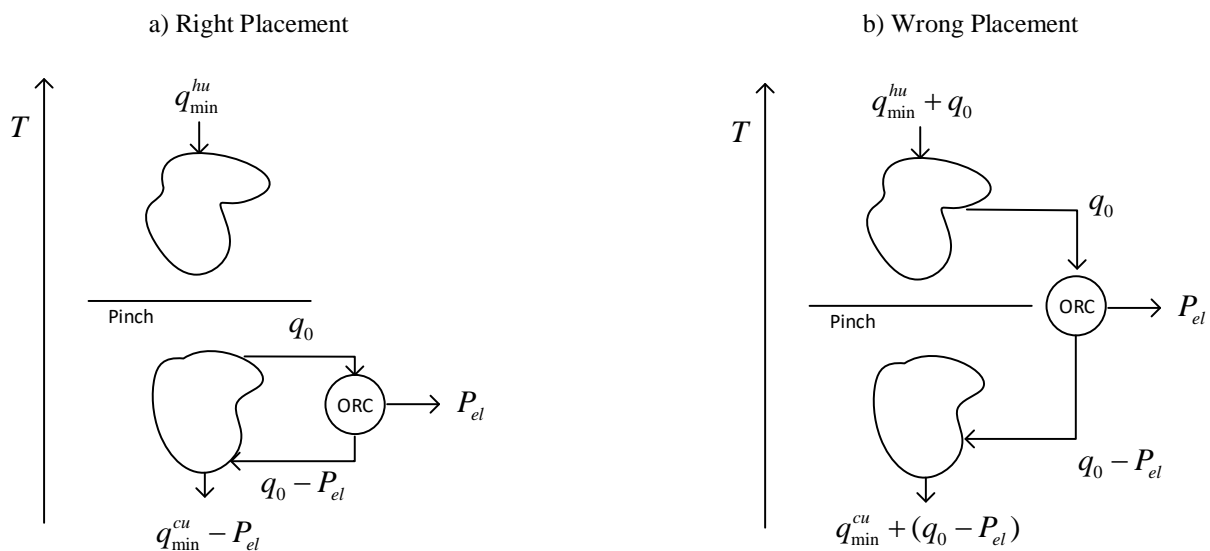


Figure 3-1. Appropriate placement of ORCs driven by waste heat according to pinch analysis.

Source: Own diagram based on Townsend and Linnhoff (1983a) and diagram from Natural Resources Canada (2012)

Desai and Bandyopadhyay (2009) used PA techniques to study the integration of ORCs into continuous HENs. They explored the opportunities for integration of ORCs using the GCCs and the PTA to rapidly evaluate different dry working fluids using different evaporation and

condensation temperatures for the ORC. They also considered other ORC configurations aside from the basic, including the recuperative cycle (referred as regenerative cycle in the article), turbine bleeding and a combination of the two. After the working fluid, ORC configuration and corresponding evaporation and condensation temperatures are determined, the HEN including the ORC is generated using the Pinch Design Method (Linnhoff and Hindmarsh 1983). Thermophysical properties of the working fluids are obtained from the software REFPROP (Huber et al. 2018).

Later, works by Hipólito-Valencia et al. (2013) first and then Chen et al. (2014), developed mathematical programming approaches to the simultaneous integration of ORCs into the background processes and the synthesis of the accompanying HEN. Both superstructures are extensions of the SYNHEAT model for the synthesis of HENs (Yee and Grossmann 1990). Hipólito-Valencia et al. (2013) focused on the optimization of the TAC of the system and neglected the latent heat of evaporation of the working fluid. In the model, the ORC structure included an economizer to pre-heat the working fluid before the evaporator with the hot working fluid exiting the turbine. Similar to the framework presented in Chapter 4, the model only allows heat exchange between the working fluid and the process streams in one dedicated stage located at the cold side of the superstructure. The authors did not calculate the thermophysical properties of the working fluids for the ORC and instead assumed values for the heat capacity of the working fluids. The superstructure was later extended by the same research group to include inter-plant heat integration (Hipólito-Valencia et al. 2014b) and absorption chillers and steam cycles (Lira-Barragán et al. 2014c). In this case, a boiler fed by renewable energies (solar thermal or biomass) or fossil fuels drives the steam cycle and the energy rejected by the cycle in the condenser acts as hot utility for the process streams, the ORC and the ABC. The ORC and the ABC are integrated in the HEN of the process streams and can be driven by energy from the process streams, or from the hot utility, depending on the process conditions and the objective function. Additionally, the study considered alternative objective functions including environmental (greenhouse gas emissions or GHGE) and social considerations (number of jobs generated by the project). The superstructure for the ORC integration was applied to a bioethanol separation process with TAC savings up to 7% in comparison with the HEN without ORC under the conditions used by the authors (Hipólito-Valencia et al. 2014c).

The superstructure proposed by Chen et al. (2014) was also an extension of the SYNHEAT model and pursued the maximization of the “Net Power” generated from the waste heat using the Peng Robinson Equations of State (PR-EOS) (Peng and Robinson 1976) to calculate,

separately from the optimization model, the thermophysical properties of the working fluid. The study considered the latent heat of evaporation and condensation of the working fluid and rightfully proved its influence on the model results. The model used a basic ORC configuration and allowed heat exchange between the working fluid and the process streams in all stages of the superstructure. The model was later extended to include transcritical ORCs (Chen et al. 2015a). A similar superstructure was later used by the same research group to study the integration ORCs into a refinery (Chen et al. 2016). In this case, the HEN was not generated and only hot streams were considered. Heat recovery loops using intermediate heat transfer fluids were used to transfer energy between the hot streams and the ORCs. Multiple ORCs with different working fluids and operating conditions could be evaluated simultaneously. The selection of the optimal working fluid and operating conditions for a given ORC was made using an iterative “trial and error” algorithm. The same algorithm is applied to the case studies in Chapter 5, with “Net Power” generated from waste heat as objective function, in order to determine the best working fluids and operating conditions for the ORCs presented in the chapter. A flow diagram of the “prescreening algorithm” is available in Chapter 5 in Figure 5-2. More recently, Elsidio et al. (2017) extended the superstructure presented by Chen et al. (2014) in order to consider multiple pressure levels for the expansion in the turbines. The properties for the working fluid are taken from REFPROP. The MINLP is then solved using metaheuristics⁹.

In order to include the optimization of the ORC configuration and operating temperatures explicitly into the optimization problem, Yu et al. (2017a) proposed a sequential method. In the first step, the ORC configuration, operating temperatures and mass flow of the working fluid in the ORC are treated as variables and optimized using the Duran-Grossmann model for the simultaneous consideration of Heat Integration and Process Synthesis¹⁰ (Duran and Grossmann 1986). The thermophysical properties of the working fluid are included explicitly in the formulation through the use of the PR-EOS (Peng and Robinson 1976). In the second step, a HEN including the ORC and process streams is generated using the transshipment model for

⁹ Metaheuristics algorithms are high-level adaptive and autonomous methodologies that apply generic heuristic rules (i.e. based on trial and error and/or rule of thumb) for the solution of computational problems (Wang 2010). Main difference with exact/deterministic methodologies is that metaheuristics do not provide information about the gap between the solutions found and the best possible solution and cannot guarantee to find the global optimum if enough time is provided (Hussain et al. 2019).

¹⁰ The original Duran-Grossmann model 1986 is a mathematical formulation used to find the required temperatures and mass flows of process streams that maximizes the heat recovery in a given chemical process without generating the HEN.

sequential synthesis of HENs (Floudas et al. 1986). The same research group also extended the formulation to include indirect heat transfer between the ORC and the process streams using hot water as an intermediate heat transfer fluid (HTF) (Yu et al. 2017b). Previously, the authors had already studied the integration of an ORC into a refinery using hot water as HTF in a HRL using graphical PA tools (Yu et al. 2016).

Kermani et al. (2018) also presented a sequential method for the integration of ORCs into HENs. In the first step, a MILP generic superstructure that includes up to five pressure levels for the turbines and consider basic cycles, superheated, regenerative, transcritical, reheating, bleeding and multi-stage cycles is optimized and the optimal configuration and operating parameters for the integrated ORC is determined. The MILP is solved using a bi-level decomposition technique, which uses a MILP solver to find the optimal ORC configuration and metaheuristics to determine the optimal operating conditions for the ORC. The properties of the working fluid are included in the formulation as piece-wise linear models. In the second step, the HEN including the ORC is generated using the transshipment model (Floudas et al. 1986). The study also considered multiple objective functions and multi-objective optimization. The formulation includes equations for the calculation of heat transfer coefficients of the working fluids in the heat exchangers (film coefficients) and an interactive database with some thermophysical properties for selected working fluids was also generated.

More recently, a number of publications discussing the ORC integration into HENs were published. Xu et al. (2020) included the ORC evaporation and condensation temperatures as variables in the model by Chen et al. (2014) and considered the total exergy destruction and the TAC as multi-objective functions. Properties of the working fluids are obtained from REFPROP. Dong et al. (2020) included the working fluid properties in the formulation using fit functions obtained from polynomial regressions of the fluid properties instead of using the highly non-linear PR-EOS. Similarly, Huang et al. (2020) presented a superstructure including HEN, steam Rankine cycle, ORC and cooling tower and considered the properties of the working fluid in the formulation using fit functions. Chamorro-Romero and Radgen (2020) extended the superstructure by Chen et al. (2014) to include indirect heat integration of ORCs into HEN using intermediate HTFs. The heat transfers between the ORCs and the HEN take place through HRLs. The operating temperatures and mass flows of the HTFs inside of the HRLs are treated as variables and determined during the optimization procedure. Additionally, a recent review by Anastasovski et al. (2020) presented a comprehensive analysis of heat integration approaches for the integration of ORCs driven by waste heat into production processes. The review focuses on the link between the ORC and the industrial processes and

the methods used for the optimization of the ORC configuration and operating parameters in the integrated system. Studies considering simultaneously the ORC integration and the HEN synthesis are also mentioned but are not the main focus of the review. Anastasovski et al. (2020) concluded that the main gap in the research is the gap of systematic methods for the integration of ORCs into batch and discontinuous processes.

Finally, last year (2021), the first work dealing with the integration of ORC into multi-period HENs was presented. Elsidio et al. (2021) extended a previous metaheuristic methodology developed for continuous processes (Elsidio et al. 2017) and later improved for better computational performance (Elsidio et al. 2019), to include multi-period operation. Two-tank storages with FTVM were considered and their temperatures were known in advance. Size of the storage was part of the variables to optimize.

3.2 Process Integration of Absorption Chillers into Heat Exchanger Networks

Only few works study the process integration of absorption chillers into heat exchanger networks. The contrast with the process integration of ORCs into HEN as discussed in the previous section is clear. Similar to ORCs, the “Appropriate Placement” rules (Townsend and Linnhoff 1983a) offer guidelines for the integration of ABCs into HENs. In general, heat pumps should transfer heat across the pinch in order to be efficient. In the case of ABCs, they behave like reversed heat pumps between the process streams located below and above the “utility pinch”, that is, the pinch generated by the cold utility. As long as the ABC transfer heat across the utility pinch, they will provide cooling without increasing the heat consumption of the system, in practice generating cooling from waste heat. As represented in Figure 3-2, the total cooling demand of the system, does not change due to the integration of the ABC, but the ABC replaces the demand of low temperature cold utility by usually cheaper higher temperature cold utility, using waste heat from the system to drive the refrigeration cycle. Similar to ORCs, the study of the process integration of ABC into HENs was in relative obscurity until Tora and El-Halwagi (2010) presented a PA approach for the integration of ABC into industrial processes.

Tora and El-Halwagi (2010) did not consider the HEN synthesis, but the study presented a systematic approach to evaluate ABC integration opportunities into industrial processes using GCCs. The utility pinch caused by the cold utility (cooling water in their case) was located on the GCC and the required cooling load and cooling temperature to be provided by the ABC was also determined from the GCCs. The available waste heat under the process pinch that could be supplied to the ABC was also calculated. The additional thermal energy required by the ABC

that could not be provided by the process streams, was supplied by solar energy, or the hot utility. A NLP determining the optimal combination of hot utility and solar energy to supply the additional energy required by the ABC was also presented. A fixed COP for the ABC was used and the objective function of the NLP was the TAC of the system.

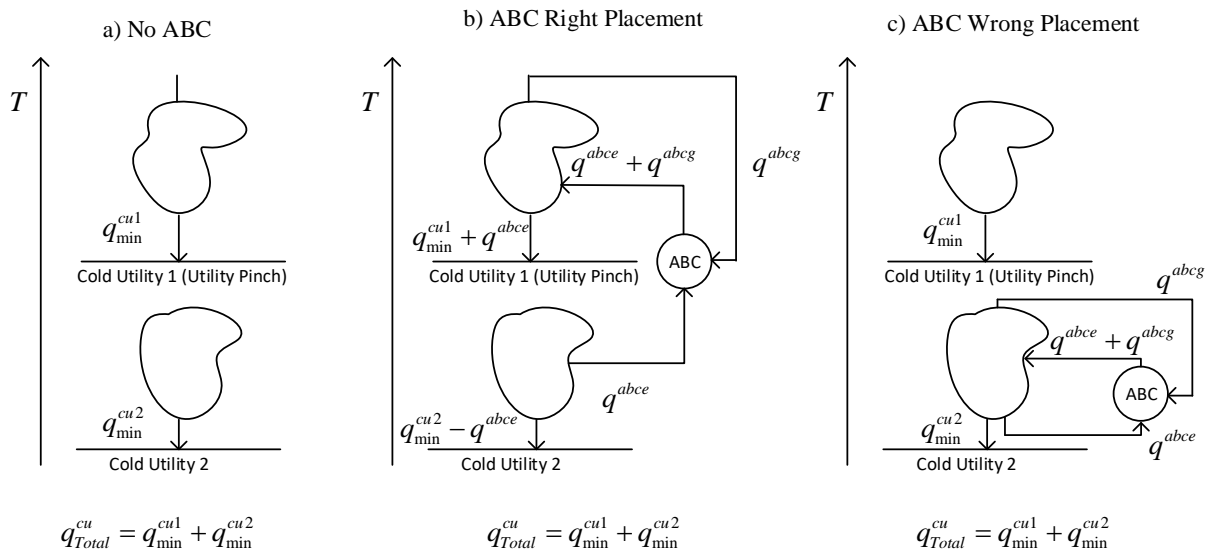


Figure 3-2. Appropriate placement of ABCs driven by waste heat according to pinch analysis.

Source: Own diagram based on Townsend and Linnhoff (1983a) and Tora and El-Halwagi (2010)

The same research group then extended the method to include multiple objectives (TAC and GHGE) in the formulation (Ponce-Ortega et al. 2011). Later, the research group presented a MP approach for the integration of ABCs into HENs (Lira-Barragán et al. 2013), based on the SYNHEAT model for the simultaneous synthesis of HENs. In their superstructure, the ABC could only exchange energy with the process streams in dedicated stages, located at the cold end of the system after the cold utility stage (ABC-Evaporator Stage) and at the hot end of the system between the hot utility stage and the first intra-process stage (ABC-Generator Stage). If the process streams were incapable to provide all the required thermal energy for the ABC, solar collectors and hot utilities could be used to supply the additional energy to the ABC. The COP of the ABC was fixed and the operating conditions of the ABC (refrigeration temperature and the temperature of the energy supplied to the ABC) were defined beforehand. Next, the formulation was extended to include the heat storage design for the solar collectors (Lira-Barragán et al. 2014b).

More recently, Sun et al. (2019) presented a superstructure for the integration of ABC into HEN considering the optimization of the operating conditions of the ABC. Instead of fixed operating conditions, the heat source temperature for the ABC, the refrigeration temperatures produced by the ABC cycle and the COP of the ABC, were treated as variables and fit functions between

the mentioned temperatures and the COP of the ABC were included in the optimization algorithm. The objective function was the TAC. The method was illustrated with a case study and the generated HEN-ABC configuration was compared with a system where a Vapor Compression Refrigeration (VCR) system was used to provide the cooling below the cold utility temperature. Later, the HEN-ABC superstructure was extended to include hybrid Compression-Absorption Cascade Refrigeration Systems (CACRS) (Sun et al. 2020a; Sun et al. 2020b). CACRS are hybrid systems combining ABC and VCR in cascade. The ABC supplies the refrigeration until a temperature of 0°C (the technical limit for the LiBr/H₂O working pair) and the VCR covers the cooling demand below that temperature.

3.3 Process Integration of Organic Rankine Cycles and Absorption Chillers into Heat Exchanger Networks (Combined Models)

Only few studies, all from the same research group, consider the simultaneous integration of ORCs and ABCs into HENs. Lira-Barragán et al. (2014c, 2014a) combined their models for stand-alone integration of ORCs and ABC into HENs into a single model considering the simultaneous integration of both WHR technologies. In their model, a steam Rankine cycle fed by fossil fuels or renewable sources generates mechanical energy and rejects thermal energy in the condenser. This rejected energy is used as hot utility for the process streams in the HEN and provides additional energy to the ORC and the ABC if necessary. The ORC and the ABC are integrated in the HEN and driven by waste heat provided by the process streams or energy take directly from the hot utility, depending on the optimization results. As with the single models for ORC and ABC integration into HENs by the same research group, thermophysical properties of the working fluids and working pairs are not considered. Later the model was extended to consider multiple industrial plants simultaneously (Hipólito-Valencia et al. 2014a).

3.4 Summary of the State-of-the-Art and Overview of Mathematical Framework

A summary of the state-of-the art of the Process Integration of ORCs and ABC into HEN is presented in Table 3-1. Only studies considering simultaneously the HEN synthesis and the integration of the ORCs, ABCs or both into HENs, are presented, as well as the main PA studies in the field. The main conclusion of the literature review is the lack of structured methods for the process integration of ORCs and ABC into HENs in discontinuous processes.

This dissertation is an effort to help to bridge that gap in the literature. Although the pinch rules for integration of ORCs and ABCs into HENs are known since the first years of PA, only in the last decade, studies considering this problematic have been published. This can be related to greater sensibilities about environmental issues and higher energy prices. Also the increase in power and availability of optimization hardware/software has given an impulse into the formulation of MP models with increasing complexity. This dissertation is also the first work on the simultaneous integration of ORC and ABC integration into HENs considering working/fluid properties. An extended table of the State-of-the-Art including other relevant articles in the field and their main contributions is presented in Appendix E.

Table 3-1. Selection of relevant studies on the Process Integration of Organic Rankine Cycles and Absorption Chillers into Heat Exchanger Networks.

	Waste Heat Recovery Technology		Approach		Type of Process		Working Fluid/Pair Properties	
	ORC	ABC	PA	MP		Cont.		Discont.
				SQ	SM			
Chamorro-Romero (2023) *	x	x		x	x	x	x	
Elsido et al. (2021)	x			x		x	x	
Sun et al.; Sun et al. (2020b; 2020a)		x		x	x		x	
Sun et al. (2019)		x		x	x		x	
Kermani et al. (2018)	x			x	x		x	
Elsido et al. (2017)	x			x	x		x	
Yu et al. (2017a)	x			x	x		x	
Chen et al. (2014)	x			x	x		x	
Lira-Barragán et al. (2014c, 2014a)	x	x		x	x			
Hipólito-Valencia et al. (2013)	x			x	x			
Lira-Barragán et al. (2013)		x		x	x			
Tora and El-Halwagi (2010)		x	(x) ²⁾		x			
Desai and Bandyopadhyay (2009)	x		x		x		x	
Townsend and Linnhoff (1983a, 1983b)	x	(x) ¹⁾	x		x			

* This work.

¹⁾ Absorption chillers were not mentioned but general pinch rules for the integration of heat pumps were provided.

²⁾ No HEN synthesis considered. Pinch rules for the integration of ABCs into HEN explicitly presented.

ORC: Organic Rankine Cycle; ABC: Absorption Refrigeration/Chiller; PA: Pinch Analysis; MP: Mathematical Programming; SQ: Sequential Method; SM: Simultaneous Method

Source: Own table

The main contribution of the works referenced in Table 3-1 are the following:

- **Townsend and Linnhoff (1983a, 1983b)** : Pinch rules for the integration of heat engines and heat pumps into industrial processes. Consideration of technical limitations and shapes of heat profiles of working fluids in steam, ORC and Brayton cycles.
- **Desai and Bandyopadhyay (2009)** : First dedicated study on the integration of ORCs into HENs using PA.

-
- **Tora and El-Halwagi (2010)** : First dedicated study on the integration of ABCs into industrial processes using PA. HEN was not generated.
 - **Lira-Barragán et al. (2013)** : First MP formulation for the integration of ABCs into HENs. ABC could be driven by process streams or hot utilities (including solar energy).
 - **Hipólito-Valencia et al. (2013)** : First MP formulation for the integration of ORCs into HENs. Extension of SYNHEAT (Yee and Grossmann, 1990).
 - **Lira-Barragán et al. (2014c, 2014a)** : First MP model for the simultaneous integration of ORCs and ABCs into HENs. Combination of Hipolito-Valencia, et-al (2013) and Lira-Barragan, et-al (2013).
 - **Chen et al. (2014)** : MP model for the integration of ORCs into HENs considering the latent heat of evaporation and thermophysical properties of the working fluids. Properties are calculated independently of the optimization model.
 - **Yu et al. (2017a)** : MP model for the integration of ORCs into HENs including working fluid properties and temperatures into the optimization problem.
 - **Elsido et al. (2017)** : MP model for the integration of ORCs into HENs considering multiple pressure levels for ORC expansion and the use of metaheuristics for the MINLP. Extension of Chen, et-al (2014).
 - **Kermani et al. (2018)** : MP model for the integration of ORCs into HENs including most of the possible ORC configurations (multiple pressure levels, regeneration, superheating, transcritical, etc.)
 - **Sun et al. (2019)** : MP model for the integration of ABCs into HENs considering the working pair properties and temperatures inside of the ABCs.
 - **Sun et al.; Sun et al. (2020b; 2020a)** : MP model for the integration of ABCs into HENs considering hybrid systems combining ABCs and VCRs.
 - **Elsido et al. (2021)**: Extension of Elsido et al. (2017) for multi-period operation. Two tank FTVM heat storages with known temperatures are considered. First work considering the integration of ORCs in HENs with multi-period operation.
 - **Chamorro-Romero (2023) ***: MP framework for the process integration of ORC, ABC or both into HENs into continuous and multi-period processes, while considering working fluid/pair properties. First formulation combining ORC, ABC and HENs while including discontinuous processes (multi-period with and without FTVM heat storage). Storage sizes and temperatures are part of the optimization variables and multiple storage levels (more than 2 storage tanks) are considered.

In this work a total of nine superstructures are developed, grouped in three categories, each of them related to the specific objectives presented in section 1.2 and depending on the type of process they are referring to (continuous processes, multi-period processes without heat storage and multi-period processes with Fixed Temperature Variable Mass [FTVM] heat storage). Each category consists of three individual models: one model describing the process integration of stand-alone ORCs, one model describing the process integration of stand-alone ABCs and a combined model for the process integration of both waste heat recovery (WHR) technologies simultaneously.

The mathematical framework developed in this dissertation is a mathematical programming approach for the integration of selected waste heat recovery technologies (ORC and ABC) into heat exchanger networks for continuous and multi-period processes with and without FTVM heat storage. The assumptions used for the mathematical framework are presented in detail in Section 1.3. The following chapter (Chapter 4) presents a complete description of the framework and in Chapter 5 the application of the framework is illustrated using examples from the literature.

4 Mathematical Framework

This chapter presents the superstructures developed for the process integration of organic Rankine cycles (ORC), absorption chillers (ABC) or both, into heat exchanger networks (HEN) for continuous and multi-period processes with and without FTVM heat storage, including the mathematical models describing the behavior of the systems. Section 4.1 introduces the methodology and general considerations and assumptions applicable to all models. Section 4.2 presents the detail description of each of the developed models, their constituting equations and their particularities. Finally, section 4.3 discusses the mathematical considerations and limitations of each of the models.

4.1 Methodology and General Assumptions

In this work a total of nine superstructures are developed, grouped in three categories, each of them related to the specific objectives presented in section 1.2 and depending on the type of process they are referring to (continuous processes, multi-period processes without heat storage and multi-period processes with Fixed Temperature Variable Mass [FTVM] heat storage). Each category consists of three individual models: one model describing the process integration of stand-alone ORCs, one model describing the process integration of stand-alone ABCs and a combined model for the process integration of both waste heat recovery (WHR) technologies simultaneously. Each of the individual models is named using short acronyms for their easy identification. The categories, models and acronyms are as follows:

- Superstructures for continuous processes
 - Process Integration of Organic Rankine Cycles (HEN-ORC)
 - Process Integration of Absorption Chillers (HEN-ABC)
 - Combined Model (HEN-WHR)
- Superstructures for multi-period processes without heat storage
 - Process Integration of Organic Rankine Cycles (MP-ORC)
 - Process Integration of Absorption Chillers (MP-ABC)
 - Combined Model (MP-WHR)
- Superstructures for multi-period processes with FTVM heat storage
 - Process Integration of Organic Rankine Cycles (MP-ST-ORC)
 - Process Integration of Absorption Chillers (MP-ST-ABC)
 - Combined Model (MP-ST-WHR)

Figure 4-1 illustrates the different models developed and their relation with the specific objectives presented in section 1.2.

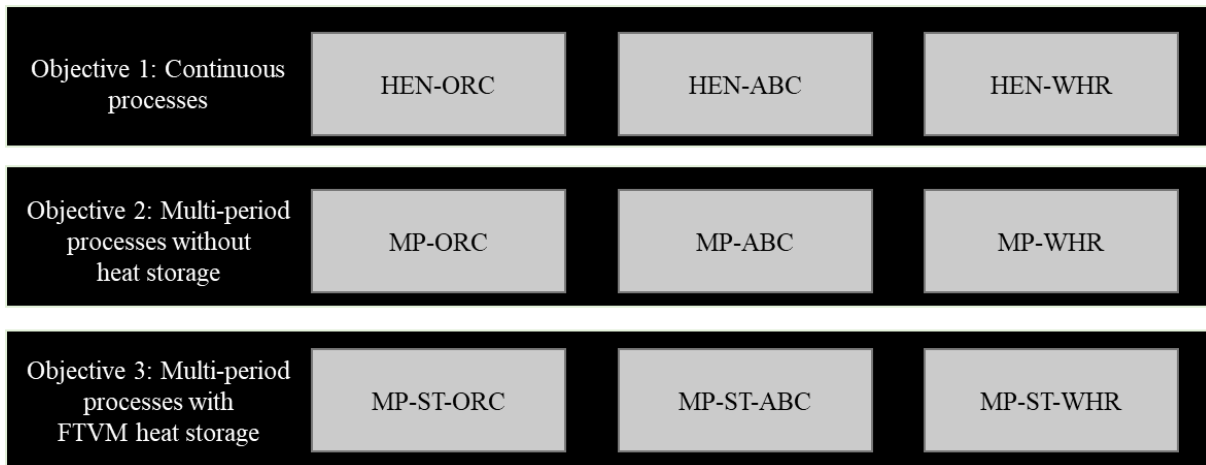


Figure 4-1. Overview of the superstructures developed in this dissertation.

Source: Own diagram

The assumptions used for the development of the nine superstructures for the process integration of ORCs, ABCs or both into HENs in continuous and multi-period processes, with and without FTVM heat storage, were already presented in section 1.3 and they were used to establish the scope of the research. Please see Section 1.3 for more information.

In the following sections, a description of the nine superstructures developed in this work is presented. As many of the modes share similar equations and terms, in the descriptions only the new equations related to each model are presented. A complete presentation of all the constituent equations for each model is provided in Appendix C.

4.2 Model Formulations

All the mathematical models developed for the process integration of WHR technologies into HENs have a similar structure. A common feature of all models is the use of energy balances and logical conditions for temperatures and heat transfer duties. Table 4-1 presents a generic depiction of the structure of the common equations used in the models. As illustrated in Table 4-1, all models contain overall energy balances for the process streams, stage energy balances for each stage in the superstructure, including utility and dedicated stages (ORC Stage, ABC-Evaporator Stage and ABC-Condenser Stage), logical relations and conditions for the temperatures of the process streams guaranteeing the feasibility of the energy transfer at different locations in the superstructure, upper limits for the heat transfer duties of each of the possible heat exchangers, equations calculating the approach temperatures at the hot and cold

ends of each possible heat exchanger in the superstructure and the objective function, in this work the “Total Annualized Cost” (TAC). Additional constraints for the models such as restricted matches, maximum number of units, etc. can also be added but are not part of the main formulation. The specific terms used in each equation, change depending on the model used. Models for ORC integration have to include terms related to the ORC-Evaporators and ORC-Condensers, as well as terms describing the behavior of ORC-Pumps and ORC-Turbines. Similarly, models including ABC integration have to contain terms describing the behavior ABC-Generators, ABC-Evaporators and the central ABC-Condenser and ABC-Absorber.

Table 4-1. Generic depiction of common equations for all superstructures for the Process Integration of Waste Heat Recovery Technologies

Overall energy balances	$\left\{ \begin{array}{l} \sum_{j \in CP} \sum_{k \in ST} q_{i,j,k} + q_i^{evap} + q_i^{cu} = F_i(T_i^{in} - T_i^{out}) \\ \dots \\ \dots \end{array} \right\}$
Stage energy balances	$\left\{ \begin{array}{l} \sum_{j \in CP} q_{i,j,k} = F_i(t_{i,k} - t_{i,k+1}) \\ \dots \\ \dots \end{array} \right\}$
Logical relations of temperatures (Process Streams)	$\left\{ \begin{array}{l} t_{i,NOK+1} \geq t_i^{orc} \geq T_i^{out} \\ \dots \\ \dots \end{array} \right\}$
Upper limits for heat exchangers duties	$\left\{ \begin{array}{l} q_{i,j,k} - \Omega z_{i,j,k} \leq 0 \\ \dots \\ \dots \end{array} \right\}$
Approach temperatures for hot and cold ends of heat exchangers	$\left\{ \begin{array}{l} \Delta T_{min} \leq dt1_{i,j,k} \leq t_{i,k} - t_{j,k} + \Gamma(1 - z_{i,j,k}) \\ \Delta T_{min} \leq dt2_{i,j,k} \leq t_{i,k+1} - t_{j,k+1} + \Gamma(1 - z_{i,j,k}) \\ \dots \\ \dots \end{array} \right\}$
Objective Function	$\{min TAC = CAPEX + OPEX\}$
Additional constraints (Optional)	$\left\{ \begin{array}{l} \sum_{j \in CP} q_j^{hu} \leq \sum_{j \in CP} q_j^{hu} (HEN) \\ \dots \\ \dots \end{array} \right\}$

Source: Own table

Aside from the common equations used in all models, specific equations depending on the WHR technologies considered (ORCs, ABCs or both), as well as the type of process (continuous or multi-period with and without heat storage) have to be included. Table 4-2 presents a generic representation of the additional equations required depending on the technologies considered. As illustrated in Table 4-2, models considering ORC integration have

to include additional mass balances for the working fluid split streams in evaporators and condensers, energy balances for pumps and turbines and calculations for approach temperatures inside of the evaporators and condensers due to the phase changes of the working fluid. As for models considering ABC integration, definitions for important parameters in the system such as the “Coefficient of Performance” (COP) of the refrigeration system and the ratio between the energy extracted in the central ABC-Condenser and the energy supplied in the ABC-Generators (in this work referred as C2G) have to be provided, as well as additional fit functions describing the physical behavior of the ABC and an overall energy balance of the absorption refrigeration cycle. As for the fit functions, they include expressions calculating COP, C2G as function of the temperatures in the system, as well as expressions for temperatures of the refrigerant solution and the refrigerant inside of the absorption cycle.

Table 4-2. *Generic depiction of specific equations for the Process Integration of Waste Heat Recovery Technologies depending on the technologies considered.*

	Mass balances stream splits	$\left\{ \begin{array}{l} \sum_{i \in HP} r_{wi} = 1 \\ \dots \\ \dots \end{array} \right\}$
ORC	Energy balances turbines/pumps	$\left\{ \begin{array}{l} W_{pump} = \dot{m}_w W_{pump} \\ \dots \\ \dots \end{array} \right\}$
	Approach temperatures evaporation/condensation	$\left\{ \begin{array}{l} \Delta T_{min} \leq dt z_i^{evap} \leq \left(t_i^{orc} + \frac{\dot{m}_w r_{wi} c_{p_{w(l)}} (T_{evap}^{out} - T_{evap}^{in})}{F_i} \right) \\ -T_{evap}^{out} + \Gamma(1 - z_i^{evap}) \\ \dots \\ \dots \end{array} \right\}$
	Definitions COP/C2G	$\left\{ \begin{array}{l} COP = \frac{\sum_{i \in HP} q_i^{abce}}{\sum_{i \in HP} q_i^{abcg}} \\ \dots \\ \dots \end{array} \right\}$
ABC	Energy balance ABC-System	$\left\{ \begin{array}{l} \sum_{i \in HP} q_i^{abcg} + \sum_{i \in HP} q_i^{abce} = q^{abcc} + q^{abca} \\ \dots \\ \dots \end{array} \right\}$
	Fit functions	$\left\{ \begin{array}{l} COP = C_1 e^{C_2 t_{gen}} + C_3 e^{C_4 t_{gen}} \\ \dots \\ \dots \end{array} \right\}$

Source: *Own table*

As for models for multi-period processes, the general equations presented in Table 4-1, as well as specific equations depending on the technology presented in Table 4-2, are also used, but they are repeated for each period of operation. That means that overall energy balances, stage energy balances, logical constraints, etc., have to be represented for each period. Most of the terms in the equations have to be also written as multi-period terms, namely, temperatures for the process streams and heat transfer duties for the heat exchangers, as they change from period to period. On the other hand, the binary terms, the temperatures and properties of the working fluid inside the ORC and the temperatures, COP and C2G of the refrigeration cycle remain independent of the periods, that is, they do not change from period to period.

Additionally, equations calculating the effective size of the components in the system (heat exchangers, turbines and pumps), to be used in cost calculations, are necessary. The effective size for a given component is the maximum size between the required sizes for the given component if each period is considered as an independent system at continuous operation. This effective size guarantees that the given component is able to perform its duty in all periods of operation (see Section 1.3). Table 4-3 presents a generic representation of these “Maximum Size” equations.

Table 4-3. *Generic depiction of "Maximum Size" equations for the Process Integration of Waste Heat Recovery Technologies into Multi-Period Processes*

Maximum size of components	$\left\{ \begin{array}{l} A_{i,j,k} \geq \frac{q_{i,j,k,p}}{U_{i,j,p} LMTD_{i,j,k,p}} \\ \dots \\ \dots \end{array} \right\}$
----------------------------	---

Source: *Own table*

In the case of multi-period processes with heat storage, additional terms have to be included into the energy balances presented in Table 4-1 in order to represent the energy exchanged between the storage system and the process streams at each period of operation. In this work, only “Fixed Temperature Variable Mass” (FTVM) storage tanks are considered. Also, extra equations describing the behavior of the storage system have to be included. Table 4-4 presents a generic representation of the additional equations required for the storage system. These equations consist of energy balances for the storage streams, equations describing the energy accumulated in the storage tanks at the end of each period, equations for the sizes of the storage tanks as well as logical conditions and relations for the hot and cold storages.

In the following sections, a detail description of the superstructures and their constituent equations is presented. The models are formulated as “Mixed Integer Non Linear Programming” (MINLP) problems, where the binary variables represent the existence of a

certain component at a certain stage of the superstructure and continuous variables are used to describe the operational conditions of the system (temperatures, mass flows, heat flows and equipment sizes).

Table 4-4. Generic depiction of equations for the Process Integration of Fixed Temperature Variable Mass (FTVM) Storage Systems

Energy balances	$\left\{ \begin{array}{l} q_{p,lv}^{charh} = \sum_{i \in HHP} \sum_{k \in ST} q_{i,k,p,lv}^{stoc} \\ \dots \\ \dots \end{array} \right\}$
Accumulated energy in tanks	$\left\{ \begin{array}{l} Q_{p,lv}^h = Q_{p-1,lv}^h + DOP_p \left((q_{p,lv}^{charh} - q_{p,lv}^{discharh}) + (q_{p,lv-1}^{charc} - q_{p,lv-1}^{discharc}) \right) \\ \dots \\ \dots \end{array} \right\}$
Maximum size	$\left\{ \begin{array}{l} \max\{Q_{p,lv}^h\} \geq Q_{p,lv}^h \\ \dots \\ \dots \end{array} \right\}$
Logical relations	$\left\{ \begin{array}{l} T_{lv}^{sth} = T_{lv-1}^{stc} \\ \dots \\ \dots \end{array} \right\}$

Source: Own table

4.2.1 Continuous Processes

4.2.1.1 Organic Rankine Cycles (HEN-ORC)

A schematic representation of the superstructure for the process integration of ORCs into HENs in continuous processes (HEN-ORC) is depicted in Figure 4-2. Not all possible matches between the process streams are included (e.g., streams splits, etc.). Also for clarity, only two hot and two cold process streams are presented, but the superstructure and its associated mathematical model are suitable for any arbitrary number of process streams.

The heat exchange between process streams takes place in the inner stages of the superstructure, also known as “Intra-Process Stages” in Figure 4-2. The heat exchange between the process streams and the ORC takes place only in the “ORC Stage”, located at the cold end of the process streams after the last intra-process stage. In the dedicated ORC stage the hot process streams exchange heat with the dry working fluid circulating in the evaporators of the ORC. The working fluid at the evaporation pressure, leaves the stage as a saturated vapor and is mixed isothermally before being expanded in the turbine. The expanded working fluid exits the turbine at the condensation pressure in a superheated stage and is cooled in the condensers by means of heat exchange with the cold process streams in the dedicated ORC stage or through heat

release to the cold utility. The working fluid leaves the stage as a saturated liquid at the condensation pressure and is again isothermally mixed before being pumped back to the evaporation pressure to restart the cycle. At the hot and cold ends of the superstructure in the “Hot and Cold Utility Stages”, utilities are used to provide or remove the remaining energy required to achieve the target temperatures of the process streams. Similar to the SYNHEAT model, in HEN-ORC the number of intra-process stages is decided beforehand and it is recommended to be greater or equal to the number of hot or cold process streams (Yee and Grossmann 1990), although in most cases, less stages will also provide viable designs.

As explained in section 4.2, the structure of the mathematical model for HEN-ORC is a combination of common equations used for all models, as presented in Table 4-1, and specific equations due to the integration of the ORC, as presented in Table 4-2. Equations (4-1) to (4-9) present the energy balances for the process streams and stages as mentioned in Table 4-1. In this formulation, equations (4-1) and (4-2) represent the overall energy balances for the hot and cold process streams $i \in HP$ and $j \in CP$. For the hot streams, the overall change in enthalpy ($F_i(T_i^{in} - T_i^{out})$) is equal to the sum of the energy exchanged with the cold streams at the intra-process stages of the superstructure ($q_{i,j,k}$), the energy transferred to the ORC through the evaporators located in the ORC stage at the cold end of the hot process stream (q_i^{evap}), and the energy rejected to the cold utility in the cold utility stage (q_i^{cu}). Similarly for the cold process streams, the overall enthalpy change ($F_j(T_j^{out} - T_j^{in})$) equals the sum of the energy exchanged with the hot streams at the intra-process stages of the superstructure ($q_{i,j,k}$), the energy rejected by the ORC system into the cold streams as heating in the ORC stage (q_j^{cond}) and the energy provided to the cold process stream by the hot utility in the hot utility stage (q_j^{hu}).

$$\sum_{j \in CP} \sum_{k \in ST} q_{i,j,k} + q_i^{evap} + q_i^{cu} = F_i(T_i^{in} - T_i^{out}) \quad (4-1)$$

$$\sum_{i \in HP} \sum_{k \in ST} q_{i,j,k} + q_j^{cond} + q_j^{hu} = F_j(T_j^{out} - T_j^{in}) \quad (4-2)$$

Equations (4-3) and (4-4) denote the energy balances for the intra-process stages. In the case of the hot process streams, the energy transferred by a hot process stream $i \in HP$ at a given stage $k \in ST$, equals the sum of the heat ($q_{i,j,k}$) exchanged between the hot stream and each of the cold process streams $j \in CP$. The enthalpy change in the hot process stream in that stage is equivalent to the product of the heat capacity flowrate of the stream (F_i) and the temperatures of the stream at the inlet ($t_{i,k}$) and outlet ($t_{i,k+1}$) of the stage. An analog equation is used to calculate the stage energy balances for the cold process streams.

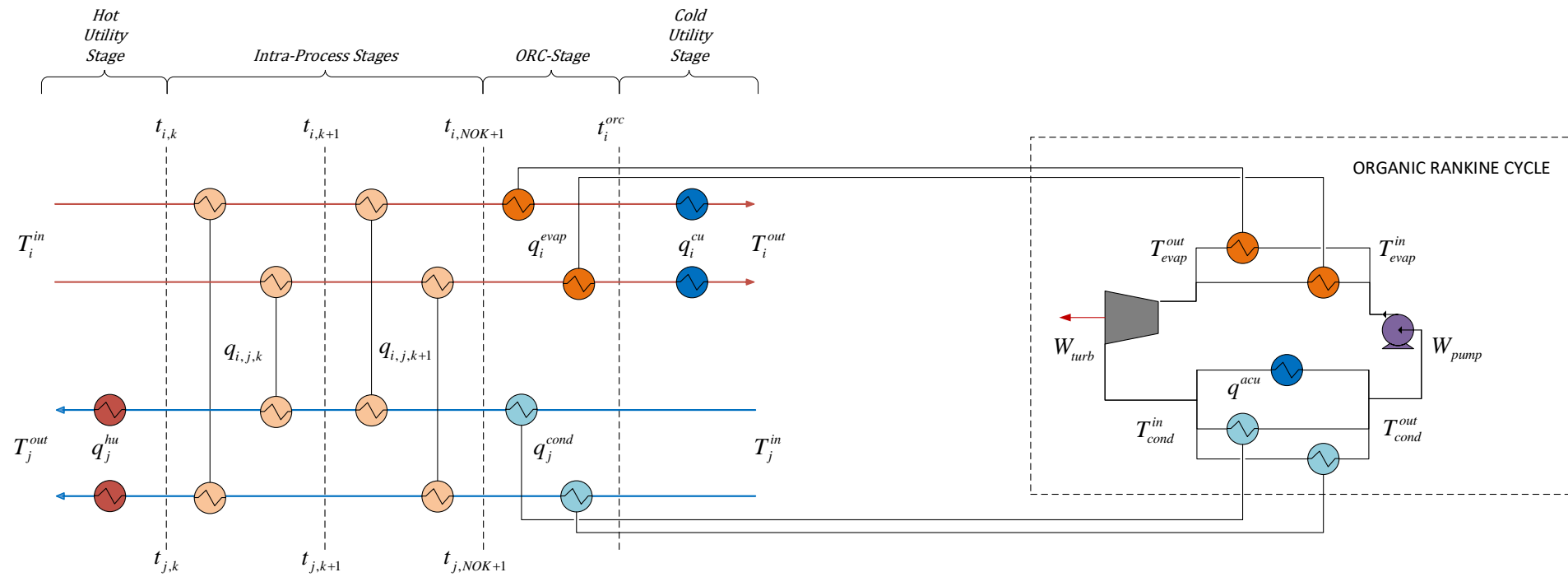


Figure 4-2. Schematic representation of the Superstructure for the Process Integration of Organic Rankine Cycles into Continuous Processes (HEN-ORC).

Source Own diagram.

$$\sum_{j \in CP} q_{i,j,k} = F_i(t_{i,k} - t_{i,k+1}) \quad (4-3)$$

$$\sum_{i \in HP} q_{i,j,k} = F_j(t_{j,k} - t_{j,k+1}) \quad (4-4)$$

Equations (4-5) and (4-6) show individual energy balances for the heat exchangers between the process streams and the utilities located in the hot and cold utility stages. In the case of the hot process streams $i \in HP$, t_i^{orc} denotes the temperature of the hot process stream after leaving the evaporator, that is, after exchanging energy with the ORC system. For the cold process streams $j \in CP$, $t_{j,1}$ denotes the temperature of the cold process stream at the first stage of the superstructure.

$$q_i^{cu} = F_i(t_i^{orc} - T_i^{out}) \quad (4-5)$$

$$q_j^{hu} = F_j(T_j^{out} - t_{j,1}) \quad (4-6)$$

Energy balances for the exchangers located in the ORC stage between the ORC working fluid, the hot process streams $i \in HP$ (evaporators) and the cold process streams $j \in CP$ (condensers) are also illustrated in equations (4-7) and (4-8). At each of the evaporators, a split fraction (r_{w_i}) of the total mass flowrate of the working fluid (\dot{m}_w), goes from a subcooled liquid state at the exit of the pump at the evaporation pressure (P_{evap}) and temperature T_{evap}^{in} to a saturated vapor at the same pressure and temperature T_{evap}^{out} , higher than T_{evap}^{in} . The average heat capacity of the working fluid at the liquid state until reaching the evaporation temperature ($cp_{w(l)}$), as well as the latent heat of vaporization at the evaporator pressure λ_{evap} are calculated separately using equations of state or extracted from properties databases. Likewise at each of the condensers, a split fraction (r_{w_j}) of the total mass flowrate of the working fluid (\dot{m}_w), goes from a superheated vapor state at the exit of the turbine at the condensation pressure (P_{cond}) and temperature T_{cond}^{in} to a saturated liquid at the same pressure and temperature T_{cond}^{out} , lower than T_{cond}^{in} . Similar to the evaporation process, the average heat capacity of the working fluid at the gas state until reaching the condensation temperature ($cp_{w(g)}$), as well as the latent heat of vaporization at the condenser pressure (λ_{cond}) are calculated separately using equations of state or extracted from properties databases. If necessary, the rest of the working fluid ($1 - \sum_{j \in CP} r_{w_j}$) is condensed at a dedicated exchanger which rejects excess energy to the cold utility, as illustrated in equation (4-9).

$$q_i^{evap} = F_i(t_{i,NOK+1} - t_i^{orc}) = \dot{m}_w r_{w_i} (cp_{w(l)}(T_{evap}^{out} - T_{evap}^{in}) + \lambda_{evap}) \quad (4-7)$$

$$q_j^{cond} = F_j(t_{j,NOK+1} - T_j^{in}) = \dot{m}_w r_{wj} (cp_{w(g)}(T_{cond}^{in} - T_{cond}^{out}) + \lambda_{cond}) \quad (4-8)$$

$$q^{acu} = \dot{m}_w \left(1 - \sum_{j \in CP} r_{wj} \right) (cp_{w(g)}(T_{cond}^{in} - T_{cond}^{out}) + \lambda_{cond}) \quad (4-9)$$

Next, and as presented in Table 4-1, logical conditions for the temperatures in the formulation are provided to guarantee the non-negativity of the heat exchanger duties calculated in equations (4-3) to (4-8). Equations (4-10) and (4-11) assign logical relations to the temperatures at the hot and cold ends of the hot process streams $i \in HP$. Equation (4-10) indicates that the temperature at the first intra-process stage ($t_{i,1}$) equals to the initial temperature of the stream (T_i^{in}). Equation (4-11) describes the logical relations between the temperatures at the cold end of the superstructure. The temperature at the last intra-process stage ($t_{i,NOK+1}$) should be greater or equal to the temperature of the stream after the ORC stage (t_i^{orc}), which likewise should be greater or equal to the target temperature of the process stream (T_i^{out}). Similarly, equations (4-12) and (4-13) assign logical relations to the temperatures at the hot and cold ends of the cold process streams $j \in CP$. In the hot end, equation (4-12) indicates that the target temperature of the stream (T_j^{in}) is greater or equal to the temperature at the first intra-process stage ($t_{j,1}$). Equation (4-13) establishes that in the cold end, the temperature at the last intra-process stage ($t_{j,NOK+1}$) should be greater or equal to the initial temperature of the cold process stream (T_j^{in}). Equations (4-14) and (4-15) describe the monotonic decrease of the temperatures of the hot and cold process streams $i \in HP$ and $j \in CP$ at each subsequent intra-process stage $k \in ST$, starting on the hot end of the model (left hand side in Figure 4-2).

$$T_i^{in} = t_{i,1} \quad (4-10)$$

$$t_{i,NOK+1} \geq t_i^{orc} \geq T_i^{out} \quad (4-11)$$

$$T_j^{out} \geq t_{j,1} \quad (4-12)$$

$$t_{j,NOK+1} \geq T_j^{in} \quad (4-13)$$

$$t_{i,k} \geq t_{i,k+1} \quad (4-14)$$

$$t_{j,k} \geq t_{j,k+1} \quad (4-15)$$

Equation (4-16) provides a generic expression for upper limits (Ω) to the heat transfer duties (q_*^\dagger) of all possible heat exchangers in the superstructure, as represented in Figure 4-2. In this expression, the binary variables (z_*^\dagger) represent the existence of the different heat exchanger units. The optimization process will decide which process units exist in the final design

depending on the objective function. Similarly, equations (4-17) and (4-18) calculate the approach temperatures at the hot and cold ends ($dt1_*^\dagger$ and $dt2_*^\dagger$) of each possible heat exchanger in the superstructure, relaxing the temperature constraints if there are no heat exchangers between the streams at the given location, and providing lower (ΔT_{min}) and upper (Γ) limits to the allowed temperature differences in the system.

In general, equations (4-16) to (4-18) are “Big-M” formulations, that is equations or constrains that are “turned on” or “turned off” depending on the value of a binary variable (z_*^\dagger). Big-M formulations are easy to implement but can lead to numerical instabilities and the performance of many of the available solvers for MILP and MINLP problems is heavily affected by the selection of suitable M values (Ω and Γ in equations (4-16) to (4-18)). From a mathematical point of view, any value of M large enough to guarantee that the constrains are active (or inactive) when $z_*^\dagger = 1$ (or $z_*^\dagger = 0$), is a suitable candidate for M, but M values that are “too big”, have a negative impact on the performance of the optimization solvers (Bonami et al. 2015). In the literature on HEN synthesis, the M values are usually defined as the “maximum possible values” for the variables in the constrains that make physical sense, that is the upper limits for the heat transfer duties values (Ω) and approach temperatures in the heat exchanger (Γ) in equations (4-16) to (4-18)), but this is a rather arbitrary choice.

Table 4-5 presents all the possible heat exchangers in the superstructures for the process integration of ORCs, ABCs or both into HENs in continuous processes (HEN-ORC, HEN-ABC and HEN-WHR) and the symbols for their heat exchanger duties, the binary variables representing their existence and the corresponding temperature differences at the hot and cold ends ($\Delta T_{Hot-End}$ and $\Delta T_{Cold-End}$) of the heat exchangers.

$$q_*^\dagger - \Omega z_*^\dagger \leq 0 \quad (4-16)$$

$$\Delta T_{min} \leq dt1_*^\dagger \leq \Delta T_{Hot-End} + \Gamma(1 - z_*^\dagger) \quad (4-17)$$

$$\Delta T_{min} \leq dt2_*^\dagger \leq \Delta T_{Cold-End} + \Gamma(1 - z_*^\dagger) \quad (4-18)$$

As mentioned in Table 4-2, due to the ORC integration, additional mass balances for the working fluid split streams in the ORC-Evaporators and ORC-Condensers should be considered. Equation (4-19) illustrates that the entire working fluid is evaporated through heat exchange with the hot process streams and the inequality in expression (4-20) indicates that part of the working fluid can condense releasing energy to the cold utility instead of exchanging heat with the cold process streams.

$$\sum_{i \in HP} r_{wi} = 1 \quad (4-19)$$

$$\sum_{j \in CP} r_{wj} \leq 1 \quad (4-20)$$

Additional equations are also required for the evaporators and condensers to guarantee that the approach temperature constraints are maintained inside of the process units during the phase change of the working fluid. Equations (4-21) and (4-22) calculate the minimum approach temperature inside of the evaporators and condensers during the phase change.

$$\Delta T_{min} \leq dt3_i^{evap} \leq \left(t_i^{orc} + \frac{\dot{m}_w r_{wi} c_{p_{w(l)}} (T_{evap}^{out} - T_{evap}^{in})}{F_i} \right) - T_{evap}^{out} + \Gamma(1 - z_i^{evap}) \quad (4-21)$$

$$\Delta T_{min} \leq dt3_j^{cond} \leq T_{cond}^{out} - \left(t_{j,NOK+1} - \frac{\dot{m}_w r_{wj} c_{p_{w(g)}} (T_{cond}^{in} - T_{cond}^{out})}{F_j} \right) + \Gamma(1 - z_j^{cond}) \quad (4-22)$$

Other specific equations required due to the ORC integration (Table 4-2) include the equations for the work generated by the turbine and required by the pump. They are calculated as the product of the mass flow of working fluid (\dot{m}_w) and the specific work required or generated per mass unit (w_{pump} and w_{turb} for the pump and turbine respectively). Equations (4-23) and (4-24) describe these relations. The specific work of turbines and pumps is calculated separately from the optimization model, as the difference between the specific enthalpies of the working fluid before and after the turbines and pumps, respectively. An extended discussion on the calculations of the thermophysical properties of the working fluids, as well as an exemplary calculation of the specific enthalpies of the working fluid at different locations in the ORC cycle including the calculation of the specific work of turbines and pumps is found in Appendix B.

$$W_{pump} = \dot{m}_w w_{pump} \quad (4-23)$$

$$W_{turb} = \dot{m}_w w_{turb} \quad (4-24)$$

For the HEN-ORC model, the objective function is the minimization of the ‘‘Total Annualized Cost’’ (TAC) of the system, which is equal to the sum of the TAC of the subsystems (HEN and ORC) as defined in equations (4-25) to (4-27). The TAC of the ORC includes the revenues due to the sale of the net electricity generated as presented in equation (4-27). In this expressions H_y indicates the hours of operation per year, e_{price} and e_{cost} the price and for the net electricity generated and consumed by the system, c_{cu} and c_{hu} the unitary costs for the cold and hot utilities, c_{fix}^{HEN} and c_{var}^{HEN} the fixed and variable cost factors for the heat exchanger units, U_*^\dagger the overall heat transfer coefficients for the heat exchangers in the superstructure and $LMTD_*^\dagger$ the

“Logarithmic Mean Temperature Differences” between the streams at a given location. An extended discussion about the $LMTD$ can be found in section 4.3. Also in the expression, c_{fix}^{turb} , c_{fix}^{pump} and c_{var}^{turb} , c_{var}^{pump} represent the fixed and variable cost factors for turbines and pumps, β^{HEN} , β^{pump} and β^{turb} the cost exponents associated to the variable costs of heat exchangers, pumps and turbines, respectively and AF the annualization factor for the equipment costs.

$$\min TAC = TAC_{HEN} + TAC_{ORC} \quad (4-25)$$

$$TAC_{HEN} = \left\{ \begin{array}{l} H_y \sum_{i \in HHP} c_{cu} q_i^{cu} + H_y \sum_{j \in CCP} c_{hu} q_j^{hu} \\ + AF \left(c_{fix}^{HEN} \left(\sum_{i \in HHP} \sum_{j \in CCP} \sum_{k \in EST} z_{i,j,k} + \sum_{i \in HHP} z_i^{cu} + \sum_{j \in CCP} z_j^{hu} \right) \right) \\ + AF \left(c_{var}^{HEN} \left(\sum_{i \in HHP} \sum_{j \in CCP} \sum_{k \in EST} \left(\frac{q_{i,j,k}}{U_{i,j,k} LMTD_{i,j,k}} \right)^{\beta^{HEN}} \right) \right) \\ \left. + \sum_{i \in HHP} \left(\frac{q_i^{cu}}{U_i^{cu} LMTD_i^{cu}} \right)^{\beta^{HEN}} + \sum_{j \in CCP} \left(\frac{q_j^{hu}}{U_j^{hu} LMTD_j^{hu}} \right)^{\beta^{HEN}} \right) \end{array} \right\} \quad (4-26)$$

$$TAC_{ORC} = \left\{ \begin{array}{l} -H_y e_{price} W_{turb} + H_y e_{cost} W_{pump} \\ + AF \left(c_{fix}^{HEN} \left(\sum_{i \in HHP} z_i^{evap} + \sum_{j \in CCP} z_j^{cond} + z^{acu} \right) \right) \\ + AF \left(c_{var}^{HEN} \left(\sum_{i \in HHP} \left(\frac{q_i^{evap}}{U_i^{evap} LMTD_i^{evap}} \right)^{\beta^{HEN}} \right) \right) \\ \left. + \sum_{j \in CCP} \left(\frac{q_j^{cond}}{U_j^{cond} LMTD_j^{cond}} \right)^{\beta^{HEN}} + \left(\frac{q^{acu}}{U^{acu} LMTD^{acu}} \right)^{\beta^{HEN}} \right) \\ + AF \left(c_{fix}^{turb} + c_{fix}^{pump} \right) + AF \left(c_{var}^{turb} W_{turb}^{\beta^{turb}} + c_{var}^{pump} W_{pump}^{\beta^{pump}} \right) \end{array} \right\} \quad (4-27)$$

4.2.1.2 Absorption Chillers (HEN-ABC)

A schematic representation of the superstructure for the process integration of ABCs into HENs in continuous processes (HEN-ABC) is depicted in Figure 4-3. Not all possible matches between the process streams are included (e.g., streams splits, etc.). Also for clarity, only two hot and two cold process streams are presented, but the superstructure and its associated mathematical model are suitable for any arbitrary number of process streams. The heat exchange between process streams takes place in the inner stages of the superstructure. Hot and

cold utilities located at their dedicated stages at the hot and cold ends of the superstructure can also provide/remove energy to/from the process streams. The heat exchange between the process streams and the fluids circulating in the ABC (“Refrigerant” and “Refrigerant Solution”) takes place in two dedicated stages located at the cold end of the hot process streams, one before and one after the cold utility stage. In the first dedicated stage, located between the cold utility and the last stage of intra-process energy exchange, the hot process streams exchange energy with the generators of the ABC. The energy from the hot process streams is used in the generators of the ABC, to evaporate the refrigerant and separate it from the weak refrigerant solution coming from the absorber. The refrigerant in gaseous state coming from the generators mixes isothermally and flows to one central condenser where it releases heat to the cold utility leaving the unit as a saturated liquid. The liquid refrigerant circulates through an expansion valve, reducing its pressure and decreasing its temperature. The cooled refrigerant flows to the evaporators where it exchanges heat with the hot process streams in the second dedicated stage, located after the cold utility stage at the cold end of the superstructure, providing cooling to the streams. The refrigerant leaving the evaporators as a saturated gas is again mixed isothermally and returns to one central absorber where it is mixed with the strong solution returning from the generators to be cooled down using the cold utility. Finally, the solution is pumped back to the generator to restart the cycle. An additional heat exchanger is used to recover heat from the strong solution returning to the absorber and preheat the weak solution flowing to the generator.

As with HEN-ORC, the structure of the mathematical model for HEN-ABC is a combination of common equations used for all models, presented in Table 4-1, and specific equations due to the integration of the ABC, presented in Table 4-2. Equations (4-28) to (4-35) present the energy balances for the process streams and stages as mentioned in Table 4-1. Equations (4-28) and (4-29) represent overall energy balances for the hot and cold process streams $i \in HP$ and $j \in CP$. Hot process streams exchange heat with cold process streams ($q_{i,j,k}$) and the cold utility (q_i^{cu}), with additional terms representing the heat exchange with the ABC at the ABC-Generator (q_i^{abcg}) and ABC-Evaporator (q_i^{abce}) stages. Cold process streams exchange heat only with hot process streams ($q_{i,j,k}$) or with the hot utility (q_j^{hu}).

$$\sum_{j \in CP} \sum_{k \in ST} q_{i,j,k} + q_i^{abcg} + q_i^{cu} + q_i^{abce} = F_i(T_i^{in} - T_i^{out}) \quad (4-28)$$

$$\sum_{i \in HP} \sum_{k \in ST} q_{i,j,k} + q_j^{hu} = F_j(T_j^{out} - T_j^{in}) \quad (4-29)$$

The energy balances for the inner stages of the superstructure, where only intra-process energy exchange occurs, are similar to those of the HEN-ORC model and are described by equations (4-30) and (4-31).

$$\sum_{j \in CP} q_{i,j,k} = F_i(t_{i,k} - t_{i,k+1}) \quad (4-30)$$

$$\sum_{i \in HP} q_{i,j,k} = F_j(t_{j,k} - t_{j,k+1}) \quad (4-31)$$

Equations (4-32) and (4-33) illustrate the energy balances for the utilities. For the cold utilities, t_i^{abcg} represents the temperature of the hot process stream $i \in HP$ after the energy exchange with the ABC-Generators, and t_i^{abce} the temperature of the hot process stream $i \in HP$ before the energy exchange with the ABC-Evaporators. In the case of the hot utilities, the energy balance is similar to the balance in the HEN-ORC model.

$$q_i^{cu} = F_i(t_i^{abcg} - t_i^{abce}) \quad (4-32)$$

$$q_j^{hu} = F_j(T_j^{out} - t_{j,1}) \quad (4-33)$$

Equations (4-34) and (4-35) describe the energy balances for ABC-Generator and ABC-Evaporator stages.

$$q_i^{abcg} = F_i(t_{i,NOK+1} - t_i^{abcg}) \quad (4-34)$$

$$q_i^{abce} = F_i(t_i^{abce} - T_i^{out}) \quad (4-35)$$

Similar to HEN-ORC, logical conditions for the temperatures in the superstructure are provided. Equations (4-36) to (4-41) assign temperatures for the hot and cold process streams $i \in HP$ and $j \in CP$ at the cold and hot ends of the superstructure and establish mathematical constraints between the stream temperatures in different locations of the system.

$$T_i^{in} = t_{i,1} \quad (4-36)$$

$$t_{i,NOK+1} \geq t_i^{abcg} \geq t_i^{abce} \geq T_i^{out} \quad (4-37)$$

$$T_j^{out} \geq t_{j,1} \quad (4-38)$$

$$t_{j,NOK+1} \geq T_j^{in} \quad (4-39)$$

$$t_{i,k} \geq t_{i,k+1} \quad (4-40)$$

$$t_{j,k} \geq t_{j,k+1} \quad (4-41)$$

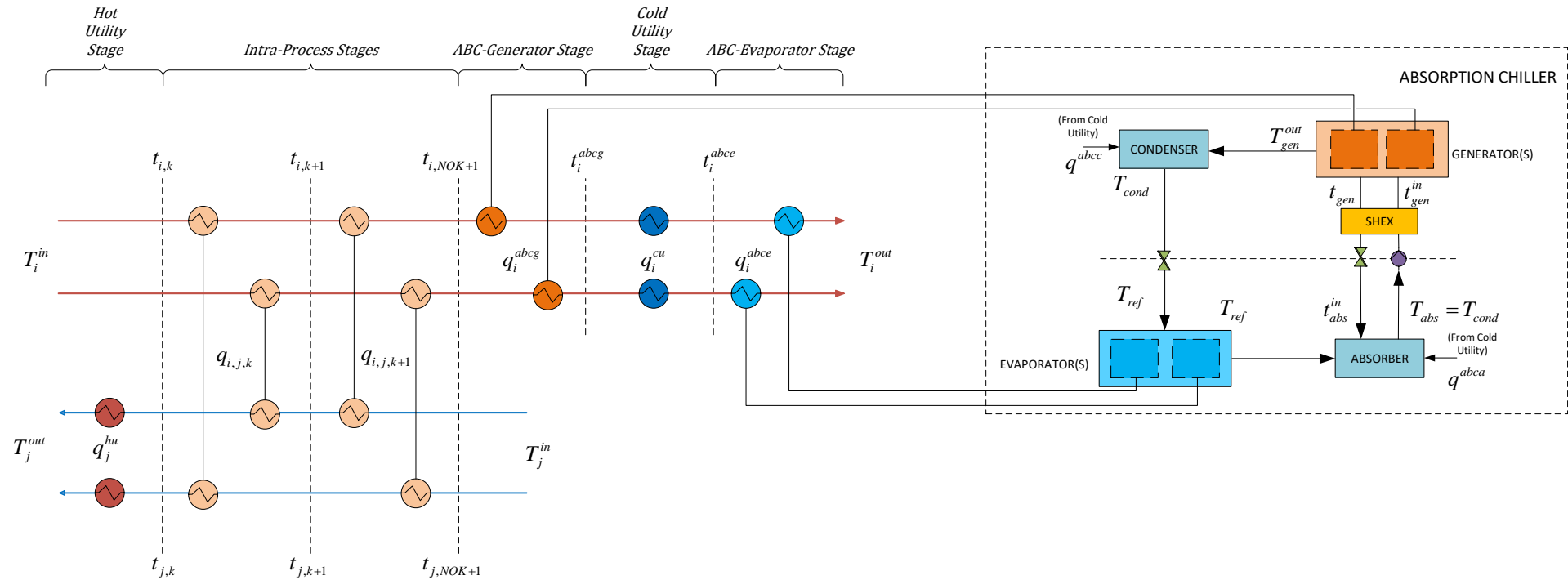


Figure 4-3. Schematic representation of the Superstructure for the Process Integration of Absorption Chillers into Continuous Processes (HEN-ABC)

Source: Own diagram

As with HEN-ORC, equations (4-42) to (4-44) offer generic expressions for the heat transfer duties and approach temperatures for every possible exchanger in the superstructure, as illustrated in Figure 4-3. For the ABC-Condenser and ABC-Absorber no binary variables have been defined. The formulation calculates their approach temperatures with the cold utility assuming that the ABC-Condenser and ABC-Absorber exist, and they are equal to $\Delta T_{Hot-End}$ and $\Delta T_{Cold-End}$ as defined in Table 4-5.

$$q_*^\dagger - \Omega z_*^\dagger \leq 0 \quad (4-42)$$

$$\Delta T_{min} \leq dt1_*^\dagger \leq \Delta T_{Hot-End} + \Gamma(1 - z_*^\dagger) \quad (4-43)$$

$$\Delta T_{min} \leq dt2_*^\dagger \leq \Delta T_{Cold-End} + \Gamma(1 - z_*^\dagger) \quad (4-44)$$

Equations (4-45) to (4-51) provide the specific additional equations required for the integration of the ABC as presented in Table 4-2. Equation (4-45) and (4-46) offer definitions for the COP and C2G of the system and equation (4-47) provides an overall energy balance for the refrigeration cycle.

$$COP \sum_{i \in HPP} q_i^{abcg} = \sum_{i \in HPP} q_i^{abce} \quad (4-45)$$

$$C2G \sum_{i \in HPP} q_i^{abcg} = q^{abcc} \quad (4-46)$$

$$\sum_{i \in HPP} q_i^{abcg} + \sum_{i \in HPP} q_i^{abce} = q^{abcc} + q^{abca} \quad (4-47)$$

Equations (4-48) to (4-51) present the generic forms of the fit functions generated for different parameters and temperatures in the absorption cycle. The *COP* and *C2G* as defined in equations (4-45) and (4-46) are functions of the temperatures of the refrigerant and refrigerant solution in different locations of the cycle. In this work, an expression describing *COP* as a function of the temperature of the refrigerant solution at the exit of the ABC-Generators (t_{gen}) is developed. This function, as described in Appendix A, is obtained by data fitting procedures and is based on a detailed mathematical simulation of the behavior of the ABC. In the simulation, the physical behavior of the system is described as a function of: 1) the temperature of the refrigerant solution at the exit of the generator (t_{gen}), 2) the refrigeration temperature, that is the target temperature of the refrigerant at the evaporator (T_{ref}), 3) the condensation temperature, described as the temperature of the refrigerant at the exit of the ABC-Condenser (T_{cond}), 4) the absorption temperature, defined as the temperature of the refrigerant solution at the exit of the ABC-Absorber (T_{abs}) and 5) the effectiveness of the ‘‘Solution Heat Exchanger’’ (ε_{SHEX}) as defined in Appendix A. The values of T_{cond} and T_{abs} have been assumed equal and

set to the initial temperature of the cold utility (T_{cu}^{in}) plus the minimum approach temperature allowed (ΔT_{min}). For more details about the simulation of the ABC please refer to Appendix A.

For the described conditions and using the assumptions and procedures in Appendix A for given refrigeration and condensation temperatures T_{ref} and T_{cond} , and a given effectiveness of the SHEX, ε_{SHEX} , a unique set of fit functions describing the behavior of the ABC is generated. All the fit functions obtained have $R^2 \geq 0.95$. In the case of $C2G$, a fit function relating its value to the COP of the ABC is also developed using similar data fitting procedures. Equation (4-48) and (4-49) present the generic form of the fit functions generated for the COP and $C2G$.

$$COP = C_1 e^{C_2 t_{gen}} + C_3 e^{C_4 t_{gen}} \quad (4-48)$$

$$C2G = C_5 COP + C_6 \quad (4-49)$$

Additional fit functions for temperatures of the refrigerant and refrigerant solution at key locations in the ABC are also generated. Equations (4-50) and (4-51) present the generic forms for the temperature of the refrigerant solution at the entry of the ABC-Generators (t_{gen}^{in}) and the entry of the ABC-Absorber (t_{abs}^{in}). These temperatures are used to calculate the LMTDs at the ABC-Generator and ABC-Absorber, and therefore to calculate their required heat transfer areas, which are necessary to determine the TAC of the system. C_1 to C_{11} are the fitting parameters for the different fit functions generated for a given ABC with refrigeration and condensation temperatures T_{ref} and T_{cond} and effectiveness of the SHEX, ε_{SHEX} .

$$t_{gen}^{in} = C_7 (t_{gen})^2 + C_8 t_{gen} + C_9 \quad (4-50)$$

$$t_{abs}^{in} = C_{10} t_{gen} + C_{11} \quad (4-51)$$

Equations (4-52) to (4-54) describe the objective function for the HEN-ABC model. In this expressions, the ‘‘Total Annualized Cost’’ (TAC) is defined as the sum of all annual operating costs for the system and the annualized capital costs of all components, including those in the ABC. Pumping cost for the ABC as well as the pump capital costs are negligible in comparison with heat exchanger costs and therefore are not taken under consideration (Mussati et al. 2016). Additionally, no fixed costs were considered for the ABC-Condenser and ABC-Absorber and only their variable costs as a function of their required heat exchanger area, are accounted in the objective function (See Section 1.3 for a detail list of all the assumptions).

$$\min TAC = TAC_{HEN} + TAC_{ABC} \quad (4-52)$$

$$TAC_{HEN} = \left\{ \begin{array}{l} H_y \sum_{i \in HP} c_{cu} q_i^{cu} + H_y \sum_{j \in CP} c_{hu} q_j^{hu} \\ + AF \left(c_{fix}^{HEN} \left(\sum_{i \in HP} \sum_{j \in CP} \sum_{k \in ST} z_{i,j,k} + \sum_{i \in HP} z_i^{cu} + \sum_{j \in CP} z_j^{hu} \right) \right) \\ + AF \left(c_{var}^{HEN} \left(\sum_{i \in HP} \sum_{j \in CP} \sum_{k \in ST} \left(\frac{q_{i,j,k}}{U_{i,j,k} LMTD_{i,j,k}} \right)^{\beta^{HEN}} \right) \right) \\ \left. \left(+ \sum_{i \in HP} \left(\frac{q_i^{cu}}{U_i^{cu} LMTD_i^{cu}} \right)^{\beta^{HEN}} + \sum_{j \in CP} \left(\frac{q_j^{hu}}{U_j^{hu} LMTD_j^{hu}} \right)^{\beta^{HEN}} \right) \right) \right\} \quad (4-53)$$

$$TAC_{ABC} = \left\{ \begin{array}{l} H_y c_{cu} (q^{abcc} + q^{abca}) \\ + AF \left(c_{fix}^{HEN} \left(\sum_{i \in HP} z_i^{abcg} + \sum_{i \in HP} z_i^{abce} \right) \right) \\ + AF \left(c_{var}^{HEN} \left(\sum_{i \in HP} \left(\frac{q_i^{abcg}}{U_i^{abcg} LMTD_i^{abcg}} \right)^{\beta^{HEN}} \right) \right) \\ \left. \left(+ \sum_{i \in HP} \left(\frac{q_i^{abce}}{U_i^{abce} LMTD_i^{abce}} \right)^{\beta^{HEN}} \right) \right) \\ \left(+ \left(\frac{q^{abcc}}{U^{abcc} LMTD^{abcc}} \right)^{\beta^{HEN}} + \left(\frac{q^{abca}}{U^{abca} LMTD^{abca}} \right)^{\beta^{HEN}} \right) \right) \right\} \quad (4-54)$$

4.2.1.3 Combined Model (HEN-WHR)

A schematic representation of the combined superstructure for the process integration of ORCs and ABCs into HENs in continuous processes (HEN-WHR) is presented in Figure 4-4. Similar to previous diagrams, not all possible matches between the process streams are included (e.g., streams splits, etc.). Also for clarity, only two hot and two cold process streams are presented, but the superstructure and its associated mathematical model are suitable for any arbitrary number of process streams. For brevity, the group of ORC and ABC is referred to simply as “Waste Heat Recovery” (WHR) system. This superstructure combines HEN-ORC and HEN-ABC and the mathematical formulation is a combination of equations from the mentioned models.

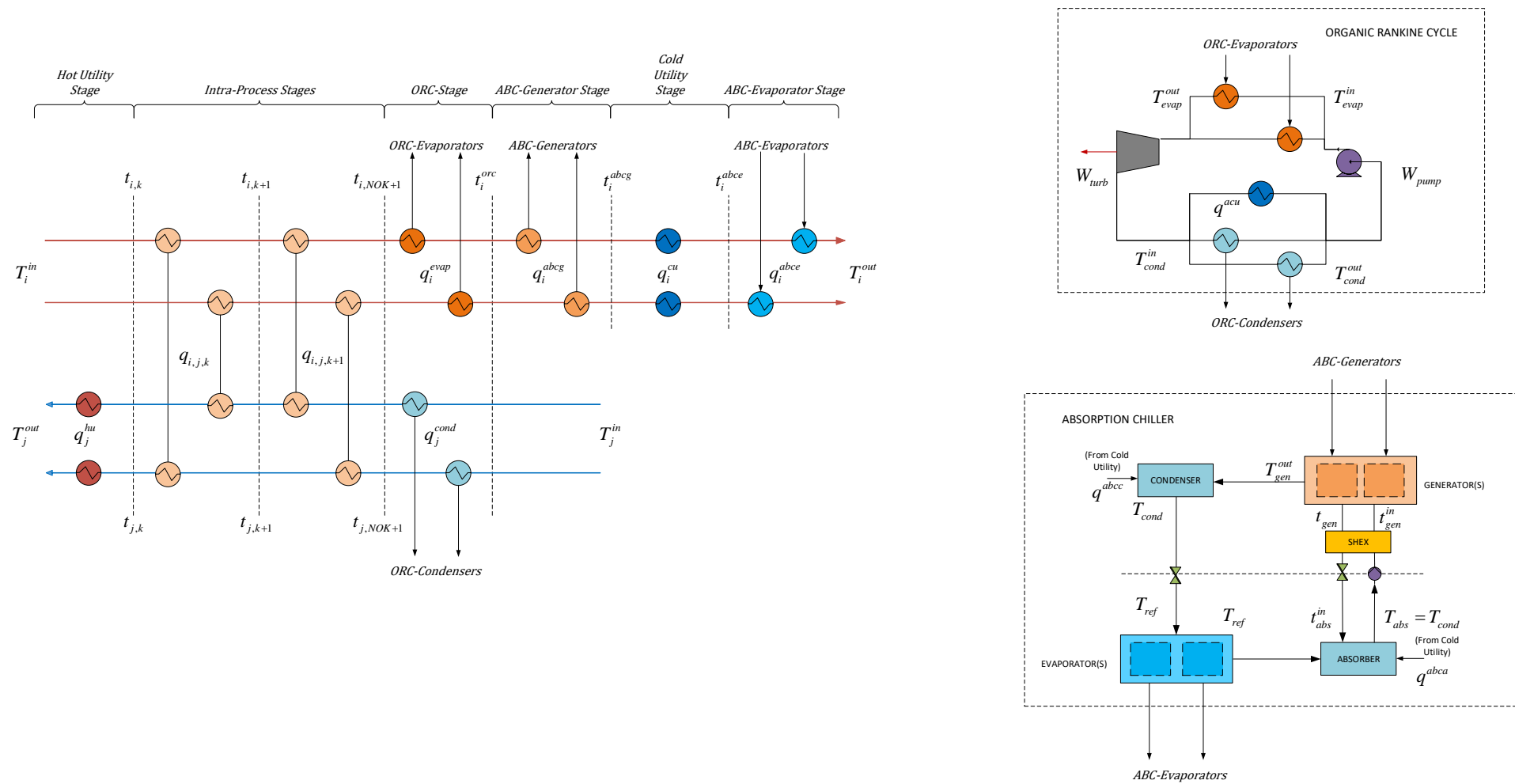


Figure 4-4. Schematic representation of the Superstructure for the Process Integration of Organic Rankine Cycles and Absorption Chillers into Continuous Processes (HEN-WHR)

Source: Own diagram

As in HEN-ORC and HEN-ABC, the heat exchange between process streams takes place in the inner stages of the superstructure. Additional dedicated stages allow the integration of the WHR technologies into the system. After exchanging energy with the cold process streams, the hot process streams can exchange heat with the dry working fluid circulating in the ORC-Evaporators in the ORC stage located directly after the last intra-process stage. This energy powers the ORC cycle as described in HEN-ORC (Section 4.2.1.1). The hot process streams can subsequently exchange energy with the refrigerant solution flowing through the ABC-Generators in their dedicated stage and then be cooled down by the cold utility. The energy supplied to the ABC-Generators powers the refrigeration cycle and generates a cooling effect in the ABC-Evaporators, as described in HEN-ABC (Section 4.2.1.2). The refrigerant can then exchange energy back with the hot process streams to provide cooling at temperatures below the temperature of the cold utility at the dedicated stage located at the cold end of the hot process streams. The cold process streams, similar to HEN-ORC, can be heated by energy from the ORC-Condensers at the ORC stage and then exchange heat with the hot process streams. The remaining energy required to achieve their target temperatures is provided by the hot utility. The energy exchange between the hot process streams and the ORC precedes the exchange between the hot process streams and the ABC, because of the higher temperatures required to drive the ORC cycle, in comparison with the absorption refrigeration cycle.

General equations as described in Table 4-1 are provided in equations (4-55) to (4-74). In the HEN-WHR formulation, equations (4-55) and (4-56) represent the overall energy balances for the process streams. The hot process streams $i \in HP$ can exchange energy with the cold process streams $j \in CP$, the ORC-Evaporator, the ABC-Generators, the cold utility and the ABC-Evaporators. As for the cold process streams $j \in CP$, they can exchange energy with the ORC-Condensers and the hot process streams $i \in HP$.

$$\sum_{j \in CP} \sum_{k \in ST} q_{i,j,k} + q_i^{evap} + q_i^{abcg} + q_i^{cu} + q_i^{abce} = F_i(T_i^{in} - T_i^{out}) \quad (4-55)$$

$$\sum_{i \in HP} \sum_{k \in ST} q_{i,j,k} + q_j^{cond} + q_j^{hu} = F_j(T_j^{out} - T_j^{in}) \quad (4-56)$$

Energy balances for each of the intra-process stages are depicted in equations (4-57) and (4-58). The energy balances are identical to those used in HEN-ORC and HEN-ABC.

$$\sum_{j \in CP} q_{i,j,k} = F_i(t_{i,k} - t_{i,k+1}) \quad (4-57)$$

$$\sum_{i \in HP} q_{i,j,k} = F_j(t_{j,k} - t_{j,k+1}) \quad (4-58)$$

The energy balances for the hot and cold utilities are identical to those used in HEN-ABC, as presented in equations (4-59) and (4-60).

$$q_i^{cu} = F_i(t_i^{abcg} - t_i^{abce}) \quad (4-59)$$

$$q_j^{hu} = F_j(T_j^{out} - t_{j,1}) \quad (4-60)$$

Equations (4-61) to (4-63) illustrate the energy balances for the ORC-Evaporators and ORC-Condensers. The equations are identical to those used in HEN-ORC.

$$q_i^{evap} = F_i(t_{i,NOK+1} - t_i^{orc}) = \dot{m}_w r_{wi} \left(cp_{w(l)}(T_{evap}^{out} - T_{evap}^{in}) + \lambda_{evap} \right) \quad (4-61)$$

$$q_j^{cond} = F_j(t_{j,NOK+1} - T_j^{in}) = \dot{m}_w r_{wj} \left(cp_{w(g)}(T_{cond}^{in} - T_{cond}^{out}) + \lambda_{cond} \right) \quad (4-62)$$

$$q^{acu} = \dot{m}_w \left(1 - \sum_{j \in CP} r_{wj} \right) \left(cp_{w(g)}(T_{cond}^{in} - T_{cond}^{out}) + \lambda_{cond} \right) \quad (4-63)$$

As for the ABC-Generators and ABC-Condensers, the energy balances, as presented in equations (4-64) and (4-65), are similar to those in HEN-ABC. In the case of the ABC-Generators a small modification to the temperatures used is needed, in order to correctly represent the new position of the ABC-Generators stage. As described before, the ABC-Generator stage in the HEN-WHR superstructure is located after the ORC stage, instead of being located directly after the last intra-process stage like in HEN-ABC.

$$q_i^{abcg} = F_i(t_i^{orc} - t_i^{abcg}) \quad (4-64)$$

$$q_i^{abce} = F_i(t_i^{abce} - T_i^{out}) \quad (4-65)$$

Equations (4-66) to (4-71) assign logical conditions for the temperatures at the hot and cold ends of the process streams and also provide logical relations between the temperatures of the process streams at different locations in the superstructure.

$$T_i^{in} = t_{i,1} \quad (4-66)$$

$$t_{i,NOK+1} \geq t_i^{orc} \geq t_i^{abcg} \geq t_i^{abce} \geq T_i^{out} \quad (4-67)$$

$$T_j^{out} \geq t_{j,1} \quad (4-68)$$

$$t_{j,NOK+1} \geq T_j^{in} \quad (4-69)$$

$$t_{i,k} \geq t_{i,k+1} \quad (4-70)$$

$$t_{j,k} \geq t_{j,k+1} \quad (4-71)$$

As with the previous models, equations (4-72) to (4-74) offer generic expressions for the heat transfer duties and approach temperatures for all the possible heat exchangers in the superstructure as illustrated in Figure 4-4. $\Delta T_{Hot-End}$ and $\Delta T_{Cold-End}$ are defined in Table 4-5.

$$q_*^\dagger - \Omega z_*^\dagger \leq 0 \quad (4-72)$$

$$\Delta T_{min} \leq dt1_*^\dagger \leq \Delta T_{Hot-End} + \Gamma(1 - z_*^\dagger) \quad (4-73)$$

$$\Delta T_{min} \leq dt2_*^\dagger \leq \Delta T_{Cold-End} + \Gamma(1 - z_*^\dagger) \quad (4-74)$$

The specific equations for HEN-WHR due to the integration of the WHR technologies are a combination of the specific equations for HEN-ORC and HEN-ABC as presented in Table 4-2. Mass balances for the working fluids in case of stream splits in the ORC-Evaporators and ORC-Condensers are provided in equations (4-75) and (4-76) and they are identical to those used in HEN-ORC.

$$\sum_{i \in HP} r_{wi} = 1 \quad (4-75)$$

$$\sum_{j \in CP} r_{wj} \leq 1 \quad (4-76)$$

As with HEN-ORC, additional equations are required to guarantee that the approach temperature constraints are maintained inside the ORC-Evaporators and ORC-Condensers during the phase change of the working fluid. Equations (4-77) and (4-78) calculate the minimum approach temperature inside of the evaporators and condensers during the phase change and are identical to the equations developed for HEN-ORC.

$$\Delta T_{min} \leq dt3_i^{evap} \leq \left(t_i^{orc} + \frac{\dot{m}_w r_{wi} cp_{w(l)}(T_{evap}^{out} - T_{evap}^{in})}{F_i} \right) - T_{evap}^{out} + \Gamma(1 - z_i^{evap}) \quad (4-77)$$

$$\Delta T_{min} \leq dt3_j^{cond} \leq T_{cond}^{out} - \left(t_{j,NOK+1} - \frac{\dot{m}_w r_{wj} cp_{w(g)}(T_{cond}^{in} - T_{cond}^{out})}{F_j} \right) + \Gamma(1 - z_j^{cond}) \quad (4-78)$$

Equations (4-79) and (4-80) calculate the work generated by the turbine and required by the pump in the ORC as a function of the mass flow of working fluid and the specific work required or generated per mass unit.

$$W_{pump} = \dot{m}_w w_{pump} \quad (4-79)$$

$$W_{turb} = \dot{m}_w w_{turb} \quad (4-80)$$

Equations (4-81) to (4-83) offer additional definitions for COP and C2G as well as a general energy balance for the refrigeration cycle in HEN-WHR. The equations are identical to those used in HEN-ABC.

$$COP \sum_{i \in HP} q_i^{abcg} = \sum_{i \in HP} q_i^{abce} \quad (4-81)$$

$$C2G \sum_{i \in HP} q_i^{abcg} = q^{abcc} \quad (4-82)$$

$$\sum_{i \in HP} q_i^{abcg} + \sum_{i \in HP} q_i^{abce} = q^{abcc} + q^{abca} \quad (4-83)$$

As with HEN-ABC, fit functions describing the physical behavior of the ABC, are presented. Equations (4-84) to (4-87) present the fit functions developed for the COP , $C2G$, t_{gen}^{in} and t_{abs}^{in} , respectively. The equations are identical to those used in HEN-ABC with C_1 to C_{11} representing the fitting parameters.

$$COP = C_1 e^{C_2 t_{gen}} + C_3 e^{C_4 t_{gen}} \quad (4-84)$$

$$C2G = C_5 COP + C_6 \quad (4-85)$$

$$t_{gen}^{in} = C_7 (t_{gen})^2 + C_8 t_{gen} + C_9 \quad (4-86)$$

$$t_{abs}^{in} = C_{10} t_{gen} + C_{11} \quad (4-87)$$

For HEN-WHR the objective function, the ‘‘Total Annualized Cost’’ (TAC), is defined as the sum of the TACs of all the constituent subsystems (HEN, ORC and ABC). Equation (4-88) presents the TAC of HEN-WHR as a combination of equations (4-89) to (4-91) for the TACs of the HEN, ORC and ABC respectively.

$$\min TAC = TAC_{HEN} + TAC_{ORC} + TAC_{ABC} \quad (4-88)$$

$$TAC_{HEN} = \left\{ \begin{array}{l} H_y \sum_{i \in HP} c_{cu} q_i^{cu} + H_y \sum_{j \in CP} c_{hu} q_j^{hu} \\ + AF \left(c_{fix}^{HEN} \left(\sum_{i \in HP} \sum_{j \in CP} \sum_{k \in ST} z_{i,j,k} + \sum_{i \in HP} z_i^{cu} + \sum_{j \in CP} z_j^{hu} \right) \right) \\ + AF \left(c_{var}^{HEN} \left(\sum_{i \in HP} \sum_{j \in CP} \sum_{k \in ST} \left(\frac{q_{i,j,k}}{U_{i,j,k} LMTD_{i,j,k}} \right)^{\beta^{HEN}} \right) \right) \\ \left(+ \sum_{i \in HP} \left(\frac{q_i^{cu}}{U_i^{cu} LMTD_i^{cu}} \right)^{\beta^{HEN}} + \sum_{j \in CP} \left(\frac{q_j^{hu}}{U_j^{hu} LMTD_j^{hu}} \right)^{\beta^{HEN}} \right) \end{array} \right\} \quad (4-89)$$

$$TAC_{ORC} = \left\{ \begin{array}{l} -H_y e_{price} W_{turb} + H_y e_{cost} W_{pump} \\ + AF \left(c_{fix}^{HEN} \left(\sum_{i \in HP} z_i^{evap} + \sum_{j \in CP} z_j^{cond} + z^{acu} \right) \right) \\ + AF \left(c_{var}^{HEN} \left(\sum_{i \in HP} \left(\frac{q_i^{evap}}{U_i^{evap} LMTD_i^{evap}} \right)^{\beta^{HEN}} \right. \right. \\ \left. \left. + \sum_{j \in CP} \left(\frac{q_j^{cond}}{U_j^{cond} LMTD_j^{cond}} \right)^{\beta^{HEN}} \right. \right. \\ \left. \left. + \left(\frac{q^{acu}}{U^{acu} LMTD^{acu}} \right)^{\beta^{HEN}} \right) \right) \\ + AF \left(c_{fix}^{turb} + c_{fix}^{pump} \right) + AF \left(c_{var}^{turb} W_{turb} \beta^{turb} + c_{var}^{pump} W_{pump} \beta^{pump} \right) \end{array} \right\} \quad (4-90)$$

$$TAC_{ABC} = \left\{ \begin{array}{l} H_y c_{cu} (q^{abcc} + q^{abca}) \\ + AF \left(c_{fix}^{HEN} \left(\sum_{i \in HP} z_i^{abcg} + \sum_{i \in HP} z_i^{abce} \right) \right) \\ + AF \left(c_{var}^{HEN} \left(\sum_{i \in HP} \left(\frac{q_i^{abcg}}{U_i^{abcg} LMTD_i^{abcg}} \right)^{\beta^{HEN}} \right. \right. \\ \left. \left. + \sum_{i \in HP} \left(\frac{q_i^{abce}}{U_i^{abce} LMTD_i^{abce}} \right)^{\beta^{HEN}} \right. \right. \\ \left. \left. + \left(\frac{q^{abcc}}{U^{abcc} LMTD^{abcc}} \right)^{\beta^{HEN}} + \left(\frac{q^{abca}}{U^{abca} LMTD^{abca}} \right)^{\beta^{HEN}} \right) \right) \end{array} \right\} \quad (4-91)$$

Table 4-5. Heat exchanger duties, binary variables and approach temperatures for all the possible heat exchangers in the Superstructures for the Process Integration of Waste Heat Recovery Technologies into Heat Exchanger Networks in Continuous Processes

Type of Heat Exchanger	Heat Exchanger Duty	Binary Variable	Appr. Temp.	Model		
				HEN-ORC	HEN-ABC	HEN-WHR
Intra-Process	$q_{i,j,k}$	$z_{i,j,k}$	$\Delta T_{Hot-End}$	$t_{i,k} - t_{j,k}$	$t_{i,k} - t_{j,k}$	$t_{i,k} - t_{j,k}$
			$\Delta T_{Cold-End}$	$t_{i,k+1} - t_{j,k+1}$	$t_{i,k+1} - t_{j,k+1}$	$t_{i,k+1} - t_{j,k+1}$
Cold Utility-Hot Process Stream	q_i^{cu}	z_i^{cu}	$\Delta T_{Hot-End}$	$t_i^{orc} - T_{cu}^{out}$	$t_i^{abcg} - T_{cu}^{out}$	$t_i^{abcg} - T_{cu}^{out}$
			$\Delta T_{Cold-End}$	$T_i^{out} - T_{cu}^{in}$	$t_i^{abce} - T_{cu}^{in}$	$t_i^{abce} - T_{cu}^{in}$
Hot Utility-Cold Process Stream	q_j^{hu}	z_j^{hu}	$\Delta T_{Hot-End}$	$T_{hu}^{in} - T_j^{out}$	$T_{hu}^{in} - T_j^{out}$	$T_{hu}^{in} - T_j^{out}$
			$\Delta T_{Cold-End}$	$T_{hu}^{out} - t_{j,1}$	$T_{hu}^{out} - t_{j,1}$	$T_{hu}^{out} - t_{j,1}$
ORC Evaporator-Hot Process Stream	q_i^{evap}	z_i^{evap}	$\Delta T_{Hot-End}$	$t_{i,NOK+1} - T_{evap}^{out}$	-	$t_{i,NOK+1} - T_{evap}^{out}$
			$\Delta T_{Cold-End}$	$t_i^{orc} - T_{evap}^{in}$	-	$t_i^{orc} - T_{evap}^{in}$
ORC Condenser-Cold Process Stream	q_j^{cond}	z_j^{cond}	$\Delta T_{Hot-End}$	$T_{cond}^{in} - t_{j,NOK+1}$	-	$T_{cond}^{in} - t_{j,NOK+1}$
			$\Delta T_{Cold-End}$	$T_{cond}^{out} - T_j^{in}$	-	$T_{cond}^{out} - T_j^{in}$
ORC Condenser-Cold Utility	q_{acu}	z_{acu}	$\Delta T_{Hot-End}$	$T_{cond}^{in} - T_{cu}^{out}$	-	$T_{cond}^{in} - T_{cu}^{out}$
			$\Delta T_{Cold-End}$	$T_{cond}^{out} - T_{cu}^{in}$	-	$T_{cond}^{out} - T_{cu}^{in}$
ABC Generator-Hot Process Stream	q_i^{abcg}	z_i^{abcg}	$\Delta T_{Hot-End}$	-	$t_{i,NOK+1} - t_{gen}$	$t_i^{orc} - t_{gen}$
			$\Delta T_{Cold-End}$	-	$t_i^{abcg} - t_{gen}^{in}$	$t_i^{abcg} - t_{gen}^{in}$
ABC Evaporator-Hot Process Stream	q_i^{abce}	z_i^{abce}	$\Delta T_{Hot-End}$	-	$t_i^{abce} - T_{ref}$	$t_i^{abce} - T_{ref}$
			$\Delta T_{Cold-End}$	-	$T_i^{out} - T_{ref}$	$T_i^{out} - T_{ref}$
ABC Absorber-Cold Utility	q^{abca}	-	$\Delta T_{Hot-End}$	-	$t_{abs}^{in} - T_{cu}^{out}$	$t_{abs}^{in} - T_{cu}^{out}$
			$\Delta T_{Cold-End}$	-	ΔT_{min}	ΔT_{min}
ABC Condenser-Cold Utility	q^{abcc}	-	$\Delta T_{Hot-End}$	-	$T_{gen}^{out} - T_{cu}^{out}$	$T_{gen}^{out} - T_{cu}^{out}$
			$\Delta T_{Cold-End}$	-	ΔT_{min}	ΔT_{min}

Source : Own table

4.2.2 Multi-Period Processes without Heat Storage (Semi-Continuous Processes)

In this section three different models are presented, describing the process integration of ORCs, ABCs or both, into HENs in multi-period processes without heat storage. For multi-period processes with long periods of operation, such as daily, weekly, monthly or seasonal variations, heat storage is usually impractical. For these semi-continuous processes, dedicated design methodologies are required.

In general, the developed superstructures are similar to those developed in the continuous cases but the mathematical descriptions contain period-dependent variables that change depending on the operating conditions and period-independent variables that remain constant throughout the different periods of operations. Additionally, and as mentioned in Table 4-3, the mathematical models for multi-period processes require additional equations calculating the effective size of the process components (heat exchangers, turbines and pumps) to be used in the cost calculations. In this work, the “Maximum Size Approach” is used. This methodology presented by Verheyen and Zhang (2006) for the synthesis of multi-period HENs, seeks to generate systems where the size of the individual units is greater or equal to the maximum size required to be able to handle the heat transfer duties in each of the periods of operation.

In order to simplify the presentation of the mathematical models and due to the similarities between the equations for the multi-period and continuous cases, in this section, only the modifications made to the equations of the continuous models are presented, as well as the specific equations due to the multi-period operation, namely the equations for the maximum size of components (Table 4-3). For a detailed presentation of all the equations, please see Appendix C, where all the equations for the superstructures developed in this work are presented explicitly.

4.2.2.1 Organic Rankine Cycles (MP-ORC)

The MP-ORC superstructure is an extension of the HEN-ORC superstructure, as presented in Figure 4-5. Similar to previous diagrams, the schematic representation of MP-ORC does not include all possible matches between the process streams (e.g., streams splits, etc.). Also for clarity, only two hot and two cold process streams are presented, but the superstructure and its associated mathematical model are suitable for any arbitrary number of process streams.

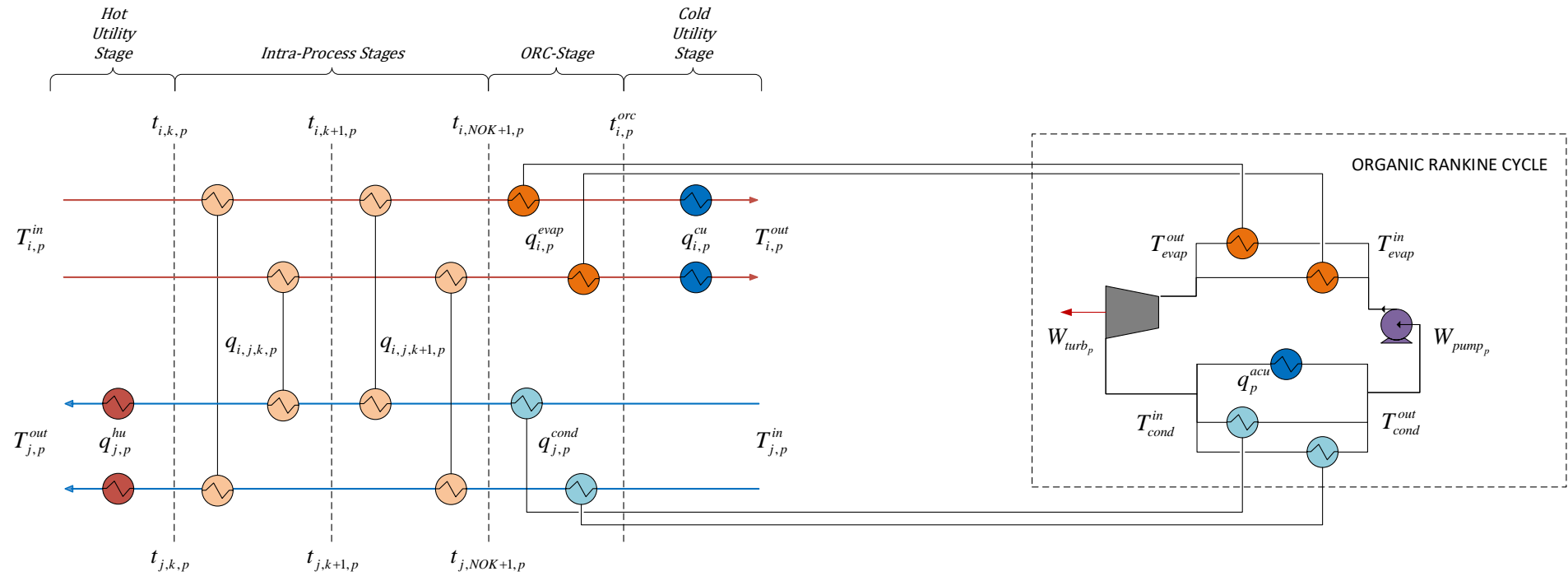


Figure 4-5. Schematic representation of the Superstructure for the Process Integration of Organic Rankine Cycles into Multi-Period Processes without Heat Storage (MP-ORC)

Source: Own diagram

As in HEN-ORC, the heat exchange between process streams takes place in the inner stages of the superstructure while the heat exchange between the process streams and the ORC takes place only in one stage located at the cold end of the streams, after the last intra-process stage. The energy supplied by the hot process streams to the ORC-Evaporators drives the ORC and generates electricity through the expansion of the working fluids in the ORC-Turbine. The expanded working fluid is then condensed by heat exchange at the ORC-Condensers with the cold process streams or the cold utility and then the saturated liquid is pumped back to the evaporation pressure to restart the cycle. The operating conditions of the process streams in each period of operation differ, but the evaporating and condensing pressures, and therefore the evaporating and condensing temperatures in the ORC, remain constant in all periods. This is visible in Figure 4-5, as the temperatures in the ORC do not have the subindex p , which represents the periods of operation.

The mathematical formulation of MP-ORC contains the equations (4-1) to (4-24) for HEN-ORC but replacing variables and parameters for the equivalent variables and parameters for the multi-period case as described in Table 4-6. As for the additional equations due to the multi-period operation, equations (4-92) to (4-94) calculate the maximum size for the different components of the system. Equation (4-92) presents a generic expression for the effective heat transfer area for each possible heat exchanger in MP-ORC, as presented in Figure 4-5. The effective area for a given heat exchanger, A_*^\dagger , is the maximum between the required heat transfer areas for each period, if they are considered separately. $q_{*,p}^\dagger$, $U_{*,p}^\dagger$ and $LMTD_{*,p}^\dagger$ represent the heat transfer duties, overall heat transfer coefficients and logarithmic mean temperature differences for each possible heat exchanger in MP-ORC at each period $p \in P$. Equations (4-93) and (4-94) use a similar approach to calculate the effective sizes for the turbines and pumps in the ORC, with W_{turb_p} and W_{pump_p} representing the power generated and required by the turbine and pump at each period of operation $p \in P$, and W_{turb}^{max} and W_{pump}^{max} indicating the effective size of these components.

$$A_*^\dagger \geq \frac{q_{*,p}^\dagger}{U_{*,p}^\dagger LMTD_{*,p}^\dagger} \quad (4-92)$$

$$W_{pump}^{max} \geq W_{pump_p} \quad (4-93)$$

$$W_{turb}^{max} \geq W_{turb_p} \quad (4-94)$$

Table 4-6. Equivalences between variables and parameters between continuous and multi-period models

Symbol		Symbol (Continuation)	
Continuous	Multi-period	Continuous	Multi-period
T_i^{in}	$T_{i,p}^{in}$	\dot{m}_w	$\dot{m}_{w,p}$
T_i^{out}	$T_{i,p}^{out}$	$dt1_{i,j,k}$	$dt1_{i,j,k,p}$
T_j^{in}	$T_{j,p}^{in}$	$dt2_{i,j,k}$	$dt2_{i,j,k,p}$
T_j^{out}	$T_{j,p}^{out}$	$dt1_i^{cu}$	$dt1_{i,p}^{cu}$
F_i	$F_{i,p}$	$dt2_i^{cu}$	$dt2_{i,p}^{cu}$
F_j	$F_{j,p}$	$dt1_j^{hu}$	$dt1_{j,p}^{hu}$
$U_{i,j,k}$	$U_{i,j,k,p}$	$dt2_j^{hu}$	$dt2_{j,p}^{hu}$
U_i^{cu}	$U_{i,p}^{cu}$	$dt1_i^{evap}$	$dt1_{i,p}^{evap}$
U_j^{hu}	$U_{j,p}^{hu}$	$dt2_i^{evap}$	$dt2_{i,p}^{evap}$
U_i^{evap}	$U_{i,p}^{evap}$	$dt3_i^{evap}$	$dt3_{i,p}^{evap}$
U_j^{cond}	$U_{j,p}^{cond}$	$dt1_j^{cond}$	$dt1_{j,p}^{cond}$
U_{acu}	U_p^{acu}	$dt2_j^{cond}$	$dt2_{j,p}^{cond}$
U_i^{abcg}	$U_{i,p}^{abcg}$	$dt3_i^{evap}$	$dt3_{i,p}^{evap}$
U_i^{abce}	$U_{i,p}^{abce}$	$dt1_{acu}$	$dt1_p^{acu}$
U_{abca}	U_p^{abca}	$dt2_{acu}$	$dt2_p^{acu}$
U_{abcc}	U_p^{abcc}	$dt1_i^{abcg}$	$dt1_{i,p}^{abcg}$
$q_{i,j,k}$	$q_{i,j,k,p}$	$dt2_i^{abcg}$	$dt2_{i,p}^{abcg}$
q_i^{cu}	$q_{i,p}^{cu}$	$dt1_i^{abce}$	$dt1_{i,p}^{abce}$
q_j^{hu}	$q_{j,p}^{hu}$	$dt2_i^{abce}$	$dt2_{i,p}^{abce}$
q_i^{evap}	$q_{i,p}^{evap}$	$dt1_p^{abca}$	$dt1_p^{abca}$
q_j^{cond}	$q_{j,p}^{cond}$	$dt2_p^{abca}$	$dt2_p^{abca}$
q_{acu}	q_p^{acu}	$dt1_p^{abcc}$	$dt1_p^{abcc}$
q_i^{abcg}	$q_{i,p}^{abcg}$	$dt2_p^{abcc}$	$dt2_p^{abcc}$
q_i^{abce}	$q_{i,p}^{abce}$	W_{pump}	$W_{pump,p}$
q_{abca}	q_p^{abca}	W_{turb}	$W_{turb,p}$
q_{abcc}	q_p^{abcc}	$LMTD_{i,j,k}$	$LMTD_{i,j,k,p}$
$t_{i,k}$	$t_{i,k,p}$	$LMTD_i^{cu}$	$LMTD_{i,p}^{cu}$
$t_{j,k}$	$t_{j,k,p}$	$LMTD_j^{hu}$	$LMTD_{j,p}^{hu}$
$t_{i,NOK+1}$	$t_{i,NOK+1,p}$	$LMTD_i^{evap}$	$LMTD_{i,p}^{evap}$
$t_{j,k,NOK+1}$	$t_{j,NOK+1,p}$	$LMTD_j^{cond}$	$LMTD_{j,p}^{cond}$
t_i^{orc}	$t_{i,p}^{orc}$	$LMTD_{acu}$	$LMTD_p^{acu}$
t_i^{abcg}	$t_{i,p}^{abcg}$	$LMTD_i^{abcg}$	$LMTD_{i,p}^{abcg}$
t_i^{abce}	$t_{i,p}^{abce}$	$LMTD_i^{abce}$	$LMTD_{i,p}^{abce}$
r_{w_i}	$r_{w_{i,p}}$	$LMTD_{abca}$	$LMTD_p^{abca}$
r_{w_j}	$r_{w_{j,p}}$	$LMTD_{abcc}$	$LMTD_p^{abcc}$

Source: Own table

Finally, the objective function for MP-ORC, the “Total Annualized Cost” (TAC), is calculated using equations (4-95) to (4-97). As with HEN-ORC, TAC is equal to the sum of the TACs of the subsystems (HEN and ORC). The weighted factor $\frac{DOP_p}{\sum_{p \in P} DOP_p}$ is included in the calculations

of the annual operating costs and the annual revenues from the sale of electricity, to take under consideration the different duration of the periods, as presented by Isafiade and Fraser (2010)¹¹.

$$\min TAC = TAC_{HEN} + TAC_{ORC} \quad (4-95)$$

$$TAC_{HEN} = \left\{ \begin{array}{l} H_y \sum_{p \in P} \left(\frac{DOP_p}{\sum_{p \in P} DOP_p} \right) \left(\sum_{j \in CP} c_{hu_p} q_{j,p}^{hu} + \sum_{i \in HP} c_{cu_p} q_{i,p}^{cu} \right) \\ + AF c_{fix}^{HEN} \left(\sum_{i \in HP} \sum_{j \in CP} \sum_{k \in ST} z_{i,j,k} + \sum_{i \in HP} z_i^{cu} + \sum_{j \in CP} z_j^{hu} \right) \\ + AF c_{var}^{HEN} \left(\sum_{i \in HP} \sum_{j \in CP} \sum_{k \in ST} (A_{i,j,k})^{\beta^{HEN}} \right. \\ \left. + \sum_{i \in HP} (A_i^{cu})^{\beta^{HEN}} + \sum_{j \in CP} (A_j^{hu})^{\beta^{HEN}} \right) \end{array} \right\} \quad (4-96)$$

$$TAC_{ORC} = \left\{ \begin{array}{l} H_y \sum_{p \in P} \left(\frac{DOP_p}{\sum_{p \in P} DOP_p} \right) (-e_{price_p} W_{turb_p} + e_{cost_p} W_{pump_p}) \\ + AF c_{fix}^{HEN} \left(\sum_{i \in HP} z_i^{evap} + \sum_{j \in CP} z_j^{cond} + z^{acu} \right) \\ + AF c_{var}^{HEN} \left(\sum_{i \in HP} (A_i^{evap})^{\beta^{HEN}} + \sum_{j \in CP} (A_j^{cond})^{\beta^{HEN}} + (A^{acu})^{\beta^{HEN}} \right) \\ + AF \left(c_{fix}^{pump} + c_{var}^{pump} (W_{pump}^{max})^{\beta^{pump}} \right) \\ + AF \left(c_{fix}^{turb} + c_{var}^{turb} (W_{turb}^{max})^{\beta^{turb}} \right) \end{array} \right\} \quad (4-97)$$

4.2.2.2 Absorption Chillers (MP-ABC)

A schematic representation of the superstructure for the process integration of ABCs into HENs in multi-period processes without heat storage (MP-ABC) is presented in Figure 4-6. Similar to previous diagrams, the schematic representation of MP-ABC does not include all possible matches between the process streams (e.g., streams splits, etc.). Also for clarity, only two hot and two cold process streams are presented, but the superstructure and its associated mathematical model are suitable for any arbitrary number of process streams. MP-ABC it is an extension of the superstructure developed for the continuous case (HEN-ABC). Intra-process energy exchange takes place in the inner stages of the superstructure. Hot process streams can

¹¹ The multi-period HEN superstructure as presented by Verheyen and Zhang 2006 ("Maximum Size Approach") used periods of operation of equal duration. The weighted factor by introduced by Isafiade and Fraser 2010 allows to consider the different duration of the periods in the optimization model.

then reject heat to the ABC-Generators located between the cold utility and the last intra-process stage. This energy drives the refrigeration cycle, separating the vapor refrigerant from the refrigerant solution in the ABC-Generators. The refrigerant flows to a central ABC-Condenser where it condenses by rejecting heat to the cold utility. The refrigerant leaves the ABC-Condenser as a saturated liquid and it is expanded in a throttle valve to generate the cooling effect. The expanded refrigerant at low temperature is then used to cool the hot process streams through heat exchange in the ABC-Evaporators, located after the cold utility stage, at the cold end of the superstructure. The refrigerant leaves the ABC-Evaporators as a saturated vapor and it is reabsorbed by the strong refrigerant solution coming from the ABC-Generators in a central ABC-Absorber. The resulting weak refrigerant solution rejects heat again to the cold utility and leaves the ABC-Absorber as a saturated liquid to be pumped back to the ABC-Generators to restart the cycle. A solution heat exchanger (SHEX) is used to preheat the weak refrigerant solution flowing to the ABC-Generators with energy provided by the strong refrigerant solution returning to the ABC-Absorbers.

Similar to MP-ORC, the temperatures inside the refrigeration cycle remain the same during all periods of operation but the temperatures of the process streams in each location of the superstructure, as well as the duties of heat exchangers (intra-process or between the process streams and the refrigeration cycle), change depending on the operating conditions. This is visible in Figure 4-6, as the temperatures in the ABC do not have the subindex p , which represents the periods of operation. As for the mathematical formulation, equations (4-28) to (4-51) from HEN-ABC are modified with the corresponding variables and parameters for the multi-period case, as presented in Table 4-6. As with MP-ORC, additional equations for the effective size of the system components, namely heat exchangers for MP-ABC, are required. Equation (4-98) presents a generic expression for the effective heat transfer areas of all possible heat exchangers in MP-ABC.

$$A_*^\dagger \geq \frac{q_{*,p}^\dagger}{U_{*,p}^\dagger LMDT_{*,p}^\dagger} \quad (4-98)$$

The objective function for MP-ABC, the “Total Annualized Cost” (TAC) as defined in equations (4-99) to (4-101), is equal to the sum of the TACs of its constituent subsystems (HEN and ABC). As with MP-ORC, the weighted factor $\frac{DOP_p}{\sum_{p \in P} DOP_p}$ is included in the calculation of the annual operating costs to take under consideration the different duration of the periods. Also similar to HEN-ABC pump capital cost, pumping costs and ABC-Condenser and ABC-Absorber fixed costs are not considered.

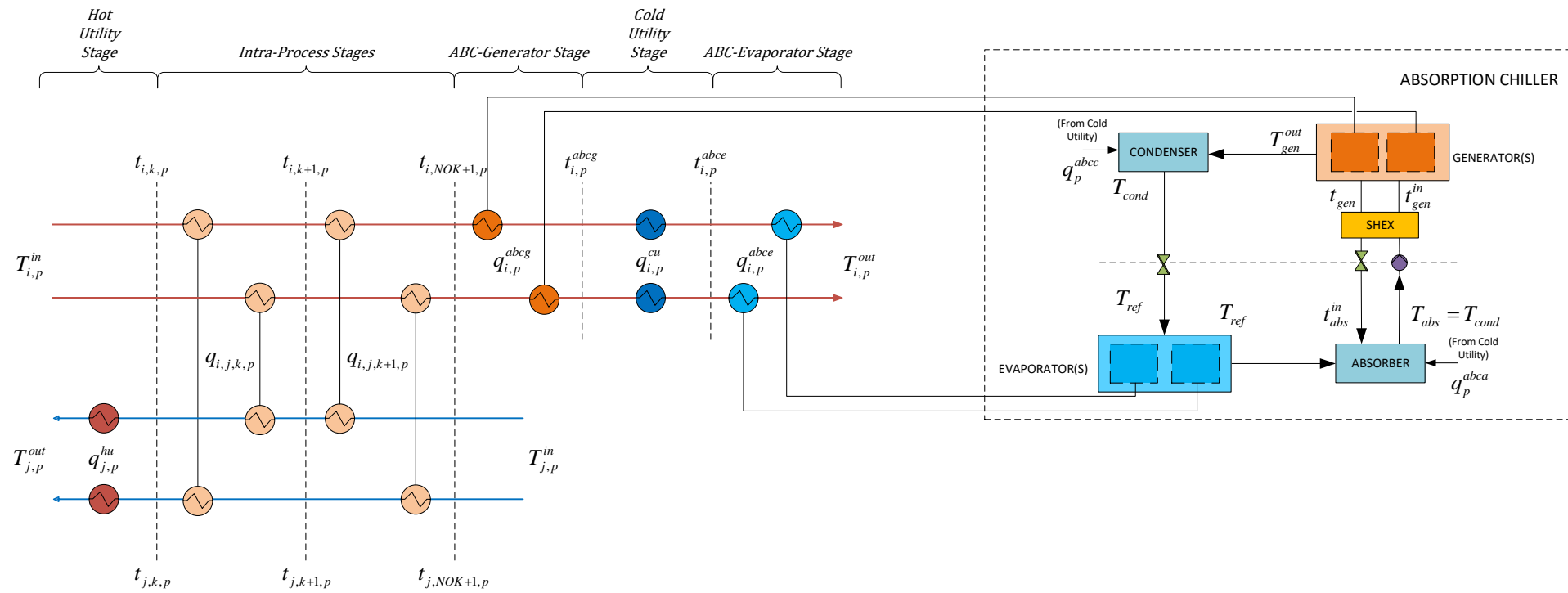


Figure 4-6. Schematic representation of the Superstructure for the Process Integration of Absorption Chillers into Multi-Period Processes without Heat Storage (MP-ABC)

Source: Own diagram

$$\min TAC = TAC_{HEN} + TAC_{ABC} \quad (4-99)$$

$$TAC_{HEN} = \left\{ \begin{array}{l} H_y \sum_{p \in P} \left(\frac{DOP_p}{\sum_{p \in P} DOP_p} \right) \left(\sum_{j \in CP} c_{hu_p} q_{j,p}^{hu} + \sum_{i \in HP} c_{cu_p} q_{i,p}^{cu} \right) \\ + AF c_{fix}^{HEN} \left(\sum_{i \in HP} \sum_{j \in CP} \sum_{k \in ST} z_{i,j,k} + \sum_{i \in HP} z_i^{cu} + \sum_{j \in CP} z_j^{hu} \right) \\ + AF c_{var}^{HEN} \left(\sum_{i \in HP} \sum_{j \in CP} \sum_{k \in ST} (A_{i,j,k})^{\beta^{HEN}} \right. \\ \left. + \sum_{i \in HP} (A_i^{cu})^{\beta^{HEN}} + \sum_{j \in CP} (A_j^{hu})^{\beta^{HEN}} \right) \end{array} \right\} \quad (4-100)$$

$$TAC_{ABC} = \left\{ \begin{array}{l} H_y \sum_{p \in P} \left(\frac{DOP_p}{\sum_{p \in P} DOP_p} \right) (c_{cu} (q_p^{abcc} + q_p^{abca})) \\ + AF c_{fix}^{HEN} \left(\sum_{i \in HP} z_i^{abcg} + \sum_{i \in HP} z_i^{abce} \right) \\ + AF c_{var}^{HEN} \left(\sum_{i \in HP} (A_i^{abcg})^{\beta^{HEN}} + \sum_{i \in HP} (A_i^{abce})^{\beta^{HEN}} \right. \\ \left. + (A^{abcc})^{\beta^{HEN}} + (A^{abca})^{\beta^{HEN}} \right) \end{array} \right\} \quad (4-101)$$

4.2.2.3 Combined Model (MP-WHR)

A schematic representation of the superstructure for the process integration of ORCs and ABCs into HENs in multi-period processes without heat storage (MP-WHR) is illustrated in Figure 4-7. Similar to previous diagrams, the schematic representation of MP-WHR does not include all possible matches between the process streams (e.g., streams splits, etc.). Also for clarity, only two hot and two cold process streams are presented, but the superstructure and its associated mathematical model are suitable for any arbitrary number of process streams.

MP-WHR is an extension of the superstructure for the continuous case (HEN-WHR). As with HEN-WHR, MP-WHR is a combination of the models for the process integration of ORCs and ABCs into HENs in multi-period processes without heat storage (MP-ORC and MP-ABC). In MP-WHR the intra-process energy exchange takes place in the inner stages of the superstructure. The energy exchange between the process streams and the working fluid circulating through the ORC occurs in a dedicated ORC stage located directly after the last intra-process stage. The energy provided to the working fluid in this stage by the hot process streams drives the power cycle, as described in MP-ORC. The hot process streams can then

supply energy to the refrigeration cycle at the ABC-Generators located between the cold utilities and the ORC stage. This energy drives the refrigeration cycle as explained in MP-ORC. The refrigeration effect generated in the cycle is then used to cool the hot process streams in the ABC-Evaporators located in the cold end of the superstructure after the cold utility. Hot utilities at the hot end of the superstructure provide the remaining energy required by the cold process streams to achieve their target temperatures.

Similar to MP-ORC and MP-ABC, the temperatures inside the ORC and refrigeration cycles remain the same during all periods of operation but the temperatures of the process streams in each location of the superstructure, as well as the duties of heat exchangers (intra-process or between the process streams and the refrigeration cycle), change depending on the operating conditions. This is visible in Figure 4-7, as the temperatures in the ORC and the ABC do not have the subindex p , which represents the periods of operation. The mathematical formulation for MP-WHR is obtained by replacing variables and parameters in equations (4-55) to (4-87) in HEN-WHR, with their multi-period counterparts as presented in Table 4-6. The additional equations for the effective size of heat exchangers, turbines and pumps are similar to those of MP-ORC and MP-ABC and presented in equations (4-102) to (4-104).

$$A_*^\dagger \geq \frac{q_{*,p}^\dagger}{U_{*,p}^\dagger LMDT_{*,p}^\dagger} \quad (4-102)$$

$$W_{pump}^{max} \geq W_{pump_p} \quad (4-103)$$

$$W_{turb}^{max} \geq W_{turb_p} \quad (4-104)$$

The MP-WHR objective function, the Total Annualized Cost (TAC), is defined as the sum of the TACs of its constituent subsystems (HEN, ORC and ABC). Equations (4-105) to (4-108) present the TAC of MP-WHR as a combination of the TACs of the HEN, ORC and ABC respectively.

$$\min TAC = TAC_{HEN} + TAC_{ORC} + TAC_{ABC} \quad (4-105)$$

$$TAC_{HEN} = \left\{ \begin{array}{l} H_y \sum_{p \in P} \left(\frac{DOP_p}{\sum_{p \in P} DOP_p} \right) \left(\sum_{j \in CP} c_{hu_p} q_{j,p}^{hu} + \sum_{i \in HP} c_{cu_p} q_{i,p}^{cu} \right) \\ + AF c_{fix}^{HEN} \left(\sum_{i \in HP} \sum_{j \in CP} \sum_{k \in ST} z_{i,j,k} + \sum_{i \in HP} z_i^{cu} + \sum_{j \in CP} z_j^{hu} \right) \\ + AF c_{var}^{HEN} \left(\sum_{i \in HP} \sum_{j \in CP} \sum_{k \in ST} (A_{i,j,k})^{\beta^{HEN}} + \sum_{i \in HP} (A_i^{cu})^{\beta^{HEN}} + \sum_{j \in CP} (A_j^{hu})^{\beta^{HEN}} \right) \end{array} \right\} \quad (4-106)$$

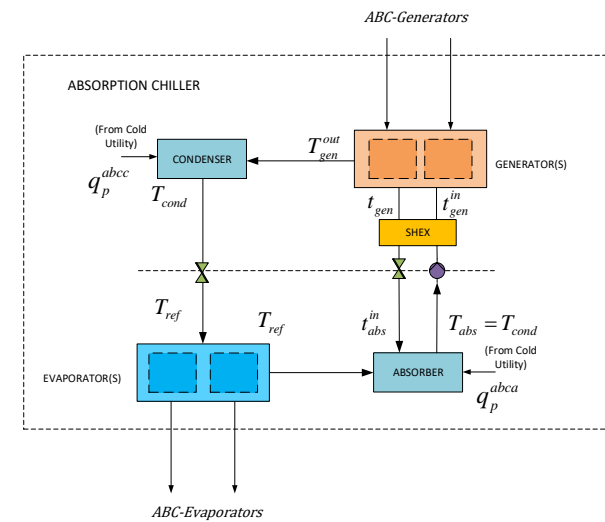
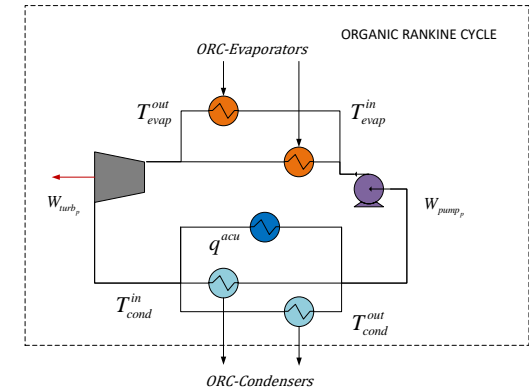
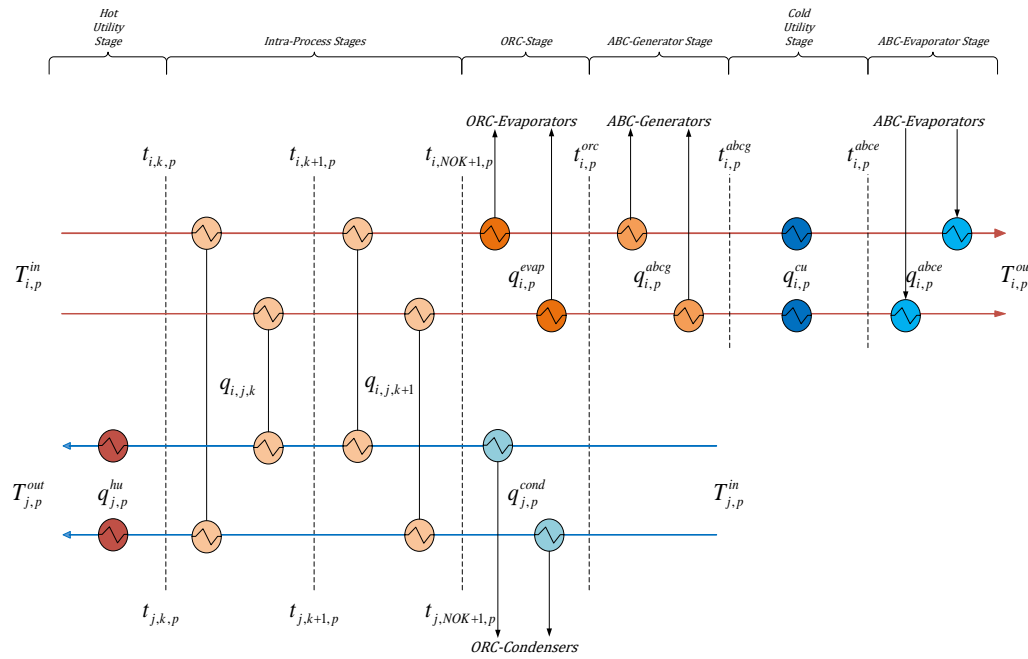


Figure 4-7. Schematic representation of the Superstructure for the Process Integration of Organic Rankine Cycles and Absorption Chillers into Multi-Period Processes without Heat Storage (MP-ABC)

Source: Own diagram

$$TAC_{ORC} = \left\{ \begin{array}{l} H_y \sum_{p \in P} \left(\frac{DOP_p}{\sum_{p \in P} DOP_p} \right) (-e_{price_p} W_{turb_p} + e_{cost_p} W_{pump_p}) \\ + AF c_{fix}^{HEN} \left(\sum_{i \in HEP} z_i^{evap} + \sum_{j \in CEP} z_j^{cond} + z_{acu} \right) \\ + AF c_{var}^{HEN} \left(\sum_{i \in HEP} (A_i^{evap})^{\beta^{HEN}} + \sum_{j \in CEP} (A_j^{cond})^{\beta^{HEN}} + (A_{acu})^{\beta^{HEN}} \right) \\ + AF \left(c_{fix}^{pump} + c_{var}^{pump} (W_{pump}^{max})^{\beta^{pump}} \right) + AF \left(c_{fix}^{turb} + c_{var}^{turb} (W_{turb}^{max})^{\beta^{turb}} \right) \end{array} \right\} \quad (4-107)$$

$$TAC_{ABC} = \left\{ \begin{array}{l} H_y \sum_{p \in P} \left(\frac{DOP_p}{\sum_{p \in P} DOP_p} \right) (c_{cu} (q_p^{abcc} + q_p^{abca})) \\ + AF c_{fix}^{HEN} \left(\sum_{i \in HEP} z_i^{abcg} + \sum_{i \in HEP} z_i^{abce} \right) \\ + AF c_{var}^{HEN} \left(\sum_{i \in HEP} (A_i^{abcg})^{\beta^{HEN}} + \sum_{i \in HEP} (A_i^{abce})^{\beta^{HEN}} \right. \\ \left. + (A^{abcc})^{\beta^{HEN}} + (A^{abca})^{\beta^{HEN}} \right) \end{array} \right\} \quad (4-108)$$

4.2.3 Multi-Period Processes with Heat Storage (Batch Processes)

In this section, the superstructures for the process integration of ORCs, ABCs or both, into HENs in multi-period processes with heat storage are provided. In this work, only “Fixed Temperature Variable Mass” (FTVM) storage tanks are considered. For multi-period process with short periods of operation and high energy consumption, the use of heat storage can be beneficial. Although numerous technologies for “Thermal Energy Storage” (TES) are available in the market, sensible storages such as the FTVM storage tanks remain the most popular alternative for industrial processes (see section 2.3.3). The FTVM storage tank models used in this work are based on the work by Beck and Hofmann (2018b) for the synthesis of HENs for multi-period process with heat storage. Beck’s model is extended to include multi-tank storage systems and then combined with the models for the process integration of ORCs, ABCs or both, into HENs in multi-period processes without heat storage developed in section 4.2.2 (MP-ORC, MP-ABC and MP-WHR) in order to generate the models presented in this section.

As with the previous superstructures, the mathematical models are formulated as “Mixed Integer Non Linear Programming” (MINLP) problems, where the binary variables (z^*) represent the existence of a certain component at a certain stage of the superstructure and continuous variables are used to describe the operational conditions of the system

(temperatures, mass flows, heat flows and equipment sizes). Additional binary variables ($y_{p,*}^{shift}$) are used to indicate if a FTVM hot storage tank is being charged or discharged in a given period and energy level. The FTVM storage tanks are fed by hot and cold storage streams that exchange energy exclusively with the process streams and only inside the intra-process stages. The tanks are organized in energy levels. In each energy level, two tanks exist, one acting like a hot storage and one as a cold storage. A tank acting as a cold storage in one energy level, is considered a hot storage in the next one. The temperatures of the tanks decrease with each increasing energy level. In each energy level, one hot storage stream flows from the hot storage tank to the cold storage tank, exchanging energy with the cold process streams in the intra-process stages. Similarly, in each energy level, one cold storage stream flows from the cold storage tank to the hot storage tank, exchanging energy with the hot process streams along the way, inside the intra-process stages. For each period, at a given energy level only one of the storage streams, either the hot storage stream or the cold storage stream, is active. The amount of energy stored/accumulated in a given storage tank at the beginning and end of the process duration (cycle) is the same. The temperatures at each storage tank remain fixed during the whole cycle and are calculated during the optimization process. Similar to the superstructures developed in section 4.2.2, and in order to simplify the presentation of the mathematical models in this section only the modifications made to the equations corresponding to the multi-period models without heat storage are presented as well as the specific equations due to the storage operation, as presented in Table 4-4. For an explicit presentation of all the equations, see Appendix C.

4.2.3.1 Storage Equations

As mentioned before, the storage system exchanges energy exclusively with the process streams and not with the working fluid in the ORC or the refrigerant or refrigerant couple in the ABCs (see Section 1.3 for a list of all the modeling assumptions used). Figure 4-8 presents a schematic representation of the superstructure for the synthesis of HENs in multi-period process with multiple FTVM heat storage tanks. This superstructure describes the interaction between the storage system and the process streams and, as mentioned before, is an extension of Beck and Hofmann (2018b), which considered two-tank systems, fluidized beds storages and latent heat storages. The integration of ORCs and ABCs does not affect the internal behavior of the storage system and therefore the equations describing their behavior are the same for all the models. As with previous diagrams, Figure 4-8 does not include all possible matches between the process streams (e.g., streams splits, etc.). Also for clarity, only two storage levels (three

storage tanks) and two hot and two cold process streams are presented, but the superstructure and its associated mathematical model are suitable for any arbitrary number of process streams and storage levels. Equations (4-109) to (4-127) are the specific equations due to the storage system as mentioned in Table 4-4 and describe its internal behavior. The equations are common to all the superstructures including FTVM heat storages and therefore will only be presented in this section. In the sections on the individual superstructures (MP-ST-ORC, MP-ST-ABC and MP-ST-WHR), the equations describing the interaction between the process streams and the storage system are presented. In principle, these equations are exclusively energy balances for the process streams. Equations (4-109) and (4-110) present overall energy balances for the hot and cold storage streams. In equation (4-109) corresponding to the cold storage streams, that is, the streams flowing from the cold to the hot storage tanks, $q_{p,lv}^{charh}$ represents the energy rate used to charge the hot storage tank in level $l \in LV$ and period $p \in P$ and it is equivalent to the energy rate used to discharge the cold storage tank in the same level $q_{p,lv}^{discharc}$. Similarly, in equation (4-110) corresponding to the hot storage stream, that is, the streams flowing from the hot to the cold storage tanks $q_{p,lv}^{charc}$ represents the energy rate used to charge the cold storage tank in level $l \in LV$ and period $p \in P$ and it is equivalent to the energy rate used to discharge the hot storage tank in the same level $q_{p,lv}^{discharh}$.

$$q_{p,lv}^{charh} = q_{p,lv}^{discharc} = \sum_{i \in HP} \sum_{k \in ST} q_{i,k,p,lv}^{stoc} \quad (4-109)$$

$$q_{p,lv}^{charc} = q_{p,lv}^{discharh} = \sum_{j \in CP} \sum_{k \in ST} q_{j,k,p,lv}^{stoh} \quad (4-110)$$

Equations (4-111) and (4-112) calculate the cumulated energy stored in a given hot or cold storage tank at the end of period $p \in P$. In these equations $Q_{p,lv}^h$ and $Q_{p,lv}^c$ represent the cumulated energy stored at the hot and cold storage tanks in level $lv \in LV$ at the end of period $p \in P$, and the terms $Q_{lv,start}^h$ and $Q_{lv,start}^c$ symbolize the cumulated energy in the tanks at the beginning of the process cycle, that is the initial state of the tanks, before any energy exchange takes place.

$$Q_{p,lv}^h = Q_{lv,start}^h + \sum_{p=1}^p q_{p,lv}^{charh} DOP_p - \sum_{p=1}^p q_{p,lv}^{discharh} DOP_p \quad (4-111)$$

$$Q_{p,lv}^c = Q_{lv,start}^c + \sum_{p=1}^p q_{p,lv}^{charc} DOP_p - \sum_{p=1}^p q_{p,lv}^{discharc} DOP_p \quad (4-112)$$

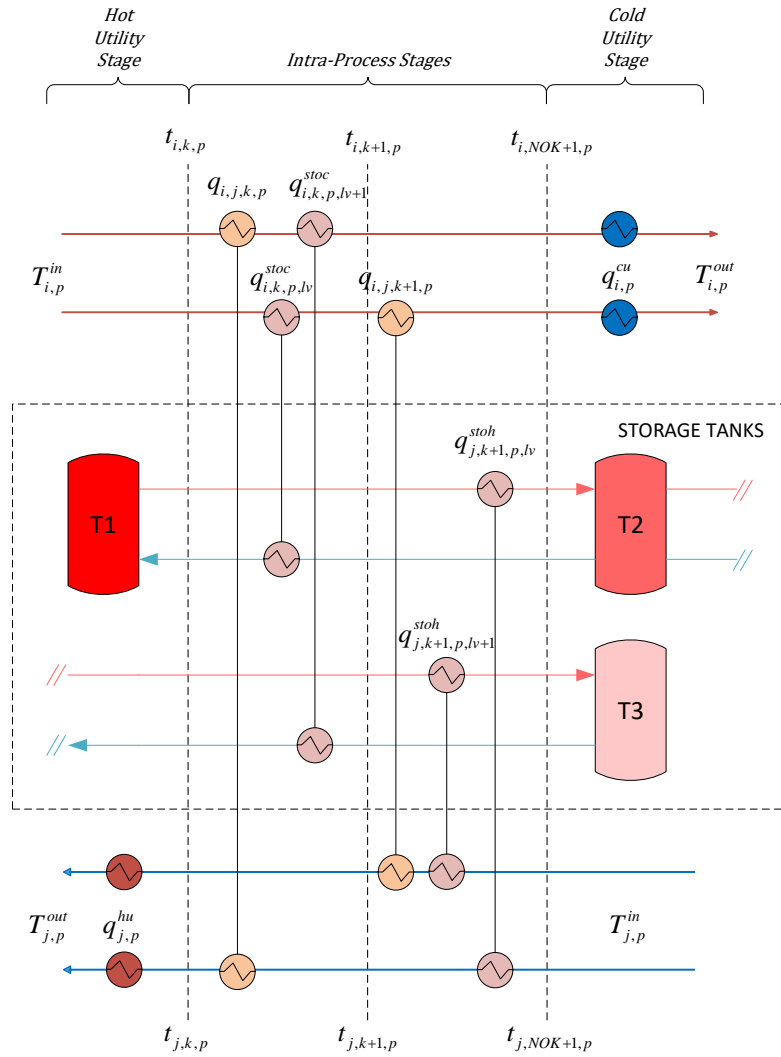


Figure 4-8. Schematic representation of the Superstructure for the Synthesis of Heat Exchanger Networks in Multi-Period Process with Fixed Temperature Variable Mass (FTVM) Heat Storage Tanks

Source: Own diagram

Equations (4-113) to (4-116) calculate the required size for the storage tanks. The difference between the maximum and minimum cumulated energy stored in a given tank during the cycle is proportional to the minimum storage mass required for the tank at the given level M_{lv}^{stoh} and M_{lv}^{stoc} , the heat capacity of the storage fluid cp_{st} , and the difference between the temperatures of hot and cold storages t_{lv}^{stoh} and t_{lv}^{stoc} in the given level. Additionally, the minimum storage volume required for a given tank, V_{lv}^{stoh} and V_{lv}^{stoc} is directly proportional to the minimum storage mass required for the tank and inversely proportional the density of the storage fluid, ρ_{st} .

$$\max\{Q_{p,l_v}^h\} - \min\{Q_{p,l_v}^h\} = (t_{lv}^{stoh} - t_{lv}^{stoc}) cp_{st} M_{lv}^{stoh} \quad (4-113)$$

$$\max\{Q_{p,l_v}^c\} - \min\{Q_{p,l_v}^c\} = (t_{lv}^{stoh} - t_{lv}^{stoc}) cp_{st} M_{lv}^{stoc} \quad (4-114)$$

$$\frac{M_{lv}^{stoh}}{\rho_{st}} = V_{lv}^{stoh} \quad (4-115)$$

$$\frac{M_{lv}^{stoc}}{\rho_{st}} = V_{lv}^{stoc} \quad (4-116)$$

Equations (4-117) to (4-127) group logical relations and conditions for different parameters of the storage system. Equations (4-117) and (4-118) assign temperatures for hot and cold storage streams at the first and last intra-process stages. Equations (4-119) and (4-120) provide monotonicity constraints to the temperatures of the hot and cold storage streams. Equations (4-121) and (4-122) establish that the cumulated energy at a given storage at the end of the process cycle should be equal to the cumulated energy at the beginning of the cycle, in order to restart the cycle. Equation (4-123) to (4-125) state that the cold storage tank in a given level acts like the hot storage tank of the next level. These equations are valid for all energy levels except the last, where the cold storage tank do not serve as a hot storage tank for another energy level. Finally, equations (4-126) and (4-127) establish that a given period of operation only one stream per level is active, the hot or the cold storage stream. Binary variable $y_{p,lv}^{charge}$ acts like a switch variable, with value 1 if the hot storage tank in the given level is charged during the period and value 0 if the hot storage tank in the given level is not charged and therefore discharged during the period. The term Ψ is an upper limit to the energy rate transferred to the storage tanks in the given period. In periods where the hot and cold streams are balanced and no charge or discharge of storages takes place, the values for the heat transfer to and from the storage streams are zero and the value of $y_{p,lv}^{charge}$ has no relevance in the calculations.

$$t_{1,lv}^{stoc} = t_{1,lv}^{stoh} = t_{lv}^{stoh} \quad (4-117)$$

$$t_{NOK+1,lv}^{stoc} = t_{NOK+1,lv}^{stoh} = t_{lv}^{stoc} \quad (4-118)$$

$$t_{k,lv}^{stoc} \geq t_{k+1,lv}^{stoc} \quad (4-119)$$

$$t_{k,lv}^{stoh} \geq t_{k+1,lv}^{stoh} \quad (4-120)$$

$$Q_{NOP,lv}^h = Q_{lv,start}^h \quad (4-121)$$

$$Q_{NOP,lv}^c = Q_{lv,start}^c \quad (4-122)$$

$$Q_{p,lv}^c = Q_{p,lv+1}^h, \forall lv < NOLV \quad (4-123)$$

$$M_{lv}^{stc} = M_{lv+1}^{sth}, \forall lv < NOLV \quad (4-124)$$

$$t_{lv}^{stc} = t_{lv+1}^{sth}, \forall lv < NOLV \quad (4-125)$$

$$q_{p,lv}^{charh} \leq \Psi y_{p,lv}^{charge} \quad (4-126)$$

$$q_{p,lv}^{charc} \leq \Psi (1 - y_{p,lv}^{charge}) \quad (4-127)$$

Finally, equations (4-128) to (4-135) calculate the heat transfer duties, approach temperatures and heat transfer areas of the individual heat exchangers located between the process streams and the storage streams.

$$q_{i,k,p,lv}^{stoc} - \Omega z_{i,k,lv}^{stoc} \leq 0 \quad (4-128)$$

$$q_{j,k,p,lv}^{stoh} - \Omega z_{j,k,lv}^{stoh} \leq 0 \quad (4-129)$$

$$\Delta T_{min} \leq dt1_{i,k,p}^{stoc} \leq t_{i,k,p} - t_{k,p,lv}^{stoc} + \Gamma(1 - z_{i,k,lv}^{stoc}) \quad (4-130)$$

$$\Delta T_{min} \leq dt2_{i,k,p}^{stoc} \leq t_{i,k+1,p} - t_{k+1,p,lv}^{stoc} + \Gamma(1 - z_{i,k,lv}^{stoc}) \quad (4-131)$$

$$\Delta T_{min} \leq dt1_{j,k,p}^{stoh} \leq t_{j,k,p} - t_{k,p,lv}^{stoh} + \Gamma(1 - z_{j,k,lv}^{stoh}) \quad (4-132)$$

$$\Delta T_{min} \leq dt2_{j,k,p}^{stoh} \leq t_{j,k+1,p} - t_{k+1,p,lv}^{stoh} + \Gamma(1 - z_{j,k,lv}^{stoh}) \quad (4-133)$$

$$A_{i,k,lv}^{stoc} \geq \frac{q_{i,k,p,lv}^{stoc}}{U_{i,k,p}^{stoc} LMTD_{i,k,p}^{stoc}}, \quad (4-134)$$

$$A_{j,k,lv}^{stoh} \geq \frac{q_{j,k,p,lv}^{stoh}}{U_{j,k,p}^{stoh} LMTD_{ijk,p}^{stoh}} \quad (4-135)$$

4.2.3.2 Organic Rankine Cycles (MP-ST-ORC)

In principle, MP-ST-ORC is similar to MP-ORC, as illustrated in Figure 4-9. As with previous diagrams, Figure 4-9 does not include all possible matches between the process streams (e.g., streams splits, etc.). Also for clarity, only two storage levels (three storage tanks) and two hot and two cold process streams are presented, but the superstructure and its associated mathematical model are suitable for any arbitrary number of process streams and storage levels.

Process streams exchange energy in the intra-process stages of the superstructure while the energy exchange between the working fluid of the ORC and the process streams takes place in a dedicated ORC stage located at the cold end of the process streams, after the last intra-process stage. The energy supplied by the hot process streams to the ORC-Evaporators drives the ORC cycle as described in HEN-ORC and MP-ORC, and the remaining energy after the expansion of the working fluid in the ORC-Turbine can be used to heat the cold process streams in the ORC-Condensers. The operating conditions in each period of operation differ but the evaporating and condensing pressures, and therefore the evaporating and condensing temperatures in the ORC, remain constant in all periods.

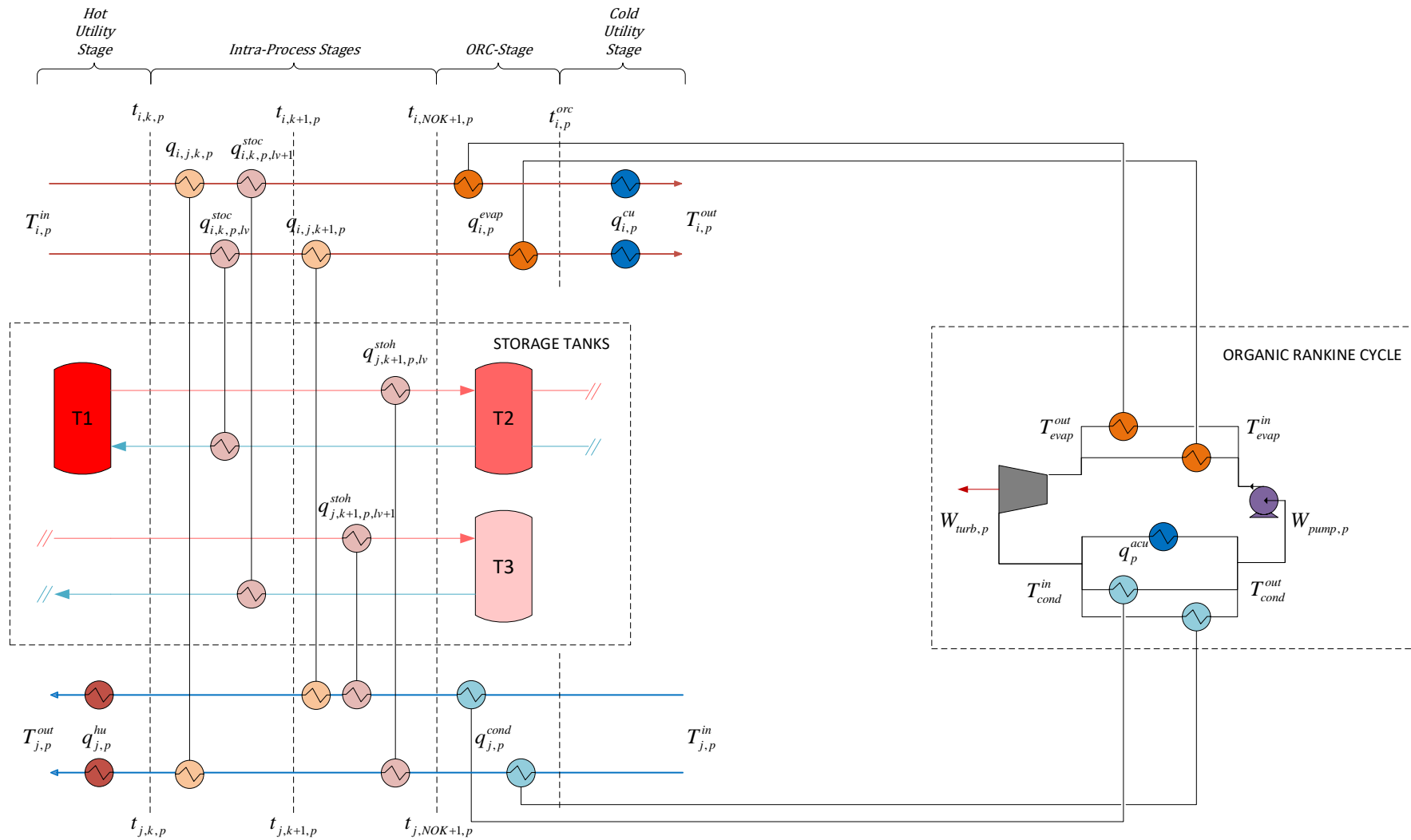


Figure 4-9. Schematic representation of the Superstructure for the Process Integration of Organic Rankine Cycles into Multi-Period Processes with FTVM Heat Storage Tanks (MP-ST-ORC)

Source: Own diagram

Additionally, the process streams can exchange heat with the storage system using heat exchangers located also in the intra-process stages. Hot process streams can exchange energy with the storage system only by supplying energy to cold storage streams, which will then be fed to the hot storage tanks in each level at their corresponding storage temperature. As a result of this mechanism, the cold storage streams will effectively charge the hot storage tanks with excess energy from the hot process streams, while simultaneously discharging the cold storage tanks. Likewise, the cold process streams can exchange energy with the storage system by receiving energy from the hot storage streams, which after releasing their energy, is fed to the cold storage tanks in each level at their corresponding storage temperature, effectively discharging the hot storage tanks while charging the cold storage tanks. At a given period and energy level, only one storage stream, hot or cold, is active, charging or discharging the hot storage tank, in that energy level, while simultaneously discharging or charging the corresponding cold storage tank. As mentioned before, the temperatures at each storage tank remain fixed during the whole cycle and are calculated during the optimization process.

The mathematical formulation for MP-ST-ORC is an extension of MP-ORC developed in section 4.2.2. Similar to MP-ORC most of the equations in MP-ST-ORC are the multi-period version of equations of the continuous HEN-ORC model, with variables and parameters adapted to the multi-period operation as presented in Table 4-6, but including terms representing the interactions between the process streams and the storage system. Additional equations describing the behavior of the storage tanks as well as the storage streams are also required as presented in Table 4-4. As mentioned before, only equations from MP-ORC that are modified to describe the interaction between the process streams and the storage system are presented in this section. For the equations describing the internal dynamics of the storage system please see section 4.2.3.1 and for an explicit presentation of all the constituent equations of MP-ST-ORC, please see Appendix C.

Equations (4-136) and (4-137) present the overall energy balances for the hot and cold process streams $i \in HP$ and $j \in CP$ at each period of operation $p \in P$. The expressions are equivalent to those used in MP-ORC but with additional terms representing the energy exchanged between the process streams and the storage system. In the overall energy balance for the hot process streams in equation (4-136), $q_{i,k,p,lv}^{stoc}$ represents the rate of the energy exchanged in stage $k \in ST$ between the hot process stream $i \in HP$ and the cold storage stream in energy level $lv \in LV$ during period $p \in P$. Similarly in equation (4-137) corresponding to the overall energy balance for the cold process streams, $q_{j,k,p,lv}^{stoh}$ represents the rate of the energy exchanged in stage $k \in$

ST between the cold process stream $j \in CP$ and the hot storage stream in energy level $lv \in LV$ during period $p \in P$. Equations (4-138) and (4-139) illustrate the energy balances for the intra-process stages for the hot and cold process streams at each period $p \in P$. At each period $p \in P$ the hot process streams $i \in HP$ in stage $k \in ST$ can exchange energy at a rate $q_{i,j,k,p}$ with each of the cold process streams $j \in CP$ or exchange energy at a rate $q_{i,k,p,lv}^{stoc}$ with the cold storage streams at each level $lv \in LV$. The enthalpy change in the hot process stream in that stage is equivalent to the product of the heat capacity flowrate of the stream at that period ($F_{i,p}$) and the temperatures of the stream at the inlet ($t_{i,k,p}$) and outlet ($t_{i,k+1,p}$) of the stage at that period.

A similar expression is used for the stage energy balance for the cold process streams, where at each period $p \in P$ the cold process streams $j \in CP$ in stage $k \in ST$ can exchange energy at a rate $q_{i,j,k,p}$ with each of the hot process streams $i \in HP$ or exchange energy at a rate $q_{i,k,p,lv}^{stoh}$ with the hot storage streams at each level $lv \in LV$. The enthalpy change in the cold process stream in that stage is equivalent to the product of the heat capacity flowrate of the stream at that period ($F_{j,p}$) and the temperatures of the stream at the inlet ($t_{j,k,p}$) and outlet ($t_{j,k+1,p}$) of the stage at that period.

$$\sum_{j \in CP} \sum_{k \in ST} q_{i,j,k,p} + \sum_{k \in ST} \sum_{lv \in LV} q_{i,k,p,lv}^{stoc} + q_{i,p}^{evap} + q_{i,p}^{cu} = F_{i,p}(T_{i,p}^{in} - T_{i,p}^{out}) \quad (4-136)$$

$$\sum_{i \in HP} \sum_{k \in ST} q_{i,j,k,p} + \sum_{k \in ST} \sum_{lv \in LV} q_{j,k,p,lv}^{stoh} + q_{j,p}^{cond} + q_{j,p}^{hu} = F_{j,p}(T_{j,p}^{out} - T_{j,p}^{in}) \quad (4-137)$$

$$\sum_{j \in CP} q_{i,j,k,p} + \sum_{lv \in LV} q_{i,k,p,lv}^{stoc} = F_{i,p}(t_{i,k,p} - t_{i,k+1,p}) \quad (4-138)$$

$$\sum_{i \in HP} q_{i,j,k,p} + \sum_{lv \in LV} q_{j,k,p,lv}^{stoh} = F_{j,p}(t_{j,k,p} - t_{j,k+1,p}) \quad (4-139)$$

For MP-ST-ORC the objective function, TAC as presented in equations (4-140) to (4-143), is defined as the sum of all annual operating costs and annualized capital costs of all subsystems, that is, the HEN, the ORC and the storage system. The costs for the storage fluid or pumping cost of the storage system are not considered (See Section 1.3 for a detail list of all the assumptions).

$$\min TAC = TAC_{HEN} + TAC_{ORC} + TAC_{STO} \quad (4-140)$$

$$TAC_{HEN} = \left\{ \begin{array}{l} H_y \sum_{p \in P} \left(\frac{DOP_p}{\sum_{p \in P} DOP_p} \right) \left(\sum_{j \in CP} c_{hu_p} q_{j,p}^{hu} + \sum_{i \in HP} c_{cu_p} q_{i,p}^{cu} \right) \\ + AF c_{fix}^{HEN} \left(\sum_{i \in HP} \sum_{j \in CP} \sum_{k \in ST} z_{i,j,k} + \sum_{i \in HP} z_i^{cu} + \sum_{j \in CP} z_j^{hu} \right) \\ + AF c_{var}^{HEN} \left(\sum_{i \in HP} \sum_{j \in CP} \sum_{k \in ST} (A_{i,j,k})^{\beta^{HEN}} \right. \\ \left. + \sum_{i \in HP} (A_i^{cu})^{\beta^{HEN}} + \sum_{j \in CP} (A_j^{hu})^{\beta^{HEN}} \right) \end{array} \right\} \quad (4-141)$$

$$TAC_{ORC} = \left\{ \begin{array}{l} H_y \sum_{p \in P} \left(\frac{DOP_p}{\sum_{p \in P} DOP_p} \right) (-e_{price_p} W_{turb_p} + e_{cost_p} W_{pump_p}) \\ + AF c_{fix}^{HEN} \left(\sum_{i \in HP} z_i^{evap} + \sum_{j \in CP} z_j^{cond} + z_{acu} \right) \\ + AF c_{var}^{HEN} \left(\sum_{i \in HP} (A_i^{evap})^{\beta^{HEN}} + \sum_{j \in CP} (A_j^{cond})^{\beta^{HEN}} + (A_{acu})^{\beta^{HEN}} \right) \\ + AF \left(c_{fix}^{pump} + c_{var}^{pump} (W_{pump}^{max})^{\beta^{pump}} \right) \\ + AF \left(c_{fix}^{turb} + c_{var}^{turb} (W_{turb}^{max})^{\beta^{turb}} \right) \end{array} \right\} \quad (4-142)$$

$$TAC_{STO} = \left\{ \begin{array}{l} AF c_{fix}^{HEN} \left(\sum_{i \in HP} \sum_{k \in ST} \sum_{lv \in LV} z_{i,k,lv}^{stoc} + \sum_{j \in CP} \sum_{k \in ST} \sum_{lv \in LV} z_{j,k,lv}^{stoh} \right) \\ + AF c_{var}^{HEN} \left(\sum_{i \in HP} \sum_{k \in ST} \sum_{lv \in LV} (A_{i,k,lv}^{stoc})^{\beta^{HEN}} + \sum_{j \in CP} \sum_{k \in ST} \sum_{lv \in LV} (A_{j,k,lv}^{stoh})^{\beta^{HEN}} \right) \\ + AF \left(\sum_{lv \in LV} c_{fix}^{sto} + c_{var}^{sto} \sum_{lv \in LV} (V_{lv}^{stoh})^{\beta^{sto}} \right) \\ + AF \left(c_{fix}^{sto} + c_{var}^{sto} (V_{NOLV}^{stoc})^{\beta^{sto}} \right) \end{array} \right\} \quad (4-143)$$

4.2.3.3 Absorption Chillers (MP-ST-ABC)

Figure 4-10 illustrates the superstructure for the process integration of ABCs into HENs in multi-period processes with FTVM heat storage (MP-ST-ABC). As with previous diagrams, Figure 4-10 does not include all possible matches between the process streams (e.g., streams splits, etc.). Also for clarity, only two storage levels (three storage tanks) and two hot and two cold process streams are presented, but the superstructure and its associated mathematical model are suitable for any arbitrary number of process streams and storage levels.

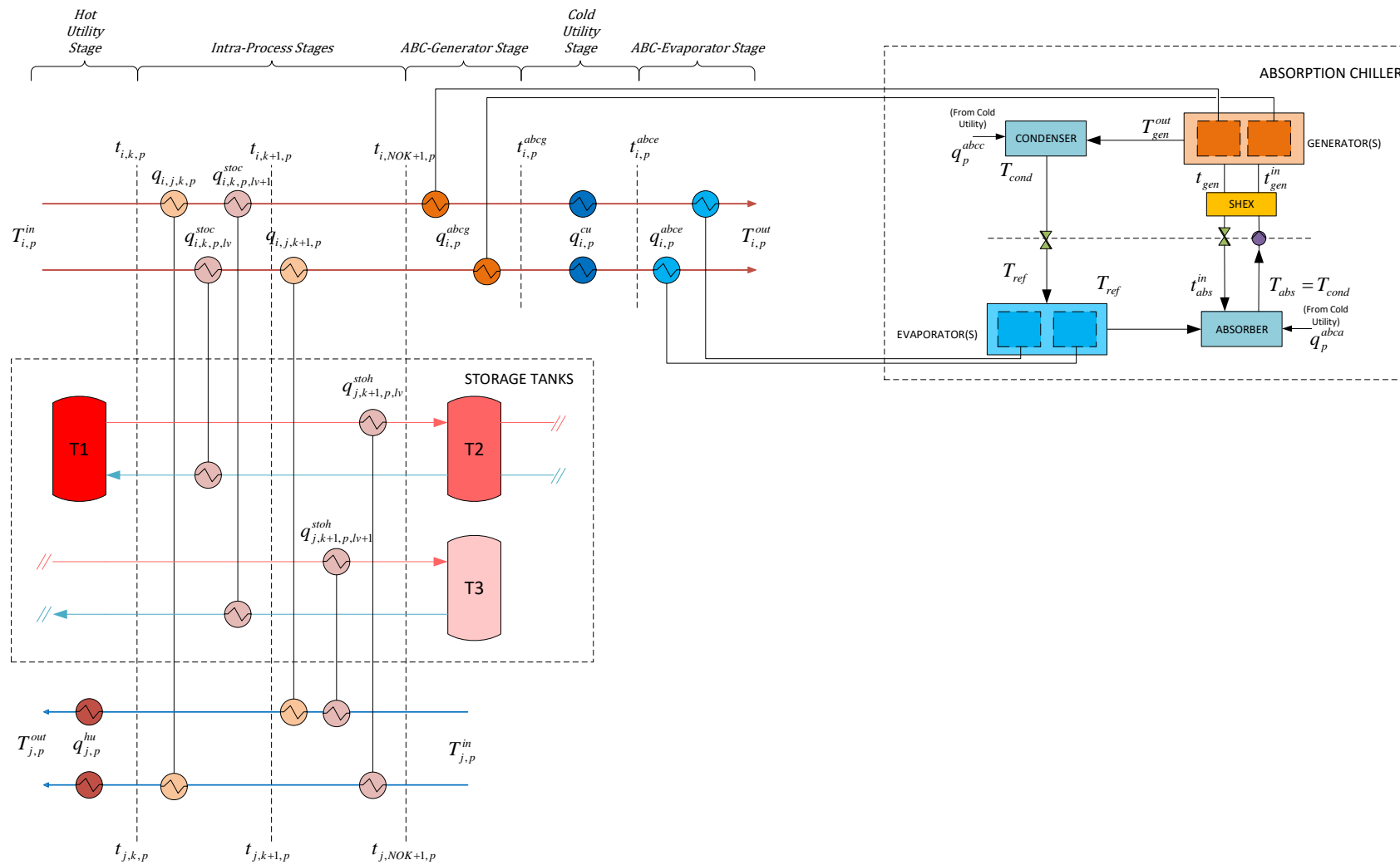


Figure 4-10. Schematic representation of the Superstructure for the Process Integration of Absorption Chillers into Multi-Period Processes with FTVM Heat Storage Tanks (MP-ST-ABC)

Source: Own diagram

Similar as with MP-ST-ORC, only the equations from MP-ABC that have been modified to describe the interaction between the process streams and the storage system are provided. In MP-ST-ABC, intra-process energy exchange and between the process streams and the storage system takes place in the inner stages of the superstructure. Hot process streams can then reject heat to the ABC-Generators located between the cold utility and the last intra-process stage. This energy drives the refrigeration cycle, as described for HEN-ABC and MP-ABC. The cooling effect generated in the refrigeration cycle can then be used to cool the hot process streams through heat exchange in the ABC-Evaporators, located after the cold utility stage, at the cold end of the superstructure. The temperatures inside the refrigeration cycle remain constant during all periods of operation but the temperatures of the process streams in each location of the superstructure as well as the duties of heat exchangers (intra-process or between the process streams and the refrigeration cycle) change depending on the operating conditions. As for the storage system, energy absorbed from the hot process streams in one period can be used to heat the cold process streams in another period through the mechanism explained in section 4.2.3.1. Appendix C provides the full mathematical description of the model.

Equations (4-144) to (4-147) provide the new energy balances for the process streams and stages due to the integration of the storage system. These equations are analogue to those presented for MP-ST-ORC.

$$\sum_{j \in CP} \sum_{k \in ST} q_{i,j,k,p} + \sum_{k \in ST} \sum_{lv \in LV} q_{i,k,p,lv}^{stoc} + q_{i,p}^{abce} + q_{i,p}^{cu} + q_{i,p}^{abcc} = F_{i,p}(T_{i,p}^{in} - T_{i,p}^{out}) \quad (4-144)$$

$$\sum_{i \in HP} \sum_{k \in ST} q_{i,j,k,p} + \sum_{k \in ST} \sum_{lv \in LV} q_{j,k,p,lv}^{stoh} + q_{j,p}^{hu} = F_{j,p}(T_{j,p}^{out} - T_{j,p}^{in}) \quad (4-145)$$

$$\sum_{j \in CP} q_{i,j,k,p} + \sum_{lv \in LV} q_{i,k,p,lv}^{stoc} = F_{i,p}(t_{i,k,p} - t_{i,k+1,p}) \quad (4-146)$$

$$\sum_{i \in HP} q_{i,j,k,p} + \sum_{lv \in LV} q_{j,k,p,lv}^{stoh} = F_{j,p}(t_{j,k,p} - t_{j,k+1,p}) \quad (4-147)$$

The objective function for MP-ST-ABC, TAC as defined in equations (4-148) to (4-151), is equal to the sum of the annual operating costs the annualized capital costs of all its constituent subsystems including the storage. Also, similarly to HEN-ABC and MP-ABC, pump capital cost, pumping costs and ABC-Condenser and ABC-Absorber fixed costs are not considered.

$$\min TAC = TAC_{HEN} + TAC_{ABC} + TAC_{sto} \quad (4-148)$$

$$TAC_{HEN} = \left\{ \begin{array}{l} H_y \sum_{p \in P} \left(\frac{DOP_p}{\sum_{p \in P} DOP_p} \right) \left(\sum_{j \in CP} c_{hu_p} q_{j,p}^{hu} + \sum_{i \in HP} c_{cu_p} q_{i,p}^{cu} \right) \\ + AF c_{fix}^{HEN} \left(\sum_{i \in HP} \sum_{j \in CP} \sum_{k \in ST} z_{i,j,k} + \sum_{i \in HP} z_i^{cu} + \sum_{j \in CP} z_j^{hu} \right) \\ + AF c_{var}^{HEN} \left(\sum_{i \in HP} \sum_{j \in CP} \sum_{k \in ST} (A_{i,j,k})^{\beta^{HEN}} \right. \\ \left. + \sum_{i \in HP} (A_i^{cu})^{\beta^{HEN}} + \sum_{j \in CP} (A_j^{hu})^{\beta^{HEN}} \right) \end{array} \right\} \quad (4-149)$$

$$TAC_{ABC} = \left\{ \begin{array}{l} H_y \sum_{p \in P} \left(\frac{DOP_p}{\sum_{p \in P} DOP_p} \right) (c_{cu} (q_p^{abcc} + q_p^{abca})) \\ + AF c_{fix}^{HEN} \left(\sum_{i \in HP} z_i^{abcg} + \sum_{i \in HP} z_i^{abce} \right) \\ + AF c_{var}^{HEN} \left(\sum_{i \in HP} (A_i^{abcg})^{\beta^{HEN}} + \sum_{i \in HP} (A_i^{abce})^{\beta^{HEN}} \right. \\ \left. + (A^{abcc})^{\beta^{HEN}} + (A^{abca})^{\beta^{HEN}} \right) \end{array} \right\} \quad (4-150)$$

$$TAC_{STO} = \left\{ \begin{array}{l} AF c_{fix}^{HEN} \left(\sum_{i \in HP} \sum_{k \in ST} \sum_{lv \in LV} z_{i,k,lv}^{stoc} + \sum_{j \in CP} \sum_{k \in ST} \sum_{lv \in LV} z_{j,k,lv}^{stoh} \right) \\ + AF c_{var}^{HEN} \left(\sum_{i \in HP} \sum_{k \in ST} \sum_{lv \in LV} (A_{i,k,lv}^{stoc})^{\beta^{HEN}} + \sum_{j \in CP} \sum_{k \in ST} \sum_{lv \in LV} (A_{j,k,lv}^{stoh})^{\beta^{HEN}} \right) \\ + AF \left(\sum_{lv \in LV} c_{fix}^{sto} + c_{var}^{sto} \sum_{lv \in LV} (V_{lv}^{stoh})^{\beta^{sto}} \right) \\ + AF (c_{fix}^{sto} + c_{var}^{sto} (V_{NOLV}^{stoc})^{\beta^{sto}}) \end{array} \right\} \quad (4-151)$$

4.2.3.4 Combined Model (MP-ST-WHR)

Figure 4-11 presents a schematic representation of the superstructure for the process integration of ORCs and ABCs into HENs in multi-period processes with FTVM heat storage (MP-ST-WHR). As with previous diagrams, Figure 4-11 does not include all possible matches between the process streams (e.g., streams splits, etc.). Also for clarity, only two storage levels (three storage tanks) and two hot and two cold process streams are presented, but the superstructure and its associated mathematical model are suitable for any arbitrary number of process streams and storage levels. The superstructure is a combination of MP-ST-ORC and MP-ST-ABC.

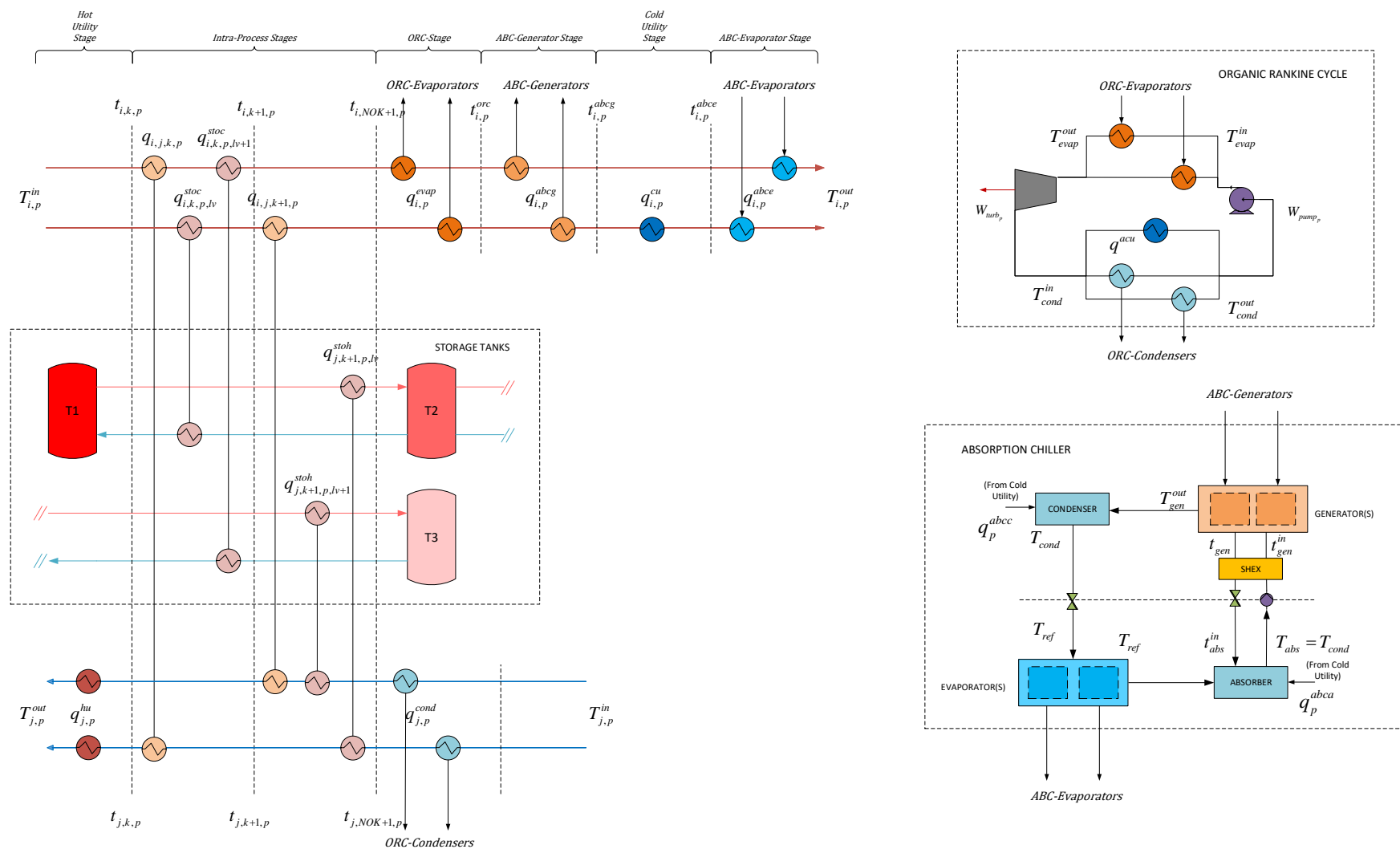


Figure 4-11. Schematic representation of the Superstructure for the Process Integration of Organic Rankine Cycles and Absorption Chillers into Multi-Period Processes with FTVM Heat Storage Tanks (MP-ST-WHR)

Source: Own diagram

In MP-ST-WHR the intra-process energy exchange takes place in the inner stages of the superstructure, where also the process streams can exchange energy with the storage system. The energy exchange between the process streams and the working fluid circulating through the ORC occurs in a dedicated ORC stage located directly after the last intra-process stage. The energy provided to the working fluid in this stage by the hot process streams drives the power cycle as described in HEN-ORC, MP-ORC and MP-ST-ORC. The hot process streams can then supply energy to the refrigeration cycle at the ABC-Generators located between the cold utilities and the ORC stage. This energy drives the refrigeration cycle as explained in HEN-ABC, MP-ABC and MP-ST-ABC. The refrigeration effect generated in the cycle is then used to cool the hot process streams in the ABC-Evaporators located in the cold end of the superstructure after the cold utility. Hot utilities at the hot end of the superstructure provide the remaining energy required by the cold process streams to achieve their target temperatures. Similar to MP-ST-ORC and MP-ST-ABC, energy absorbed in the storage system from the hot process streams in one period can be used to heat the cold process streams in another period through the mechanism explained in section 4.2.3.1. Equations (4-152) to (4-155) provide the new overall energy balances for the process streams and the energy balances for each on the intra-process stages in the superstructure. An explicit presentation of all the equations in MP-ST-WHR is available in Appendix C.

$$\sum_{j \in CP} \sum_{k \in ST} q_{i,j,k,p} + \sum_{k \in ST} \sum_{lv \in LV} q_{i,k,p,lv}^{stoc} + q_{i,p}^{evap} + q_{i,p}^{abce} + q_{i,p}^{cu} + q_{i,p}^{abcc} = F_{i,p} (T_{i,p}^{in} - T_{i,p}^{out}) \quad (4-152)$$

$$\sum_{i \in HCP} \sum_{k \in ST} q_{i,j,k,p} + \sum_{k \in ST} \sum_{lv \in LV} q_{j,k,p,lv}^{stoh} + q_{j,p}^{cond} + q_{j,p}^{hu} = F_{j,p} (T_{j,p}^{out} - T_{j,p}^{in}) \quad (4-153)$$

$$\sum_{j \in CP} q_{i,j,k,p} + \sum_{lv \in LV} q_{i,k,p,lv}^{stoc} = F_{i,p} (t_{i,k,p} - t_{i,k+1,p}) \quad (4-154)$$

$$\sum_{i \in HCP} q_{i,j,k,p} + \sum_{lv \in LV} q_{j,k,p,lv}^{stoh} = F_{j,p} (t_{j,k,p} - t_{j,k+1,p}) \quad (4-155)$$

As for MP-ST-WHR objective function, the Total Annualized Cost (TAC) is defined as the sum of the TACs of all subsystems including the storage. Equations (4-156) to (4-160) present the TAC of MP-ST-WHR.

$$\min TAC = TAC_{HEN} + TAC_{ORC} + TAC_{ABC} + TAC_{Sto} \quad (4-156)$$

$$TAC_{HEN} = \left\{ \begin{array}{l} H_y \sum_{p \in P} \left(\frac{DOP_p}{\sum_{p \in P} DOP_p} \right) \left(\sum_{j \in CP} c_{hu_p} q_{j,p}^{hu} + \sum_{i \in HP} c_{cu_p} q_{i,p}^{cu} \right) \\ + AF c_{fix}^{HEN} \left(\sum_{i \in HP} \sum_{j \in CP} \sum_{k \in ST} z_{i,j,k} + \sum_{i \in HP} z_i^{cu} + \sum_{j \in CP} z_j^{hu} \right) \\ + AF c_{var}^{HEN} \left(\sum_{i \in HP} \sum_{j \in CP} \sum_{k \in ST} (A_{i,j,k})^{\beta^{HEN}} \right. \\ \left. + \sum_{i \in HP} (A_i^{cu})^{\beta^{HEN}} + \sum_{j \in CP} (A_j^{hu})^{\beta^{HEN}} \right) \end{array} \right\} \quad (4-157)$$

$$TAC_{ORC} = \left\{ \begin{array}{l} H_y \sum_{p \in P} \left(\frac{DOP_p}{\sum_{p \in P} DOP_p} \right) (-e_{price_p} W_{turb_p} + e_{cost_p} W_{pump_p}) \\ + AF c_{fix}^{HEN} \left(\sum_{i \in HP} z_i^{evap} + \sum_{j \in CP} z_j^{cond} + z_{acu} \right) \\ + AF c_{var}^{HEN} \left(\sum_{i \in HP} (A_i^{evap})^{\beta^{HEN}} + \sum_{j \in CP} (A_j^{cond})^{\beta^{HEN}} + (A_{acu})^{\beta^{HEN}} \right) \\ + AF \left(c_{fix}^{pump} + c_{var}^{pump} (W_{pump}^{max})^{\beta^{pump}} \right) \\ + AF \left(c_{fix}^{turb} + c_{var}^{turb} (W_{turb}^{max})^{\beta^{turb}} \right) \end{array} \right\} \quad (4-158)$$

$$TAC_{ABC} = \left\{ \begin{array}{l} H_y \sum_{p \in P} \left(\frac{DOP_p}{\sum_{p \in P} DOP_p} \right) (c_{cu} (q_p^{abcc} + q_p^{abca})) \\ + AF c_{fix}^{HEN} \left(\sum_{i \in HP} z_i^{abcg} + \sum_{i \in HP} z_i^{abce} \right) \\ + AF c_{var}^{HEN} \left(\sum_{i \in HP} (A_i^{abcg})^{\beta^{HEN}} + \sum_{i \in HP} (A_i^{abce})^{\beta^{HEN}} \right) \\ + (A^{abcc})^{\beta^{HEN}} + (A^{abca})^{\beta^{HEN}} \end{array} \right\} \quad (4-159)$$

$$TAC_{STO} = \left\{ \begin{array}{l} AF c_{fix}^{HEN} \left(\sum_{i \in HP} \sum_{k \in ST} \sum_{lv \in LV} z_{i,k,lv}^{stoc} + \sum_{j \in CP} \sum_{k \in ST} \sum_{lv \in LV} z_{j,k,lv}^{stoh} \right) \\ + AF c_{var}^{HEN} \left(\sum_{i \in HP} \sum_{k \in ST} \sum_{lv \in LV} (A_{i,k,lv}^{stoc})^{\beta^{HEN}} + \sum_{j \in CP} \sum_{k \in ST} \sum_{lv \in LV} (A_{j,k,lv}^{stoh})^{\beta^{HEN}} \right) \\ + AF \left(\sum_{lv \in LV} c_{fix}^{sto} + c_{var}^{sto} \sum_{lv \in LV} (V_{lv}^{stoh})^{\beta^{sto}} \right) \\ + AF (c_{fix}^{sto} + c_{var}^{sto} (V_{NOLV}^{stoc})^{\beta^{sto}}) \end{array} \right\} \quad (4-160)$$

4.3 Mathematical Considerations and Models Limitations

As mentioned in section 2.4.2 the MINLP SYNHEAT model for the synthesis of HENs is an NP-Hard problem in the strong sense (Furman and Sahinidis 2001), that is, no known algorithm exists that can provide an exact solution (deterministic) to the problem in a computationally efficient way. All the models developed in this chapter are an extension of the SYNHEAT model and therefore they are also NP-Hard problems. That being said, a number of strategies have been developed to facilitate the generation of good local solutions for SYNHEAT and they can be adapted to solve the models developed in this chapter. The possible strategies include the linearization of non-linear terms in the formulation (Beck and Hofmann 2018a), the sequential solution of an MILP version (removing non-linear terms in the objective function) and then a NLP version of the problem with binary variables fixed to the results of the previous MILP problem in order to generate an initial feasible solution (Escobar and Trierweiler 2013) and heuristic rules for the initialization of the MINLP problem (Yee and Grossmann 1990). These procedures seek to transform the MINLP into an MILP that can be then solved to global optimality without requiring initial values (simplification) or to generate good starting points for the MINLP in order to facilitate the generation of good local solutions (initialization).

Even after using simplification and initialization strategies, MP methods for the synthesis of HENs (simultaneous or sequential) are rarely applied to problems with more than 30 streams for continuous processes, which is a relatively low number for industrial applications. For discontinuous processes the maximum number of streams that the MP formulations can handle is notably lower. Approximations with relatively large optimality gaps¹² (10% or more) help to decrease the computational effort (and time) required to obtain local solutions but in general the application of MP methods to large scale real-life industrial problems is impractical (Chen et al. 2015b).

Another mathematical limitation of the SYNHEAT model, and therefore the extensions presented in this chapter, is the approximation of the LMTD for the calculation of heat transfer areas of heat exchangers. The LMTD as defined in equation (4-161), is a discontinuous function which creates numerical problems for most of the available commercial solvers when the approach temperatures at both ends of a given heat exchanger are equal (division by zero). In

¹² Optimality gap is defined as the difference between the best known upper and lower bounds of an optimization problem. In percentage form (relative gap) represents the ratio between the difference of the upper and lower bounds and the upper bound (in case of minimization).

order to solve this, approximations to the LMTD such as the Paterson (Paterson 1984) and Chen (Chen 1987) approximations are used.

Equations (4-162) and (4-163) present the Paterson and Chen approximations, respectively. In most of the reviewed literature as well as in this work, the Chen approximation is used to calculate the LMTD. Figure 4-12 presents a comparison between different approximations to the LMTD, including the approximation using the arithmetic mean of the approach temperatures. From the diagram is clear that the simple arithmetic mean between $\Delta T_{Hot-End}$ and $\Delta T_{Cold-End}$ is a bad approximation of the LMTD. Paterson's provide more accurate results and a small overestimation of the LMTD (underestimating the heat transfer area) and Chen's a simpler formulation and a small underestimation of the LMTD (overestimating the heat transfer area). For conservative estimations of TAC, Chen's is preferred as it underestimates the LMTD, overestimating the calculated heat transfer area (and therefore TAC).

$$LMTD (\Delta T_{Hot-End}, \Delta T_{Cold-End}) = \begin{cases} \frac{\Delta T_{Hot-End} - \Delta T_{Cold-End}}{\ln \left(\frac{\Delta T_{Hot-End}}{\Delta T_{Cold-End}} \right)}, & \text{if } \Delta T_{Hot-End} \neq \Delta T_{Cold-End} \\ \Delta T_{Hot-End} = \Delta T_{Cold-End}, & \text{if } \Delta T_{Hot-End} = \Delta T_{Cold-End} \end{cases} \quad (4-161)$$

$$LMTD (\Delta T_{Hot-End}, \Delta T_{Cold-End}) = \frac{1}{6} (\Delta T_{Hot-End} + \Delta T_{Cold-End}) + \frac{2}{3} (\Delta T_{Hot-End} \Delta T_{Cold-End})^{\frac{1}{2}} \quad (4-162)$$

$$LMTD (\Delta T_{Hot-End}, \Delta T_{Cold-End}) = \left(\Delta T_{Hot-End} \Delta T_{Cold-End} \left(\frac{\Delta T_{Hot-End} + \Delta T_{Cold-End}}{2} \right) \right)^{\frac{1}{3}} \quad (4-163)$$

Other mathematical or structural limitations inherited from the SYNHEAT model and applicable to the nine superstructures developed in this work include the isothermal mixing assumption and the disregard of configurations with stream splits going through multiple heat exchangers (Yee and Grossmann 1990).

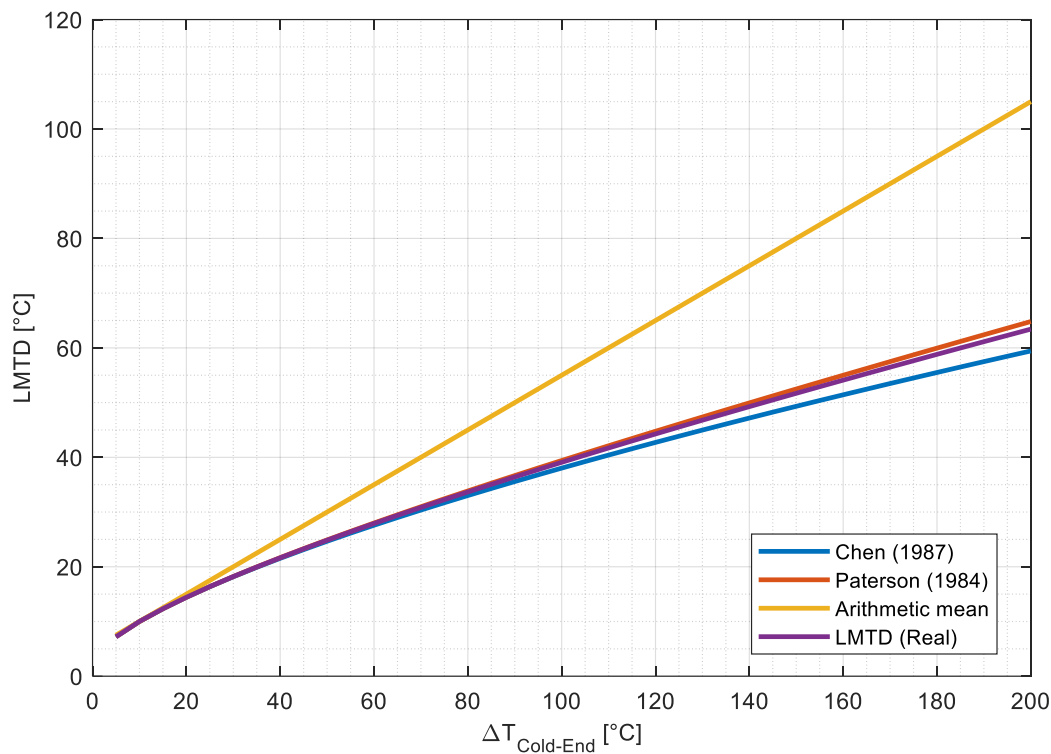


Figure 4-12. Approximations to the logarithmic mean temperature difference. $\Delta T_{\text{Hot-End}} = 10^{\circ}\text{C}$ (Fixed).

Source: Own diagram based on Verheyen and Zhang (2006)

Finally, some model limitations are not a product of the computational effort required or numerical complications but are the product of the design of the superstructures. The main structural limitation of the nine superstructures presented in this work is that they only allow heat exchange between the process streams and the WHR technologies on dedicated stages located at the cold end of the superstructure, before and/or after the cold utility stage. This limitation simplifies the mathematical formulation and decreases the computational effort required to solve the MINLP models in comparison with superstructures allowing heat transfer between process streams and WHR technologies in any stage, at the cost of neglecting possible configurations that could be beneficial to the system performance. Without the use of linearization or simplification techniques, superstructures allowing the integration of WHR technologies in any stage, in particular for multi-period processes, are impractical, due to the sheer number of variables involved, as well as the complexity of the mathematical formulations.

Other structural limitations are the interactions between the WHR technologies and between the WHR technologies and the storage system. For the continuous models as well as the models for multi-period processes without heat storage, alternative superstructures could be proposed that consider the interaction between the ORC and the ABC. Examples include the use of the heat rejected from the ORC-Condenser to drive the ABC-Generators or the use of the

refrigeration effect of the ABC to decrease the condensation temperature at the ORC, etc. Additionally, more complex configurations for the ORC (with regeneration, recuperation, multiple pressure levels, etc.) and ABC (double effect, triple effect, etc.) could be included in future studies. The direct interaction between the storage system and the WHR technologies is also not considered in this work, but could be an area of future research. Some works considering the integration of ORCs into industrial processes (without considering the HEN synthesis) have already proposed the use of storage tanks between the process streams and the ORCs in order to limit/damp the fluctuation of its operational parameters (Pili et al. 2017; Pantaleo et al. 2017; Lecompte 2017; Jiménez-Arreola et al. 2018).

5 Applications of the Framework

In this chapter, the superstructures developed for the process integration of ORCs, ABCs or both into HENs in continuous and multi-period processes, with and without FTVM heat storage, are applied to three case studies from the literature. The objective of this chapter is to illustrate the use of the methodology and to discuss possible issues and limitations of the methodology when applied to real industrial cases.

Due to the nature of the MINLP problems in this work, global optimality cannot be guaranteed unless all the possible solutions to the problem are evaluated. This process is resource intensive requiring a large CPU time and memory and therefore unfit to be used on complex problems with a high number of decision variables. Therefore, the results provided in this chapter have to be considered as local optima. For all models and case studies, a maximum CPU time of 3600 s and a minimum optimality gap of 10% was set. The only exception is the prescreening algorithm (see section 5.1.1) used to find the appropriated working fluid and ORC operating temperatures for the case studies, where a optimality gap of 5% was implemented. The optimization is terminated if either of the conditions is fulfilled. If the model does not reach a solution within the accepted tolerance in the maximum time, the best available solution is provided, together with its relative gap to the best known lower bound (best possible solution).

In this work, for all the developed models and case studies, pinch limits to the utility consumptions are used as constraints. That means that the systems generate electricity or cooling without increasing the utility consumption of the system, in practice generating useful work or cooling from waste heat. The results of the optimization problems are presented using summary tables, while only grid diagrams corresponding to the combined models (HEN-WHR, MP-WHR and MP-ST-WHR) are presented in the main body of the dissertation. For additional diagrams please see Appendix D. A complete list of all modeling assumptions is founded in Section 1.3. All models were implemented in GAMS (version 25.1.1) using the global solver BARON to solve the MINLP. The optimizations were performed on a Windows machine with an Intel(R) Core(TM) i7-6600U 2.60 GHz CPU and 12 GB RAM.

5.1 Case Study 1 (Continuous Process)

Table 5-1 presents the information of the process streams for Case Study 1. The problem is an adaptation from a case study published by Hellwig (1998) and it has 8 hot streams and 5 cold streams. The problem is based on selected streams from two different process lines in a refinery (Ripke et al. 1994). Table 5-2 provides design parameters of the system, namely information on the economics of the equipment units and processes for Case Studies 1 and 2.

Table 5-1. Stream data Case Study 1. 8H5C.

Stream	T ⁱⁿ (°C)	T ^{out} (°C)	F (kW/°C)	ΔH (kW)
H1	138.0	134.7	767.6	-2 533.1
H2	135.0	134.3	2 397.1	-1 678.0
H3	134.7	32.0	14.3	-1 468.6
H4	134.3	32.0	9.5	-971.9
H5	107.0	106.9	5 160.0	-516.0
H6	92.0	91.9	16 550.0	-1 655.0
H7	91.9	28.0	13.1	-837.1
H8	106.9	30.0	4.1	-315.3
C1	15.0	142.0	11.6	1 473.2
C2	184.0	186.0	1 999.5	3 999.0
C3	15.0	100.0	10.4	884.0
C4	115.0	117.0	1 363.5	2 727.0
C5	143.0	145.0	1 651.0	3 302.0
HU	255.0	255.0	-	-
CU ^{1), 2)}	10.0/30.0	10.0/30.0	-	-

¹⁾ The cold utility temperature is set to 10.0°C for the stand-alone HEN and HEN-ORC. For models involving absorption chillers (HEN-ABC and HEN-WHR) this temperature is set to 30.0°C.

²⁾ Film coefficients for all streams are $h = 1.0 \text{ kW/m}^2\text{°C}$

Source: Own table with data from Hellwig (1998)

Table 5-2. Design parameters for Case Study 1 and 2

Parameter	General	Heat Exchanger	Turbine	Pump
AF (a ⁻¹)	0.23	-	-	-
Hy (h/a)	8 000	-	-	-
C _{hu} (€/kWh)	0.01	-	-	-
C _{cu} (€/kWh)	0.001	-	-	-
e ^{cost} /e ^{price} (€/kWh)	0.2	-	-	-
Eff. SHEX (ε _{SHEX})	0.7	-	-	-
C _{fix} (€)	-	2 500.0	4 000.0	1 200.0
C _{var} (€/m ^{2β} ; €/kW ^β) ¹⁾	-	1 650.0	2000.0	750.0
β	-	0.65	0.65	0.65
Isentropic Eff. (ε)	-	-	0.8	0.65

¹⁾ Generic units are used for the variable cost coefficients, to generate cost calculations in Euros (€). For heat exchangers €/m^{2β} and for turbines and pumps €/kW^β are used.

Source: Own table

Using $\Delta T_{min} = 15.0 \text{ °C}$ for the minimum approach temperatures between process streams, the pinch analysis of the system provides minimum utility targets of 7 521.4 kW (hot utility) and

5 109.2 kW (cold utility) with a pinch temperature of 130.5 °C, as seen in Figure 5-1. Excess heat is available for heat recovery on the heat surplus region below the pinch at a high temperature as indicated by the high pinch temperature of 130.5 °C, and therefore the integration of an ORC can be an option. Also depending on the available temperature of the cold utility, the integration of an ABC to supply cooling from the waste heat can be explored. Additionally, from the shape of the Grand Composite Curve (GCC) around the pinch area, the use of a heat pump may be beneficial. This option was already explored by Ripke et al. (1994) in their work as well as possible process modifications to decrease the utility consumption of the process. In this work these options are not studied and the focus is set on the integration of ORCs and ABCs. In the following sections, the process integration of ORCs, ABCs and both, into HENs in continuous processes is analyzed with help of the mathematical models developed in section 4.2.1 (HEN-ORC, HEN-ABC and HEN-WHR).

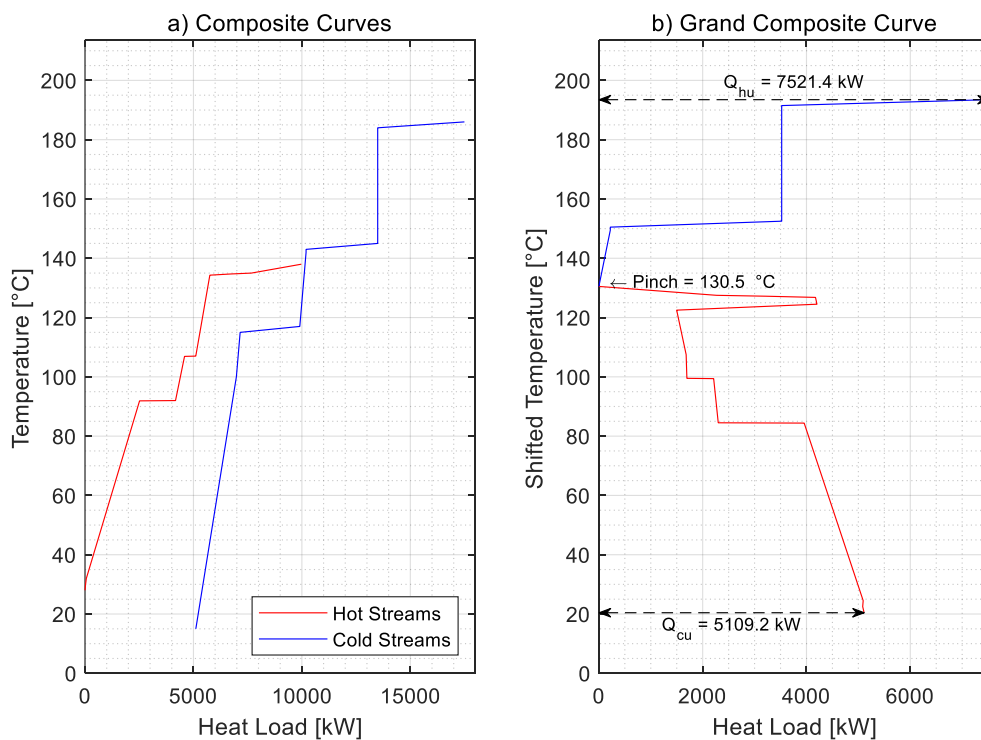


Figure 5-1. Pinch analysis for Case Study 1 ($\Delta T_{min} = 15.0$ °C).

Source: Own diagram

First, the stand-alone HEN minimizing the TAC of the system is generated using SYNHEAT. For comparison purposes two HEN designs are presented. “HEN Design 1” (HEN1) has available a cold utility with a temperature of $T_{cu}^{out} = T_{cu}^{in} = 10$ °C. On the other hand, “HEN Design 2” (HEN2) has available a cold utility with a temperature of $T_{cu}^{out} = T_{cu}^{in} = 30$ °C. In both cases the cold utility cost are set to $C_{cu} = 0.001$ €/kWh as presented in Table 5-2. The additional

cooling below 45°C ($T_{cu}^{in} + \Delta T_{min}$) required to reach its hot process streams targets (T_i^{out}), will be provided by a vapor compression refrigeration system (VCR). The following assumptions are used in the calculations involving VCR systems¹³:

- The capital cost of the VCR system is neglected in the calculations of the TAC of HEN2 (TAC2), as it is considered low in comparison with its operative costs. These neglected capital costs include the costs associated with the areas of the additional heat exchangers required by the VCR system to supply cooling to the hot process streams (i.e. between the VCR Evaporators and the process streams and between the VCR Condenser and the cold utility). The calculated TAC2 is considered a lower limit to the real TAC of a system involving HEN plus VCR system.
- As a simplification, the areas of the additional heat exchangers required by the VCR system are also not included in the total heat transfer areas calculated for HEN2 as presented in Table 5-3. Even then, the areas of HEN1 and HEN2 are not equal, as the cold utility temperature available in HEN2 is higher than in HEN1 and therefore larger heat exchanger areas are required in the cold utility heat exchangers. Additionally, the number of heat exchangers between the 2 designs also can vary.
- The VCR system generates cooling at 10°C (temperature of the available cold utility in HEN1) using the available cold utility at HEN2 at 30°C as heat source.
- The operative cost of the VCR system is equal to the cost of the electricity required to drive the VCR system with an assumed COP of 7.08. This assumed COP is equal to 50% of the ideal COP ($\text{COP}_{ideal} = 14.16$) of a VCR operating between 30°C (temperature of the available cold utility in HEN2) and 10°C (temperature of the available cold utility in HEN1).

For SYNHEAT, the number of stages was arbitrarily set to 3. The effect of a different number of stages is explored in Section 5.4. In total, the model consists of 530 equations with 705 variables (133 integer variables). The results of the optimization problem are summarized in Table 5-3. In the case of HEN1 all the cooling requirements are satisfied by the cold utility at 10°C . In the case of HEN2, 4 820.6 kW of cooling are provided by the cold utility at 30°C and 288.6 kW are provided by the VCR system at 10°C , but the sum of both consumptions is equal to the cold utility target as defined by PA and therefore equal to the cold utility consumption of

¹³ VCR assumptions are not presented in Section 1.3 as they are not part of the models developed in this dissertation, but are used in the calculation of the reference HENs (HEN1 and HEN2) which are only presented for comparison purposes.

HEN1 (5 109.2 kW). The TAC calculated for HEN2 (TAC2) underestimates the real cost of HEN2 as does not include capital cost for the VCR. Even then, the calculated TAC2 can be considered a lower limit to the real TAC of a system involving HEN plus VCR system. Another observation from Table 5-3, is that the OPEX for the HEN is significantly higher than the CAPEX (almost 10 times higher) and therefore investments decreasing the operational costs of the system should be prioritized.

Table 5-3. Results of stand-alone Heat Exchanger Network for Case Study 1

	HEN1	HEN2
$T_{cu}^{out} = T_{cu}^{in}$ (°C)	10°C	30°C
Hot Utility Consumption (kW)	7 521.4	7 521.4
Cold Utility Consumption (kW)	5 109.2	4 820.6
VCR Cooling Duty (kW)	-	288.6
Operative Expenditure /OPEX (€/a)	642 585.6	705 503.1
Hot Utility Expenditure (€/a)	601 712.0	601 712.0
Cold Utility Expenditure (€/a)	40 873.6	38 564.6
VCR Operative Expenditure (€/a)	-	65 226.5
Capital Expenditure /CAPEX (€/a)	73 677.8	85 798.3
Total Annualized Cost (TAC)	716 263.4	791 301.4
Area (m ²)	757.5	909.4
Number of Units	14	16
Termination Criteria	Tolerance	Tolerance
CPU Time (s)	2.2	7.7

Source: Own table

5.1.1 Process Integration of Organic Rankine Cycle

HEN-ORC is used to study the process integration of ORCs into HENs in continuous processes. As presented in section 2.3.5.1., the selection of the appropriated working fluid and the optimal operating temperatures for the ORC are key elements of the process integration of ORC into HENs. In this work, a prescreening algorithm for selecting the working fluid of the ORC and the evaporation and condensation temperatures of the ORC was implemented. This iterative algorithm is based on the work of Chen et al. (2016) and it is presented in Figure 5-2. In this case the HEN-ORC model was solved iteratively for different working fluids and operating temperatures with the net power as the objective function and with constraints limiting the utility consumption of HEN-ORC to the pinch targets for the standalone HEN. This process finds the working fluid and operating temperatures with the best performance when the ORC is powered exclusively by waste heat. Finally, HEN-ORC was optimized with TAC as the objective function and the working fluid and operating temperatures for the ORC found in the prescreening step.

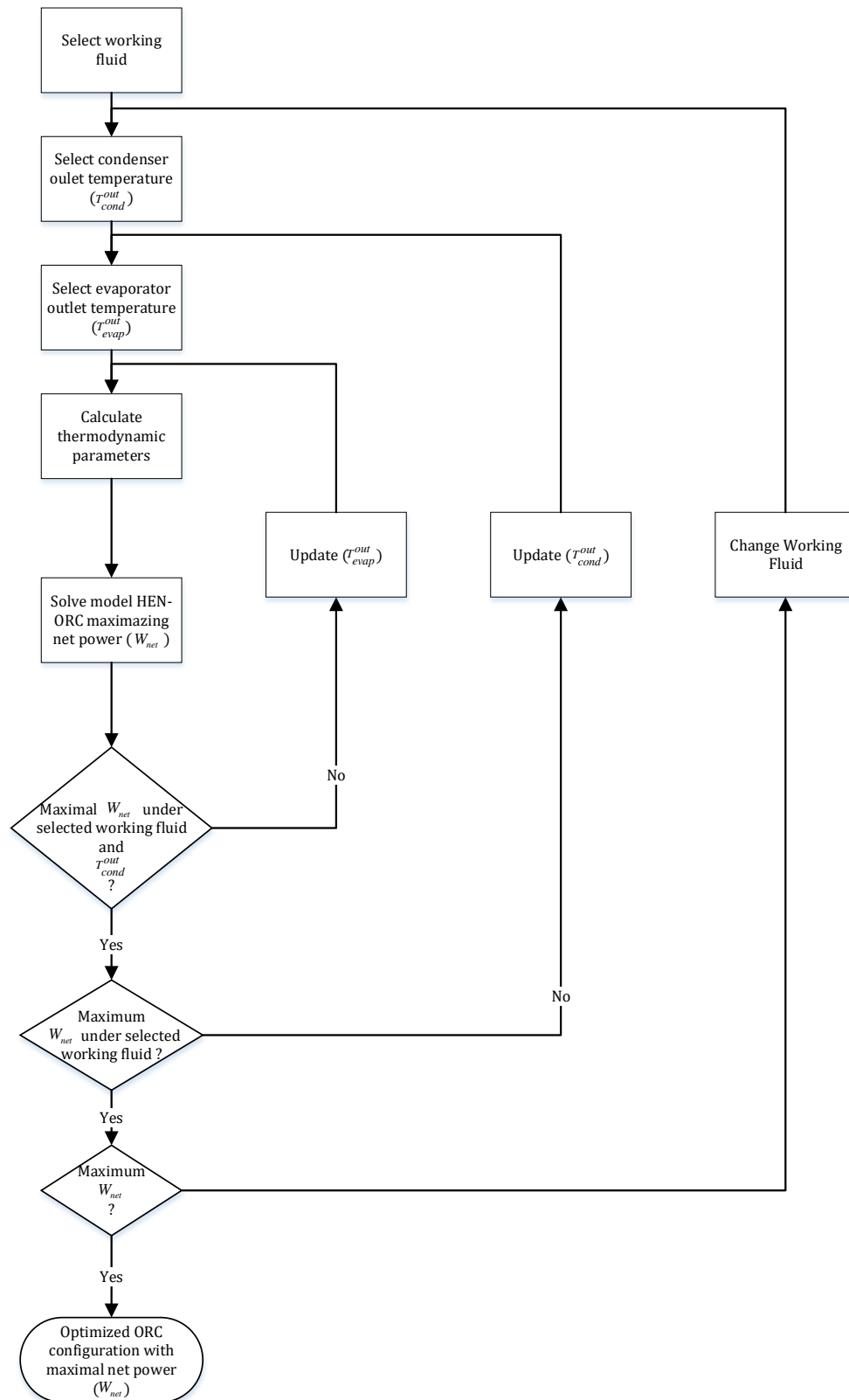


Figure 5-2. Prescreening algorithm for the selection of the ORC working fluid and operating temperatures

Source: Own diagram based on Chen et al. (2016)

The prescreening algorithm was implemented using MATLAB R2018a for the iteration loop, and GAMS (version 25.1.1) and the global solver BARON with an optimality gap of 5% were

used to solve the MINLP. A $\Delta T_{min} = 15.0\text{ }^{\circ}\text{C}$ was used for all matches, including those between the working fluid and the process streams or utilities. In total, the HEN-ORC consists of 616 equations with 678 variables (147 integer variables), with two additional equations establishing the upper limits to the utility consumption (pinch targets).

For Case Study 1, results for the prescreening process are summarized in Table 5-4. Six typical working fluids used in ORC applications according to Thurairaja et al. (2019) were tested. The evaporation and condensation temperatures for all working fluids were tested in the intervals $T_{evap}^{out} \in [80.0 ; 120.0]^{\circ}\text{C}$ and $T_{cond}^{out} \in [25.0 ; 60.0]^{\circ}\text{C}$. This selection is based on the GCC in Figure 5-1 and heuristic considerations. The evaporation temperature should be below the pinch temperature ($130.5\text{ }^{\circ}\text{C}$) to avoid cross-pinch heat transfer but it should be hot enough to drive the ORC. On the other hand, the condensation temperature should be as low as possible but high enough to be able to be cooled by the cold utility. Additionally, higher condensation temperatures allow the cold process streams to be heated by the working fluid at the exit of the turbine, decreasing the hot utility consumption of the system.

Table 5-4. Results of working fluids prescreening for Case Study 1

Working Fluid	n-butane	n-pentane	n-hexane	R113	R123	R600a
T_{evap}^{out} ($^{\circ}\text{C}$)	87.41	86.18	85.75	85.76	86.54	88.01
P_{evap} (kPa)	1 189.28	480.04	168.34	304.47	575.21	1 582.51
T_{cond}^{out} ($^{\circ}\text{C}$)	25.00	25.00	25.00	25.00	25.00	25.00
P_{cond} (kPa)	244.46	76.51	20.27	44.18	91.31	351.48
Net Power (kW)	282.49	276.62	281.73	284.88	284.76	282.51

Source: Own table

According to the results of the prescreening in Table 5-4, the working fluid with the highest net power generated is R113 with 284.88 kW. The operating conditions for the ORC are, in this case, an evaporation temperature of 85.76°C (304.47 kPa) and a condensation temperature of 25.0°C (44.18 kPa). The optimal temperatures for the evaporation and condensation for all fluids are similar. As for the condensation temperature (25°C), it corresponds to the lowest condensation temperature considered, which is to be expected, as the ORC efficiency increases with low condensation temperatures. As for the evaporation temperature (87.76°C), it corresponds roughly to the temperature of stream H6 as presented in Table 5-1. This is to be expected as stream H6 has by far the highest energy surplus of the streams located under the pinch, as presented in Table 5-1 and illustrated in the GCC of Figure 5-1. Using R113 as working fluid with the operating temperatures found in the prescreening, HEN-ORC was solved with TAC as the objective function. In total, HEN-ORC consists of 895 equations with 918 variables (147 integer variables) plus two additional equations to set the upper limits to the

utility consumption. Results for HEN-ORC for Case Study 1 are summarized in Table 5-5 and the grid diagram for the generated configuration is presented in Appendix D.

Table 5-5. Results of HEN-ORC for Case Study 1

Operating Conditions ORC	
Working Fluid	R113
P_{evap} (kPa)	304.47
P_{cond} (kPa)	44.18
T_{evap}^{in} (°C)	25.15
T_{evap}^{out} (°C)	85.76
T_{cond}^{in} (°C)	51.18
T_{cond}^{out} (°C)	25.00
Results	
Hot Utility Consumption (kW)	7 521.4
Cold Utility Consumption (kW)	4 824.3
W_{net} (kW)	284.9
W_{turb} (kW)	287.8
W_{pump} (kW)	2.9
OPEX (€/a)	640 307.1
CAPEX (€/a)	116 455.2
Electricity Sales (€/a)	-455 813.5
TAC (€/a)	300 948.8
Area (m ²)	1 000.9
Number of Units	20
η_{orc}	11.6%
Termination Criteria	Tolerance
Optimality Gap (%) /CPU Time (s)	393.9

Source: Own table

Compared with HEN1, as presented in Table 5-3 (HEN with cold utility available at 10°C, without need of VCR), the results for HEN-ORC show a reduction of 58.0% in the TAC of the system (300 948.8 €/a instead of 716 263.4 €/a), without increasing its utility consumption. This means that the electricity is generated from waste heat that would otherwise be rejected. The integration of the ORC has a significant impact on the economics of the design and it is highly beneficial to the performance of the system. The number of units and required heat transfer area in HEN-ORC (20 units and 1 000.9 m²) are significantly higher than for the stand-alone HEN1 (14 units and 757.5 m²), but the increased capital costs due to the additional heat exchangers, turbines and pumps, are compensated by the revenues from the electricity sales. An additional benefit is the decrease in the cold utility consumption as the new system rejects 4 824.3 kW instead of 5 109.2 kW to the cold utility.

5.1.2 Process Integration of Absorption Chillers

The process integration of ABCs into HENs in continuous process is studied using HEN-ABC. LiBr/H₂O is used exclusively as the refrigerant couple for the developed models and its properties are calculated using appropriated empirical correlations. The cold utility temperature available in this case is 30.0°C, as indicated in Table 5-1. The refrigeration temperature to be generated by the ABC (T_{ref}) is set to 10.0°C, and the minimum temperature difference for all matches in the system is set to $\Delta T_{min} = 15.0^\circ C$. HEN-ABC is designed to be implemented in situations where a cooling temperature below the available cold utility temperature is required.

In total, HEN-ABC consists of 621 equations with 796 variables (149 integer variables) plus two additional equations to set the upper limits to the utility consumption to the pinch targets. Results for HEN-ABC for Case Study 1 are summarized in Table 5-6 and the grid diagram is presented in Appendix D.

Table 5-6. Results of HEN-ABC for Case Study 1

Operating Conditions ABC	
T_{ref} (°C)	10.0
Results	
Hot Utility Consumption (kW)	7 521.4
Cold Utility Consumption (kW)	5 109.2
Cooling Generated (kW)	401.9
OPEX (€/a)	642 585.6
CAPEX (€/a)	93 195.5
TAC (€/a)	735 781.1
Area (m ²)	903.3
Number of Units	19
Termination Criteria	Tolerance
Optimality Gap (%) /CPU Time (s)	15

Source: Own table

Compared with HEN2 as presented in Table 5-3 (HEN with cold utility available at 30°C and therefore requiring a VCR system for additional refrigeration), the TAC of HEN-ABC is 7.0 % lower (735 781.1 €/a instead of 791 301.4 €/a) due to the replacement of electricity with waste heat as driving force for the refrigeration cycle. The calculated savings would be higher if the capital costs of the VCR were also considered. The main difference between HEN-ABC and the stand-alone HEN2 is that HEN-ABC is capable of generating 401.9 kW of cooling at 10°C from the waste heat, to be reused in the system when cooling below the cold utility temperature of 30.0°C is required.

5.1.3 Process Integration of Waste Heat Recovery Technologies (Combined Model)

The process integration of ORCs and ABCs into HENs in continuous process is studied using HEN-WHR. The conditions are similar to those of HEN-ORC and HEN-ABC. $\Delta T_{min} = 15.0^{\circ}\text{C}$ is used for all matches in the system. For HEN-WHR the cold utility temperature is set as 30.0°C , like in HEN-ABC. Similar to HEN-ORC, the working fluid for the ORC is R113 with evaporation temperature of 85.76°C (304.47 kPa) and condensation temperature of 45°C (91.64 kPa). The condensation temperature is 45°C instead of 25°C , as in HEN-ORC, because it is the lowest condensation temperature that can be achieved with the available cold utility for the given ΔT_{min} .

In total, the model consists of 986 equations with 1 129 variables (163 integer variables) plus two additional equations establishing the upper limits to the utility consumption. Results for HEN-WHR for Case Study 1 are summarized in Table 5-7. Figure 5-3 illustrates the grid diagram for the optimal design and Table 5-8 presents information about the individual heat exchangers that were calculated using HEN-WHR.

Table 5-7. Results of HEN-WHR for Case Study 1

Operating Conditions WHR	
T_{ref} ($^{\circ}\text{C}$)	10.0
Working Fluid	R113
P_{evap} (kPa)	304.47
P_{cond} (kPa)	91.64
T_{evap}^{in} ($^{\circ}\text{C}$)	45.16
T_{evap}^{out} ($^{\circ}\text{C}$)	85.76
T_{cond}^{in} ($^{\circ}\text{C}$)	63.19
T_{cond}^{out} ($^{\circ}\text{C}$)	45.00
Results	
Hot Utility Consumption (kW)	7 521.4
Cold Utility Consumption (kW)	4 953.0
Cooling Generated (kW)	288.6
W_{net} (kW)	156.3
W_{turb} (kW)	158.7
W_{pump} (kW)	2.4
OPEX (€/a)	641 335.7
CAPEX (€/a)	127 654.3
Electricity Sales (€/a)	-250 014.9
TAC (€/a)	518 975.1
Area (m^2)	1 127.4
Number of Units	25
η_{orc}	8.0%
Termination Criteria	Time Limit
Optimality Gap (%) /CPU Time (s)	18.2%

Source: Own table

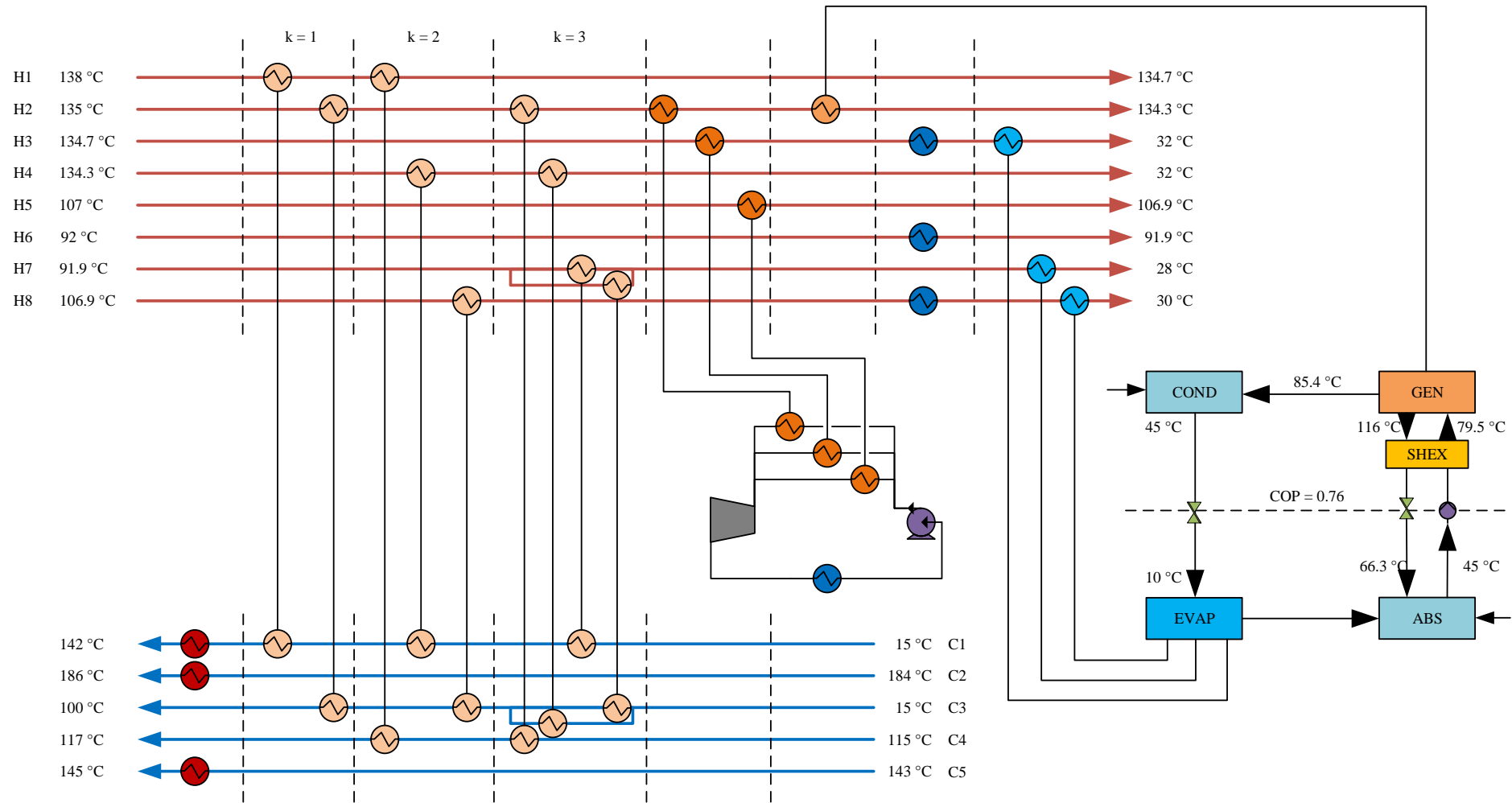


Figure 5-3. Grid diagram of HEN-WHR for Case Study 1

Source: Own diagram

Table 5-8. Heat exchanger information for HEN-WHR in Case Study 1

Type of Heat Exchanger	Match	Area (m ²)	Heat Exchanger Duty (kW)
Intra-Process (i,j,k)	1,1,1	13.2	133.1
	2,3,1	8.3	178.0
	1,4,2	238.4	2 399.9
	4,1,2	43.1	401.6
	8,3,2	6.5	62.2
	2,4,3	33.2	327.1
	4,3,3	71.0	567.4
	7,1,3	92.4	718.0
	7,3,3	9.8	76.4
Hot Utility (j)	1	3.6	220.4
	2	114.3	3 999.0
	5	59.5	3 302.0
Cold Utility (i)	3	39.8	642.6
	6	53.4	1 655.0
	8	11.8	194.6
ORC Evaporator (i)	2	23.6	794.0
	3	27.3	369.6
	5	27.2	516.0
ORC Cold Utility		221.7	1 793.3
ABC- Generator (i)	2	22.7	378.9
ABC-Evaporator (i)	3	13.3	185.8
	7	4.2	40.6
	8	4.6	62.2
ABC-Condenser		19.9	306.1
ABC-Absorber		30.0	361.4

Source: Own table

Compared with HEN2 (HEN including refrigeration costs if provided by a VCR), as presented in Table 5-3, HEN-WHR has a decrease of 34.4 % in TAC (518 975.1 €/a instead of 791 301.4 €/a) and generates 288.6 kW of cooling at 10.0°C and 156.3 kW of electric power from waste heat. The results show clearly the benefits of the integration of ORCs and ABCs into the system. Comparing HEN-WHR with HEN-ORC, the generated electricity decreases, as only 156.3 kW instead of 284.9 kW of power are generated. The 45% drop in power generated is due to two main factors: 1) some waste heat is used to generate cooling instead of electricity due to the integration of the ABC and 2) the increase in the working fluid condensation temperature, from 25.0° in HEN-ORC to 45.0°C in HEN-WHR, which decreases the efficiency of the ORC cycle by 31% (8.0% instead of 11.6%). As for the comparison between HEN-WHR and HEN-ABC, HEN-WHR generates less cooling at 10°C (288.6 kW instead of 401.9 kW) but the generated electricity by the ORC largely improves the economics of the design (TAC 518 975.1 €/a instead of 735 791.1 €/a)

5.2 Case Study 2 (Semi-Continuous Process)

Table 5-9 presents the information of the process streams for Case Study 2. The problem is an adaptation of Case Study 1 and was first used by Hellwig (1998) to illustrate the use of the OMNIUM method for the design of HENs for non-continuous operations. According to Hellwig, process streams H5 to H8 and C3 to C5 operate discontinuously, only from 6:00 to 22:00 daily, while the rest of the streams have a continuous operation. The design parameters are the same as in Case Study 1, as presented in Table 5-2, and $\Delta T_{min} = 15.0^{\circ}\text{C}$ is used for all matches in the system. From a practical point on view, the process can be divided in 2 clear periods of operation: From 22:00 to 6:00 and from 6:00 to 22:00. However, in this work 3 periods of operations are used, the same number as in the original data as presented by Hellwig (1998). The 3 periods of operation are: From 0:00 to 6:00, from 6:00 to 22:00 and from 22:00 to 24:00, to then restart the cycle again, as represented in the event diagram in Figure 5-4.

Table 5-9. Stream data Case Study 2. 8H5C Discontinuous

Stream	T^{in} ($^{\circ}\text{C}$)	T^{out} ($^{\circ}\text{C}$)	F (kW/ $^{\circ}\text{C}$)	t_{start} (h)	t_{end} (h)	Δt (h)
H1	138.0	134.7	767.6	0	24	24
H2	135.0	134.3	2 397.1	0	24	24
H3	134.7	32.0	14.3	0	24	24
H4	134.3	32.0	9.5	0	24	24
H5	107.0	106.9	5 160.0	6	22	16
H6	92.0	91.9	16 550.0	6	22	16
H7	91.9	28.0	13.1	6	22	16
H8	106.9	30.0	4.1	6	22	16
C1	15.0	142.0	11.6	0	24	24
C2	184.0	186.0	1 999.5	0	24	24
C3	15.0	100.0	10.4	6	22	16
C4	115.0	117.0	1 363.5	6	22	16
C5	143.0	145.0	1 651.0	6	22	16
HU	255.0	255.0	-	-	-	-
CU ^{1, 2)}	10.0/30.0	10.0/30.0	-	-	-	-

¹⁾ The cold utility temperature is set to 10.0°C for the stand-alone hen and HEN-ORC. For models involving absorption chillers (MP-ABC and MP-WHR) this temperature is set to 30.0°C .

²⁾ Film coefficients for all streams are $h = 1.0 \text{ kW/m}^2\text{C}$

Source: Own table

Figure 5-5 presents the GCCs for the different periods. As the periods are independent of each other (no heat storage considered), the “Time Slide Model” (TSM) is used to calculate the utility targets in each period. In the TSM, each period is treated as an independent problem and the utility targets for each period are calculated using the “Problem Table Algorithm” (PTA). Using PTA and considering the duration of the periods, the utility targets are presented in Table 5-10. Per cycle, the hot utility target is 154 097.6 kWh and the cold utility target is 123 468.8 kWh.

These values are used as limits for the utility consumption in the different models used in this case study.

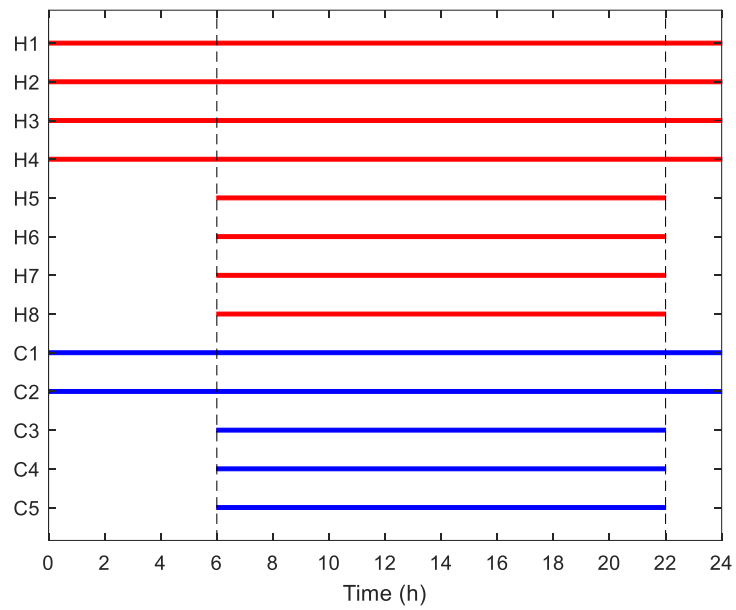


Figure 5-4. Event diagram of Case Study 2

Source: Own diagram

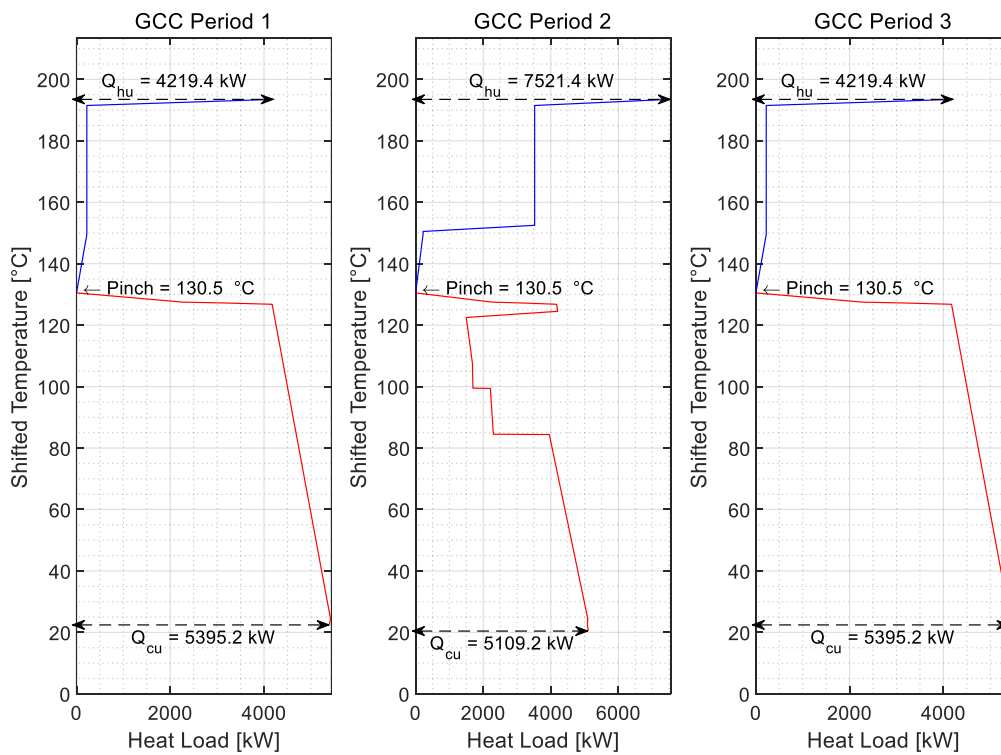


Figure 5-5. Grand Composite Curves for the different periods of operation in Case Study 2 ($\Delta T_{min} = 15.0^{\circ}\text{C}$)

Source: Own diagram

Table 5-10. Energy targets Case Study 2 according to TSM

	Hot Utility Target		Cold Utility Target	
	Heat Flow (kW)	Heat Load (kWh)	Heat Flow (kW)	Heat Load (kWh)
Period 1	4 219.4	25 316.4	5 395.2	32 371.2
Period 2	7 521.4	120 342.4	5 109.2	81 747.2
Period 3	4 219.4	8 438.8	5 395.2	10 790.4
	Total Per Cycle	154 097.6	Total Per Cycle	124 908.8

Source: Own table

As before, the stand-alone HEN minimizing the TAC of the system is generated. In this case, the multi-period stage-wise superstructure for the synthesis of HENs developed by Verheyen and Zhang (2006) using the “Maximum Area” approach, is implemented. As with Case Study 1 two HEN designs are presented for comparison purposes. “HEN Design 1” (HEN1) has available a cold utility with a temperature of $T_{cu}^{out} = T_{cu}^{in} = 10^{\circ}\text{C}$. On the other hand, “HEN Design 2” (HEN2) has available a cold utility with a temperature of $T_{cu}^{out} = T_{cu}^{in} = 30^{\circ}\text{C}$. The additional cooling below 45°C ($T_{cu}^{in} + \Delta T_{min}$) required to reach its hot process streams targets (T_i^{out}), will be provided by a vapor compression refrigeration system (VCR). The modeling assumption for the VCR are the same as with Case Study 1 as presented in Section 5.1. These assumptions include a COP = 7.08 for the VCR and the no consideration of the capital costs and heat transfer areas associated with the VCR. As with the continuous case, the number of stages was arbitrary set to 3. In total, the model consists of 2 386 equations with 2 099 variables (173 integer variables). The results of the optimization problem are summarized in Table 5-11.

Table 5-11. Results of stand-alone Heat Exchanger Network for Case Study 2

	HEN1	HEN2
$T_{cu}^{out} = T_{cu}^{in}$ ($^{\circ}\text{C}$)	10 $^{\circ}\text{C}$	30 $^{\circ}\text{C}$
Average Hot Utility Consumption (kW)	6 420.7	6 420.7
Hot Utility Consumption per Cycle (kWh)	154 097.6	154 097.6
Average Cold Utility Consumption (kW)	5 204.5	4 950.2
Cold Utility Consumption per Cycle (kWh)	124 908.8	118 804.2
Average VCR Cooling Duty (kW)	-	254.4
VCR Cooling Duty per Cycle (kWh)	-	6 104.6
Operative Expenditure /OPEX ($\text{€}/\text{a}$)	555 294.9	610 742.4
Hot Utility Expenditure ($\text{€}/\text{a}$)	513 658.7	513 658.7
Cold Utility Expenditure ($\text{€}/\text{a}$)	41 636.3	39 601.4
VCR Operative Expenditure ($\text{€}/\text{a}$)	-	57 482.3
Capital Expenditure /CAPEX ($\text{€}/\text{a}$)	75 981.1	88 683.3
Total Annualized Cost (TAC)	631 276.1	699 425.6
Area (m^2)	760.2	908.5
Number of Units	15	17
Termination Criteria	Tolerance	Tolerance
CPU Time (s)	9.3	24.2

Source: Own table

Compared with the results of HEN1 in the continuous case presented in Table 5-3, the TAC of the multi-period HEN is 11.9% lower (631 276.1 €/a instead of 716 263.4 €/a) due to the decrease in the average hot and cold utility consumptions in the system. A slight increase in the CAPEX (75 981.1 €/a instead of 73 677.8 €/a) is caused by the increase in the number of heat transfer units required in the multi-period case (15 instead of 14). HEN2 (HEN with cold utility available at 30°C and therefore requiring a VCR system for additional refrigeration) behave similarly to HEN1, with an overall reduction of 11.6 % in the TAC of the multi-period case in comparison with the continuous operation (699 425.6 €/a instead of 791 301.4 €/a) and an slightly increase in the CAPEX (88 683.3 €/a instead of 85 798.3 €/a). In all periods of operation, there is a surplus of energy below the pinch at a high pinch temperature and therefore the integration of ORCs can be beneficial to the system. In the following sections, the process integration of ORCs, ABCs and both, into HENs in multi-period processes without FTVM heat storage (semi-continuous processes) is analyzed with help of the mathematical models developed in section 4.2.2 (MP-ORC, MP-ABC and MP-WHR).

5.2.1 Process Integration of Organic Rankine Cycle

As with the continuous case, the prescreening algorithm presented in section 5.1.1 is used to determine the operating conditions of the ORC as well as the appropriate working fluid for the system. The objective function is the average net power generated during a cycle. In Case Study 2, the pinch temperatures for all periods are the same (130.5 °C) and equal to the pinch temperature in Case Study 1, therefore the same temperature intervals for the evaporation and condensation temperatures as in Case Study 1 are tested; that is, the evaporation and condensation temperatures for all working fluids are tested in the intervals $T_{evap}^{out} \in [80.0 ; 120.0]^{\circ}C$ and $T_{cond}^{out} \in [25.0 ; 60.0]^{\circ}C$. As upper limits for the utility consumption for the prescreening algorithm, the pinch targets per cycle as presented in Table 5-10 are used. In cases where the pinch temperature differs in each period, it is recommended to test T_{evap}^{out} up until the maximum pinch temperature among all periods. Table 5-12 presents the results of the prescreening algorithm for Case Study 2 using the same working fluids tested in Case Study 1.

Table 5-12 Results of working fluids prescreening for Case Study 2

Working Fluid	n-butane	n-pentane	n-hexane	R113	R123	R600a
T_{evap}^{out} (°C)	91.92	91.90	91.92	91.08	91.61	90.96
P_{evap} (kPa)	1 304.69	550.48	199.46	348.28	649.03	1 676.52
T_{cond}^{out} (°C)	25.00	25.00	25.00	25.00	25.00	25.00
P_{cond} (kPa)	244.46	76.51	20.27	44.18	91.31	351.48
Average Net Power (kW)	362.77	367.29	371.16	373.33	375.40	355.11

Source: Own table

Different than in Case Study 1, the best working fluid for Case Study 2 is R123 instead of R113. Again, the best condensation temperature for all working fluids, 25.0°C (91.31 kPa for R123), is the lowest temperature evaluated and the calculated evaporation temperatures are similar among all the working fluids. For R123 in Case Study 2, the evaporation temperature 91.61 °C (649.03 kPa), is higher than the evaporation temperature calculated for R113 in Case Study 1. This is explained by the shape of the GCC in periods 1 and 3 in Figure 5-5, where higher temperatures are available for the waste heat recovery under the pinch in comparison with period 2, which is equivalent to the GCC for Case Study 1, as presented in Figure 5-1. Using R123 as working fluid with the operating temperatures found in the prescreening, MP-ORC is solved with TAC as the objective function. In total, MP-ORC consists of 2 713 equations with 2 402 variables (187 integer variables) plus two additional equations to set the upper limits to the utility consumption. Results for MP-ORC for Case Study 2 are summarized in Table 5-13 and the grid diagram for the generated configuration is presented in Appendix D.

Table 5-13. Results of MP-ORC for Case Study 2

Operating Conditions ORC	
Working Fluid	R123
P_{evap} (kPa)	649.03
P_{cond} (kPa)	91.31
T_{evap}^{in} (°C)	25.40
T_{evap}^{out} (°C)	91.61
T_{cond}^{in} (°C)	45.07
T_{cond}^{out} (°C)	25.00
Results	
Average Hot Utility Consumption (kW)	6 420.7
Hot Utility Consumption per Cycle (kWh)	154 097.6
Average Cold Utility Consumption (kW)	4 830.0
Cold Utility Consumption per Cycle (kWh)	115 919.3
\bar{W}_{net} (kW)	374.6
\bar{W}_{turb} (kW)	382.9
\bar{W}_{pump} (kW)	8.2
W_{net} (kWh)	8 991.1
W_{turb} (kWh)	9 188.6
W_{pump} (kWh)	197.5
OPEX (€/a)	552 318.4
CAPEX (€/a)	141 928.6
Electricity Sales (€/a)	-599 409.6
TAC (€/a)	94 817.4
Area (m ²)	1 226.6
Number of Units	22
η_{orc}	12.3
Termination Criteria	Time Limit
Optimality Gap (%) /CPU Time (s)	80.5

Source: Own table

Compared with the stand-alone multi-period HEN1 in Table 5-11, the integration of ORCs again decreases the TAC of the system by generating electricity from waste heat. The effect of the ORC integration is even larger than in the continuous case presented in Case Study 1, as an 85.0% drop in the TAC of the system (from 631 276.1 €/a to 94 817.4 €/a) is achieved (only a 58.0% drop in TAC in HEN-ORC in Case Study 1). The reason for this improvement is, as mentioned before, the availability of high temperature waste heat in periods 1 and 3. This waste heat at high temperature, increases the evaporation temperature of the system as compared with the continuous case (91.61 °C instead of 85.76°C), increasing the ORC efficiency ($\eta_{orc} = 12.3\%$ instead of 11.6%). Additionally, the amount of waste heat available in Case Study 2 is slightly higher than the waste heat available in Case Study 1, as visible from the cold utility targets (5 204.5 kW in average in Case Study 2 instead of 5 019.2 kW in Case Study 1).

5.2.2 Process Integration of Absorption Chillers

As in Case Study 1, the cold utility temperature available in this case is 30.0 °C, as indicated in Table 5-9. The refrigeration temperature to be generated by the ABC (T_{ref}) is set to 10.0 °C and $\Delta T_{min} = 15.0$ °C for all matches. In total, the model consists of 2 747 equations with 2 390 variables (189 integer variables) with two additional equations establishing the upper limits to the utility consumption. Results for MP-ABC for Case Study 2 are summarized in Table 5-14 and the grid diagrams for the generated configurations are presented in Appendix D.

Table 5-14. Results of MP-ABC for Case Study 2

Operating Conditions ABC	
T_{ref} (°C)	10.0
Results	
Average Hot Utility Consumption (kW)	6 420.7
Hot Utility Consumption per Cycle (kWh)	154 097.6
Average Cold Utility Consumption (kW)	5 204.5
Cold Utility Consumption per Cycle (kWh)	124 908.8
Average Cooling Generated (kW)	333.9
Cooling Generated (kWh)	8 014.1
OPEX (€/a)	555 294.9
CAPEX (€/a)	100 768.4
TAC (€/a)	656 063.3
Area (m ²)	1 014.0
Number of Units	20
Termination Criteria	Tolerance
Optimality Gap (%) /CPU Time (s)	2 680.1

Source: Own table

Compared with HEN2 (HEN with cold utility available at 30°C and therefore requiring a VCR system for additional refrigeration), as presented in Table 5-11, MP-ABC has at least a reduction of 6.2% in the TAC of the system (656 063.3 €/a instead of 699 425.6 €/a) due to the replacement of electricity by waste heat as driving force for the refrigeration cycle. The calculated savings would be higher if the capital costs of the VCR were also considered.

MP-ABC is able to generate in average 333.9 kW of cooling at 10°C from waste heat, which otherwise would have to be provided by the VCR system using electricity. Compared with the continuous case in Case Study 1, MP-ABC has a lower TAC, mainly due to the lower OPEX (555 294.9 €/a instead of 642 585.6 €/a in HEN-ABC) as the utility consumption in the multi-period case is lower than in the continuous case.

5.2.3 Process Integration of Waste Heat Recovery Technologies (Combined Model)

The conditions for MP-WHR are similar to those of MP-ORC and MP-ABC. $\Delta T_{min} = 15.0$ °C is used for all matches in the system. The cold utility temperature is set as 30.0 °C, like in MP-ABC. The working fluid for the ORC is R123 with evaporation temperature of 91.61°C (649.03 kPa) and condensation temperature of 45°C (181.69 kPa). The condensation temperature, 45.0 °C, is the lowest temperature that can be achieved with the available cold utility. The model consists of 3 089 equations with 2 653 variables (163 integer variables), with two additional equations for the upper limits to the utility consumption. Results for MP-WHR for Case Study 2 are summarized in Table 5-15. Table 5-16 and Table 5-17 present detailed information about the design and Figure 5-6 illustrates the grid diagram for the configuration.

Compared with HEN2 (HEN with cold utility available at 30°C and therefore requiring a VCR system for additional refrigeration), as presented in Table 5-11, MP-WHR has a decrease of 53.4% in TAC (325 784.8 €/a instead of 699 425.6 €/a) and generates in average 240.7 kW of electric power and 254.4 kW of cooling at 10.0°C from waste heat. The results show clearly the benefits of the integration of ORCs and ABCs into the system. As expected, the heat exchanger duties as well as the energy generated and consumed by turbines and pumps, varies depending on the period of operation, with 12 out of 27 heat exchanger units in the system operating only during period 2.

Comparing MP-WHR with MP-ORC, the electricity generated decreases by 35.7 %, as only 240.7 kW instead of 374.6 kW of power are generated. Similar to HEN-WHR, the drop in power generated by MP-WHR is produced by two main factors: 1) some waste heat is used to generate cooling instead of electricity due to the integration of the ABC and 2) the increase in

the working fluid condensation temperature, from 25° in MP-ORC to 45°C in MP-WHR, which decreases the efficiency of the ORC cycle in 28.2% (8.8% instead of 12.3%). As for the comparison between MP-WHR and MP-ABC, MP-WHR generates less cooling at 10°C (in average 254.4 kW instead of 333.9 kW) but the generated electricity largely improves the economics of the design (TAC 325 784.8 €/a instead of 656 063.3€/a).

Table 5-15. Results of MP-WHR for Case Study 2

Operating Conditions WHR	
T_{ref} (°C)	10.0
Working Fluid	R123
P_{evap} (kPa)	649.03
P_{cond} (kPa)	181.69
T_{evap}^{in} (°C)	45.38
T_{evap}^{out} (°C)	91.61
T_{cond}^{in} (°C)	59.70
T_{cond}^{out} (°C)	45.00
Results	
Average Hot Utility Consumption (kW)	6 420.7
Hot Utility Consumption per Cycle (kWh)	154 097.6
Average Cold Utility Consumption (kW)	4 830.0
Cold Utility Consumption per Cycle (kWh)	119 135.4
Average Cooling Generated (kW)	254.4
Cooling Generated (kWh)	6 104.6
\bar{W}_{net} (kW)	240.7
\bar{W}_{turb} (kW)	248.8
\bar{W}_{pump} (kW)	7.1
W_{net} (kWh)	5 776.6
W_{turb} (kWh)	5 946.2
W_{pump} (kWh)	169.7
OPEX (€/a)	553 370.5
CAPEX (€/a)	157 517.7
Electricity Sales (€/a)	-385 103.4
TAC (€/a)	325 784.8
Area (m ²)	1 453.3
Number of Units	27
η_{orc}	8.8
Termination Criteria	Time Limit
Optimality Gap (%) /CPU Time (s)	43.6

Source: Own table

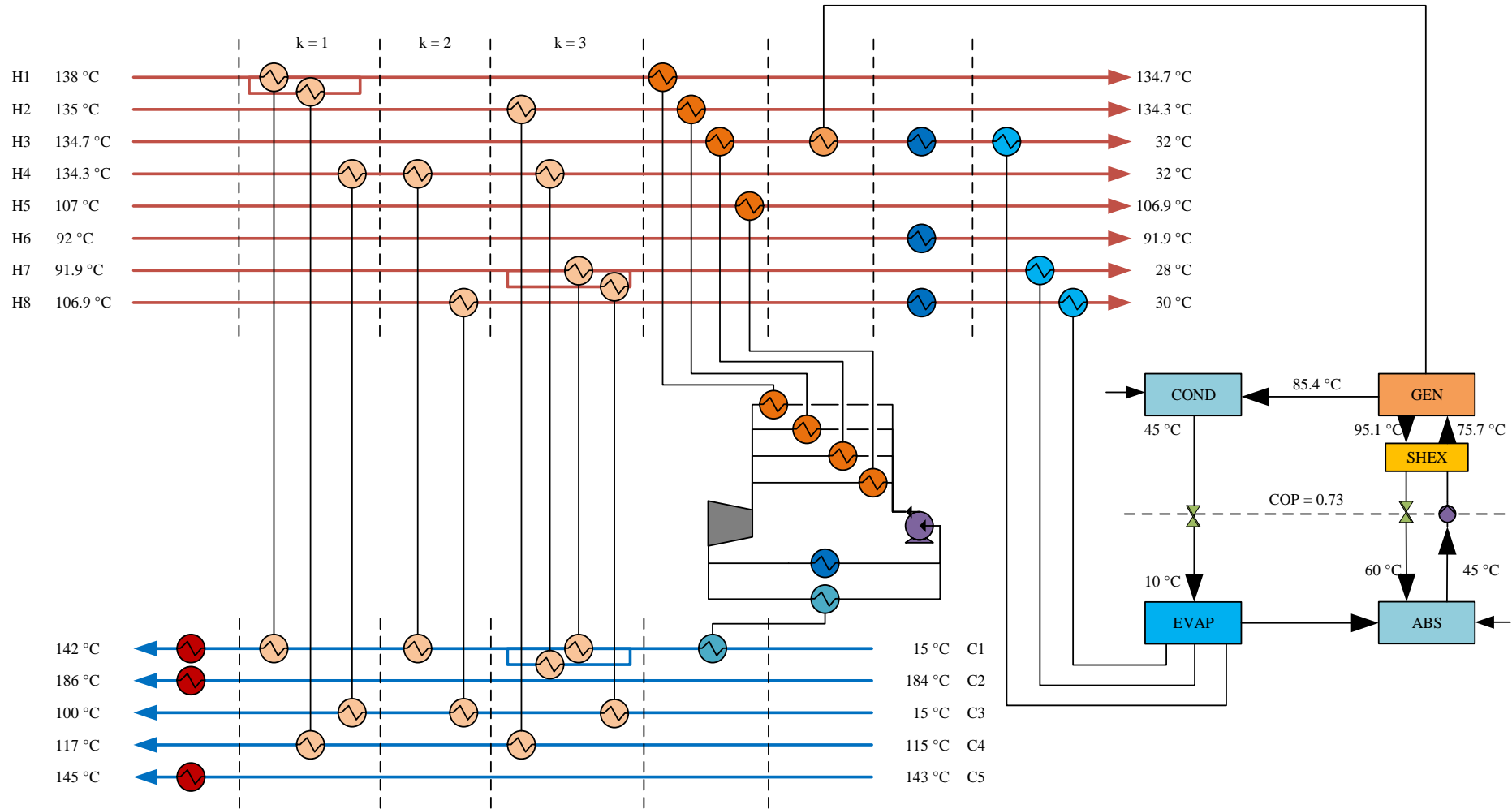


Figure 5-6. Grid diagram MP-WHR for Case Study 2

Source: Own diagram

Table 5-16. Heat exchanger information for MP-WHR in Case Study 2

Type of Heat Exchanger	Match	Maximum Area (m ²)	Heat Exchanger Duty (kW)		
			Period 1	Period 2	Period 3
Intra-Process (i,j,k)	1,1,1	24.4	260.6	311.2	260.6
	1,4,1	102.4	-	1 049.0	-
	4,3,1	10.6	-	178.0	-
	4,1,2	26.2	274.2	223.6	274.2
	8,3,2	6.5	-	62.2	-
	2,4,3	176.3	-	1 678.0	-
	4,1,3	71.0	694.8	567.4	694.8
	7,1,3	19.4	-	150.7	-
	7,3,3	82.8	-	643.8	-
Hot Utility (j)	1	3.6	220.4	220.4	220.4
	2	52.9	3 999.0	3 999.0	3 999.0
	5	14.3	-	3 302.0	-
Cold Utility (i)	3	40.1	652.8	652.8	652.8
	6	53.4	-	1 655.0	-
	8	11.8	-	194.6	-
ORC Evaporator (i)	1	69.6	2 272.4	1 172.8	2 272.4
	2	52.9	1 678.0	-	1 678.0
	3	14.3	375.3	234.8	375.3
	5	31.1	-	516.0	-
ORC Condenser (j)	1	1.3	23.2	-	23.2
ORC Cold Utility		364.5	3920.6	1753.8	3 920.6
ABC- Generator (i)	3	31.2	254.1	394.6	254.1
ABC-Evaporator (i)	3	13.3	185.8	185.8	185.8
	7	4.2	-	40.6	-
	8	4.6	-	62.2	-
ABC-Condenser		19.9	197.1	306.1	197.1
ABC-Absorber		34.8	242.8	377.1	242.8

Source: Own table

Table 5-17. Turbine and pump information for MP-WHR in Case Study 2

Type of Component	Maximum Duty (kW)	Duty (kW)		
		Period 1	Period 2	Period 3
Turbine	393.4	393.4	175.0	393.4
Pump	11.2	11.2	5.0	11.2

Source: Own table

5.3 Case Study 3 (Batch Process)

Table 5-18 presents the information of the process streams for Case Study 3. The problem is an adaptation from a problem first used by Chaturvedi et al. (2016) to illustrate a methodology for batch heat integration with direct storage of product streams. In total 3 hot streams and 2 cold streams are part of the process, which is characterized by four different periods of operation, as represented in the event diagram of Figure 5-7. Design parameters for the system, including

economic parameters for the cost calculations of heat exchangers, turbines pumps and storage tanks, are presented in Table 5-19.

Table 5-18. Stream data Case Study 3. 3H2C

Stream	T ⁱⁿ (°C)	T ^{out} (°C)	F (kW/°C)	t _{start} (h)	t _{end} (h)	Δt (h)
H1	170.0	60.0	4.00	0	10	10
H2	190.0	20.0	3.00	0	8	8
H3	130.0	100.0	1.67	5	8	3
C1	80.0	140.0	8.00	0	8	8
C2	10.0	135.0	10.00	2.5	5	2.5
HU	200.0	200.0	-	-	-	-
CU ^{1), 2)}	5.0/20.0	5.0/20.0	-	-	-	-

¹⁾ The cold utility temperature is set to 5.0°C for the stand-alone HEN and MP-ST-ORC. For models involving absorption chillers (MP-ST-ABC and MP-ST-WHR) this temperature is set to 20.0°C.
²⁾ Film coefficients for all streams are $h = 1.0 \text{ kW/m}^2\text{°C}$

Source: Own table

For the Pinch Analysis, $\Delta T_{min} = 10.0^\circ\text{C}$ is used for all matches in the system. The cold utility temperature is set to 20.0 °C for the models involving absorption chillers (MP-ST-ABC and MP-ST-WHR) and 5.0 °C for the rest (stand-alone HEN and MP-ST-ORC). Energy targets are obtained using both, the Time Slice Model (TSM), for the case when no heat storage is available, and the Time Average Model (TAM), for the case when heat storage is allowed. In TAM, the energy targets are calculated as if the process were a continuous process, where the heat flows of the streams are the weighted averages (time averages) of the heat flows of the streams over the duration of the batch cycle. Table 5-20 presents the calculated energy targets.

Table 5-19. Design parameters for Case Study 3

Parameter	General	Heat Exchanger	Storage Tanks	Turbine	Pump
AF (a ⁻¹)	0.23	-	-	-	-
Hy (h/a)	8 000	-	-	-	-
C _{hu} (€/kWh)	0.05	-	-	-	-
C _{cu} (€/kWh)	0.01	-	-	-	-
e ^{cost} /e ^{price} (€/kWh)	0.2	-	-	-	-
Eff. SHEX (ε _{SHEX})	0.7	-	-	-	-
C _{fix} (€)	-	1 600.0	0.0	4 000.0	1 200.0
C _{var} (€/m ^{2β} ; €/m ^{3β} ; €/kW ^β) ¹⁾	-	210.0	2 500.0	2 000.0	750.0
β	-	0.95	0.95	0.95	0.95
Isentropic Eff. (ε)	-	-	-	0.8	0.65
cp _{st} (kJ/kg°C)	4.2	-	-	-	-
ρ _{st} (kg/m ³)	885.2	-	-	-	-

¹⁾ Generic units are used for the variable cost coefficients, to generate cost calculations in Euros (€). For heat exchangers €/m^{2β}, for storage tanks €/m^{3β}, and for turbines and pumps €/kW^β are used.

Source: Own table

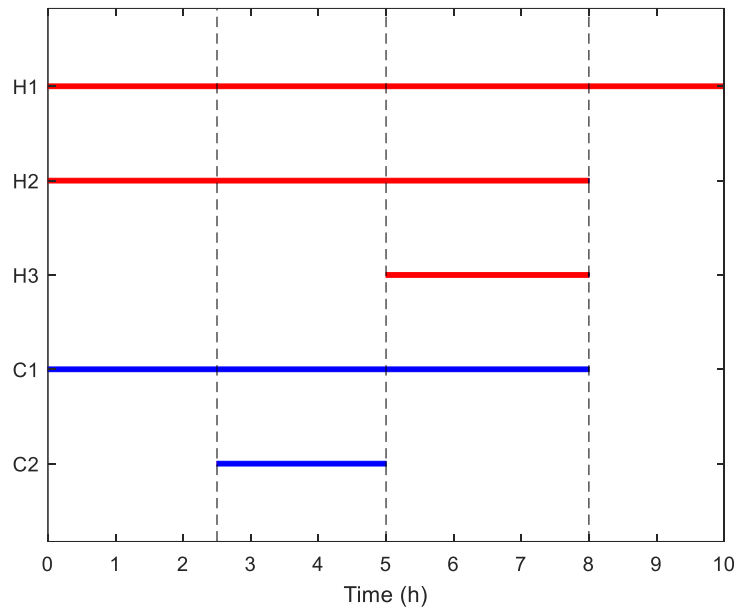


Figure 5-7. Event diagram Case Study 3

Source: Own diagram

Table 5-20. Energy targets Case Study 3 according to TAM and TSM

	TAM	TSM
Hot Utility Target (kWh)	0	1 950.0
Cold Utility Target (kWh)	1 655.3	3 615.3

Source: Own table

From the GCCs for the different periods of operation presented in Figure 5-8, it is clear that the use of heat storage is key for the efficient design of the HEN, as three of the periods have a significant heat surplus and only one of the periods has external heating needs. As illustrated in the time-averaged GGC in Figure 5-9 and the TAM targets in Table 5-20, heat storage could allow the system to operate without hot utility consumption. The pinch temperature of the time-averaged process streams is 185.0 °C, which indicates the availability of high temperature excess energy, but the shape of the GGCs (V-shape between 85.0 °C and 165.0 °C) also indicates that most of this excess energy can be recovered internally in the system through heat exchange with the help of the heat storage system.

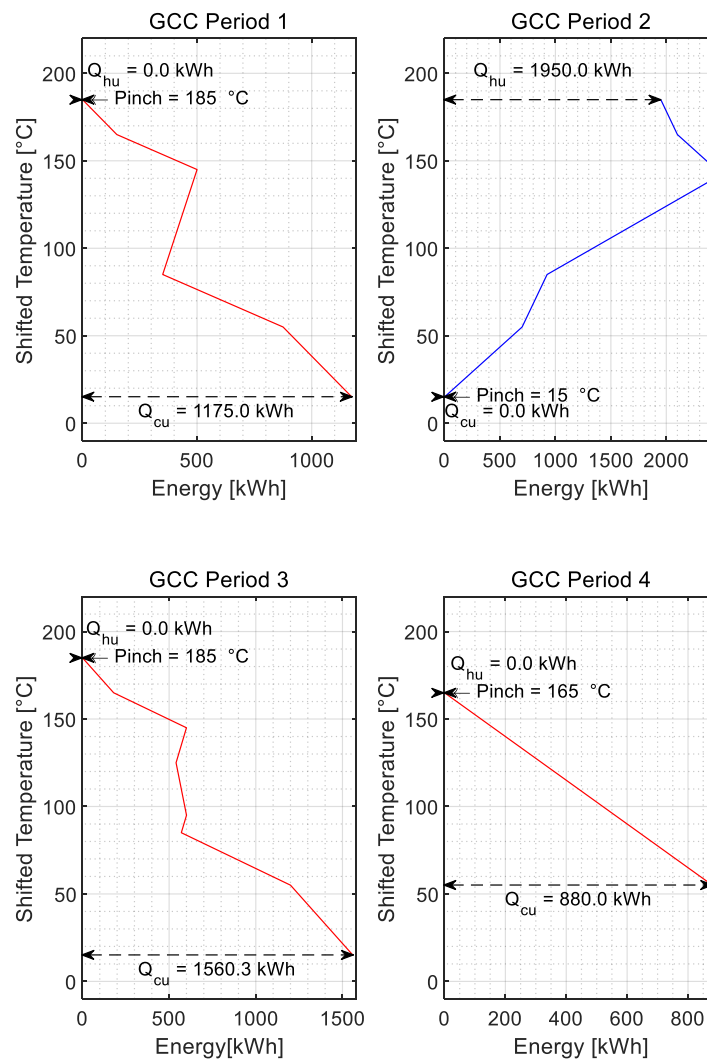


Figure 5-8. Grand Composite Curves for the different periods of operation in Case Study 3 ($\Delta T_{min} = 10^\circ\text{C}$)
 Source: Own diagram

A stand-alone HEN using heat storage and based on the modified Beck's model as presented in section 4.2.3.1 is generated. The number of energy levels for the storage system is set to 1 (two storage tanks). Again, two HEN designs are presented for comparison purposes. "HEN Design 1" (HEN1) has available a cold utility with a temperature of $T_{cu}^{out} = T_{cu}^{in} = 5^\circ\text{C}$. On the other hand, "HEN Design 2" (HEN2) has available a cold utility with a temperature of $T_{cu}^{out} = T_{cu}^{in} = 20^\circ\text{C}$. The additional cooling below 30°C ($T_{cu}^{in} + \Delta T_{min}$) required to reach its hot process streams targets (T_i^{out}), will be provided by a vapor compression refrigeration system (VCR). The modeling assumptions for the VCR are similar to those used in Case Study 1 and Case Study 2 as presented in Sections 5.1 and 5.2. These assumptions include a $\text{COP} = 9.27$ calculated as the 50% of the ideal COP ($\text{COP}_{ideal} = 18.54$) of a VCR operating between 20°C (temperature of the

available cold utility in HEN2) and 5°C (temperature of the available cold utility in HEN1). No capital costs or heat transfer areas associated with the VCR system are considered.

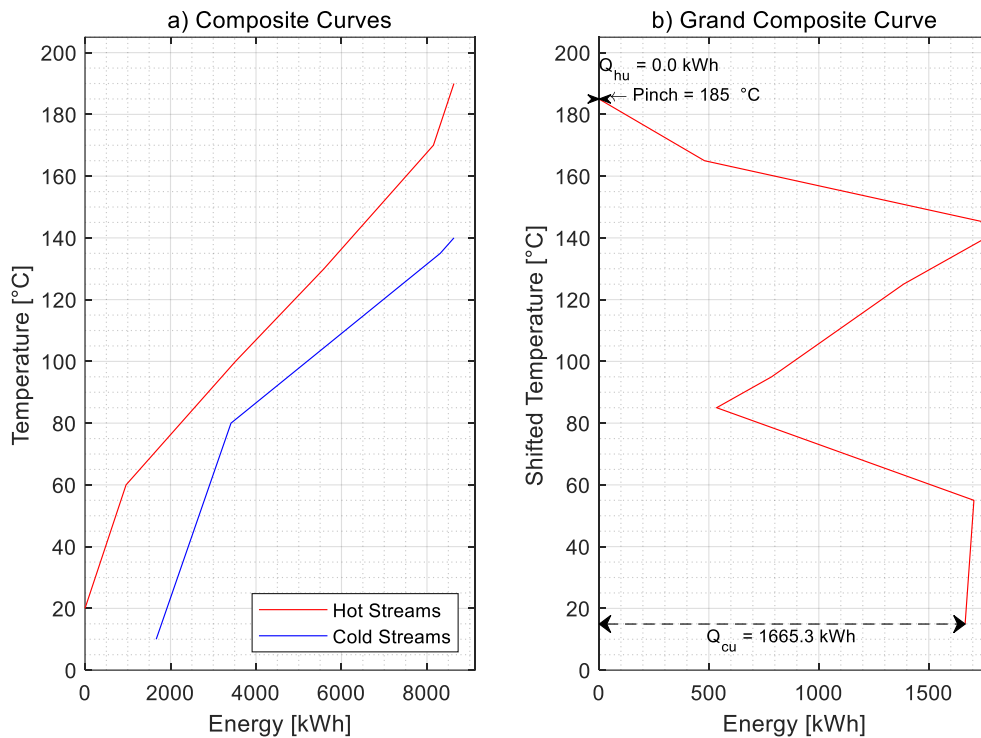


Figure 5-9. Pinch analysis of the time-averaged process streams in Case Study 3 ($\Delta T_{min} = 10.0^{\circ}\text{C}$) ($\Delta T_{min} = 10.0^{\circ}\text{C}$)

Source: Own diagram

The number of stages was arbitrarily set to 3. In total, the model consists of 1 085 equations with 865 variables (53 integer variables). The results of the optimization problem are summarized in Table 5-21.

One important conclusion from Table 5-21 is that only one energy level (two storage tanks) is enough to reach the TAM targets. This is not always the case and in general increasing the number of energy levels improves the energy recovery on the system, while simultaneously increasing the capital costs.

Table 5-21. Results of stand-alone Heat Exchanger Network with Heat Storage for Case Study 3

	HEN1	HEN2
$T_{cu}^{out} = T_{cu}^{in}$ (°C)	5°C	20°C
Average Hot Utility Consumption (kW)	0.0	0.0
Hot Utility Consumption per Cycle (kWh)	0.0	0.0
Average Cold Utility Consumption (kW)	166.5	142.5
Cold Utility Consumption per Cycle (kWh)	1 665.3	1425.3
Average VCR Cooling Duty (kW)	-	24.0
VCR Cooling Duty per Cycle (kWh)	-	240.0
Operative Expenditure /OPEX (€/a)	13 322.4	15 544.8
Hot Utility Expenditure (€/a)	0.0	0.0
Cold Utility Expenditure (€/a)	13 322.4	11 402.4
VCR Operative Expenditure (€/a)	-	4 142.4
Capital Expenditure /CAPEX (€/a)	31 239.9	37 447.5
Total Annualized Cost (TAC)	44 562.3	52 992.3
Area (m ²)	252.1	379.9
Storage Volume (m ³)	33.9	37.1
Number of Units	11	11
Termination Criteria	Time Limit	Time Limit
CPU Time (s)	36.41	58.39

Source: Own table

5.3.1 Process Integration of Organic Rankine Cycle

The prescreening algorithm presented in section 5.1.1 is used to determine the operating conditions of the ORC as well as the appropriate working fluid for the system. The time-averaged streams used to calculate the TAM targets are used as input for the algorithm, as they account for the existence of heat storage in the system. The objective function is the average net power generated during a cycle. The evaporation and condensation temperatures for all working fluids are tested in the intervals $T_{evap}^{out} \in [60.0 ; 175.0]^{\circ}\text{C}$ and $T_{cond}^{out} \in [20.0 ; 80.0]^{\circ}\text{C}$. As upper limits for the utility consumption for the prescreening algorithm, the TAM targets per cycle as presented in Table 5-20 are used. Table 5-22 presents the results of the prescreening algorithm for Case Study 3 using the same working fluids evaluated in Case Studies 1 and 2.

Table 5-22. Results of working fluids prescreening for Case Study 3

Working Fluid	n-butane	n-pentane	n-hexane	R113	R123	R600a
T_{evap}^{out} (°C)	60.00	60.00	60.00	60.00	60.00	60.00
P_{evap} (kPa)	641.42	240.09	76.64	148.24	286.00	871.30
T_{cond}^{out} (°C)	20.00	20.00	20.00	20.00	20.00	20.00
P_{cond} (kPa)	208.63	63.32	16.25	36.14	75.56	302.90
Average Net Power (kW)	13.97	13.32	13.84	13.65	13.86	13.66

Source: Own table

For this case, n-butane is the working fluid with the best performance. As with the previous case studies, the best condensation temperature for all working fluids, 20.0°C (208.63 kPa), is

the lowest temperature evaluated, and the calculated evaporation temperatures are similar among all the working fluids. In Case Study 3, the optimal evaporation temperature, 60.00 °C (641.42 kPa), is the same regardless of the working fluid. This result is in concordance with the GGC for the time-averaged process streams, which indicates that most of the heat available at temperatures higher than 85.0 °C is recovered internally through heat exchange with the help of the heat storage system, and only the heat below 85.0 °C is available to be used by the WHR technologies, including the ORC.

In total, the model consists of 1 562 equations with 1 236 variables (59 integer variables), plus two additional equations to set the TAM limits to the utility consumption. Results for MP-ST-ORC for Case Study 3 are summarized in Table 5-23 and the grid diagrams for the generated configuration are presented in Appendix D.

Table 5-23. Results of MP-ST-ORC for Case Study 3

Operating Conditions ORC	
Working Fluid	n-Butane
P_{evap} (kPa)	641.42
P_{cond} (kPa)	208.63
T_{evap}^{in} (°C)	20.36
T_{evap}^{out} (°C)	60.00
T_{cond}^{in} (°C)	32.35
T_{cond}^{out} (°C)	20.00
Results	
Average Hot Utility Consumption (kW)	0.0
Hot Utility Consumption per Cycle (kWh)	0.0
Average Cold Utility Consumption (kW)	157.8
Cold Utility Consumption per Cycle (kWh)	1 575.8
\bar{W}_{net} (kW)	9.0
\bar{W}_{turb} (kW)	9.2
\bar{W}_{pump} (kW)	0.28
W_{net} (kWh)	89.5
W_{turb} (kWh)	90.3
W_{pump} (kWh)	2.8
OPEX (€/a)	12 606.2
CAPEX (€/a)	39 631.5
Electricity Sales (€/a)	-14 321.7
TAC (€/a)	37 916.0
Area (m ²)	345.8
Storage Volume (m ³)	32.1
Number of Units	13
η_{orc}	8.4
Termination Criteria	Time Limit
Optimality Gap (%) /CPU Time (s)	67.20

Source: Own table

Compared with HEN1 as presented in Table 5-21 (TAC1), the results for MP-ST-ORC show a reduction of 14.9 % in the TAC of the system (37 916.0 €/a instead of 44 562.3 €/a), without increasing its utility consumption. The system generates in average 9.0 kW of electricity from waste heat, which would otherwise be rejected. The low temperature at which the waste heat is available, influences negatively the efficiency of the cycle and only 8.4% of the energy fed to the ORC is transformed to electricity. The generated system has only two heat exchanger units more than the stand-alone HEN (13 instead of 11) and, although the heat transfer area required increases by 37.2 % (345.8 m² instead of 252.1 m²), the required heat storage volume decreases slightly by 5.3% (32.1 m³ instead of 33.9 m³). In general, the integration of the ORC has again a positive impact on the economics of the design, as the increased CAPEX (39 631.5 €/a instead of 31 239.9 €/a) is offset by the sales from the electricity generated by the ORC (14 321.7 €/a).

5.3.2 Process Integration of Absorption Chillers

The cold utility temperature available in this case is 20.0°C, as indicated in Table 5-18. The refrigeration temperature to be generated by the ABC (T_{ref}) is set to 5.0°C and $\Delta T_{min} = 10.0^\circ\text{C}$ is used for all matches. In total, the model consists of 1 283 equations with 1 001 variables (53 integer variables) plus two equations for the TAM limits to the utility consumption. Results for MP-ST-ABC for Case Study 3 are summarized in Table 5-24 and the grid diagrams for the generated configuration is presented in Appendix D.

Table 5-24. Results of MP-ST-ABC for Case Study 3

Operating Conditions ABC	
T_{ref} (°C)	5
Results	
Average Hot Utility Consumption (kW)	0.0
Hot Utility Consumption per Cycle (kWh)	0.0
Average Cold Utility Consumption (kW)	166.5
Cold Utility Consumption per Cycle (kWh)	1 665.3
Average Cooling Generated (kW)	30.0
Cooling Generated per Cycle (kWh)	300.0
OPEX (€/a)	13 322.4
CAPEX (€/a)	35 649.1
TAC (€/a)	48 971.4
Area (m ²)	292.3
Storage Volume (m ³)	35.1
Number of Units	17
Termination Criteria	Time Limit
Optimality Gap (%) /CPU Time (s)	43.18

Source: Own table

Compared with HEN2 (HEN with cold utility available at 30°C and therefore requiring a VCR system for additional refrigeration) as presented in Table 5-21, MP-ST-ABC has a 7.6% lower

TAC (48 971.4 €/a instead of 52 992.3 €/a) due to the replacement of electricity for waste heat as driving force for the refrigeration cycle. The calculated savings would be higher if the capital costs of the VCR were also considered.

The system has also an increase in the required heat transfer area (292.3 m² instead of 252.1 m²), the number of heat transfer units (17 instead of 11) and in storage volume (35.1 m³ instead of 33.9 m³). Even then, MP-ST-ABC is able to generate in average 30.0 kW of cooling at 5.0 °C from waste heat, which otherwise would have to be provided by the VCR system using electricity.

5.3.3 Process Integration of Waste Heat Recovery Technologies (Combined Model)

In this case, the conditions are similar to those of MP-ST-ORC and MP-ST-ABC. $\Delta T_{min} = 10.0$ °C is used for all matches in the system. The cold utility temperature is set to 20.0 °C, like in MP-ST-ABC. The working fluid for the ORC is n-Butane with an evaporation temperature of 60.0 °C (641.42 kPa) and a condensation temperature of 30.0 °C (284.81 kPa). In total, the model consists of 1 483 equations with 1 178 variables (59 integer variables), plus two equations for the TAM limits to the utility consumption. Results for MP-ST-WHR for Case Study 3 are summarized in Table 5-25. Table 5-26 and Table 5-27 present detailed information about the design and Figure 5-10 illustrates the grid diagram for the configuration.

Compared with HEN2 (HEN with cold utility available at 30°C and therefore requiring a VCR system for additional refrigeration) as presented in Table 5-21, MP-ST-WHR has a slight decrease of 5.9 % in TAC (49 846.4 €/a instead of 52 992.3 €/a) and it is able to generate in average 3.2 kW of electric power and 30.0 kW of cooling at 5.0°C from waste heat.

Comparing MP-ST-WHR with MP-ST-ORC, the electricity generated decreases in 64.4 % (3.2 kW instead of 9.0 kW). Similar to HEN-WHR and MP-WHR, the drop in power generated by MP-ST-WHR is produced by the use of a part of the waste heat to drive the ABC instead of generating electricity and the increase in the working fluid condensation temperature for the ORC, which decreases the efficiency of the ORC cycle (6.4% instead of 8.4) and the amount of waste heat available for the ORC. As for the comparison between MP-ST-WHR and MP-ST-ABC, both configurations generate the same amount of cooling at 5°C (in average 30.0 kW in both cases) but the integration of the ORC increases by 1.8% the TAC of the system (49 846.4 €/a instead of 48 971.4 €/a), as the generated electricity in MP-ST-ORC is unable to offset the increases in the capital cost of the system due to the ORC.

The heat exchanger information for MP-ST-WHR in Table 5-26 shows, as with Case Study 2, that the heat exchanger duties vary depending on the period of operation, with none of the heat exchangers operating in all the periods. A similar behavior is observed in turbines and pumps as presented in Table 5-27, as their duties change depending on the operating period.

Table 5-25. Results of MP-ST-WHR for Case Study 3

Operating Conditions WHR	
T_{ref} (°C)	5.00
Working Fluid	n-Butane
P_{evap} (kPa)	641.42
P_{cond} (kPa)	284.81
T_{evap}^{in} (°C)	30.31
T_{evap}^{out} (°C)	60.00
T_{cond}^{in} (°C)	39.44
T_{cond}^{out} (°C)	30.00
Results	
Average Hot Utility Consumption (kW)	0.0
Hot Utility Consumption per Cycle (kWh)	0.0
Average Cold Utility Consumption (kW)	163.3
Cold Utility Consumption per Cycle (kWh)	1 633.3
Average Cooling Generated (kW)	30.0
Cooling Generated per Cycle (kWh)	300.0
\bar{W}_{net} (kW)	3.2
\bar{W}_{turb} (kW)	3.3
\bar{W}_{pump} (kW)	0.1
W_{net} (kWh)	32.0
W_{turb} (kWh)	33.2
W_{pump} (kWh)	1.1
OPEX (€/a)	13 066.2
CAPEX (€/a)	41 906.0
Electricity Sales (€/a)	-5 125.7
TAC (€/a)	49 846.4
Area (m ²)	386.5
Storage Volume (m ³)	34.8
Number of Units	16
η_{orc}	6.4
Termination Criteria	Time Limit
Optimality Gap (%) /CPU Time (s)	82.57

Source: Own table

Table 5-26. Heat exchanger information for MP-ST-WHR in Case Study 3

Type of Heat Exchanger	Match	Maximum Area (m ²)	Heat Exchanger Duty (kW)			
			Period 1	Period 2	Period 3	Period 4
Intra-Process (i,j,k)	2,1,1	10.9	163.0	135.0	163.0	-
	1,1,2	28.8	180.0	320.0	180.0	-
	2,1,2	21.4	137.1	-	137.1	-
	2,2,3	47.8	-	345.0	-	-
Cold Utility (i)	1	2.0	7.1	7.1	7.1	45.1
Hot Streams to Cold Sto. Streams (i,k,l _v)	1,1,1	16.0	140.0	-	134.8	320.0
	2,3,1	24.3	120.7	-	159.5	-
	3,2,1	4.0	-	-	50.1	-
Cold Streams to Hot Sto. Streams (j,k,l _v)	1,2,1	1.2	-	25.0	-	-
	2,3,1	171.8	-	905.0	-	-
ORC-Evaporator (i)	1	4.3	-	74.9	54.2	74.9
ORC-Cold Utility		9.9	-	70.1	50.7	70.1
ABC-Generator (i)	1	13.7	112.9	37.9	63.9	-
ABC-Evaporator (i)	2	6.6	80.3	30.0	50.5	-
ABC-Condenser		8.9	93.0	31.3	52.6	-
ABC-Absorber		15.0	109.1	36.7	61.8	-

Source: Own table

Table 5-27. Turbine and pump information for MP-ST-WHR in Case Study 3

Type of Component	Maximum Duty (kW)	Duty (kW)			
		Period 1	Period 2	Period 3	Period 4
Turbine	5.0	0.0	5.0	3.6	5.0
Pump	0.2	0.0	0.2	0.1	0.2

Source: Own table

5.4 Sensitivity Analysis

In this section, an exemplary sensitivity analysis of one of the nine developed models is performed. The objective of this analysis is to study the effect of the variation of key design parameters in the synthesis results. From the nine developed models, HEN-WHR, as used in Case Study 1, is used for the sensitivity analysis because it combines good computational performance (low optimality gaps after 3600 s of computational time) and a reasonable complexity as it combines 3 of the 4 studied subsystems (HEN, ORC and ABC).

The sensitivity analysis is divided into three parts corresponding to a) economical parameters, b) key temperatures inside the subsystems (ORC and ABC) and c) the minimum approach temperatures between different stream types in the system.

5.4.1 Economical parameters

The economical parameters considered and their variation range are presented in Table 5-28. All the selected parameters appear in the objective function for HEN-WHR as presented in equations (4-88) to (4-91) in Section 4.2.1.3. The selected parameters do not influence the amount of waste heat available in the system nor the performance of the ORC and ABC but influence the TAC of the design by changing its economics (CAPEX and OPEX).

Table 5-28. *Economical parameters for the sensitivity analysis of model HEN-WHR.*

Parameter	Symbol	Unit	Nominal Value	Lower Limit (%)	Upper Limit (%)
Annualization Factor	AF	(a ⁻¹)	0.23	70	130
Hours of Operation	Hy	(h/a)	8 000	70	100
Hot Utility Cost	C _{hu}	(€/kWh)	0.01	70	130
Cold Utility Cost	C _{cu}	(€/kWh)	0.001	70	130
Electricity Cost/Price	e ^{cost} /e ^{price}	(€/kWh)	0.2	70	130
Capital cost exponent	β	-	0.65	70	130

Source: *Own table*

The results of the sensitivity analysis for Case Study 1 with the HEN-WHR model using economical parameters are presented in Figure 5-11 and Figure 5-12. From the studied parameters, the “Hot Utility Cost” (C_{hu}) has the biggest impact on the TAC of the system. As expected the “Hot Utility Cost” has a linear relation with TAC, as the hot utility consumption of the system is fixed to its “hot utility target” as calculated with pinch analysis (See modeling assumptions in Section 1.3). A similar linear relation can be seen for other of the studied variables with exception of the capital cost exponent (β) which presents an exponential relation with TAC. In this case, as with Case Study 1, the same capital cost exponent was used by all components. The only variable with an inverse relation with TAC is the electricity cost, as for the same amount of energy recovered by the ORC, increasing electricity costs decrease the TAC of the system by decreasing its OPEX.

It is clear from Figure 5-12, that variations on the selected parameters do not influence the net power generated by the system (W_{net}) nor the total heat transfer area of the design. The small discrepancies between the values reported for the Total Heat Transfer Area and W_{net} for different percentages of the nominal values in Figure 5-12 are explained by the numerical precision of the solver used and the relatively large optimality gap used for the optimizations (10 %). From the variables in Table 5-28, two (i.e. Annualization Factor and Capital Cost Exponent) have an influence solely on the CAPEX of the system, while the other 4 variables in Table 5-28 (hours of operation, electricity cost and hot and cold utility cost) only affect the OPEX. None of the variables affects simultaneously both TAC components.

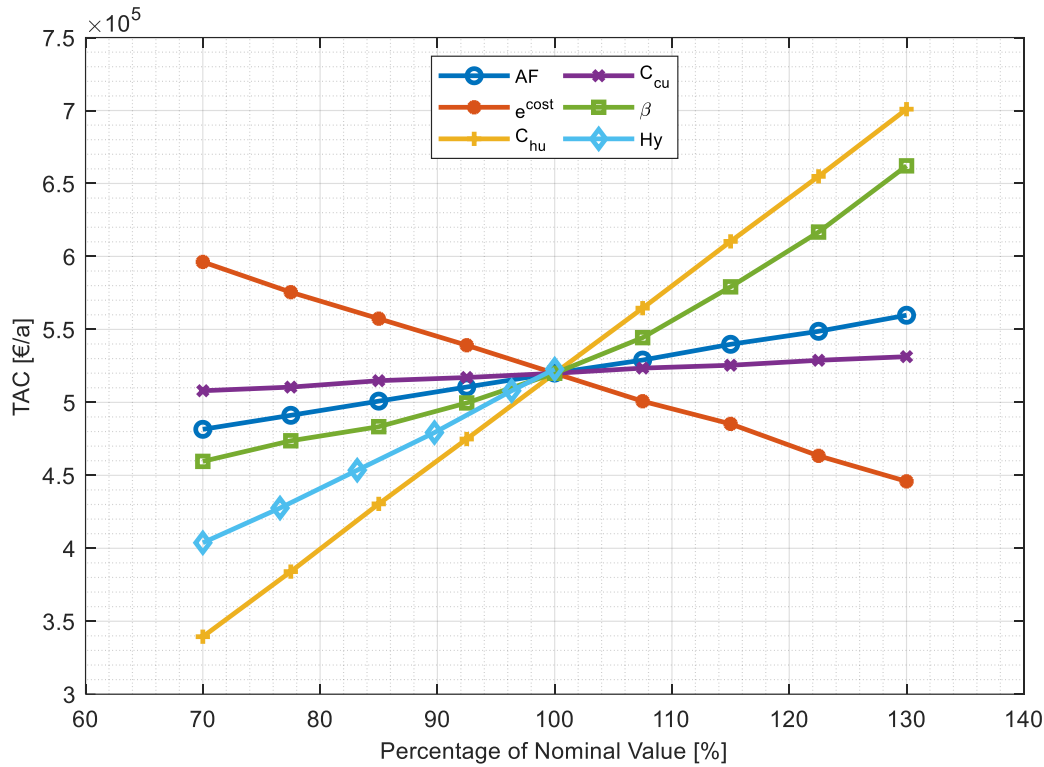


Figure 5-11. Sensitivity analysis of the Total Annualized Cost (TAC) of the system generated using HEN-WHR for Case Study 1 (Economical Parameters).

Source: Own diagram

5.4.2 Key temperatures in the subsystems ORC and ABC

Three key temperatures in the system are used to study the behavior of the HEN-WHR model. These temperatures are the evaporation (T_{evap}^{out}) and condensation (T_{cond}^{out}) temperatures in the ORC (as defined at the exit of the ORC-Evaporator and ORC-Condenser respectively) and the refrigeration temperature (T_{ref}) as used in the evaporator in the ABC. The temperatures considered and their variation range are presented in Table 5-29. The selected parameters do not influence the amount of waste heat available in the system but they affect the performance of the ORC and ABC, therefore changing the system designs and their economic performance. For consistency, the range of variation for the ORC evaporation temperatures is the same as the one used in the prescreening procedure as presented in Section 5.1.1 ($T_{evap}^{out} \in [80.0 ; 120.0]^{\circ}C$). Condensation temperatures lower than the nominal value are not considered, as the nominal value ($T_{cond}^{out} = 45^{\circ}C$) is the lowest temperature that can be achieved in the ORC condenser using the available cold utility in HEN-WHR ($T_{cu}^{out} = T_{cu}^{in} = 30^{\circ}C$) with the given minimum approach temperature ($\Delta T_{min} = 15.0^{\circ}C$).

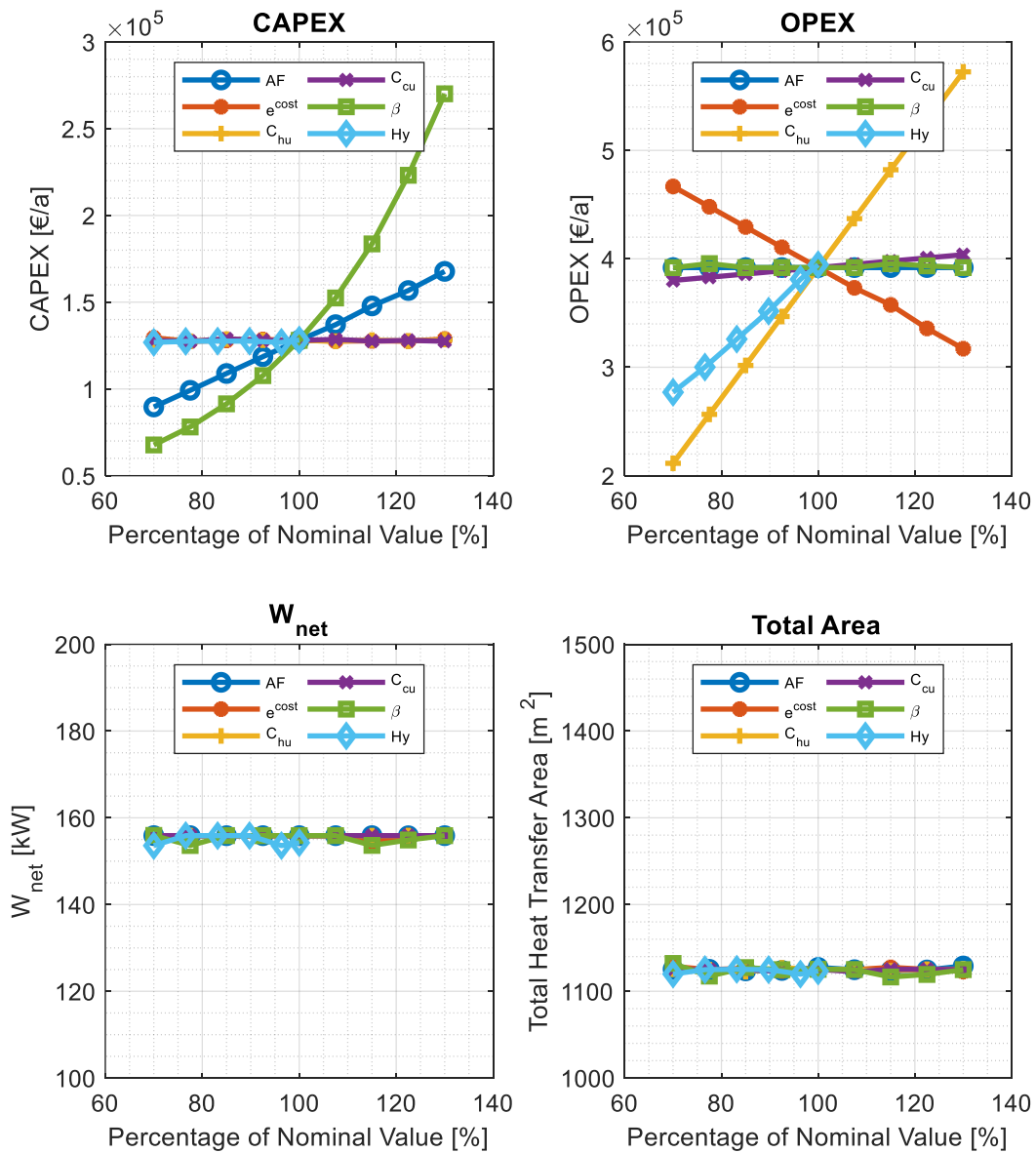


Figure 5-12. Sensitivity analysis of multiple design variables of the system as generated using HEN-WHR for Case Study 1 (Economical Parameters).

Source: Own diagram

Table 5-29. Key temperatures used for the sensitivity analysis of model HEN-WHR.

Parameter	Symbol	Unit	Nominal Value	Lower Limit (%)	Upper Limit (%)
Evaporation Temperature (ORC)	T_{evap}^{out}	°C	85.76	93.28	139.93
Condensation Temperature (ORC)	T_{cond}^{out}	°C	45.00	100	130
Refrigeration Temperature (ABC)	T_{ref}	°C	10.00	70	130

Source: Own table

The results of the sensitivity analysis for Case Study 1 with the HEN-WHR model using the parameters in Table 5-29 are presented in Figure 5-13 and Figure 5-14. Higher ORC condensation temperatures (T_{cond}^{out}) have a negative impact on the TAC of the system as they decrease the amount of net power generated by the ORC. This effect can be explained by a reduction of the energy available for the ORC and a decrease in the efficiency of the ORC. The variation of the refrigeration temperature (T_{ref}) have a minimal impact on the TAC of the system by slightly increasing or decreasing the total heat transfer areas of the designs. An interesting behaviour is obtained by increasing the ORC evaporation temperature (T_{evap}^{out}), as it tends to increase the net power (W_{net}) generated, to decrease the OPEX and to improve the TAC of the system. This behaviour is not linear and for this particular case study (Case Study 1) and model (HEN-WHR) it can be described as a trend instead of a direct relationship.

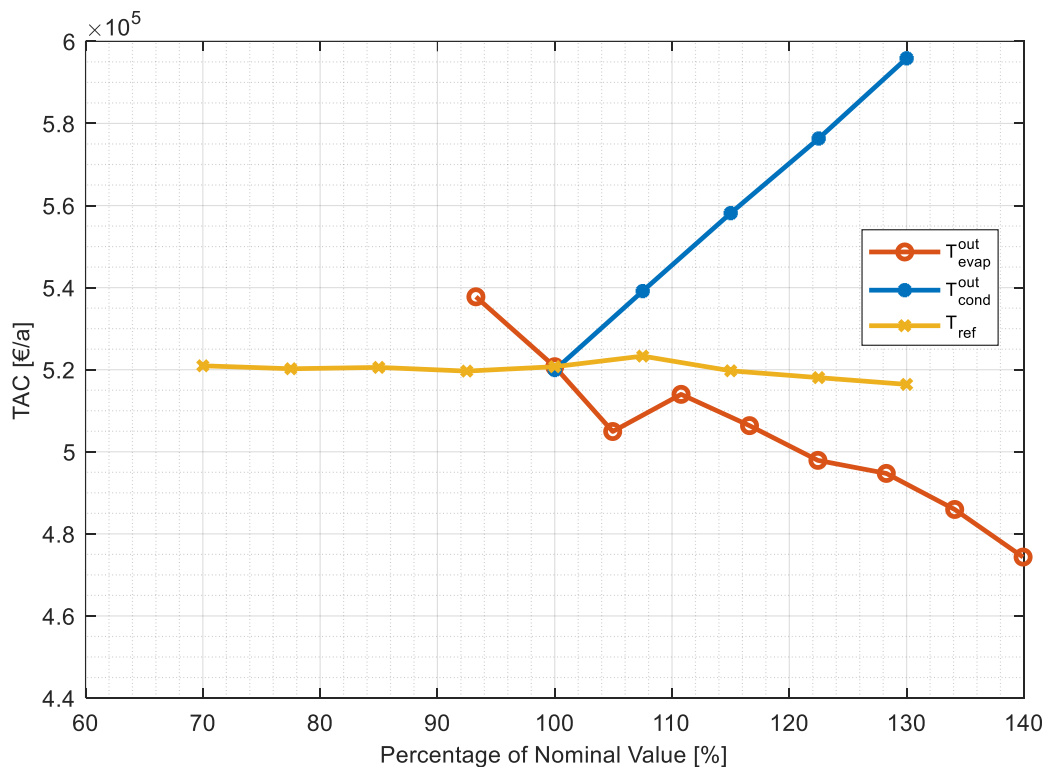


Figure 5-13. Sensitivity analysis of the Total Annualized Cost (TAC) of the system generated using HEN-WHR for Case Study 1 (Key temperatures in the subsystems ORC and ABC).

Source: Own diagram

Another interesting finding is that the nominal T_{evap}^{out} used in Case Study 1 for HEN-WHR is not the optimal evaporation temperature, as higher temperature values have better thermodynamical and economical performances. This is expected as the nominal evaporation temperature used ($T_{evap}^{out} = 85.76$ °C) was obtained using the prescreening algorithm with the HEN-ORC model and W_{net} as the objective function. For HEN-WHR a new application of the

prescreening algorithm is required in order to find its “optimal” (in relation to W_{net}) operating conditions. In Section 5.1 the same evaporation temperature was used for the 2 models (HEN-ORC and HEN-WHR) in order to have a direct comparison between the systems designs. The irregular behaviour of TAC and W_{net} with the increasing T_{evap}^{out} highlights the need to incorporate the operating conditions of the ORC in the optimization model. This extension is recommended as a future area of research (Section 6.2).

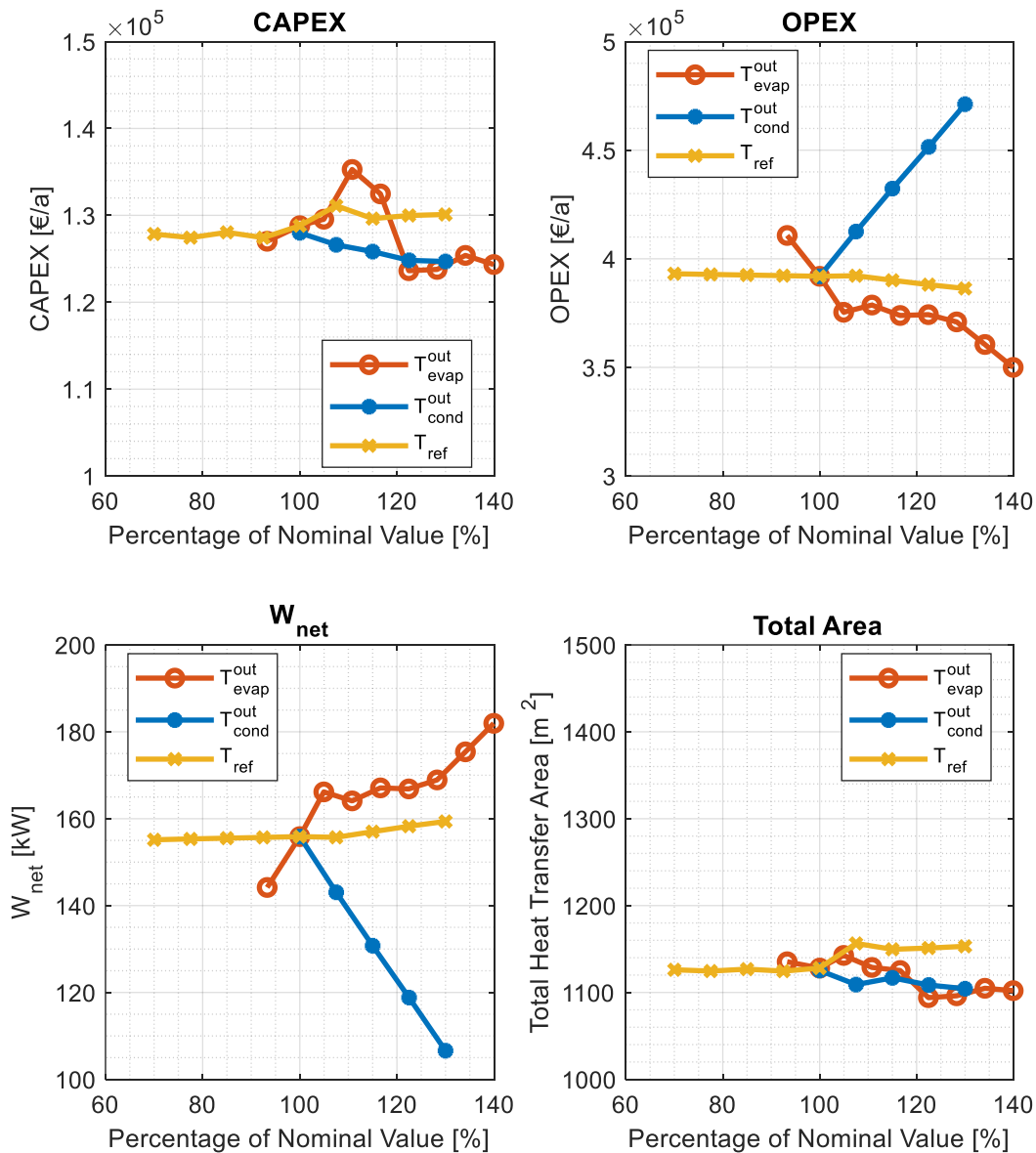


Figure 5-14. Sensitivity Analysis of multiple design variables of the system as generated using HEN-WHR for Case Study 1 (Key temperatures in the subsystems ORC and ABC).

Source: Own diagram

5.4.3 Minimum approach temperatures

Variations in the minimum approach temperatures between the process streams including utilites (ΔT_{min}^{HEN}), the process streams (including utilites) and the ORC working fluid (ΔT_{min}^{ORC}) and the process streams (including utilites) and the ABC working pair (ΔT_{min}^{ABC}) are also studied as part of the sensitivity analysis. In the case studies presented in this chapter, all the minimum approach temperatures in their respective systems were set to the same value and treated as equal ($\Delta T_{min} = 15.0^\circ\text{C}$ for Case Study 1 and Case Study 2, and $\Delta T_{min} = 10.0^\circ\text{C}$ for Case Study 3), but in the most general case, minimum approach temperatures for each match in the system can be defined. Table 5-30 presents the minimum approach temperatures considered and their variation range. In this sensitivity analysis, the hot and cold utility are treated as part of the process streams. ΔT_{min}^{ORC} is limited to values lower than the nominal, as the condensation temperature of the working fluid is set to 45°C and it requires cooling from the cold utility at 30°C . A ΔT_{min}^{ORC} higher than the nominal (15°C) would therefore force the cold process streams to provide the whole cooling requirement for the ORC, which is impractical. A similar limitation is presented in ΔT_{min}^{ABC} , which cannot be higher than 115% of the nominal value in order to avoid crystallization. Higher values of ΔT_{min}^{ABC} increase the condensation (T_{cond}) and absorption (T_{abs}) temperatures of the ABC as defined in Section 4.2.1.2 and Section 1.3 (Cold utility temperature 30°C plus minimum approach temperature). For a given refrigeration temperature (T_{ref}) there is a maximum condensation/absorption temperature above which crystallization occurs and the ABC cycle is not able to generate the required cooling.

Table 5-30. Minimum approach temperatures used for the sensitivity analysis of model HEN-WHR.

Minimum Approach Temperature	Symbol	Unit	Nominal Value	Lower Limit (%)	Upper Limit (%)
Process Streams-Process Streams	ΔT_{min}^{HEN}	$^\circ\text{C}$	15.00	70	130
Process Streams-ORC	ΔT_{min}^{ORC}	$^\circ\text{C}$	15.00	70	100
Process Streams-ABC	ΔT_{min}^{ABC}	$^\circ\text{C}$	15.00	70	115

Source: Own table

The results of the sensitivity analysis for Case Study 1 with the HEN-WHR model using the parameters in Table 5-30 are presented in Figure 5-15 and Figure 5-16. ΔT_{min}^{HEN} and ΔT_{min}^{ORC} behave similarly, with higher values increasing the TAC of the system as they increase its OPEX. This growth in the OPEX is mainly caused by a decrease in the net power generated by the ORC as higher values of ΔT_{min}^{HEN} and ΔT_{min}^{ORC} decrease the amount of energy available to be used by the ORC. ΔT_{min}^{ABC} has similar trends and higher values increase the TAC of the system by increasing its OPEX due to the reduction of the net power generated by the ORC. An

interesting behaviour takes places with ΔT_{min}^{ABC} lower than 77.5 % of the nominal value ($\Delta T_{min}^{ABC} = 11.625\text{ }^{\circ}\text{C}$) as below this minimum approach temperature, the ABC can be driven by the hot stream H6 ($T^{in} = 92^{\circ}\text{C}$ and $T^{out} = 91.9^{\circ}\text{C}$ in Table 5-1) leaving additional energy available to the ORC, which for higher values of ΔT_{min}^{ABC} is used to drive the ABC and now can instead be fed to the ORC to generate additional net power.

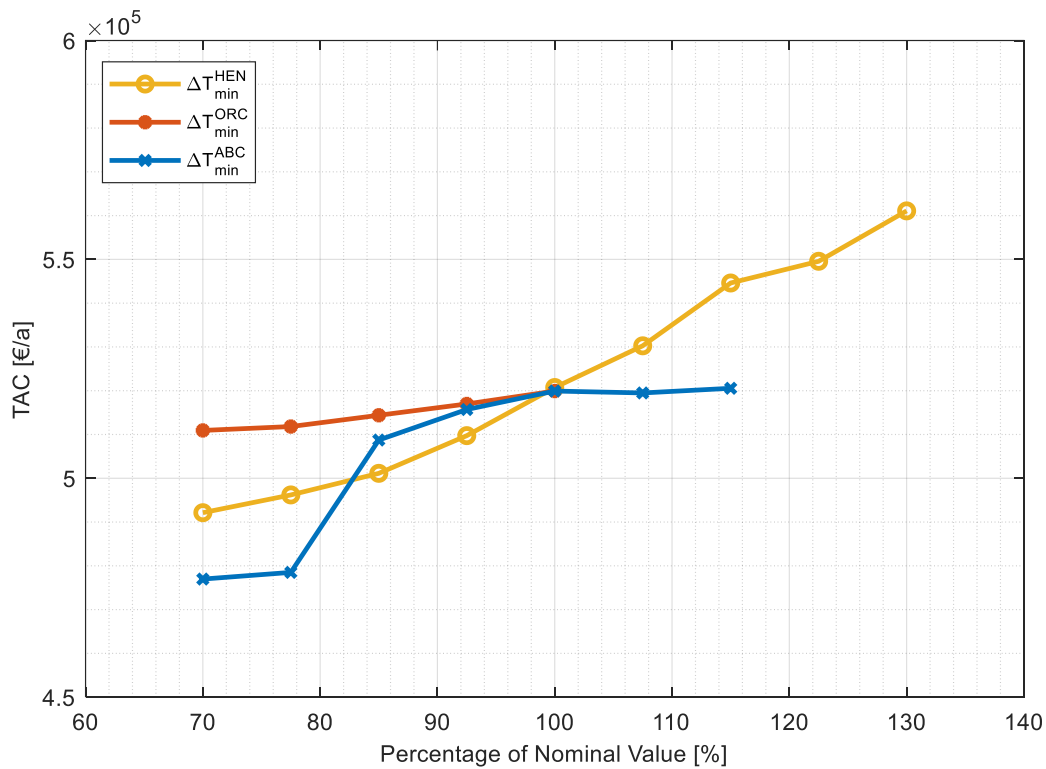


Figure 5-15. Sensitivity Analysis of the Total Annualized Cost (TAC) of the system generated using HEN-WHR for Case Study 1 (Minimum approach temperatures between different stream types).

Source: Own diagram

5.4.4 General comments on the sensitivity analysis

The results of the sensitivity analysis of the HEN-WHR model as used for Case Study 1 show the effects of different parameters in the optimization procedure and its corresponding system designs. The multitude of parameters and complex interactions between them have been evaluated in a fast and direct way with help of the mathematical model. The results of the sensitivity analysis can only be interpreted on the context of Case Study 1 and the HEN-WHR model and the effect of the different parameters in the behavior of the variables can differ if different input data or models are used.

As for the sensitivity analysis of HEN-WHR using Case Study 1, the parameters “Hot Utility Cost” (C_{hu}), “Hours of Operation per Year” (H_y) and “ORC Condensation Temperature”

(T_{cond}^{out}) have the biggest impact on the TAC of the system, while the “ABC Refrigeration Temperature” (T_{ref}) has the smallest. An important finding of the sensitivity analysis is, that the nominal “ORC Evaporation Temperature” used ($T_{evap}^{out} = 85.76\text{ }^{\circ}\text{C}$) is not optimal and higher temperatures tend to generate designs with better TAC. This result highlights the need to incorporate the operating conditions of the ORC in the optimization model.

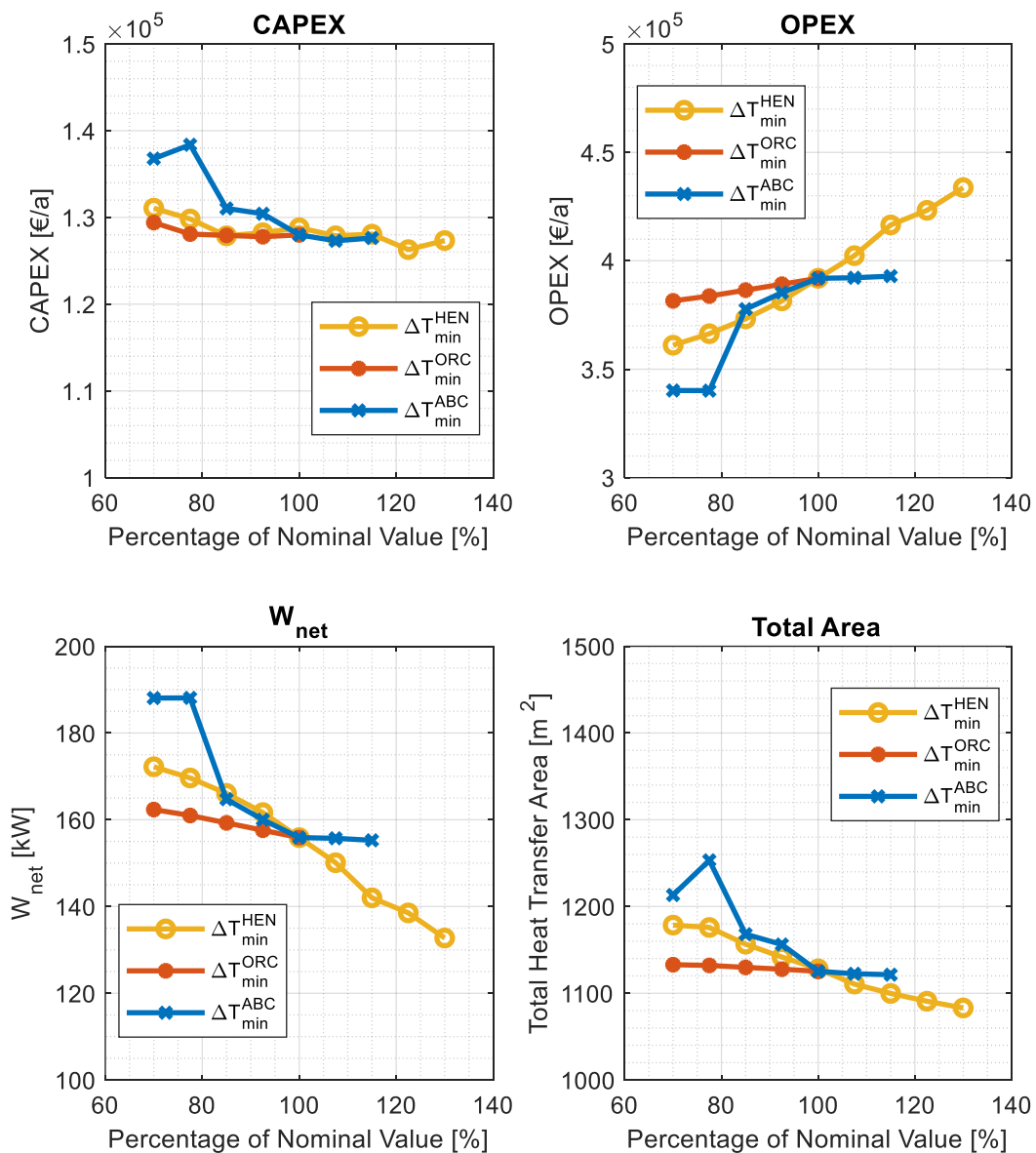


Figure 5-16. Sensitivity Analysis of multiple design variables of the system as generated using HEN-WHR for Case Study 1 (Minimum approach temperatures between different stream types).

Source: Own diagram

Another interesting parameter to study is the number of intra-process stages in the superstructure. Figure 5-17 and Figure 5-18 present the results of the sensitivity analysis of the number of intra-process stages for HEN-WHR as used in Case Study 1. The results show that starting on 3 stages the optimization results stay constant and additional stages do not improve the system designs. In the case of only 2 intra-process stages a small penalty in the TAC exist as the net power generated by the ORC is lower than with 3 or more stages. Additionally, the number of heat transfer units in the system designs increases with increasing number of stages. This is typical of mathematical programming techniques and it is referred to as “Spaghettification”. Although starting from 3 stages, all the designs have similar TACs, in practice the systems with less heat transfer units are preferable as they simplify the control and operation the system.

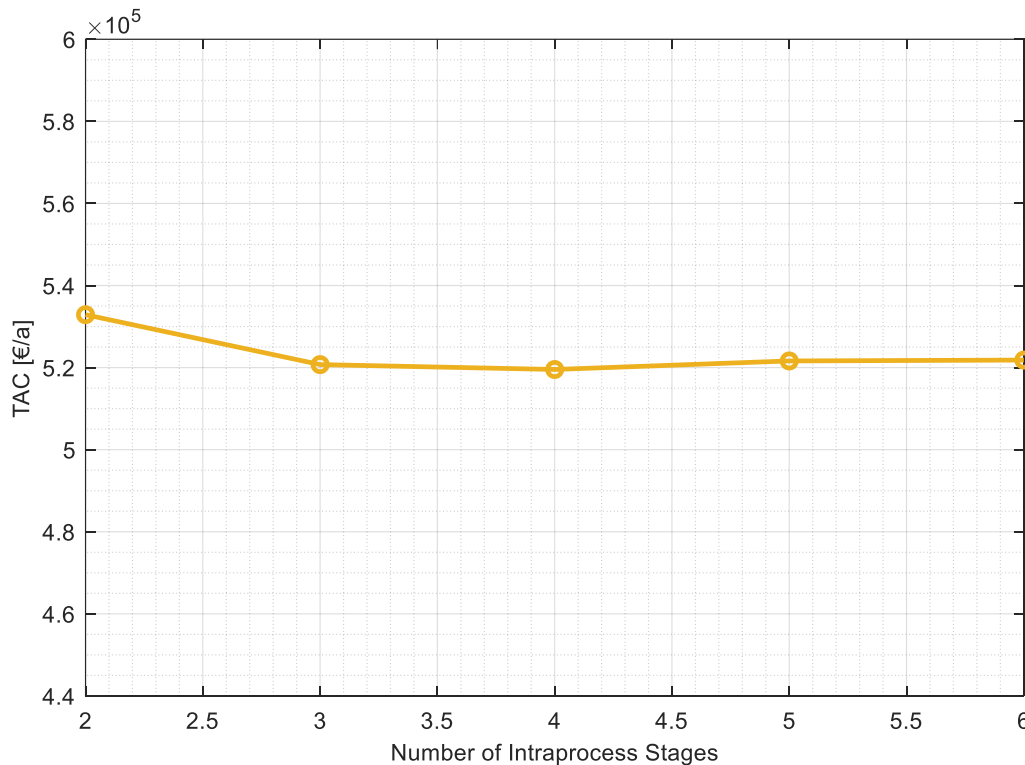


Figure 5-17. Sensitivity Analysis of the Total Annualized Cost (TAC) of the system generated using HEN-WHR for Case Study 1 (Number of intraprocess stages in the superstructure).

Source: Own diagram

In general, the minimum number of stages required to generate a system with minimum TAC (optimal number of stages) depends on the process streams studied and the model used. Ideally, multiple runs of the models with different number of stages should be performed to find the optimal number of stages. As mentioned before the results presented in this sensitivity analysis

are only to be interpreted in the context of the input data for Case Study 1 and using the HEN-WHR model.

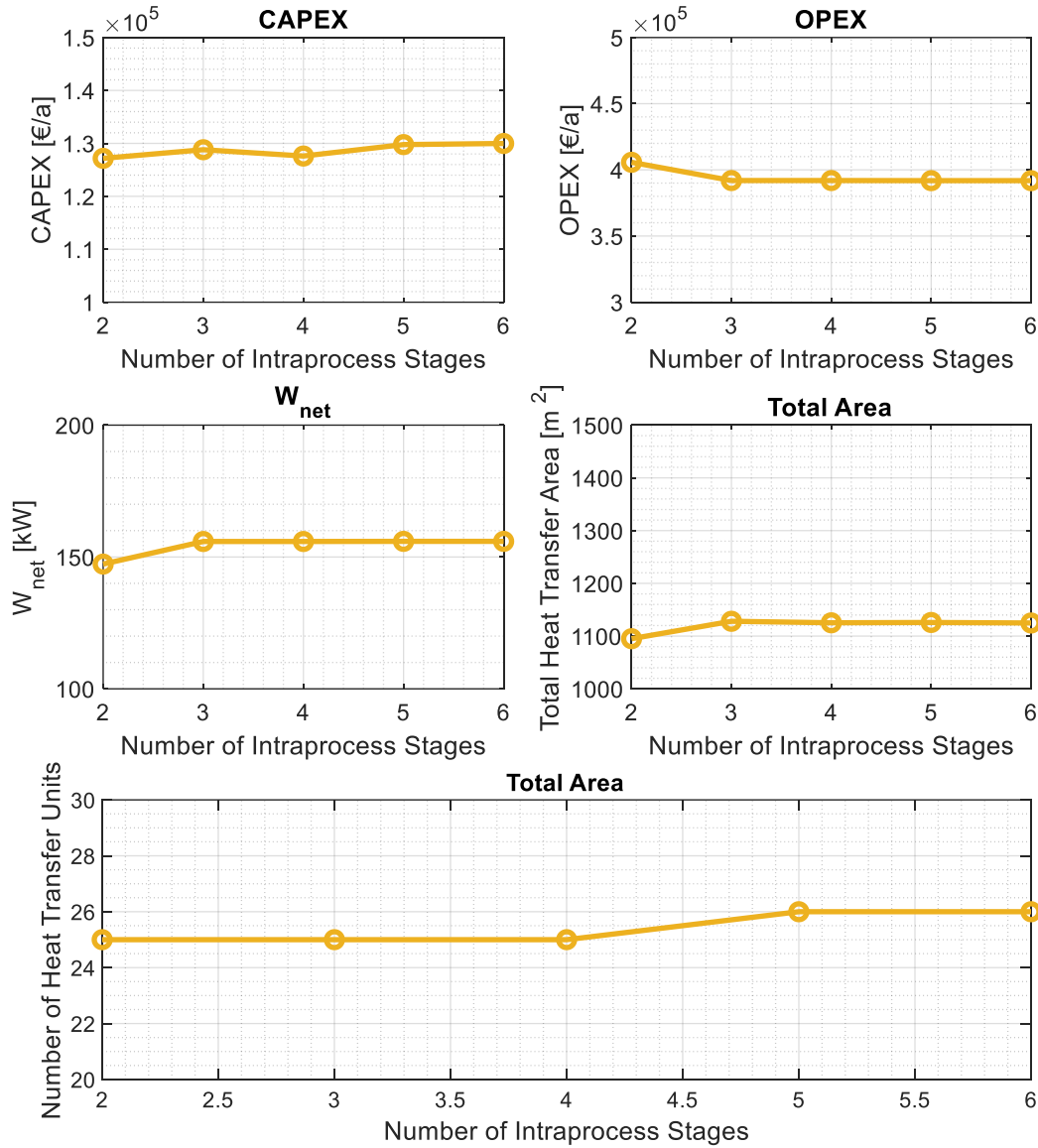


Figure 5-18. Sensitivity Analysis of multiple design variables of the system as generated using HEN-WHR for Case Study 1 (Number of intraprocess stages in the superstructure).

Source: Own diagram

5.5 Critical Discussion

The application of the nine structures developed in Chapter 4 for the process integration of organic Rankine cycles, absorption chillers or both, into heat exchanger networks for continuous and multi-period processes with and without FTVM heat storage, was illustrated with three case studies from the literature. For each model a local optimum is reported, which minimizes the TAC of the system while integrating WHR technologies without increasing its utility consumption. As a result, the generated designs produce electricity, cooling or both from waste heat that otherwise would be rejected through the cold utility. Additionally, an exemplary sensitivity analysis of one of the developed models (HEN-WHR) was presented, in order to illustrate the effect of different parameters in the optimization results.

Some general comments from the results of the case studies are presented below, including the calculation of CO₂ savings due to the integration of the WHR technologies into the HENs, in comparison with the stand-alone HENs.

- As expected even with the 10% optimality gap, most of the optima generated in the case studies do not reach the required tolerance before the time limit, and instead they generate local solutions that cannot be proved to be less than 10% off from the global optimum. The effect is more visible in multi-period processes where only 1 out of 6 optima reaches the tolerance required.
- It is important to emphasize that big optimality gaps do not indicate if the reported solutions are close or far to the global optimum. They only indicate that the solver was unable to “prove” that the reported solution is less than 10% off from the global optimum. Although the solver BARON includes some mathematical procedures to help with the “proving process”, in the most general case for complex MINLP a global optimum can only be calculated if all the possible configurations are evaluated. Even in the simplest case for continuous processes without including the utilities or the WHR technologies, the synthesis of HENs is a combinatorial problem, that is the number of possible configurations of the system is equal to $(N_{Hot}N_{Cold}N_{Stages})!$. For Case Study 1 that number is up to 120! (6.7E198). In practice, the evaluation of all possible configurations is impossible.
- Although the solver BARON does not require initial values to perform the optimization, good initial values help the solver to find good local optima faster. For the case studies presented, a simple initialization procedure was used. First the models are solved without including the capital costs in the objective functions. The binary variables from this solution are then fixed and the resulting NLP is then optimized. The solution obtained to this NLP

including the binary variables from the first optimization are used as initial points for the final MINLP.

- The number of heat exchanger units when using mathematical programming approaches tends to be high (“Spaghettification”). This can be solved by introducing a limit to the number of units in the system. For the most general case (MP-ST-WHR superstructure), equation (5-1) sets that limit to the number of heat exchanger units (N_{Limit}). The effects of this limit to the number of heat exchanger units in the TAC and performance of the system should be evaluated in case-by-case basis.

$$\begin{aligned} \sum_{i \in HHP} \sum_{j \in CP} \sum_{k \in ST} z_{i,j,k} + \sum_{i \in HHP} z_i^{cu} + \sum_{j \in CP} z_j^{hu} + \sum_{i \in HHP} z_i^{evap} + \sum_{j \in CP} z_j^{cond} + z^{acu} \\ + \sum_{i \in HHP} z_i^{abcg} + \sum_{i \in HHP} z_i^{abce} \leq N_{Limit} \end{aligned} \quad (5-1)$$

- The results obtained in the case studies can be further optimized using post-optimization strategies. By fixing the objective value generated by the models and using it as a constraint instead, it is possible to find other attractive system configurations. This strategy takes advantage of the fact that the number of variables in the models is always higher than the number of equations and therefore multiple solutions for the optimization problems exist that generate the same objective value. For example, by fixing the objective value obtained for TAC and using the minimum number of units or the minimum heat transfer area as objective functions instead, it is possible to find more attractive system configurations for real-life operation.
- In multi-period models, heat exchangers tend to operate only in some periods of operation. The reuse of heat exchangers for different matches, that is, the reuse of heat exchanger for different pairs of streams at different locations in the system, each period depending on their availability has the potential to decrease the number of units required, and therefore the capital costs of the HEN. Possible disadvantages of this method include but are not limited to the need of cleaning procedures for the heat exchangers with their associated additional costs. The integration of this “timesharing mechanism”, as presented by Sadeli and Chang (2012), to the models developed in this work, constitutes an area of future research.
- Although the integration of ORCs into HEN has a positive effect on the economics of the design in the case studies presented, the evaluation has to be done on a case-by-case basis. For batch processes where capital costs represent a large share of the investment cost, and

the energy costs only represent a small fraction of the TAC, the integration of ORCs could increase the CAPEX of the system without significant gains due to electricity revenues.

- For processes with cooling requirements and waste heat availability, the integration of ABCs into the HENs can be an interesting option. The ABCs do not change the required cooling load, but exchange expensive low temperature cold utility or cooling generated by VCR system with a cheaper cold utility at a higher temperature. Similar to ORCs the economics of the design have to be evaluated in a case-by-case basis.
- In their current configuration, the models integrating both ORCs and ABCs into HENs do not use at full extend the opportunities for additional synergies between the ORC and the ABC. Future improvements to the combined models, using the cooling generated by the ABC to decrease the condensation temperature of the ORC, have the potential to achieve a greater integration between the studied technologies and therefore improve the economic performance of the designs.
- It is possible to quantify, with certain assumptions, the environmental impact of the integrated designs presented in this chapter. Table 5-31 presents the CO₂ savings of the integrated designs in comparison with the stand-alone HENs (HEN1 and HEN2). The calculations are based on the emission factor of the German electricity mix for 2019 (0.401 kg/kWh), the electricity and cooling generated using waste heat for the different models and the assumed COPs for the cooling below the cold utility temperature, when provided by VCR systems as presented in each of the individual case studies (COP_{VCR} = 7.08 for Case Studies 1 and 2 and COP_{VCR} = 9.27 for Case Study 3).

Table 5-31. CO₂-Savings of the integrated designs in comparison with the stand-alone HENs

		CO ₂ Savings (t/a)		
		Electricity	Cooling	Total
Case Study 1	HEN-ORC	914.0	-	914.0
	HEN-ABC	-	182.1	182.1
	HEN-WHR	501.4	130.8	632.2
Case Study 2	MP-ORC	1 201.7	-	1 201.7
	MP-ABC	-	151.3	151.3
	MP-WHR	772.2	115.3	887.4
Case Study 3	MP-ST-ORC	28.9	-	28.9
	MP-ST-ABC	-	10.4	10.4
	MP-ST-WHR	10.3	10.4	20.7

Source: Own table

- Although not presented in the case studies, the models developed in this work are suitable, to some extent, for retrofit analysis of existing HENs. Similar to the use of the SYNHEAT model for the retrofit of HENs in continuous processes (Björk and Nordman 2005), by

fixing the binary variables representing the existing heat exchangers in the HEN and small modifications in the cost and area equations (e.g., capital cost of existing heat exchangers should be zero if their new required area is lower than their current area), it is possible to explore other configurations for the HEN while exploring opportunities for the integration of ORCs and ABCs into the background processes. The use of the models in their current configuration for retrofit is however limited, as they do not allow for exploring some retrofit options such as the relocation of existing heat exchangers and non-isothermal mixing of streams.

- The exemplary sensitivity analysis shows the effect of some model parameters in the optimization results for HEN-WHR. In the most general case, the results of the sensitivity analysis are not transferable due to the complex interactions between the subsystems. A case-by-case analysis of the models and input data is necessary in order to find the best operating conditions for each particular design.

In order to evaluate the economical, technical and/or environmental performance of the generated designs, three different parameters (one for each considered aspect) are used. To evaluate the economic performance of the systems integrating exclusively ORC (HEN-ORC, MP-ORC and MP-ST-ORC) the difference between the TAC of the combined designs and the TAC of HEN1 (TAC of the stand-alone HEN if no refrigeration is required) is used. In the case of systems involving ABCs (HEN-ABC, HEN-WHR, MP-ABC, MP-WHR, MP-ST-ABC and MP-ST-WHR), the difference between the TAC of the combined designs and the TAC of HEN2 (TAC of the stand-alone HEN including the refrigeration costs if provided by a VCR) is used.

In order to evaluate the technical performance of the systems, an efficiency ratio between the useful work recovered from the waste heat and the amount of waste heat available, as indicated by the cold utility target for the process, is used. The useful work for the ORC subsystem is defined by its net power generated and for the ABC subsystem equals to the refrigeration duty provided to the hot process streams at the ABC-Evaporators. For multi-period processes the average power and average refrigeration duties per cycle are used. By definition, this ratio for stand-alone HENs is zero, as they do not generate any useful work (electricity or cooling) from the available waste heat. The efficiency ratio is presented in equation (5-2).

$$Effic. Ratio = \frac{W_{net} + \sum_{i \in HP} q_i^{abce}}{\sum_{i \in HP} q_i^{cu}} \quad (5-2)$$

Finally, in order to evaluate the environmental performance of the designs, the CO₂-savings calculated in Table 5-31 are used.

Table 5-32. *Economical, technical and environmental evaluation of the results of the case studies.*

		TAC Savings		Efficiency Ratio	CO ₂ Savings (t/a)
		€/a	%		
Case Study 1	HEN-ORC	415 314.6	58.0%	5.6%	914
	HEN-ABC	55 520.3	7.0%	7.9%	182.1
	HEN-WHR	272 326.3	34.4%	8.7%	632.2
Case Study 2	MP-ORC	536 458.7	85.0%	7.2%	1 201.7
	MP-ABC	43 362.3	6.2%	6.4%	151.3
	MP-WHR	373 640.8	53.4%	9.5%	887.4
Case Study 3	MP-ST-ORC	6 646.3	14.9%	5.4%	28.9
	MP-ST-ABC	4 020.9	7.6%	18.0%	10.4
	MP-ST-WHR	3 145.9	5.9%	19.9%	20.7

Source: *Own table*

The results of the case studies as presented in Table 5-32 support the idea that combined design approaches are able to generate economically, technically and/or environmentally attractive system designs. For all the case studies presented, a reduction in the TAC of the systems (economically attractive) and CO₂-savings (environmentally attractive) were achieved by the combined designs in comparison with the stand-alone HEN designs (in the case of HEN-ORC, MP-ORC and MP-ST-ORC), or in comparison with the stand-alone HEN designs with cooling below the cold utility temperature provided by a VCR (in the case of HEN-ABC, HEN-WHR, MP-ABC, MP-WHR, MP-ST-ABC and MP-ST-WHR). Additionally in all combined designs, a share of the waste heat that would be otherwise rejected to the cold utility, was transformed into useful work (electricity or cooling). In average 9.8% of the waste heat available in the case studies was transformed into useful work (technically attractive).

6 Conclusions and Future Work

6.1 Conclusions

The overarching research question for this dissertation is:

“Can a combined design methodology considering simultaneously the synthesis of heat exchanger networks and the process integration of organic Rankine cycles, absorption chillers or both into the background processes in continuous and multi-period operation with and without FTVM heat storage, generate system designs that are economically, technically and/or environmentally more attractive than systems solely factoring heat exchanger networks?”

In order to answer this question, a mathematical framework for the process integration of ORCs, ABCs or both, into HENs in continuous and multi-period processes with and without FTVM heat storage was presented. As outlined in section 1.4, Chapter 2 introduced fundamental concepts of waste heat recovery and HEN synthesis (Process Integration), Chapter 3 presented the State-of-the-Art of the integration of ORCs and ABCs into HENs and Chapter 4 presented the nine superstructures developed for the process integration of ORCs and ABCs into HENs in continuous and multi-period processes with and without FTVM heat storage, including a discussion about the mathematical considerations and limitations of the nine superstructures. Finally, in Chapter 5, three case studies from the literature were used to illustrate the use and possibilities of the nine individual superstructures developed in this work and an exemplary sensitivity analysis for one of the developed superstructures was presented to highlight the influence that key parameters in the system have in the optimization results. At the end of the chapter, general comments about the results of the case studies and the performance of the mathematical models were presented.

The developed superstructures with their corresponding mathematical models, have proved to be useful for the relatively quick evaluation of combined designs integrating ORCs, ABCs, or both, into HENs in continuous and multi-period processes with and without FTVM heat storage. Although the specific economical, technical and/or environmental benefits from the generated designs have to be evaluated on a case-by-case basis, depending on the process considered and the economic and design parameters of the system, the results of this dissertation establish that at least for some cases (as the ones presented in the case studies), a combined design methodology considering simultaneously the synthesis of HENs and the process integration of ORCs, ABCs and FTVM heat storage into the background processes in systems with continuous or multi-period operation, is able to generate system designs that are economically,

technically and environmentally more attractive than systems solely factoring the stand-alone HEN. This allows to answer the overarching research question of this dissertation affirmatively.

6.2 Future Work

The main objective of this research was the generation of a mathematical framework for the process integration of ORCs, ABCs or both technologies into HENs, in continuous and multi-period processes with and without FTVM heat storage, and it was accomplished successfully. However, the mathematical framework has a number of limitations due to the assumptions made during the development of the superstructures and it can be improved to include more complex configurations or other attractive WHR technologies. Possible directions for future work, expanding upon the mathematical framework developed in this dissertation include but are not limited to:

- Inclusion of additional WHR technologies into the mathematical framework, with special emphasis on the process integration of heat pumps, as they have been successfully implemented in industrial processes worldwide.
- Integration of WHR in all locations in the superstructures and not only in the dedicated-stages.
- Linearization and simplification methodologies in order to reduce the computational complexity of the mathematical problems and limit the size of their solution search space.
- Integration of working fluid/working pair properties in the optimization. In this work, the operating conditions for working fluids and working pairs are decided beforehand and are not part of the optimization problem. By fully integrating working fluid/working pairs properties in the optimization model, it is possible to treat temperatures and pressures inside the ORCs and ABCs as optimization variables in order to find the best operating conditions for the systems.
- Consideration of other heat storage technologies. Mathematical formulations including latent heat storages, as well as VTVM (Variable Temperature Variable Mass) or VTFM (Variable Temperature Fixed Mass) storages are suggested topics for future works.
- For models including ORCs, the inclusion of other ORC configurations aside of the basic cycle, like regenerative, recuperative or transcritical cycles.
- For models including ABCs, the consideration of multi-effect ABCs and a rigorous analysis of the crystallization of LiBr in the refrigeration cycle.
- The consideration of transient and partial-load effects in the multi-period systems. As presented in this work, no transient or partial load effects have been considered. Even then,

turbine and pump efficiencies are known to be a function of the load in the system and varying the mass flow in the cycles can have an important effect on the performance of their components. Additionally, transient effects due to the change in operating conditions have not been considered but they could have a considerable influence on the performance of some system components.

- For multi-period processes, the consideration of the “timesharing mechanism” as presented by Sadeli and Chang (2012), in order to reuse heat exchangers in different matches each period, depending on the needs of the process. This methodology has the potential to improve the CAPEX of the systems, and therefore their TAC.
- Other configurations considering more complex integrations between the different WHR technologies used in the superstructures (ORCs and ABCs) can also be explored. Examples of such alternative configurations include the use of the heat rejected from the ORC-Condenser to drive the ABC-Generators, or the use of the refrigeration effect at the ABC-Evaporator to decrease the condensation temperature at the ORC-Condenser, etc.
- Similarly, alternative configurations exploring better integration opportunities between the WHR technologies and the storage systems can also be explored. As presently constructed, the direct interaction between the storage system and the WHR technologies was not considered in the mathematical framework developed in this dissertation. As mentioned in section 4.3, some works considering the integration of ORCs into industrial processes (without considering the HEN synthesis) have already proposed the use of storage tanks between the process streams and the ORCs in order to limit/damp the fluctuation of its operational parameters (Pili et al. 2017; Pantaleo et al. 2017; Lecompte 2017; Jiménez-Arreola et al. 2018), with positive results, including the decrease on the required size for the ORC.
- Adaptation of the mathematical framework for the study of retrofit problems. Although, in their current configuration, the superstructures can be used to evaluate some retrofit options, they do not include attractive retrofit measures, such as the relocation of existing heat exchangers, or the non-isothermal mixing of streams.
- Use of intermediate heats transfer fluids for the process integration of the WHR technologies into the HEN. As presented by Chamorro-Romero and Radgen (2020) for the integration of ORC into HENs in continuous processes, the use of intermediate heat transfer fluids allows to consider system designs where the physical location of the ORC is far from the process streams, or where a direct heat exchange between the WHR technologies and the process streams is undesirable, due to safety and/or controllability reasons. The

extension of the mathematical framework developed in this work to include this type of indirect heat integration between the WHR and the process streams constitutes therefore a future research opportunity.

6.3 Final Remarks

It is clear from the results of this dissertation, that combined design methodologies, considering the process integration of ORCs, ABCs or both, into HENs for continuous and multi-period processes with and without FTVM heat storage, can generate economically, technically or environmentally attractive system designs. The simultaneous consideration of different technologies and subsystems generate synergies that would be neglected if a traditional hierarchical/sequential approach was applied or if only the stand-alone HEN were considered. Additionally, compared with Pinch Analysis, the mathematical nature of the methodology allows to calculate multiple variables/parameters of the system simultaneously while considering the interaction between the different subsystems in a direct and flexible way. The next steps in this area of research include but are not limited, to the consideration of other WHR technologies that were not included in this work, as well as the consideration of linearization and simplification strategies in order to be able to handle industrial-size problems within reasonable computational time and with reasonable computational resources. The developed mathematical framework, allows for the relatively quick analysis of this integrated designs, under the limitations and assumptions used to for development of the framework. This work does not claim to be able to generate the best possible configurations for a given system, but allows the easy evaluation of different design options for systems integrating ORCs and ABCs into HEN for continuous and multi-period processes with and without FTVM heat storage.

7 Bibliography

- Aaltola, Juha (2003): Simultaneous synthesis of flexible heat exchanger networks. Dissertation. Helsinki University of Technology, Espoo, Finland. Laboratory of Energy Engineering and Environmental Protection.
- Abdelouadoud, Yasmina; Lucas, Edward; Krummenacher, Pierre; Olsen, Donald; Wellig, Beat (2019): Batch process heat storage integration. A simple and effective graphical approach. In *Energy* 185, pp. 804–818. DOI: 10.1016/j.energy.2019.06.180.
- Abou Elmaaty, Talal M.; Kabeel, A. E.; Mahgoub, M. (2017): Corrugated plate heat exchanger review. In *Renewable and Sustainable Energy Reviews* 70, pp. 852–860. DOI: 10.1016/j.rser.2016.11.266.
- Ainger, A. (1830): Notice on the ‘Economy of the Steam Engine’. In Royal Institution of Great Britain (Ed.): *Quarterly Journal of Science, Literature and the Arts*. London ((Jan. - June)).
- Airò Farulla, Girolama; Cellura, Maurizio; Guarino, Francesco; Ferraro, Marco (2020): A Review of Thermochemical Energy Storage Systems for Power Grid Support. In *Applied Sciences* 10 (9), p. 3142. DOI: 10.3390/app10093142.
- Alefeld, G. (1982): Regeln für den Entwurf von mehrstufigen Absorptionswärmepumpen. In *Brennst.-Wärme-Kraft* 34 (2), pp. 64–73.
- Alefeld, G. (1983): Double effect, triple effect and quadruple effect absorption machines. In : *Proc. of the 16th Int. Congress of Refrigeration, Paris, vol. 2*, pp. 951–956.
- Almendros-Ibáñez, J. A.; Fernández-Torrijos, M.; Díaz-Heras, M.; Belmonte, J. F.; Sobrino, C. (2019): A review of solar thermal energy storage in beds of particles: Packed and fluidized beds. In *Solar Energy* 192, pp. 193–237. DOI: 10.1016/j.solener.2018.05.047.
- Alves, Joao J.; Towler, Gavin P. (2002): Analysis of Refinery Hydrogen Distribution Systems. In *Ind. Eng. Chem. Res.* 41 (23), pp. 5759–5769. DOI: 10.1021/ie010558v.
- Ammar, Yasmine; Joyce, Sharon; Norman, Rosemary; Wang, Yaodong; Roskilly, Anthony P. (2012): Low grade thermal energy sources and uses from the process industry in the UK. In *Applied Energy* 89 (1), pp. 3–20. DOI: 10.1016/j.apenergy.2011.06.003.
- Anastasovski, Aleksandar; Rasković, Predrag; Guzović, Zvonimir (2020): A review of heat integration approaches for organic rankine cycle with waste heat in production processes.

- In *Energy Conversion and Management* 221, p. 113175. DOI: 10.1016/j.enconman.2020.113175.
- Atkins, Martin J.; Walmsley, Michael R.W.; Neale, James R. (2010): The challenge of integrating non-continuous processes – milk powder plant case study. In *Journal of Cleaner Production* 18 (9), pp. 927–934. DOI: 10.1016/j.jclepro.2009.12.008.
- Atkins, Martin J.; Walmsley, Michael R.W.; Neale, James R. (2012): Process integration between individual plants at a large dairy factory by the application of heat recovery loops and transient stream analysis. In *Journal of Cleaner Production* 34, pp. 21–28. DOI: 10.1016/j.jclepro.2012.01.026.
- Ausfelder, Florian; Beilmann, Christian; Bertau, Martin; Bräuninger, Sigmar; Heinzl, Angelika; Hoer, Renate et al. (2015): Energiespeicherung als Element einer sicheren Energieversorgung. In *Chemie Ingenieur Technik* 87 (1-2), pp. 17–89. DOI: 10.1002/cite.201400183.
- Bao, Junjiang; Zhao, Li (2013): A review of working fluid and expander selections for organic Rankine cycle. In *Renewable and Sustainable Energy Reviews* 24, pp. 325–342. DOI: 10.1016/j.rser.2013.03.040.
- Barker, Mike; Rawtani, Jawahar; Mackay, Steve (2005): Introduction. In : Practical Batch Process Management: Elsevier, pp. 1–16.
- Bauer, Thomas; Steinmann, Wolf-Dieter; Laing, Doerte; Tamme, Rainer (2012): THERMAL ENERGY STORAGE MATERIALS AND SYSTEMS. In *Annual Rev Heat Transfer* 15 (15), pp. 131–177. DOI: 10.1615/AnnualRevHeatTransfer.2012004651.
- Beck, Anton; Hofmann, René (2018a): A Novel Approach for Linearization of a MINLP Stage-Wise Superstructure Formulation. In *Computers & Chemical Engineering* 112, pp. 17–26. DOI: 10.1016/j.compchemeng.2018.01.010.
- Beck, Anton; Hofmann, René (2018b): Extensions for Multi-Period MINLP Superstructure Formulation for Integration of Thermal Energy Storages in Industrial Processes. In : 28th European Symposium on Computer Aided Process Engineering, vol. 43: Elsevier (Computer Aided Chemical Engineering), pp. 1335–1340.
- Beck, Anton; Hofmann, René (2019): A sequential approach for integration of multiple thermal energy storages with fixed mass and variable temperature. In *Applied Thermal Engineering* 148, pp. 278–294. DOI: 10.1016/j.applthermaleng.2018.11.039.

- Becker, Helen Carla (2012): Methodology and Thermo-Economic Optimization for Integration of Industrial Heat Pumps. Dissertation.
- Bendig, Matthias; Maréchal, François; Favrat, Daniel (2013): Defining “Waste Heat” for industrial processes. In *Applied Thermal Engineering* 61 (1), pp. 134–142. DOI: 10.1016/j.applthermaleng.2013.03.020.
- Berntsson, Thore; Åsblad, Anders (2015): Annex XV: Industrial Excess Heat - Technologies and Applications. Supported by Denmark, Germany, Norway, Portugal, US and Sweden. Final Report - Phase 1. Industrial Energy-Related Technologies and Systems (IETS). An Implementing Agreement established under the auspices of the International Energy Agency (IEA). Sweden. Available online at <https://iea-industry.org/app/uploads/annex-15-final-report-phase-1-appendix-1.pdf>, checked on 11/6/2020.
- Björk, Kaj-Mikael; Nordman, Roger (2005): Solving large-scale retrofit heat exchanger network synthesis problems with mathematical optimization methods. In *Chemical Engineering and Processing: Process Intensification* 44 (8), pp. 869–876. DOI: 10.1016/j.cep.2004.09.005.
- Blesl; M; Kempe; S; Ohl; Fahl et al. (2008): Wärmeatlas Baden-Württemberg. Erstellung eines Leitfadens und Umsetzung für Modellregionen. Institut für Energiewirtschaft und Rationelle Energieanwendung (IER). Universität Stuttgart.
- Bonami, Pierre; Lodi, Andrea; Tramontani, Andrea; Wiese, Sven (2015): On mathematical programming with indicator constraints. In *Math. Program.* 151 (1), pp. 191–223. DOI: 10.1007/s10107-015-0891-4.
- Braimakis, Konstantinos; Karellas, Sotirios (2018): Energetic optimization of regenerative Organic Rankine Cycle (ORC) configurations. In *Energy Conversion and Management* 159, pp. 353–370. DOI: 10.1016/j.enconman.2017.12.093.
- Branchini, Lisa; Pascale, Andrea de; Peretto, Antonio (2013): Systematic comparison of ORC configurations by means of comprehensive performance indexes. In *Applied Thermal Engineering* 61 (2), pp. 129–140. DOI: 10.1016/j.applthermaleng.2013.07.039.
- Broberg Viklund, Sarah; Johansson, Maria T. (2014): Technologies for utilization of industrial excess heat. Potentials for energy recovery and CO₂ emission reduction. In *Energy Conversion and Management* 77, pp. 369–379. DOI: 10.1016/j.enconman.2013.09.052.
- Bronicki, L. Y. (2017): History of Organic Rankine Cycle systems. In : Organic Rankine Cycle (ORC) Power Systems: Elsevier, pp. 25–66.

- Brückner, Sarah; Arbter, Rene; Pehnt, Martin; Laevemann, Eberhard (2017): Industrial waste heat potential in Germany—a bottom-up analysis. In *Energy Efficiency* 10 (2), pp. 513–525. DOI: 10.1007/s12053-016-9463-6.
- Brückner, Sarah; Liu, Selina; Miró, Laia; Radspieler, Michael; Cabeza, Luisa F.; Lävemann, Eberhard (2015): Industrial waste heat recovery technologies. An economic analysis of heat transformation technologies. In *Applied Energy* 151, pp. 157–167. DOI: 10.1016/j.apenergy.2015.01.147.
- Brückner, Sarah; Miró, Laia; Cabeza, Luisa F.; Pehnt, Martin; Laevemann, Eberhard (2014): Methods to estimate the industrial waste heat potential of regions – A categorization and literature review. In *Renewable and Sustainable Energy Reviews* 38, pp. 164–171. DOI: 10.1016/j.rser.2014.04.078.
- Brunner, F.; Krummenacher, P.; Wellig, B. (2015): Einführung in die Prozessintegration mit der Pinch-Methode. Handbuch für die Analyse von kontinuierlichen Prozessen und Batch-Prozessen. Zweite Auflage. Bundesamt für Energie BFE.
- Buffa, Simone; Cozzini, Marco; D’Antoni, Matteo; Baratieri, Marco; Fedrizzi, Roberto (2019): 5th generation district heating and cooling systems: A review of existing cases in Europe. In *Renewable and Sustainable Energy Reviews* 104, pp. 504–522. DOI: 10.1016/j.rser.2018.12.059.
- Butturi, M. A.; Lolli, F.; Sellitto, M. A.; Balugani, E.; Gamberini, R.; Rimini, B. (2019): Renewable energy in eco-industrial parks and urban-industrial symbiosis: A literature review and a conceptual synthesis. In *Applied Energy* 255, p. 113825. DOI: 10.1016/j.apenergy.2019.113825.
- Carré, Ferdinand (1860): Improvement in apparatus for freezing liquids. Patent no. US30201A.
- Cerda, Jaime; Westerberg, Arthur W.; Mason, David; Linnhoff, Bodo (1983): Minimum utility usage in heat exchanger network synthesis A transportation problem. In *Chemical Engineering Science* 38 (3), pp. 373–387. DOI: 10.1016/0009-2509(83)80156-0.
- Cerda, Jaime; Westerburg, Arthur W. (1983): Synthesizing heat exchanger networks having restricted stream/stream matches using transportation problem formulations. In *Chemical Engineering Science* 38 (10), pp. 1723–1740. DOI: 10.1016/0009-2509(83)85029-5.
- Chamorro-Romero, Luis; Radgen, Peter (2020): Optimal Integration of Organic Rankine Cycles with Heat Exchanger Networks Using Intermediate Heat Transfer Fluids. In *I* 81, pp. 991–996. DOI: 10.3303/CET2081166.

- Chandra, Yogender Pal; Matuska, Tomas (2019): Stratification analysis of domestic hot water storage tanks: A comprehensive review. In *Energy and Buildings* 187, pp. 110–131. DOI: 10.1016/j.enbuild.2019.01.052.
- Chen, Cheng-Liang; Chang, Feng-Yi; Chao, Tzu-Hsiang; Chen, Hui-Chu; Lee, Jui-Yuan (2014): Heat-Exchanger Network Synthesis Involving Organic Rankine Cycle for Waste Heat Recovery. In *Ind. Eng. Chem. Res.* 53 (44), pp. 16924–16936. DOI: 10.1021/ie500301s.
- Chen, Cheng-Liang; Ciou, Ying-Jyuan (2008): Design and Optimization of Indirect Energy Storage Systems for Batch Process Plants. In *Ind. Eng. Chem. Res.* 47 (14), pp. 4817–4829. DOI: 10.1021/ie0710667.
- Chen, Cheng-Liang; Ciou, Ying-Jyuan (2009): Design of Indirect Heat Recovery Systems with Variable-Temperature Storage for Batch Plants. In *Ind. Eng. Chem. Res.* 48 (9), pp. 4375–4387. DOI: 10.1021/ie8013633.
- Chen, Cheng-Liang; Hung, Ping-Sung (2004): Simultaneous Synthesis of Flexible Heat-Exchange Networks with Uncertain Source-Stream Temperatures and Flow Rates. In *Ind. Eng. Chem. Res.* 43 (18), pp. 5916–5928. DOI: 10.1021/ie030701f.
- Chen, Cheng-Liang; Li, Po-Yi; Chen, Hui-Chu; Lee, Jui-Yuan (2015a): Synthesis of transcritical ORC-integrated heat exchanger networks for waste heat recovery. In : 12th International Symposium on Process Systems Engineering and 25th European Symposium on Computer Aided Process Engineering, vol. 37: Elsevier (Computer Aided Chemical Engineering), pp. 1073–1078.
- Chen, Cheng-Liang; Li, Po-Yi; Le, Si Nguyen Tien (2016): Organic Rankine Cycle for Waste Heat Recovery in a Refinery. In *Ind. Eng. Chem. Res.* 55 (12), pp. 3262–3275. DOI: 10.1021/acs.iecr.5b03381.
- Chen, J.J.J. (1987): Comments on improvements on a replacement for the logarithmic mean. In *Chemical Engineering Science* 42 (10), pp. 2488–2489. DOI: 10.1016/0009-2509(87)80128-8.
- Chen, Li-Ting (1988): A new ejector-absorber cycle to improve the COP of an absorption refrigeration system. In *Applied Energy* 30 (1), pp. 37–51. DOI: 10.1016/0306-2619(88)90053-0.
- Chen, N. H. (1965): Generalized Correlation for Latent Heat of Vaporization. In *J. Chem. Eng. Data* 10 (2), pp. 207–210. DOI: 10.1021/je60025a047.

- Chen, X.; Wang, R. Z.; Du, S. (2017): Heat integration of ammonia-water absorption refrigeration system through heat-exchanger network analysis. In *Energy* 141, pp. 1585–1599. DOI: 10.1016/j.energy.2017.11.100.
- Chen, Yang; Grossmann, Ignacio E.; Miller, David C. (2015b): Computational strategies for large-scale MILP transshipment models for heat exchanger network synthesis. In *Computers & Chemical Engineering* 82, pp. 68–83. DOI: 10.1016/j.compchemeng.2015.05.015.
- Chertow, Marian R. (2004): Industrial Symbiosis. In Cutler J. Cleveland (Ed.): *Encyclopedia of energy*, vol. 3. Amsterdam: Elsevier, pp. 407–415.
- Choudhury, B.; Chatterjee, P. K.; Sarkar, J. P. (2010): Review paper on solar-powered air-conditioning through adsorption route. In *Renewable and Sustainable Energy Reviews* 14 (8), pp. 2189–2195. DOI: 10.1016/j.rser.2010.03.025.
- Chowdhury, Jahedul Islam; Hu, Yukun; Haltas, Ismail; Balta-Ozkan, Nazmiye; Matthew, George, JR.; Varga, Liz (2018): Reducing industrial energy demand in the UK: A review of energy efficiency technologies and energy saving potential in selected sectors. In *Renewable and Sustainable Energy Reviews* 94, pp. 1153–1178. DOI: 10.1016/j.rser.2018.06.040.
- Chys, M.; van den Broek, M.; Vanslambrouck, B.; Paepe, M. de (2012): Potential of zeotropic mixtures as working fluids in organic Rankine cycles. In *Energy* 44 (1), pp. 623–632. DOI: 10.1016/j.energy.2012.05.030.
- Ciric, A. R.; Floudas, C. A. (1991): Heat exchanger network synthesis without decomposition. In *Computers & Chemical Engineering* 15 (6), pp. 385–396. DOI: 10.1016/0098-1354(91)87017-4.
- Clausius, R. (1854): Ueber eine veränderte Form des zweiten Hauptsatzes der mechanischen Wärmetheorie. In *Ann. Phys. Chem.* 169 (12), pp. 481–506. DOI: 10.1002/andp.18541691202.
- Clayton, R. W. (1986): Cost reductions on an edible oil refinery identified by a process integration study at Van den Berghs and Jurgens Ltd. Original report prepared by Linnhoff-March Consultants Ltd. Energy Technology Support Unit, Harwell (UK). United Kingdom. Available online at <https://www.osti.gov/etdeweb/biblio/7794571>.
- Corominas, J.; Espuña, A.; Puigjaner, L. (1993): A new look at energy integration in multiproduct batch processes. In *Computers & Chemical Engineering* 17, S15-S20. DOI: 10.1016/0098-1354(93)80202-X.

- Corominas, J.; Espuña, A.; Puigjaner, L. (1994): Method to incorporate energy integration considerations in multiproduct batch processes. In *Computers & Chemical Engineering* 18 (11-12), pp. 1043–1055. DOI: 10.1016/0098-1354(94)E0016-G.
- Darvish, Kamyar; Ehyaei, Mehdi; Atabi, Farideh; Rosen, Marc (2015): Selection of Optimum Working Fluid for Organic Rankine Cycles by Exergy and Exergy-Economic Analyses. In *Sustainability* 7 (11), pp. 15362–15383. DOI: 10.3390/su71115362.
- Desai, Nishith B.; Bandyopadhyay, Santanu (2009): Process integration of organic Rankine cycle. In *Energy* 34 (10), pp. 1674–1686. DOI: 10.1016/j.energy.2009.04.037.
- Desrochers, Pierre (2001): Cities and Industrial Symbiosis: Some Historical Perspectives and Policy Implications. In *Journal of Industrial Ecology* 5 (4), pp. 29–44. DOI: 10.1162/10881980160084024.
- Dhole, Vikas R.; Linnhoff, Bodo (1993): Total site targets for fuel, co-generation, emissions, and cooling. In *Computers & Chemical Engineering* 17, S101-S109. DOI: 10.1016/0098-1354(93)80214-8.
- Dinker, Abhay; Agarwal, Madhu; Agarwal, G. D. (2017): Heat storage materials, geometry and applications. A review. In *Journal of the Energy Institute* 90 (1), pp. 1–11. DOI: 10.1016/j.joei.2015.10.002.
- Dong, Xuan; Liao, Zuwei; Sun, Jingyuan; Huang, Zhengliang; Jiang, Binbo; Wang, Jingdai; Yang, Yongrong (2020): Simultaneous Optimization of a Heat Exchanger Network and Operating Conditions of Organic Rankine Cycle. In *Ind. Eng. Chem. Res.* 59 (25), pp. 11596–11609. DOI: 10.1021/acs.iecr.0c01708.
- Duran, M. A.; Grossmann, I. E. (1986): Simultaneous optimization and heat integration of chemical processes. In *AIChE J.* 32 (1), pp. 123–138. DOI: 10.1002/aic.690320114.
- El-Halwagi, Mahmoud M.; Manousiouthakis, Vasilios (1989): Synthesis of mass exchange networks. In *AIChE J.* 35 (8), pp. 1233–1244. DOI: 10.1002/aic.690350802.
- Elsido, Cristina; Martelli, Emanuele; Grossmann, Ignacio E. (2019): A bilevel decomposition method for the simultaneous heat integration and synthesis of steam/organic Rankine cycles. In *Computers & Chemical Engineering* 128, pp. 228–245. DOI: 10.1016/j.compchemeng.2019.05.041.
- Elsido, Cristina; Martelli, Emanuele; Grossmann, Ignacio E. (2021): Multiperiod optimization of heat exchanger networks with integrated thermodynamic cycles and thermal storages. In

- Computers & Chemical Engineering* 149, p. 107293. DOI: 10.1016/j.compchemeng.2021.107293.
- Elsido, Cristina; Mian, Alberto; Martelli, Emanuele (2017): A systematic methodology for the techno-economic optimization of Organic Rankine Cycles. In *Energy Procedia* 129, pp. 26–33. DOI: 10.1016/j.egypro.2017.09.171.
- Escobar, Marcelo; Trierweiler, Jorge O. (2013): Optimal heat exchanger network synthesis. A case study comparison. In *Applied Thermal Engineering* 51 (1-2), pp. 801–826. DOI: 10.1016/j.applthermaleng.2012.10.022.
- Fang, Hao; Xia, Jianjun; Jiang, Yi (2015): Key issues and solutions in a district heating system using low-grade industrial waste heat. In *Energy* 86, pp. 589–602. DOI: 10.1016/j.energy.2015.04.052.
- Fang, Hao; Xia, Jianjun; Zhu, Kan; Su, Yingbo; Jiang, Yi (2013): Industrial waste heat utilization for low temperature district heating. In *Energy Policy* 62, pp. 236–246. DOI: 10.1016/j.enpol.2013.06.104.
- Feng, Yongqiang; Hung, TzuChen; Greg, Kowalski; Zhang, Yaning; Li, Bingxi; Yang, Jinfu (2015): Thermoeconomic comparison between pure and mixture working fluids of organic Rankine cycles (ORCs) for low temperature waste heat recovery. In *Energy Conversion and Management* 106, pp. 859–872. DOI: 10.1016/j.enconman.2015.09.042.
- Fernandes, M. S.; Brites, G.J.V.N.; Costa, J. J.; Gaspar, A. R.; Costa, V.A.F. (2014): Review and future trends of solar adsorption refrigeration systems. In *Renewable and Sustainable Energy Reviews* 39, pp. 102–123. DOI: 10.1016/j.rser.2014.07.081.
- Fertahi, Saïf ed-Dîn; Jamil, A.; Benbassou, A. (2018): Review on Solar Thermal Stratified Storage Tanks (STSST): Insight on stratification studies and efficiency indicators. In *Solar Energy* 176, pp. 126–145. DOI: 10.1016/j.solener.2018.10.028.
- Floudas, C. A.; Ciric, A. R.; Grossmann, I. E. (1986): Automatic synthesis of optimum heat exchanger network configurations. In *AIChE J.* 32 (2), pp. 276–290. DOI: 10.1002/aic.690320215.
- Floudas, Christodoulos A.; Grossmann, Ignacio E. (1986): Synthesis of flexible heat exchanger networks for multiperiod operation. In *Computers & Chemical Engineering* 10 (2), pp. 153–168. DOI: 10.1016/0098-1354(86)85027-X.

- Floudas, Christodoulos A.; Grossmann, Ignacio E. (1987): Automatic generation of multiperiod heat exchanger network configurations. In *Computers & Chemical Engineering* 11 (2), pp. 123–142. DOI: 10.1016/0098-1354(87)80013-3.
- Foo, Dominic Chwan Yee; Kazantzi, Vasiliki; El-Halwagi, Mahmoud M.; Abdul Manan, Zainuddin (2006): Surplus diagram and cascade analysis technique for targeting property-based material reuse network. In *Chemical Engineering Science* 61 (8), pp. 2626–2642. DOI: 10.1016/j.ces.2005.11.010.
- Forman, Clemens; Muritala, Ibrahim Kolawole; Pardemann, Robert; Meyer, Bernd (2016): Estimating the global waste heat potential. In *Renewable and Sustainable Energy Reviews* 57, pp. 1568–1579. DOI: 10.1016/j.rser.2015.12.192.
- Fraunhofer ISI; TEP Energy GmbH; University Utrecht; ARMINES (2017): Profile of heating and cooling demand in 2015. Edited by Tobias Fleiter. Heat Roadmap Europe.
- Fulton (1851): On P. V. Du Trembley's combined vapor engine. In *Journal of the Franklin Institute* 52 (3), pp. 194–195. DOI: 10.1016/0016-0032(51)90194-9.
- Furman, Kevin C.; Sahinidis, Nikolaos V. (2001): Computational complexity of heat exchanger network synthesis. In *Computers & Chemical Engineering* 25 (9-10), pp. 1371–1390. DOI: 10.1016/S0098-1354(01)00681-0.
- Gabathuler, Hans Rudolf (1994): Elektrizität und Wärme. Grundlagen und Zusammenhänge. Bern: Eidg. Drucksachen- und Materialzentrale (RAVEL im Wärmesektor, H. 1).
- Gautam, Abhishek; Saini, R. P. (2020): A review on technical, applications and economic aspect of packed bed solar thermal energy storage system. In *Journal of Energy Storage* 27, p. 101046. DOI: 10.1016/j.est.2019.101046.
- Gilani, Syed Ihtsham-ul-Haq; Ahmed, Mojahid Sidahmed Mohammed Salih (2015): Solution Crystallization Detection for Double-effect LiBr-H₂O Steam Absorption Chiller. In *Energy Procedia* 75, pp. 1522–1528. DOI: 10.1016/j.egypro.2015.07.304.
- Glasser, L. (2004): Water, Water, Everywhere: Phase Diagrams of Ordinary Water Substance. In *J. Chem. Educ.* 81 (3), p. 414. DOI: 10.1021/ed081p414.
- Gomri, Rabah (2009): Second law comparison of single effect and double effect vapour absorption refrigeration systems. In *Energy Conversion and Management* 50 (5), pp. 1279–1287. DOI: 10.1016/j.enconman.2009.01.019.

- Gomri, Rabah (2010): Investigation of the potential of application of single effect and multiple effect absorption cooling systems. In *Energy Conversion and Management* 51 (8), pp. 1629–1636. DOI: 10.1016/j.enconman.2009.12.039.
- Gundersen, Truls (2002): A Process Integration PRIMER. 3rd. International Energy Agency. Trondheim, Norway. Available online at https://iea-industry.org/app/uploads/a-process-integration-primer-iea-t-gundersen_2002.pdf, checked on 12/15/2020.
- Heberle, Florian; Preißinger, Markus; Brüggemann, Dieter (2012): Zeotropic mixtures as working fluids in Organic Rankine Cycles for low-enthalpy geothermal resources. In *Renewable Energy* 37 (1), pp. 364–370. DOI: 10.1016/j.renene.2011.06.044.
- Hellwig, Tillmann (1998): OMNIUM: ein Verfahren zur Optimierung der Abwärmenutzung in Industriebetrieben. Dissertation. Universität Stuttgart, Stuttgart. Institut für Energiewirtschaft und Rationelle Energieanwendung (IER).
- Heyden, Erik (2016): Kostenoptimale Abwärmerückgewinnung durch integriert-iteratives Systemdesign (KOARiiS) : ein Verfahren zur energetisch-ökonomischen Bewertung industrieller Abwärmepotenziale. Dissertation. Universität Stuttgart, Stuttgart. Institut für Energiewirtschaft und Rationelle Energieanwendung,
- Hipólito-Valencia, Brígido J.; Rubio-Castro, Eusiel; Ponce-Ortega, José M.; Serna-González, Medardo; Nápoles-Rivera, Fabricio; El-Halwagi, Mahmoud M. (2013): Optimal integration of organic Rankine cycles with industrial processes. In *Energy Conversion and Management* 73, pp. 285–302. DOI: 10.1016/j.enconman.2013.04.036.
- Hipólito-Valencia, Brígido Jesús; Lira-Barragán, Luis Fernando; Ponce-Ortega, José María; Serna-González, Medardo; El-Halwagi, Mahmoud M. (2014a): Multiobjective design of interplant trigeneration systems. In *AIChE J.* 60 (1), pp. 213–236. DOI: 10.1002/aic.14292.
- Hipólito-Valencia, Brígido Jesús; Rubio-Castro, Eusiel; Ponce-Ortega, José María; Serna-González, Medardo; Nápoles-Rivera, Fabricio; El-Halwagi, Mahmoud M. (2014b): Optimal design of inter-plant waste energy integration. In *Applied Thermal Engineering* 62 (2), pp. 633–652. DOI: 10.1016/j.applthermaleng.2013.10.015.
- Hipólito-Valencia, Brígido Jesús; Vázquez-Ojeda, María; Segovia-Hernández, Juan Gabriel; Ponce-Ortega, José María (2014c): Waste Heat Recovery through Organic Rankine Cycles in the Bioethanol Separation Process. In *Ind. Eng. Chem. Res.* 53 (16), pp. 6773–6788. DOI: 10.1021/ie404202a.

- Hofmann, René; Dusek, Sabrina; Gruber, Stephan; Drexler-Schmid, Gerwin (2019): Design Optimization of a Hybrid Steam-PCM Thermal Energy Storage for Industrial Applications. In *Energies* 12 (5), p. 898. DOI: 10.3390/en12050898.
- Hohmann, Edward (1971): Optimum networks for heat exchange. Dissertation. University of Southern California, Los Angeles. Available online at <http://digitallibrary.usc.edu/cdm/ref/collection/p15799coll17/id/211425>, checked on 12/16/2020.
- Huang, Xiaojian; Lu, Pei; Luo, Xianglong; Chen, Jianyong; Yang, Zhi; Liang, Yingzong et al. (2020): Synthesis and simultaneous MINLP optimization of heat exchanger network, steam Rankine cycle, and organic Rankine cycle. In *Energy* 195, p. 116922. DOI: 10.1016/j.energy.2020.116922.
- Huber, Marcia; Harvey, Allan; Lemmon, Eric; Hardin, Gary; Bell, Ian; McLinden, Mark (2018): NIST Reference Fluid Thermodynamic and Transport Properties Database (REFPROP) Version 10 - SRD 23.
- Hung, T. C.; Wang, S. K.; Kuo, C. H.; Pei, B. S.; Tsai, K. F. (2010): A study of organic working fluids on system efficiency of an ORC using low-grade energy sources. In *Energy* 35 (3), pp. 1403–1411. DOI: 10.1016/j.energy.2009.11.025.
- Hung, Tzu-Chen (2001): Waste heat recovery of organic Rankine cycle using dry fluids. In *Energy Conversion and Management* 42 (5), pp. 539–553. DOI: 10.1016/S0196-8904(00)00081-9.
- Hussain, Kashif; Mohd Salleh, Mohd Najib; Cheng, Shi; Shi, Yuhui (2019): Metaheuristic research: a comprehensive survey. In *Artif Intell Rev* 52 (4), pp. 2191–2233. DOI: 10.1007/s10462-017-9605-z.
- Imran, Muhammad; Park, Byung Sik; Kim, Hyouck Ju; Lee, Dong Hyun; Usman, Muhammad; Heo, Manki (2014): Thermo-economic optimization of Regenerative Organic Rankine Cycle for waste heat recovery applications. In *Energy Conversion and Management* 87, pp. 107–118. DOI: 10.1016/j.enconman.2014.06.091.
- International Renewable Energy Agency (2013): IRENA-IEA-ETSAP Technology Brief 4: Thermal Storage.
- IPCC (2018): Global Warming of 1.5°C. An IPCC Special Report on the impacts of global warming of 1.5°C above pre-industrial levels and related global greenhouse gas emission pathways, in the context of strengthening the global response to the threat of climate change,

- sustainable development, and efforts to eradicate poverty. Edited by V. Masson-Delmotte, P. Zhai, H.-O. Pörtner, D. Roberts, J. Skea, P.R. Shukla et al. IPCC.
- Irvine, Thomas F.; Liley, Peter E. (1984): Steam and gas Tables with computer equations. Orlando, Fla.: Acad. Press.
- Isafiade, A. J.; Fraser, D. M. (2010): Interval based MINLP superstructure synthesis of heat exchanger networks for multi-period operations. In *Chemical Engineering Research and Design* 88 (10), pp. 1329–1341. DOI: 10.1016/j.cherd.2010.02.019.
- Isafiade, Adeniyi; Bogataj, Milos; Fraser, Duncan; Kravanja, Zdravko (2015): Optimal synthesis of heat exchanger networks for multi-period operations involving single and multiple utilities. In *Chemical Engineering Science* 127, pp. 175–188. DOI: 10.1016/j.ces.2014.12.037.
- Isafiade, Adeniyi J.; Short, Michael (2016): Simultaneous synthesis of flexible heat exchanger networks for unequal multi-period operations. In *Process Safety and Environmental Protection* 103, pp. 377–390. DOI: 10.1016/j.psep.2016.04.021.
- Isafiade, Adeniyi Jide (2017): Synthesis of Flexible Multi-Period Heat Exchanger Networks Using a Reduced MINLP Superstructure Approach. In *Process Integr Optim Sustain* 1 (3), pp. 203–211. DOI: 10.1007/s41660-017-0014-1.
- I-ThERM Consortium (2016): Industrial Thermal Energy Recovery conversion and Management (I-ThERM). Literature review of energy use and potential for heat recovery in the EU28 Report. Edited by Cyprus University of Technology (CUT).
- Jarimi, Hasila; Aydin, Devrim; Yanan, Zhang; Ozankaya, Gorkem; Chen, Xiangjie; Riffat, Saffa (2019): Review on the recent progress of thermochemical materials and processes for solar thermal energy storage and industrial waste heat recovery. In *International Journal of Low-Carbon Technologies* 14 (1), pp. 44–69. DOI: 10.1093/ijlct/cty052.
- Jawahar, C. P.; Saravanan, R. (2010): Generator absorber heat exchange based absorption cycle—A review. In *Renewable and Sustainable Energy Reviews* 14 (8), pp. 2372–2382. DOI: 10.1016/j.rser.2010.05.002.
- Jiang, Da; Chang, Chuei-Tin (2013): A New Approach to Generate Flexible Multiperiod Heat Exchanger Network Designs with Timesharing Mechanisms. In *Ind. Eng. Chem. Res.* 52 (10), pp. 3794–3804. DOI: 10.1021/ie301075v.

- Jiang, Da; Chang, Chuei-Tin (2015): An algorithmic approach to generate timesharing schemes for multi-period HEN designs. In *Chemical Engineering Research and Design* 93, pp. 402–410. DOI: 10.1016/j.cherd.2014.04.011.
- Jiménez-Arreola, Manuel; Pili, Roberto; Dal Magro, Fabio; Wieland, Christoph; Rajoo, Srithar; Romagnoli, Alessandro (2018): Thermal power fluctuations in waste heat to power systems. An overview on the challenges and current solutions. In *Applied Thermal Engineering*. DOI: 10.1016/j.applthermaleng.2018.02.033.
- Johnson, Ilona; Choate, William T.; Davidson, Amber (2008): Waste Heat Recovery: Technology and Opportunities in U.S. Industry. U.S. Department of Energy. United States.
- Jouhara, Hussam; Khordehghah, Navid; Almahmoud, Sulaiman; Delpech, Bertrand; Chauhan, Amisha; Tassou, Savvas A. (2018): Waste heat recovery technologies and applications. In *Thermal Science and Engineering Progress* 6, pp. 268–289. DOI: 10.1016/j.tsep.2018.04.017.
- Jouhara, Hussam; Żabnieńska-Góra, Alina; Khordehghah, Navid; Ahmad, Darem; Lipinski, Tom (2020): Latent thermal energy storage technologies and applications: A review. In *International Journal of Thermofluids* 5-6, p. 100039. DOI: 10.1016/j.ijft.2020.100039.
- Kaita, Y. (2001): Thermodynamic properties of lithium bromide–water solutions at high temperatures. In *International Journal of Refrigeration* 24 (5), pp. 374–390. DOI: 10.1016/S0140-7007(00)00039-6.
- Kalina, A. I. (1984): Combined-Cycle System With Novel Bottoming Cycle. In *Journal of Engineering for Gas Turbines and Power* 106 (4), pp. 737–742. DOI: 10.1115/1.3239632.
- Kemp, I. C. (1990): Applications of the time-dependent cascade analysis in process integration. In *Heat Recovery Systems and CHP* 10 (4), pp. 423–435. DOI: 10.1016/0890-4332(90)90091-W.
- Kemp, Ian C. (2007): Pinch Analysis and Process Integration: Elsevier.
- Kermani, Maziar; Wallerand, Anna S.; Kantor, Ivan D.; Maréchal, François (2018): Generic superstructure synthesis of organic Rankine cycles for waste heat recovery in industrial processes. In *Applied Energy* 212, pp. 1203–1225. DOI: 10.1016/j.apenergy.2017.12.094.
- Klemes, J. (Ed.) (2013): Handbook of Process Integration (PI). Minimisation Of Energy And Water Use, Waste And Emissions. Burlington: Elsevier Science (Woodhead Publishing Series in Energy).

- Klemeš, Jiří Jaromír; Kravanja, Zdravko (2013): Forty years of Heat Integration. Pinch Analysis (PA) and Mathematical Programming (MP). In *Current Opinion in Chemical Engineering* 2 (4), pp. 461–474. DOI: 10.1016/j.coche.2013.10.003.
- Klemeš, Jiří Jaromír; Varbanov, Petar Sabev; Kravanja, Zdravko (2013): Recent developments in Process Integration. In *Chemical Engineering Research and Design* 91 (10), pp. 2037–2053. DOI: 10.1016/j.cherd.2013.08.019.
- Klemeš, Jiří Jaromír; Varbanov, Petar Sabev; Walmsley, Timothy G.; Jia, Xuexiu (2018): New directions in the implementation of Pinch Methodology (PM). In *Renewable and Sustainable Energy Reviews* 98, pp. 439–468. DOI: 10.1016/j.rser.2018.09.030.
- Koçak, Burcu; Fernandez, Ana Ines; Paksoy, Halime (2020): Review on sensible thermal energy storage for industrial solar applications and sustainability aspects. In *Solar Energy* 209, pp. 135–169. DOI: 10.1016/j.solener.2020.08.081.
- Kolasiński, Piotr (2020): The Method of the Working Fluid Selection for Organic Rankine Cycle (ORC) Systems Employing Volumetric Expanders. In *Energies* 13 (3), p. 573. DOI: 10.3390/en13030573.
- Kondili, E.; Pantelides, C. C.; Sargent, R.W.H. (1993): A general algorithm for short-term scheduling of batch operations—I. MILP formulation. In *Computers & Chemical Engineering* 17 (2), pp. 211–227. DOI: 10.1016/0098-1354(93)80015-F.
- Krummenacher, Pierre (1999): Energy Integration of Industrial Batch Processes (PinchBATCH) - Phase 2. Swiss Federal Institute of Technology - Lausanne (EPFL).
- Krummenacher, Pierre; Favrat, Daniel (2001): Indirect and Mixed Direct-Indirect Heat Integration of Batch Processes Based on Pinch Analysis. In *International journal of applied thermodynamics* (3), pp. 135–143.
- Kuhn, Harold W. (2012): A tale of three eras: The discovery and rediscovery of the Hungarian Method. In *European Journal of Operational Research* 219 (3), pp. 641–651. DOI: 10.1016/j.ejor.2011.11.008.
- Lawal, Musa; Wan Alwi, Sharifah Rafidah; Manan, Zainuddin Abdul; Ho, Wai Shin (2021): Industrial symbiosis tools—A review. In *Journal of Cleaner Production* 280, p. 124327. DOI: 10.1016/j.jclepro.2020.124327.

- Lecompte, S.; Ameel, B.; Ziviani, D.; van den Broek, M.; Paepe, M. de (2014): Exergy analysis of zeotropic mixtures as working fluids in Organic Rankine Cycles. In *Energy Conversion and Management* 85, pp. 727–739. DOI: 10.1016/j.enconman.2014.02.028.
- Lecompte, Steven (2017): Potential of Organic Rankine Cycles (ORC) for Waste Heat Recovery on an Electric Arc Furnace (EAF).
- Lecompte, Steven; Huisseune, Henk; van den Broek, Martijn; Vanslambrouck, Bruno; Paepe, Michel de (2015): Review of organic Rankine cycle (ORC) architectures for waste heat recovery. In *Renewable and Sustainable Energy Reviews* 47, pp. 448–461. DOI: 10.1016/j.rser.2015.03.089.
- Lee, Jui-Yuan; Seid, Esmael R.; Majozi, Thokozani (2015): Heat integration of intermittently available continuous streams in multipurpose batch plants. In *Computers & Chemical Engineering* 74, pp. 100–114. DOI: 10.1016/j.compchemeng.2014.12.003.
- Lee, Jui-Yuan; Seid, Esmael R.; Majozi, Thokozani (2016): An improved model for Heat Integration of intermittent process streams in multipurpose batch plants. In *Applied Thermal Engineering* 105, pp. 822–838. DOI: 10.1016/j.applthermaleng.2016.05.131.
- Liao, Xiaohong; Radermacher, Reinhard (2007): Absorption chiller crystallization control strategies for integrated cooling heating and power systems. In *International Journal of Refrigeration* 30 (5), pp. 904–911. DOI: 10.1016/j.ijrefrig.2006.10.009.
- Liew, Peng Yen; Theo, Wai Lip; Wan Alwi, Sharifah Rafidah; Lim, Jeng Shiun; Abdul Manan, Zainuddin; Klemeš, Jiří Jaromír; Varbanov, Petar Sabev (2017): Total Site Heat Integration planning and design for industrial, urban and renewable systems. In *Renewable and Sustainable Energy Reviews* 68, pp. 964–985. DOI: 10.1016/j.rser.2016.05.086.
- Linnhoff, B.; Ashton, G.J.; Obeng, E.D.A. (1988): Process integration of batch processes. In P. R. Crump (Ed.): Understanding process integration II. A two-day symposium ... held at the University of Manchester Institute for Science and Technology (UMIST), 22 - 23 March 1988. 1. ed. Rugby: Inst. of Chemical Engineers (EFCE event, 385).
- Linnhoff, B.; Hindmarsh, E. (1983): The pinch design method for heat exchanger networks. In *Chemical Engineering Science* 38 (5), pp. 745–763. DOI: 10.1016/0009-2509(83)80185-7.
- Linnhoff, Bodo (1979): Thermodynamic Analysis in the Design of Process Network. Dissertation. University of Leeds, Leeds, UK. Department of Chemical Engineering.

- Linnhoff, Bodo; Flower, John R. (1978a): Synthesis of heat exchanger networks. I. Systematic generation of energy optimal networks. In *AIChE J.* 24 (4), pp. 633–642. DOI: 10.1002/aic.690240411.
- Linnhoff, Bodo; Flower, John R. (1978b): Synthesis of heat exchanger networks: II. Evolutionary generation of networks with various criteria of optimality. In *AIChE J.* 24 (4), pp. 642–654. DOI: 10.1002/aic.690240412.
- Lira-Barragán, Luis Fernando; Ponce-Ortega, José María; Serna-González, Medardo; El-Halwagi, Mahmoud M. (2013): Synthesis of integrated absorption refrigeration systems involving economic and environmental objectives and quantifying social benefits. In *Applied Thermal Engineering* 52 (2), pp. 402–419. DOI: 10.1016/j.applthermaleng.2012.11.047.
- Lira-Barragán, Luis Fernando; Ponce-Ortega, José María; Serna-González, Medardo; El-Halwagi, Mahmoud M. (2014a): Optimal design of process energy systems integrating sustainable considerations. In *Energy* 76, pp. 139–160. DOI: 10.1016/j.energy.2014.04.111.
- Lira-Barragán, Luis Fernando; Ponce-Ortega, José María; Serna-González, Medardo; El-Halwagi, Mahmoud M. (2014b): Optimum heat storage design for solar-driven absorption refrigerators integrated with heat exchanger networks. In *AIChE J.* 60 (3), pp. 909–930. DOI: 10.1002/aic.14308.
- Lira-Barragán, Luis Fernando; Ponce-Ortega, José María; Serna-González, Medardo; El-Halwagi, Mahmoud M. (2014c): Sustainable Integration of Trigeneration Systems with Heat Exchanger Networks. In *Ind. Eng. Chem. Res.* 53 (7), pp. 2732–2750. DOI: 10.1021/ie4021232.
- Liu, Bo-Tau; Chien, Kuo-Hsiang; Wang, Chi-Chuan (2004): Effect of working fluids on organic Rankine cycle for waste heat recovery. In *Energy* 29 (8), pp. 1207–1217. DOI: 10.1016/j.energy.2004.01.004.
- Ludwig, Jens (2012): Energieeffizienz durch Planung betriebsübergreifender Prozessintegration mit der Pinch-Analyse. Dissertation. Karlsruher Institut für Technologie (KIT), Karlsruhe. Institut für Industriebetriebslehre und Industrielle Produktion (IIP).
- Lund, Henrik; Werner, Sven; Wiltshire, Robin; Svendsen, Svend; Thorsen, Jan Eric; Hvelplund, Frede; Mathiesen, Brian Vad (2014): 4th Generation District Heating (4GDH). In *Energy* 68, pp. 1–11. DOI: 10.1016/j.energy.2014.02.089.

- Mahmoudi, A.; Fazli, M.; Morad, M. R. (2018): A recent review of waste heat recovery by Organic Rankine Cycle. In *Applied Thermal Engineering* 143, pp. 660–675. DOI: 10.1016/j.applthermaleng.2018.07.136.
- Majozi, T.; Zhu, X. X. (2001): A Novel Continuous-Time MILP Formulation for Multipurpose Batch Plants. 1. Short-Term Scheduling. In *Ind. Eng. Chem. Res.* 40 (25), pp. 5935–5949. DOI: 10.1021/ie0005452.
- Majozi, Thokozani (2006): Heat integration of multipurpose batch plants using a continuous-time framework. In *Applied Thermal Engineering* 26 (13), pp. 1369–1377. DOI: 10.1016/j.applthermaleng.2005.05.027.
- Majozi, Thokozani (2009): Minimization of energy use in multipurpose batch plants using heat storage. An aspect of cleaner production. In *Journal of Cleaner Production* 17 (10), pp. 945–950. DOI: 10.1016/j.jclepro.2009.02.013.
- Martelli, Emanuele; Amaldi, Edoardo (2014): PGS-COM: A hybrid method for constrained non-smooth black-box optimization problems. In *Computers & Chemical Engineering* 63, pp. 108–139. DOI: 10.1016/j.compchemeng.2013.12.014.
- Mathiesen, B.V.; Bertelsen, N.; Schneider, N.C.A.; García, L.S.; Paardekooper, S.; Thellufsen, J.Z.; Djørup, S.R. (2019): Towards a decarbonised heating and cooling sector in Europe: Unlocking the potential of energy efficiency and district energy. Aalborg Universitet.
- Mavromatis, S. P.; Kokossis, A. C. (1998): Conceptual optimisation of utility networks for operational variations—I. targets and level optimisation. In *Chemical Engineering Science* 53 (8), pp. 1585–1608. DOI: 10.1016/S0009-2509(97)00431-4.
- Mazhar, Abdur Rehman; Liu, Shuli; Shukla, Ashish (2018): A state of art review on the district heating systems. In *Renewable and Sustainable Energy Reviews* 96, pp. 420–439. DOI: 10.1016/j.rser.2018.08.005.
- Mewes, D.; Mayinger, F.; Mehling, Harald; Cabeza, Luisa F. (2008): Heat and cold storage with PCM. Berlin, Heidelberg: Springer Berlin Heidelberg.
- Mian, Alberto; Martelli, Emanuele; Maréchal, Francois (2016): Multi-period Sequential Synthesis of Heat Exchanger Networks and Utility Systems including storages. In : 26th European Symposium on Computer Aided Process Engineering, vol. 38: Elsevier (Computer Aided Chemical Engineering), pp. 967–972.

- Mian, Alberto; Martelli, Emanuele; Maréchal, François (2015): Framework for the Multiperiod Sequential Synthesis of Heat Exchanger Networks with Selection, Design, and Scheduling of Multiple Utilities. In *Ind. Eng. Chem. Res.* 55 (1), pp. 168–186. DOI: 10.1021/acs.iecr.5b02104.
- Mikielewicz, Dariusz; Mikielewicz, Jarosław (2010): A thermodynamic criterion for selection of working fluid for subcritical and supercritical domestic micro CHP. In *Applied Thermal Engineering* 30 (16), pp. 2357–2362. DOI: 10.1016/j.applthermaleng.2010.05.035.
- Miranda, Camila B.; Costa, Caliane B. B.; Caballero, Jose A.; Ravagnani, Mauro A. S. S. (2016): Heat Exchanger Network Optimization for Multiple Period Operations. In *Ind. Eng. Chem. Res.* 55 (39), pp. 10301–10315. DOI: 10.1021/acs.iecr.6b01117.
- Miró, Laia; Gasia, Jaume; Cabeza, Luisa F. (2016): Thermal energy storage (TES) for industrial waste heat (IWH) recovery. A review. In *Applied Energy* 179, pp. 284–301. DOI: 10.1016/j.apenergy.2016.06.147.
- Modi, Anish; Haglind, Fredrik (2017): A review of recent research on the use of zeotropic mixtures in power generation systems. In *Energy Conversion and Management* 138, pp. 603–626. DOI: 10.1016/j.enconman.2017.02.032.
- Mussati, Sergio F.; Gernaey, Krist V.; Morosuk, Tatiana; Mussati, Miguel C. (2016): NLP modeling for the optimization of LiBr-H₂O absorption refrigeration systems with exergy loss rate, heat transfer area, and cost as single objective functions. In *Energy Conversion and Management* 127, pp. 526–544. DOI: 10.1016/j.enconman.2016.09.021.
- Natural Resources Canada (2012): Pinch Analysis, for the Efficient Use of Energy, Water & Hydrogen: Natural Resources Canada.
- Nguyen, Thu-Trang; Martin, Viktoria; Malmquist, Anders; Silva, Carlos A.S. (2017): A review on technology maturity of small scale energy storage technologies. In *Renew. Energy Environ. Sustain.* 2, p. 36. DOI: 10.1051/rees/2017039.
- Nikbakhti, Rasoul; Wang, Xiaolin; Hussein, Ahmed Kadhim; Iranmanesh, Aghil (2020): Absorption cooling systems – Review of various techniques for energy performance enhancement. In *Alexandria Engineering Journal* 59 (2), pp. 707–738. DOI: 10.1016/j.aej.2020.01.036.
- Ojha, Manish Kumar; Shukla, Anoop Kumar; Verma, Puneet; Kannojiya, Ravindra (2020): Recent progress and outlook of solar adsorption refrigeration systems. In *Materials Today: Proceedings*. DOI: 10.1016/j.matpr.2020.09.593.

- Olsen, Donald; Liem, Peter; Abdelouadoud, Yasmina; Wellig, Beat (2017): Thermal Energy Storage Integration Based on Pinch Analysis - Methodology and Application. In *Chemie Ingenieur Technik* 89 (5), pp. 598–606. DOI: 10.1002/cite.201600103.
- Oluleye, Oluwagbemisola (2015): Integration of Waste Heat Recovery in Process Sites. A thesis submitted to The University of Manchester for the degree of Doctor of Philosophy in the Faculty of Engineering and Physical Sciences. Dissertation. University of Manchester, Manchester, UK. School of Chemical Engineering and Analytical Science. Available online at <https://www.escholar.manchester.ac.uk/api/datastream?publicationPid=uk-ac-man-scw:298679&datastreamId=FULL-TEXT.PDF>, checked on 9/19/2017.
- Ormat Technologies Inc. (2020). Available online at <https://www.ormat.com/en/company/welcome/profile/>, checked on 12/8/2020.
- Pantaleo, A. M.; Fordham, J.; Oyewunmi, O. A.; Markides, C. N. (2017): Intermittent waste heat recovery. Investment profitability of ORC cogeneration for batch, gas-fired coffee roasting. In *Energy Procedia* 129, pp. 575–582. DOI: 10.1016/j.egypro.2017.09.209.
- Papadopoulos, Athanasios I.; Gkouletsos, Dimitris; Champilomatis, Vassilis; Giannakakis, Alexandros; Kousidis, Vergis; Hassan, Ibrahim; Seferlis, Panos (2020): Systematic assessment of working fluid mixtures for absorption refrigeration based on techno-economic, environmental, health and safety performance. In *Energy Conversion and Management* 223, p. 113262. DOI: 10.1016/j.enconman.2020.113262.
- Papadopoulos, Athanasios I.; Kyriakides, Alexios-Spyridon; Seferlis, Panos; Hassan, Ibrahim (2019): Absorption refrigeration processes with organic working fluid mixtures- a review. In *Renewable and Sustainable Energy Reviews* 109, pp. 239–270. DOI: 10.1016/j.rser.2019.04.016.
- Papageorgiou, Lazaros G.; Shah, Nilay; Pantelides, Constantinos C. (1994): Optimal Scheduling of Heat-Integrated Multipurpose Plants. In *Ind. Eng. Chem. Res.* 33 (12), pp. 3168–3186. DOI: 10.1021/ie00036a036.
- Papapetrou, Michael; Kosmadakis, George; Cipollina, Andrea; La Commare, Umberto; Micale, Giorgio (2018): Industrial waste heat: Estimation of the technically available resource in the EU per industrial sector, temperature level and country. In *Applied Thermal Engineering* 138, pp. 207–216. DOI: 10.1016/j.applthermaleng.2018.04.043.

- Papoulias, Soterios A.; Grossmann, Ignacio E. (1983): A structural optimization approach in process synthesis—II. In *Computers & Chemical Engineering* 7 (6), pp. 707–721. DOI: 10.1016/0098-1354(83)85023-6.
- Paterson, W. R. (1984): A replacement for the logarithmic mean. In *Chemical Engineering Science* 39 (11), pp. 1635–1636. DOI: 10.1016/0009-2509(84)80090-1.
- Pavão, Leandro V.; Miranda, Camila B.; Costa, Caliane B.B.; Ravagnani, Mauro A.S.S. (2018): Synthesis of multiperiod heat exchanger networks with timesharing mechanisms using meta-heuristics. In *Applied Thermal Engineering* 128, pp. 637–652. DOI: 10.1016/j.applthermaleng.2017.09.002.
- Peesel, Ron-H.; Philipp, Matthias; Schumm, Gregor; Hesselbach, Jens; Walmsley, Timothy G. (2016): Energy Efficiency Measures for Batch Retort Sterilization in the Food Processing Industry. In *Chemical Engineering Transactions* 52, pp. 163–168. DOI: 10.3303/CET1652028.
- Pehnt, Martin; Bödeker, Jan; Arens, Marlene; Jochem, Eberhard; Idrissova, Farikha (2010): Die Nutzung industrieller Abwärme technisch-wirtschaftliche Potenziale und energiepolitische Umsetzung (2010). „Wissenschaftliche Begleitforschung zu übergreifenden technischen, ökologischen, ökonomischen und strategischen Aspekten des nationalen Teils der Klimaschutzinitiative“. ifeu - Institut für Energie- und Umweltforschung Heidelberg; Fraunhofer Fraunhofer-Institut für System- und Innovationsforschung; IREES GmbH. Heidelberg, Karlsruhe.
- Peng, Ding-Yu; Robinson, Donald B. (1976): A New Two-Constant Equation of State. In *Ind. Eng. Chem. Fund.* 15 (1), pp. 59–64. DOI: 10.1021/i160057a011.
- Perry, Simon; Klemeš, Jiří; Bulatov, Igor (2008): Integrating waste and renewable energy to reduce the carbon footprint of locally integrated energy sectors. In *Energy* 33 (10), pp. 1489–1497. DOI: 10.1016/j.energy.2008.03.008.
- Persson, U.; Möller, B.; Werner, S. (2014): Heat Roadmap Europe: Identifying strategic heat synergy regions. In *Energy Policy* 74, pp. 663–681. DOI: 10.1016/j.enpol.2014.07.015.
- Pieper, Christoph (2019): Transformation of the German energy system - Towards photovoltaic and wind power. Technology Readiness Levels 2018. Dissertation. Technische Universität Dresden, Dresden. Institut für Verfahrenstechnik und Umwelttechnik.

- Pili, Roberto; Romagnoli, Alessandro; Spliethoff, Hartmut; Wieland, Christoph (2017): Techno-Economic Analysis of Waste Heat Recovery with ORC from Fluctuating Industrial Sources. In *Energy Procedia* 129, pp. 503–510. DOI: 10.1016/j.egypro.2017.09.170.
- Poling, Bruce E.; Prausnitz, John M.; O’Connell, John P. (2001): The properties of gases and liquids. 5. ed. New York: McGraw-Hill.
- Ponce-Ortega, José María; Tora, Eman A.; González-Campos, J. Betzabe; El-Halwagi, Mahmoud M. (2011): Integration of Renewable Energy with Industrial Absorption Refrigeration Systems. Systematic Design and Operation with Technical, Economic, and Environmental Objectives. In *Ind. Eng. Chem. Res.* 50 (16), pp. 9667–9684. DOI: 10.1021/ie200141j.
- Qiu, Guoquan; Liu, Hao; Riffat, Saffa (2011): Expanders for micro-CHP systems with organic Rankine cycle. In *Applied Thermal Engineering* 31 (16), pp. 3301–3307. DOI: 10.1016/j.applthermaleng.2011.06.008.
- Quoilin, Sylvain (2011): Sustainable energy conversion through the use of Organic Rankine Cycles for waste heat recovery and solar applications. Dissertation. University of Liège, Liège, Belgium. Faculty of Applied Science.
- Rayegan, R.; Tao, Y. X. (2011): A procedure to select working fluids for Solar Organic Rankine Cycles (ORCs). In *Renewable Energy* 36 (2), pp. 659–670. DOI: 10.1016/j.renene.2010.07.010.
- Reif-Acherman, Simón (2012): The early ice making systems in the nineteenth century. In *International Journal of Refrigeration* 35 (5), pp. 1224–1252. DOI: 10.1016/j.ijrefrig.2012.03.003.
- Ripke, M.; Menzler, G.; Roth, H.; Lucas, K. (1994): Primärenergieeinsparung durch Standortintegration; Primary energy savings through location integration. In *Brennst.-Wärme-Kraft* 46 (3), pp. 82–86.
- Hannah Ritchie, Max Roser and Pablo Rosado (2020): "CO₂ and Greenhouse Gas Emissions". Available online at <https://ourworldindata.org/co2-and-greenhouse-gas-emissions>, checked on 01/27/2021.
- Roos, Philipp; Haselbacher, Andreas (2021): Thermocline control through multi-tank thermal-energy storage systems. In *Applied Energy* 281, p. 115971. DOI: 10.1016/j.apenergy.2020.115971.

- Sadeli, Efrat; Chang, Chuei-Tin (2012): Heuristic Approach to Incorporate Timesharing Schemes in Multiperiod Heat Exchanger Network Designs. In *Ind. Eng. Chem. Res.* 51 (23), pp. 7967–7987. DOI: 10.1021/ie202171g.
- Sarbu, Ioan; Sebarchievici, Calin (2015): General review of solar-powered closed sorption refrigeration systems. In *Energy Conversion and Management* 105, pp. 403–422. DOI: 10.1016/j.enconman.2015.07.084.
- Sarbu, Ioan; Sebarchievici, Calin (2018): A Comprehensive Review of Thermal Energy Storage. In *Sustainability* 10 (2), p. 191. DOI: 10.3390/su10010191.
- Sebelebele, Nthabiseng; Majozi, Thokozani (2017): Heat integration of multipurpose batch plants through multiple heat storage vessels. In *Computers & Chemical Engineering* 106, pp. 269–285. DOI: 10.1016/j.compchemeng.2017.06.007.
- Seid, Reshid; Majozi, Thokozani (2012): A robust mathematical formulation for multipurpose batch plants. In *Chemical Engineering Science* 68 (1), pp. 36–53. DOI: 10.1016/j.ces.2011.08.050.
- Seid, Reshid; Majozi, Thokozani (2014a): Heat integration in multipurpose batch plants using a robust scheduling framework. In *Energy* 71, pp. 302–320. DOI: 10.1016/j.energy.2014.04.058.
- Seid, Reshid; Majozi, Thokozani (2014b): Optimization of energy and water use in multipurpose batch plants using an improved mathematical formulation. In *Chemical Engineering Science* 111, pp. 335–349. DOI: 10.1016/j.ces.2014.02.036.
- Shmroukh, Ahmed N.; Ali, Ahmed Hamza H.; Ookawara, Shinichi (2015): Adsorption working pairs for adsorption cooling chillers: A review based on adsorption capacity and environmental impact. In *Renewable and Sustainable Energy Reviews* 50, pp. 445–456. DOI: 10.1016/j.rser.2015.05.035.
- Short, Michael; Isafiade, Adeniyi J.; Fraser, Duncan M.; Kravanja, Zdravko (2016a): Synthesis of heat exchanger networks using mathematical programming and heuristics in a two-step optimisation procedure with detailed exchanger design. In *Chemical Engineering Science* 144, pp. 372–385. DOI: 10.1016/j.ces.2016.01.045.
- Short, Michael; Isafiade, Adeniyi J.; Fraser, Duncan M.; Kravanja, Zdravko (2016b): Two-step hybrid approach for the synthesis of multi-period heat exchanger networks with detailed exchanger design. In *Applied Thermal Engineering* 105, pp. 807–821. DOI: 10.1016/j.applthermaleng.2016.05.065.

- Shu, Gequn; Yu, Guopeng; Tian, Hua; Wei, Haiqiao; Liang, Xingyu (2014): A Multi-Approach Evaluation System (MA-ES) of Organic Rankine Cycles (ORC) used in waste heat utilization. In *Applied Energy* 132, pp. 325–338. DOI: 10.1016/j.apenergy.2014.07.007.
- Singhvi, A.; Shenoy, U. V. (2002): Aggregate Planning in Supply Chains by Pinch Analysis. In *Chemical Engineering Research and Design* 80 (6), pp. 597–605. DOI: 10.1205/026387602760312791.
- Smith, Robin (2005): Chemical process design and integration. Chichester, West Sussex: Wiley.
- Sözen, Adnan (2001): Effect of heat exchangers on performance of absorption refrigeration systems. In *Energy Conversion and Management* 42 (14), pp. 1699–1716. DOI: 10.1016/S0196-8904(00)00151-5.
- Stamp, Jane; Majozi, Thokozani (2011): Optimum heat storage design for heat integrated multipurpose batch plants. In *Energy* 36 (8), pp. 5119–5131. DOI: 10.1016/j.energy.2011.06.009.
- Stamp, Jane D.; Majozi, Thokozani (2017): Long-term heat integration in multipurpose batch plants using heat storage. In *Journal of Cleaner Production* 142, pp. 1492–1509. DOI: 10.1016/j.jclepro.2016.11.155.
- Stampfli, Jan A.; Lucas, Edward J.; Ong, Benjamin H.Y.; Olsen, Donald G.; Krummenacher, Pierre; Wellig, Beat (2020): Optimization of volume-limited thermal energy storage in non-continuous processes. In *Energy* 203, p. 117805. DOI: 10.1016/j.energy.2020.117805.
- Statistisches Bundesamt (2019): Energieverbrauch in der Industrie 2018 um 2,3 % gegenüber dem Vorjahr gesunken. Pressemitteilung Nr. 502. Available online at https://www.destatis.de/DE/Presse/Pressemitteilungen/2019/12/PD19_502_435.html, checked on 11/11/2020.
- Stijepovic, Mirko Z.; Linke, Patrick; Papadopoulos, Athanasios I.; Grujic, Aleksandar S. (2012): On the role of working fluid properties in Organic Rankine Cycle performance. In *Applied Thermal Engineering* 36, pp. 406–413. DOI: 10.1016/j.applthermaleng.2011.10.057.
- Stoltze, S; Mikkelsen, J.; Lorentzen, B.; Petersen, P.M.; Qvale, B. (1995): Waste-Heat Recovery in Batch Processes Using Heat Storage. In *Journal of Energy Resources Technologies* 117 (2). Available online at <http://energyresources.asmedigitalcollection.asme.org/>, checked on 11/9/2017.

- Sun, Da-Wen (1997): Thermodynamic design data and optimum design maps for absorption refrigeration systems. In *Applied Thermal Engineering* 17 (3), pp. 211–221. DOI: 10.1016/S1359-4311(96)00041-5.
- Sun, Da-Wen; Eames, Ian W.; Aphornratana, Satha (1996): Evaluation of a novel combined ejector-absorption refrigeration cycle — I: computer simulation. In *International Journal of Refrigeration* 19 (3), pp. 172–180. DOI: 10.1016/0140-7007(96)00010-2.
- Sun, Jian; Fu, Lin; Zhang, Shigang (2012): A review of working fluids of absorption cycles. In *Renewable and Sustainable Energy Reviews* 16 (4), pp. 1899–1906. DOI: 10.1016/j.rser.2012.01.011.
- Sun, Xiaojing; Liu, Linlin; Dong, Yachao; Zhuang, Yu; Zhang, Lei; Du, Jian (2020a): Superstructure-Based Simultaneous Optimization of a Heat Exchanger Network and a Compression–Absorption Cascade Refrigeration System for Heat Recovery. In *Ind. Eng. Chem. Res.* 59 (36), pp. 16017–16028. DOI: 10.1021/acs.iecr.0c02776.
- Sun, Xiaojing; Liu, Linlin; Sheng, Yao; Zhang, Lei; Du, Jian (2019): Heat Exchanger Network Synthesis with Absorption Refrigeration Cycle Integrated Considering the Optimization of Operating Condition. In *I* 76, pp. 301–306. DOI: 10.3303/CET1976051.
- Sun, Xiaojing; Liu, Linlin; Zhuang, Yu; Zhang, Lei; Du, Jian (2020b): Heat Exchanger Network Synthesis Integrated with Compression–Absorption Cascade Refrigeration System. In *Processes* 8 (2), p. 210. DOI: 10.3390/pr8020210.
- Tabor, H.; Bronicki, L. (1961): Small turbine for solar energy power package. UN Conference on New Sources of Energy. United Nations. Rome, 1961.
- Tabor, H.; Bronicki, L. (1965): Establishing Criteria for Fluids for Small Vapor Turbines. In *SAE Transactions* 73, pp. 561–575. DOI: 10.4271/640823.
- Tan, Raymond R.; Foo, Dominic C.Y. (2007): Pinch analysis approach to carbon-constrained energy sector planning. In *Energy* 32 (8), pp. 1422–1429. DOI: 10.1016/j.energy.2006.09.018.
- Tartière, Thomas; Astolfi, Marco (2017): A World Overview of the Organic Rankine Cycle Market. In *Energy Procedia* 129, pp. 2–9. DOI: 10.1016/j.egypro.2017.09.159.
- Tchanche, Bertrand Fankam; Papadakis, George; Lambrinos, Gregory; Frangoudakis, Antonios (2009): Fluid selection for a low-temperature solar organic Rankine cycle. In *Applied*

- Thermal Engineering* 29 (11-12), pp. 2468–2476. DOI: 10.1016/j.applthermaleng.2008.12.025.
- Tchernev, D.I. (1978): Solar energy application of natural zeolites. In *Natural zeolites: Occurrence, properties, use* 474, p. 485.
- Thurairaja, Kankeyan; Wijewardane, Anusha; Jayasekara, Saliya; Ranasinghe, Chathura (2019): Working Fluid Selection and Performance Evaluation of ORC. In *Energy Procedia* 156, pp. 244–248. DOI: 10.1016/j.egypro.2018.11.136.
- Tora, E. A.; El-Halwagi, M. M. (2010): Integration of Solar Energy into Absorption Refrigerators and Industrial Processes (9). Available online at <https://onlinelibrary.wiley.com/doi/epdf/10.1002/ceat.201000048>, updated on 1/15/2021, checked on 1/15/2021.
- Townsend, D. W.; Linnhoff, Bodo (1983a): Heat and power networks in process design. Part I: Criteria for placement of heat engines and heat pumps in process networks. In *AIChE J.* 29 (5), pp. 742–748. DOI: 10.1002/aic.690290508.
- Townsend, D. W.; Linnhoff, Bodo (1983b): Heat and power networks in process design. Part II: Design procedure for equipment selection and process matching. In *AIChE J.* 29 (5), pp. 748–771. DOI: 10.1002/aic.690290509.
- Uhlenbruck, S.; Vogel, R.; Lucas, K. (2000): Heat Integration of Batch Processes. In *Chem. Eng. Technol.* 23 (3), pp. 226–229. DOI: 10.1002/(SICI)1521-4125(200003)23:3<226::AID-CEAT226>3.0.CO;2-K.
- UNFCCC (2015): Adoption of the Paris Agreement. Report No. FCCC/CP/2015/L.9/ Rev.1. Available online at https://unfccc.int/files/essential_background/convention/application/pdf/english_paris_agreement.pdf, checked on 1/26/2021.
- Vanslambrouck, B.; Vankeirsbilck, I.; van den Broek, M.; Gusev, S.; De Paepe, M. (2012): Efficiency comparison between the steam cycle and the organic rankine cycle for small scale power generation. In *Renewable Energy World Conference & Expo North America, Proceedings*. Available online at <https://biblio.ugent.be/publication/3078894>, checked on 2020.
- Varbanov, Petar Sabev (2013): Basic Process Integration Terminology. In J. Klemes (Ed.): *Handbook of Process Integration (PI). Minimisation Of Energy And Water Use, Waste And Emissions*. Burlington: Elsevier Science (Woodhead Publishing Series in Energy), pp. 28–78.

- Vaselenak, Jane A.; Grossmann, Ignacio E.; Westerberg, Arthur W. (1986): Heat integration in batch processing. In *Ind. Eng. Chem. Proc. Des. Dev.* 25 (2), pp. 357–366. DOI: 10.1021/i200033a004.
- Verheyen, N.; Zhang, W. (2006): Design of flexible heat exchanger network for multi-period operation. In *Chemical Engineering Science* 61 (23), pp. 7730–7753. DOI: 10.1016/j.ces.2006.08.043.
- Vivian, Jacopo; Manente, Giovanni; Lazzaretto, Andrea (2015): A general framework to select working fluid and configuration of ORCs for low-to-medium temperature heat sources. In *Applied Energy* 156, pp. 727–746. DOI: 10.1016/j.apenergy.2015.07.005.
- Vliet, G. C.; Lawson, M. B.; Lithgow, R. A. (1980): Water-lithium bromide double-effect absorption cooling analysis. Final report. Texas Univ., Austin (USA). Center for Energy Studies. United States.
- Wagner, W. (1973): New vapour pressure measurements for argon and nitrogen and a new method for establishing rational vapour pressure equations. In *Cryogenics* 13 (8), pp. 470–482. DOI: 10.1016/0011-2275(73)90003-9.
- Walmsley, Michael R.W.; John Atkins, Martin; Walmsley, Timothy G. (2013a): Application of Heat Recovery Loops to Semi-continuous Processes for Process Integration. In : *Handbook of Process Integration (PI)*: Elsevier, pp. 594–629.
- Walmsley, Michael R.W.; Walmsley, Timothy G.; Atkins, Martin J.; Neale, James R. (2013b): Methods for improving heat exchanger area distribution and storage temperature selection in heat recovery loops. In *Energy* 55, pp. 15–22. DOI: 10.1016/j.energy.2013.02.050.
- Walmsley, Timothy G.; Walmsley, Michael R.W.; Atkins, Martin J.; Neale, James R. (2014): Integration of industrial solar and gaseous waste heat into heat recovery loops using constant and variable temperature storage. In *Energy* 75, pp. 53–67. DOI: 10.1016/j.energy.2014.01.103.
- Wang, E. H.; Zhang, H. G.; Fan, B. Y.; Ouyang, M. G.; Zhao, Y.; Mu, Q. H. (2011): Study of working fluid selection of organic Rankine cycle (ORC) for engine waste heat recovery. In *Energy* 36 (5), pp. 3406–3418. DOI: 10.1016/j.energy.2011.03.041.
- Wang, Yingxu (2010): A Sociopsychological Perspective on Collective Intelligence in Metaheuristic Computing. In *International Journal of Applied Metaheuristic Computing (IJAMC)* 1 (1), pp. 110–128. DOI: 10.4018/jamc.2010102606.

- Watson, K. M. (1943): Thermodynamics of the Liquid State. In *Ind. Eng. Chem.* 35 (4), pp. 398–406. DOI: 10.1021/ie50400a004.
- Werner, Sven (2017): International review of district heating and cooling. In *Energy* 137, pp. 617–631. DOI: 10.1016/j.energy.2017.04.045.
- Wiltshire, Robin (2016): Advanced District Heating and Cooling (DHC) Systems. Chapter 1. Historical development of district heating and characteristics of a modern district heating system. Burlington: Elsevier (Woodhead Publishing Series in Energy Ser, number 87).
- Wolf, Stefan (2017): Integration von Wärmepumpen in industrielle Produktionssysteme : Potenziale und Instrumente zur Potenzialerschließung. Dissertation. Universität Stuttgart, Stuttgart. Institut für Energiewirtschaft und Rationelle Energieanwendung.
- Wonchala, Jason; Hazledine, Maxwell; Goni Boulama, Kiari (2014): Solution procedure and performance evaluation for a water–LiBr absorption refrigeration machine. In *Energy* 65, pp. 272–284. DOI: 10.1016/j.energy.2013.11.087.
- Xu, Yanyan; Wang, Lei; Chen, Yuting; Ye, Shuang; Huang, Weiguang (2020): Simultaneous Optimization Method for Directly Integrating ORC with HEN to Achieve Exergy-Economy Multiobjective. In *Ind. Eng. Chem. Res.* 59 (49), pp. 21488–21501. DOI: 10.1021/acs.iecr.0c04039.
- Xu, Z. Y.; Wang, R. Z.; Yang, Chun (2019): Perspectives for low-temperature waste heat recovery. In *Energy* 176, pp. 1037–1043. DOI: 10.1016/j.energy.2019.04.001.
- Yang, Mina; Lee, Seung Yeob; Chung, Jin Taek; Kang, Yong Tae (2017): High efficiency H₂O/LiBr double effect absorption cycles with multi-heat sources for tri-generation application. In *Applied Energy* 187, pp. 243–254. DOI: 10.1016/j.apenergy.2016.11.067.
- Yee, T. F.; Grossmann, I. E. (1990): Simultaneous optimization models for heat integration—II. Heat exchanger network synthesis. In *Computers & Chemical Engineering* 14 (10), pp. 1165–1184. DOI: 10.1016/0098-1354(90)85010-8.
- Yu, Haoshui; Eason, John; Biegler, Lorenz T.; Feng, Xiao (2017a): Process integration and superstructure optimization of Organic Rankine Cycles (ORCs) with heat exchanger network synthesis. In *Computers & Chemical Engineering* 107, pp. 257–270. DOI: 10.1016/j.compchemeng.2017.05.013.
- Yu, Haoshui; Eason, John; Biegler, Lorenz T.; Feng, Xiao (2017b): Simultaneous heat integration and techno-economic optimization of Organic Rankine Cycle (ORC) for

multiple waste heat stream recovery. In *Energy* 119, pp. 322–333. DOI: 10.1016/j.energy.2016.12.061.

Yu, Haoshui; Feng, Xiao; Wang, Yufei; Biegler, Lorenz T.; Eason, John (2016): A systematic method to customize an efficient organic Rankine cycle (ORC) to recover waste heat in refineries. In *Applied Energy* 179, pp. 302–315. DOI: 10.1016/j.apenergy.2016.06.093.

Zhang, Xinxin; He, Maogang; Zhang, Ying (2012): A review of research on the Kalina cycle. In *Renewable and Sustainable Energy Reviews* 16 (7), pp. 5309–5318. DOI: 10.1016/j.rser.2012.05.040.

Zhelev, T. K.; Ntlhakana, J. L. (1999): Energy-environment closed-loop through Oxygen Pinch. In *Computers & Chemical Engineering* 23, S79-S83. DOI: 10.1016/S0098-1354(99)80021-0.

Zogg, Martin (2008): History of heat pumps. Swiss contributions and international milestones. Swiss Federal Office of Energy SFOE. Oberburg, Switzerland. Available online at <https://www.osti.gov/etdeweb/biblio/21381633>.

Appendix A Modeling of Single-Effect Absorption Chiller

Appendix A describes the procedure for the mathematical modeling of single-effect absorption chillers as used in the mathematical framework developed in Chapter 4. The objective of the modeling is to generate fit functions for the coefficient of performance of the ABC (COP), the ratio between the cooling demand at the ABC-Condenser and the heating demand at the ABC-Generator ($C2G$), the temperature of the refrigerant solution at the entry of the ABC-Generators (t_{gen}^{in} , location 3 at Figure A-1) and temperature of the strong refrigerant solution at the entry of the ABC-Absorber (t_{abs}^{in} , location 10 at Figure A-1). These four variables are used in the mathematical framework developed in Chapter 4 to describe the physical behaviour of the ABC and its interaction with the HEN. These variables are period independent and remain constant during the whole duration of the cycle in the case of multi-period processes. The structure of the fit functions and the mathematical definitions for COP and G2G were presented in Chapter 4. For clarity, the expressions are repeated below.

$$COP \sum_{i \in HP} q_i^{abcg} = \sum_{i \in HP} q_i^{abce} \quad (A-1)$$

$$C2G \sum_{i \in HP} q_i^{abcg} = q^{abcc} \quad (A-2)$$

$$COP = C_1 e^{C_2 t_{gen}} + C_3 e^{C_4 t_{gen}} \quad (A-3)$$

$$C2G = C_5 COP + C_6 \quad (A-4)$$

$$t_{gen}^{in} = C_7 (t_{gen})^2 + C_8 t_{gen} + C_9 \quad (A-5)$$

$$t_{abs}^{in} = C_{10} t_{gen} + C_{11} \quad (A-6)$$

For for given refrigeration and condensation temperatures, T_{ref} , and T_{cond} , and a given effectiveness of the SHEX, ε_{SHEX} , a unique set of fit functions describing the behavior of the ABC is generated. The structure of the fit functions is based on the observation of multiple simulations of the behaviour of the system for different sets of T_{ref} , T_{cond} and ε_{SHEX} . The structure of the fit functions guarantees a good fit with the simulation results from the detailed simulation as presented in this appendix ($R^2 \geq 0.95$).

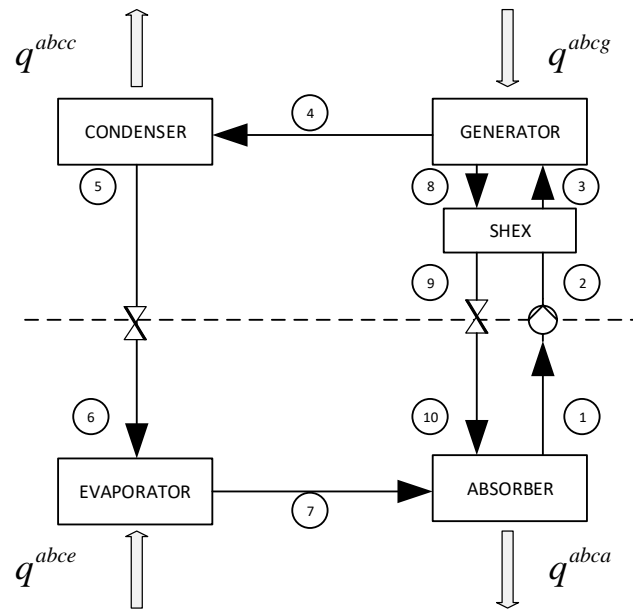


Figure A-1. Schematic representation of a single-effect absorption chiller

Source: Own diagram

The assumptions used for the mathematical modeling of the absorption chiller were presented in Section 1.3 and used to define the scope of the research. For clarity, the assumptions are repeated as following.

- Refrigerant couple is set as LiBr/H₂O.
- Only single-effect absorption chillers are considered.
- Refrigerant and refrigerant solution properties are taken from experimental correlations. For the LiBr/H₂O solution properties are taken from the correlations by Sun (1997). Properties for pure H₂O inside the absorption cycle are obtained from Irvine and Liley (1984).
- Condenser and absorber temperatures are the same and they are defined by the available cold utility and the minimum approach temperature allowed in the system.
- Evaporator (refrigeration) temperature is set in advance.
- Mixing of streams after the generators and evaporators takes place isothermally.
- Concentration of LiBr in solution remains always between 0.4 and 0.7 in mass, to avoid crystallization.
- Refrigerant (H₂O) leaves condenser and evaporators at a saturated state (as liquid and vapor respectively).
- H₂O leaves the generator as a superheated steam at the generator pressure and at the equilibrium temperature of the LiBr/H₂O solution (Wonchala et al. 2014).

- Refrigerant solution (LiBr/H₂O) leaves absorber and the generators at a saturated state (as liquid and vapor respectively).
- Efficiency of “Solution Heat Exchanger” (SHEX) is set in advance.
- Area of SHEX and pumping cost of ABC are neglected in the cost calculations (Mussati et al. 2016).

Figure A-1 presents a schematic representation of a single-effect absorption chiller. Equations (A-7) to (A-24) describe the physical behaviour of the ABC according to the assumptions provided previously and the numbering of the locations as illustrated in Figure A-1. The equations are based on mass and energy balances for all the components of the ABC.

$$m_1 = m_7 + m_{10} \quad (A-7)$$

$$m_{10}X_{ws} = m_1X_{ss} \quad (A-8)$$

$$q^{abca} = m_7h_7 + m_{10}h_{10} - m_1h_1 \quad (A-9)$$

$$m_1 = m_2 \quad (A-10)$$

$$W_{pump} = (m_2h_2 - m_1h_1) / \eta_{pump} \quad (A-11)$$

$$q^{shex} = m_3h_3 - m_2h_2 = m_9h_9 - m_8h_8 \quad (A-12)$$

$$\varepsilon_{shex} = \frac{h_8 - h_7}{h_8 - h_2} \quad (A-13)$$

$$m_3 = m_4 + m_8 \quad (A-14)$$

$$m_3X_{ws} = m_8X_{ss} \quad (A-15)$$

$$q^{abcg} = m_4h_4 + m_8h_8 - m_3h_3 \quad (A-16)$$

$$m_9 = m_{10} \quad (A-17)$$

$$m_9h_9 = m_{10}h_{10} \quad (A-18)$$

$$m_4 = m_5 \quad (A-19)$$

$$q^{abcc} = m_4h_4 - m_5h_5 \quad (A-20)$$

$$m_5 = m_6 \quad (A-21)$$

$$m_5h_5 = m_6h_6 \quad (A-22)$$

$$m_6 = m_7 \quad (A-23)$$

$$q^{abce} = m_7 h_7 - m_6 h_6 \quad (A-24)$$

Any property database or empirical correlations can be used for the fluid properties required for the modeling of the ABC (mainly enthalpies of the refrigerant and refrigerant solution) at different locations of the superstructure, without loss of generality. In this dissertation, empirical correlations by Sun (1997) and Irvine and Liley (1984) are used to calculate the thermophysical properties of the LiBr/H₂O solution and the refrigerant H₂O respectively. Below, the empirical correlations are presented explicitly.

- H₂O (Steam Properties):

- Saturation pressure P_{sat} [kPa] for $273.15 \text{ K} < T < 600 \text{ K}$

$$\ln P_{sat}(T) = \sum_{n=0}^9 A_n T^n + \frac{A_{10}}{T - A_{11}} \quad (A-25)$$

Table A-1. Coefficients for the calculation of the saturation pressure of H₂O.

n	A_n
0	1.04592E1
1	-4.04897E-3
2	-4.17520E-5
3	3.68510E-7
4	-1.01520E-9
5	8.65310E-13
6	9.03668E-16
7	-1.99690E-18
8	7.79287E-22
9	1.91482E-25
10	-3.96870E3
11	-3.95735E1

Source: Own table

- Saturation temperature T_{sat} [K]

$$T_{sat}(P) = A + \frac{B}{\ln P + C} \quad (A-26)$$

Table A-2. Coefficients for the calculation of the saturation temperature of H₂O.

	$P < 12330 \text{ kPa}$	$P \geq 12330 \text{ kPa}$
A	4.26776E1	-3.87592E2
B	-3.89270E2	-1.25875E4
C	-9.48654E1	-1.52578E1

Source: Own table

- Specific enthalpy at saturation h_{sat} [kJ/kg]

$$h_{sat}(T_r) = 2.0993E3 \left(\sum_{n=1}^7 A_n T_r^n + B T_r^{\frac{7}{8}} + C T_r^{\frac{5}{6}} + D T_r^{\frac{1}{3}} + E \right) \quad (A-27)$$

Table A-3. Coefficients for the calculation of the specific enthalpy at saturation of H₂O (Part 1).

n	A _n		
	Liquid		Gas
	273.15 K < T < 300 K	300K < T < 600 K	273.15 K < T < 647 K
1	6.24698837E2	-2.67172935E0	-4.81351884E0
2	-2.34385369E3	6.22640035E0	2.69411792E0
3	-9.50812101E3	-1.31789573E1	-7.39064542E0
4	7.16287928E4	-1.91322436E0	1.04961689E1
5	-1.63535221E5	6.87937653E1	-5.46840036E0
6	1.66531093E5	-1.24819906E2	0
7	-6.47854585E4	7.21435404E1	0

Source: Own table

Table A-4. Coefficients for the calculation of the specific enthalpy at saturation of H₂O (Part 2).

	Liquid		Gas
	273.15 K < T < 300 K	300K < T < 600 K	273.15 K < T < 647 K
	B	0	0
C	0	0	5.08441288E0
D	0	0	4.57874342E-1
E	0	8.839230108E-1	1

Source: Own table

And:

$$T_r = \frac{647.3 - T}{647.3} \quad (A-28)$$

- Specific enthalpy of supersaturated vapor h_{super} [kJ/kg]

$$h_{super}(P, T) = \left[\sum_{n=0}^2 A_n T^n \right] - A_3 e^{\frac{T_{sat}-T}{45}} \quad (A-29)$$

With:

$$A_0 = B_{11} + B_{12}P + B_{13}P^2 \quad (A-30)$$

$$A_1 = B_{21} + B_{22}P + B_{23}P^2 \quad (A-31)$$

$$A_2 = B_{31} + B_{32}P + B_{33}P^2 \quad (A-32)$$

$$A_3 = B_{41} + B_{42}P + B_{43}P^2 + B_{44}T^4 + B_{45}T^5 \quad (A-33)$$

And B_{ij} :

Table A-5. Coefficients for the calculation of the specific enthalpy of superheated H₂O.

	j=1	j=2	j=3	j=4	j=5
i=1	2.0412100E3	-4.0400210E1	-4.8095000E-1	-	-
i=2	1.6106930E0	5.4720510E-2	7.5175370E-4	-	-
i=3	3.3831170E-4	-1.9757360E-5	-2.8740900E-7	-	-
i=4	1.7078200E3	-1.6994190E1	6.2746295E-2	1.0284259E-4	6.4561298E-8

Source: Own table

- LiBr/H₂O (Solution Properties):

The equations are valid for $0\text{ }^{\circ}\text{C} \leq T \leq 180\text{ }^{\circ}\text{C}$ and $0 \leq X_{\text{LiBr}} \leq 70\%$.

- Dew temperature T_{dew} [$^{\circ}\text{F}$]

$$T_{\text{dew}}(T, X_{\text{LiBr}}) = \sum_{i=0}^5 \sum_{j=0}^2 A_{ij} X_{\text{LiBr}}^i T^j \quad (\text{A-34})$$

With X_{LiBr} [%] and A_{ij} :

Table A-6. Coefficients for the calculation of dew temperature of LiBr/H₂O solution.

	j=0	j=1	j=2
i=0	-1.313448E-1	9.967944E-1	1.978788E-5
i=1	1.820914E-1	1.778069E-3	-1.779481E-5
i=2	-5.177356E-2	-2.216697E-4	2.002427E-6
i=3	2.827426E-3	5.913618E-6	-7.667546E-8
i=4	-6.380541E-5	-7.308556E-8	1.201525E-9
i=5	4.340498E-7	2.788472E-10	-6.64171E-12

Source: Own table

- Solution enthalpy h_{sol} [kJ/kg]

$$h_{\text{sol}}(T, X_{\text{LiBr}}) = \sum_{i=0}^5 \sum_{j=0}^2 A_{ij} X_{\text{LiBr}}^i T^j \quad (\text{A-35})$$

With T [$^{\circ}\text{C}$], X_{LiBr} [%] and A_{ij} :

Table A-7. Coefficients for the calculation of specific enthalpy of LiBr/H₂O solution.

	j=0	j=1	j=2
i=0	1.134125E0	4.124891E0	5.743693E-4
i=1	-4.800450E-1	-7.643903E-2	5.870921E-5
i=2	-2.161438E-3	2.589577E-3	-7.375319E-6
i=3	2.336235E-4	-9.500522E-5	3.277592E-7
i=4	-1.188679E-5	1.708026E-6	-6.062304E-9
i=5	2.291532E-7	-1.102363E-8	3.901897E-11

Source: Own table

- Solution density ρ_{sol} [kg/m^3]

$$\rho_{sol}(T, X_{LiBr}) = \sum_{i=0}^4 \sum_{j=0}^2 A_{ij} X_{LiBr}^i T^j \quad (A-36)$$

With T [$^{\circ}C$], X_{LiBr} [%] and A_{ij} :

Table A-8. Coefficients for the calculation of density of LiBr/H₂O solution.

	j=0	j=1	j=2
i=0	9.939006E-1	-5.631094E-4	1.392527E-6
i=1	1.046888E-2	1.633541E-5	-2.801009E-7
i=2	-1.667939E-4	-1.110273E-6	1.734979E-8
i=3	5.332835E-6	2.882292E-8	-4.232988E-10
i=4	-3.440005E-8	-2.523579E-10	3.503024E-12

Source: Own table

Equations (A-7) to (A-24) and the empirical correlations in expressions (A-25) to (A-36), provide a complete description of the physical behavior of the system. In order to generate the fit functions for a given set of sets of T_{ref} (equivalent to T_7 in Figure A-1), T_{cond} (equivalent to T_5 in Figure A-1) and ε_{SHEX} , multiple simulations for the ABC with varying generator temperatures, t_{gen} (equivalent to T_8 in Figure A-1) are performed. From the result of the simulations, data fitting procedures are performed in order to generate the fit coefficients, C_1 to C_{11} .

Figure A-2 illustrates the results of the data fitting procedure for the sets of ($T_{ref}, T_{cond}, \varepsilon_{SHEX}$) used in the case studies in Chapter 5 and Table A-9 presents the coefficients C_1 to C_{11} generated for the fit functions. For all fit functions $R^2 \geq 0,95$.

Table A-9. Coefficients for the fitting functions generated for the case studies.

	Case Study 1-2 (10 $^{\circ}C$;45 $^{\circ}C$;0.7)	Case Study 3 (5 $^{\circ}C$;30 $^{\circ}C$;0.7)
C_1	7.354E-1	8.230E-1
C_2	2.127E-4	-1.422E-4
C_3	-1.322E13	-3.147E12
C_4	-3.617E-1	-5.084E-1
C_5	1.061E0	1.042E0
C_6	-1.805E-6	-3.647E-6
C_7	-6.746E-3	-7.080E-3
C_8	1.469E0	1.240E0
C_9	-2.969E0	1.421E0
C_{10}	3.178E-1	3.115E-1
C_{11}	2.988E1	2.022E1

Source: Own table

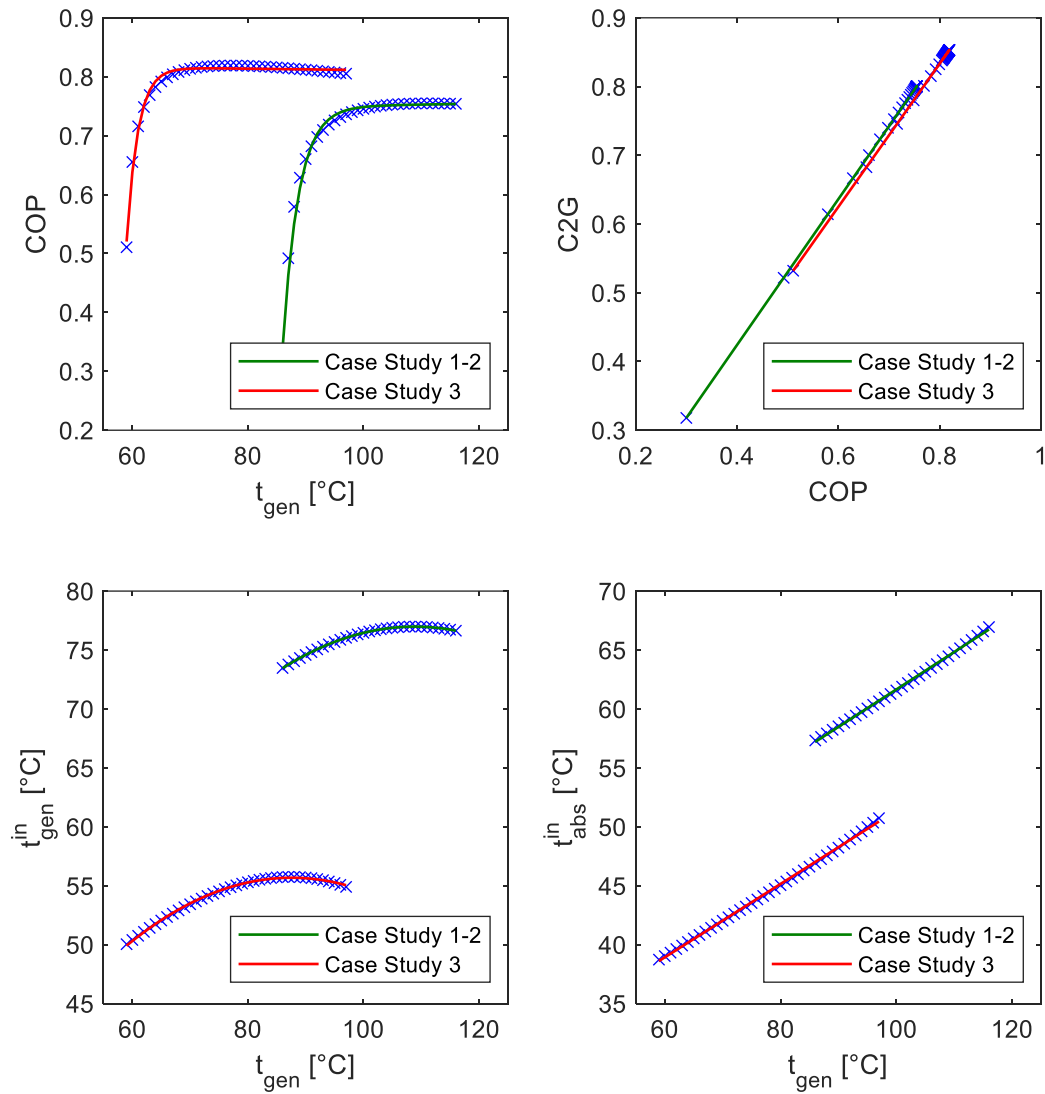


Figure A-2. Results for the data fitting procedures for the case studies.

Source: Own diagram

Appendix B Thermophysical properties of ORC Working Fluids

Appendix B describes the calculation of the thermophysical properties of the working fluids used in the case studies in Chapter 5 and presents a database of the parameters used in their calculation. In general, the mathematical framework developed in Chapter 4 can be used for any dry working fluid with known thermophysical properties. The properties can be extracted directly from property databases like REFPROP or calculated using empirical correlations and equations of state. This work uses the Peng Robinson Equations of State (PR-EOS) in order to calculate the specific enthalpies and entropies of the dry working fluids in each point of the ORC cycle. As for the ideal gas heat capacities, vapor pressures and latent heats of evaporation/condensation of the working fluids, appropriated empirical correlations as presented in the reference book “The Properties of Gas and Liquids” by Poling et al. (2001) are used. Expressions (B-1) to (B-5) present the PR-EOS and its constituent parameters.

$$P = \frac{V}{V - b} - \frac{aV}{RT(V^2 + 2bV - b^2)} \quad (B-1)$$

$$a = 0.45724 \frac{(RT_c)^2}{P_c} \alpha \quad (B-2)$$

$$b = 0.0778 \frac{RT_c}{P_c} \quad (B-3)$$

$$\alpha = \left[1 + \kappa \left(1 - \left(\frac{T}{T_c} \right)^{0.5} \right) \right]^2 \quad (B-4)$$

$$\kappa = 0.37464 + 1.54226\omega - 0.26992\omega^2 \quad (B-5)$$

By itself the PR-EOS is unable to calculate the specific enthalpies and entropies of real fluids. Departure functions based on the PR-EOS calculate the deviation of the real fluids from the properties of an ideal gas with the same critical temperature, critical pressure and acentric factor. Expressions (B-6) to (B-16) calculate the molar enthalpies and entropies, $h \left[\frac{J}{mol} \right]$ and $s \left[\frac{J}{mol K} \right]$ of real fluids with the reference temperature and pressure, T_0 and P_0 , based on the ideal gas properties and the departure functions. The ideal gas properties are expressed as a function of the molar heat capacity at constant pressure, which is calculated using polynomial empirical correlations (temperature-dependent) as presented by Poling et al. (2001). The compressibility factor (Z) used in the calculations is defined as the real roots of the cubical equation (B-12), with the maximum value corresponding to the gas state and the minimum value corresponding to the liquid state.

$$h = h_{IG} + h_{dep} \quad (B-6)$$

$$h_{IG} = \int_{T_0}^T cp_0(T) dT \quad (B-7)$$

$$h_{dep} = RT(Z - 1) + \frac{T \left(\frac{da}{dT} \right) - a}{2\sqrt{2}b} \ln \left(\frac{Z + (1 + \sqrt{2})B}{Z + (1 - \sqrt{2})B} \right) \quad (B-8)$$

$$s = s_{IG} + s_{dep} \quad (B-9)$$

$$s_{IG} = \int_{T_0}^T cp_0(T) \frac{dT}{T} - R \ln \left(\frac{P}{P_0} \right) \quad (B-10)$$

$$s_{dep} = R \ln(Z - B) + \frac{\left(\frac{da}{dT} \right)}{2\sqrt{2}b} \ln \left(\frac{Z + (1 + \sqrt{2})B}{Z + (1 - \sqrt{2})B} \right) \quad (B-11)$$

$$0 = Z^3 + (B - 1)Z^2 + (A - 3B^2 - 2B)Z + (B^3 + B^2 - AB) \quad (B-12)$$

$$A = \frac{aP}{(RT)^2} \quad (B-13)$$

$$B = \frac{bP}{RT} \quad (B-14)$$

$$\frac{da}{dT} = -0,45724 \frac{\kappa R^2 T_c}{P_c} \left(\frac{T}{T_c} \right)^{-0,5} \left[1 + \kappa \left(1 - \left(\frac{T}{T_c} \right)^{0,5} \right) \right] \quad (B-15)$$

$$\frac{cp_0(T)}{R} = a_0 + a_1T + a_2T^2 + a_3T^3 + a_4T^4 \quad (B-16)$$

The vapor pressure of the working fluids is calculated with the ‘‘Wagner Equation’’(Wagner 1973) as presented in equations (B-17) and (B-18). The latent heat of evaporation/condensation for a given fluid is calculated using the empirical equations (B-19) to (B-21), first proposed by Watson (1943) and Chen (1965). In these equations T_b represent the normal boiling point of the fluid.

$$\ln(P) = T_c \frac{w_1\tau + w_2\tau^{1.5} + w_3\tau^3 + w_4\tau^5}{T} \quad (B-17)$$

$$\tau = 1 - \frac{T}{T_c} \quad (B-18)$$

$$\lambda = \lambda_b \left(\frac{T_c - T}{T_c - T_b} \right)^{0.38} \quad (B-19)$$

$$\lambda_b = RT_b \frac{3.978 T_{br} - 3.958 + 1.555 \ln P_c}{1.07 - T_{br}} \quad (B-20)$$

$$T_{br} = \frac{T_b}{T_c} \quad (B-21)$$

The parameters used for the calculation of the thermophysical properties of the working fluids evaluated in Chapter 5 are presented in Table B-1. Coefficient units are arbitrary, in such a manner that the results of the calculations are in SI units.

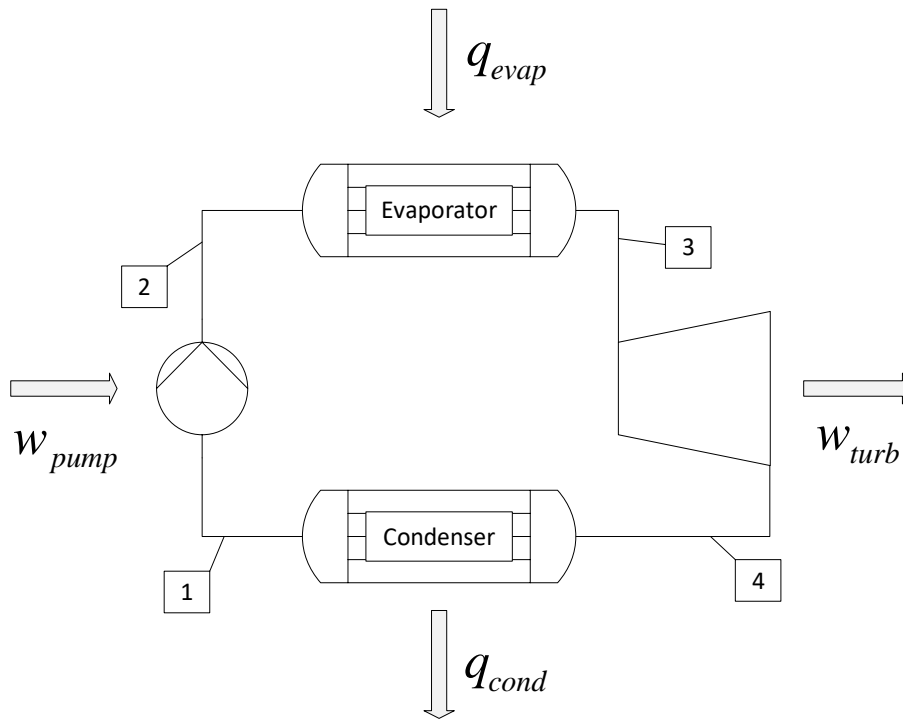
Table B-1. Parameters for the calculation of thermophysical properties of selected working fluids

Name	n-butane	n-pentane	n-hexane	R113	R123	R-600a
M [kg/mol]	58.123	72.15	87.177	187.375	152.931	58.123
T_b [K]	272.66	309.22	341.88	320.74	300.81	261.34
T_c [K]	425.12	469.7	507.6	487.4	456.9	407.85
P_c [Pa]	3796000	3770000	3025000	3378000	3674000	3640000
ω	0.2	0.252	0.3	0.249	0.282	0.186
a_0	5.547	7.554	8.831	2.133	2.996	3.351
a_1	5.536	-0.368	-0.166	66.238	39.49	17.883
a_2	8.057	11.846	14.302	-8.916	-2.743	5.477
a_3	-10.571	-14.939	-18.314	6.14	-0.122	-8.099
a_4	4.134	5.753	7.124	-1.683	0.572	3.243
w_1	-7.01763	-7.30698	-7.53998	-7.2	-7.437	-6.89609
w_2	1.6777	1.75845	1.83759	1.497	1.796	1.53762
w_3	-1.9739	-2.1629	-2.5438	-2.031	-2.505	-1.72907
w_4	-2.172	-2.913	-3.163	-3.249	-3.282	-2.56103

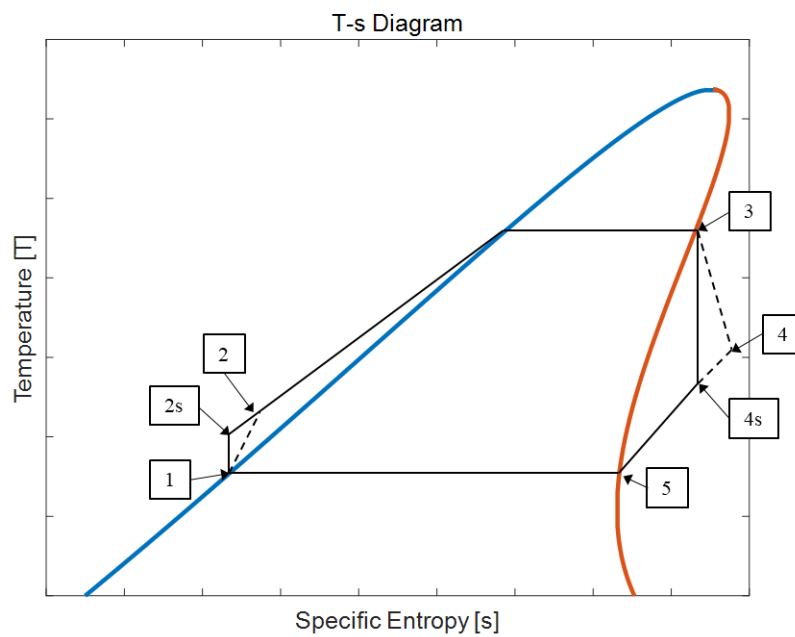
Source: Own table

Using the thermophysical properties as defined in this appendix and energy balances in each of the ORC components, it is possible to calculate the specific work of turbines (w_{turb}) and pumps (w_{pump}) as used in the ORC models (HEN-ORC, HEN-WHR, MP-ORC, MP-WHR, MP-ST-ORC and MP-ST-WHR). For illustrative purposes the calculation will be performed for Case Study 1 and HEN-ORC (Working fluid R113), but similar procedures are used for all the ORC models and Case Studies. Figure B-1 presents the basic ORC cycle as used in this work, and the temperature-enthalpy diagram for a generic dry fluid, as well as an enumeration of the different positions in the cycle. Following are a calculation of the different parameters and properties of the working fluid in each of the positions in the cycle.

- Position 1
 - $T_1 = 25^\circ\text{C}$ (given)
 - $P_1 = 44.18$ kPa (Calculated using Equation B-17)
 - $h_1 = -2.7996\text{E}+04$ [J/mol] (Calculated using Equation B-6)
 - $s_1 = -93.9813$ [J/mol K] (Calculated using Equation B-9)



a) Schematic representation of a basic ORC Cycle



b) T-s Diagram of a basic ORC cycle

Figure B-1. Basic ORC cycle.

Source: Own diagrams based on Hung (2001).

- Position 2s
 - $T_{2s} = 25.06^{\circ}\text{C}$ (Calculated from Equation B-9 using s_{2s} and pressure P_{2s})
 - $P_{2s} = 304.47 \text{ kPa}$ (Calculated using Equation B-17 with the evaporation temperature $T_3 = 85.76^{\circ}\text{C}$, which is given)
 - $h_{2s} = -2.7968\text{E}+04 \text{ [J/mol]}$ (Calculated using Equation B-6)

- $s_{2s} = s_1 = -93.9813$ [J/mol K] (Isentropic compression)
- Position 3
 - $T_3 = 85.76^\circ\text{C}$ (given)
 - $P_3 = 304.47$ kPa (Calculated using Equation B-17)
 - $h_3 = 7.4630\text{E}+03$ [J/mol] (Calculated using Equation B-6)
 - $s_3 = 23.6586$ [J/mol K] (Calculated using Equation B-9)
- Position 4s
 - $T_{4s} = 43.45^\circ\text{C}$ (Calculated from Equation B-9 using s_{4s} and pressure P_{4s})
 - $P_{4s} = P_1 = 44.18$ kPa (Condensation pressure)
 - $h_2 = -2.7968\text{E}+04$ [J/mol] (Calculated using Equation B-6)
 - $s_{4s} = s_3 = 23.6586$ [J/mol K] (Isentropic expansion)
- Position 5
 - $T_5 = T_1 = 25^\circ\text{C}$ (given)
 - $P_5 = P_1 = 44.18$ kPa (Calculated using Equation B-17)
 - $h_5 = h_1 = -2.7996\text{E}+04$ [J/mol] (Same temperature and pressure)
 - $s_5 = 15.7846$ [J/mol K] (calculated using Equation B-9)

For positions 2 and 4 the values and definitions of isentropic efficiencies for turbines and pumps are necessary. Equations B-22 and B-23 present the definitions for the isentropic efficiencies.

$$\eta_{pump} = \frac{h_{2s} - h_1}{h_2 - h_1} \quad (B-22)$$

$$\eta_{turb} = \frac{h_4 - h_3}{h_{4s} - h_3} \quad (B-23)$$

Using the definitions and the values presented in Table 5-2 for the isentropic efficiencies of turbines and pumps in Case Study 1 (0.8 and 0.65 respectively) it is possible to calculate h_2 and h_4 . With these enthalpies and knowing the evaporation and condensation pressures, it is possible to calculate the rest of the working fluid properties.

- Position 2
 - $T_2 = 25.15^\circ\text{C}$ (Calculated from Equation B-6)
 - $P_2 = P_{2s} = 304.47$ kPa
 - $h_2 = -2.7954\text{E}+04$ [J/mol] (Calculated from Equation B-22)

- Position 4
 - $T_2 = 51.18^\circ\text{C}$ (Calculated from Equation B-6)
 - $P_4 = P_{4s} = 44.18 \text{ kPa}$
 - $h_4 = 3.3231\text{E}+03 \text{ [J/mol]}$ (Calculated from Equation B-22)

With the enthalpies in each point of the cycle, the specific work of turbines (w_{turb}) and pumps (w_{pump}) are calculated using equations B-24 and B-25.

$$w_{pump} = h_2 - h_1 \quad (B-24)$$

$$w_{turb} = h_4 - h_3 \quad (B-25)$$

For Case Study 1 and HEN-ORC the specific work of turbines (w_{turb}) and pumps (w_{pump}) are:

- $w_{pump} = -2.7954\text{E}+04 - (-2.7996\text{E}+04) \text{ [J/mol]} = 41.9544 \text{ [J/mol]} = 0.2239 \text{ [kJ/kg]}$
- $w_{turb} = 3.3231\text{E}+03 - 7.4630\text{E}+03 \text{ [J/mol]} = -4.1399\text{E}+03 \text{ [J/mol]} = 22.0942 \text{ [kJ/kg]}$

Appendix C Explicit presentation of Mathematical Models

C.1 SYNHEAT

- Sets

$$HP = \{i: i \text{ is a hot process stream}\}$$

$$CP = \{j: j \text{ is a cold process stream}\}$$

$$ST = \{k: k \text{ is a stage of the superstructure, } k = 1, \dots, NOK\}$$

- Equations

$$\sum_{j \in CP} \sum_{k \in ST} q_{i,j,k} + q_i^{cu} = F_i(T_i^{in} - T_i^{out}), \quad i \in HP \quad (C-1)$$

$$\sum_{i \in HP} \sum_{k \in ST} q_{i,j,k} + q_j^{hu} = F_j(T_j^{out} - T_j^{in}), \quad j \in CP \quad (C-2)$$

$$\sum_{j \in CP} q_{i,j,k} = F_i(t_{i,k} - t_{i,k+1}), \quad i \in HP, k \in ST \quad (C-3)$$

$$\sum_{i \in HP} q_{i,j,k} = F_j(t_{j,k} - t_{j,k+1}), \quad j \in CP, k \in ST \quad (C-4)$$

$$q_i^{cu} = F_i(t_{i,NOK+1} - T_i^{out}), \quad i \in HP \quad (C-5)$$

$$q_j^{hu} = F_j(T_j^{out} - t_{j,1}), \quad j \in CP \quad (C-6)$$

$$T_i^{in} = t_{i,1}, \quad i \in HP \quad (C-7)$$

$$T_j^{in} = t_{j,NOK+1}, \quad j \in CP \quad (C-8)$$

$$t_{i,k} \geq t_{i,k+1}, \quad i \in HP, k \in ST \quad (C-9)$$

$$t_{j,k} \geq t_{j,k+1}, \quad j \in CP, k \in ST \quad (C-10)$$

$$T_i^{out} \leq t_{i,NOK+1}, \quad i \in HP \quad (C-11)$$

$$T_j^{out} \geq t_{j,1}, \quad j \in CP \quad (C-12)$$

$$q_{i,j,k} - \Omega z_{i,j,k} \leq 0, \quad i \in HP, j \in CP, k \in ST \quad (C-13)$$

$$q_i^{cu} - \Omega z_i^{cu} \leq 0, \quad i \in HP \quad (C-14)$$

$$q_j^{hu} - \Omega z_j^{hu} \leq 0, \quad j \in CP \quad (C-15)$$

$$\Delta T_{min} \leq dt1_{i,j,k} \leq t_{i,k} - t_{j,k} + \Gamma(1 - z_{i,j,k}), \quad i \in HP, j \in CP, k \in ST \quad (C-16)$$

$$\Delta T_{min} \leq dt2_{i,j,k} \leq t_{i,k+1} - t_{j,k+1} + \Gamma(1 - z_{i,j,k}), \quad i \in HP, j \in CP, k \in ST \quad (C-17)$$

$$\Delta T_{min} \leq dt1_i^{cu} \leq t_{i,NOK+1} - T_{cu}^{out} + \Gamma(1 - z_i^{cu}), \quad i \in HP \quad (C-18)$$

$$\Delta T_{min} \leq dt2_i^{cu} \leq T_i^{out} - T_{cu}^{in} + \Gamma(1 - z_i^{cu}), \quad i \in HP \quad (C-19)$$

$$\Delta T_{min} \leq dt1_j^{hu} \leq T_{hu}^{in} - T_j^{out} + \Gamma(1 - z_j^{hu}), \quad j \in CP \quad (C-20)$$

$$\Delta T_{min} \leq dt2_j^{hu} \leq T_{hu}^{out} - t_{j,1} + \Gamma(1 - z_j^{hu}), \quad j \in CP \quad (C-21)$$

$\min TAC$

$$= \left\{ \begin{array}{l} H_y \sum_{i \in HP} c_{cu} q_i^{cu} + H_y \sum_{j \in CP} c_{hu} q_j^{hu} \\ + AF \left(c_{fix}^{HEN} \left(\sum_{i \in HP} \sum_{j \in CP} \sum_{k \in ST} z_{i,j,k} + \sum_{i \in HP} z_i^{cu} + \sum_{j \in CP} z_j^{hu} \right) \right) \\ + AF \left(c_{var}^{HEN} \left(\sum_{i \in HP} \sum_{j \in CP} \sum_{k \in ST} \left(\frac{q_{i,j,k}}{U_{i,j,k} LMTD_{i,j,k}} \right)^\beta + \sum_{i \in HP} \left(\frac{q_i^{cu}}{U_i^{cu} LMTD_i^{cu}} \right)^\beta \right) \right. \\ \left. + \sum_{j \in CP} \left(\frac{q_j^{hu}}{U_j^{hu} LMTD_j^{hu}} \right)^\beta \right) \end{array} \right\} \quad (C-22)$$

C.2 HEN-ORC

- Sets

$$HP = \{i: i \text{ is a hot process stream}\}$$

$$CP = \{j: j \text{ is a cold process stream}\}$$

$$ST = \{k: k \text{ is a stage of the superstructure, } k = 1, \dots, NOK\}$$

- Equations

$$\sum_{j \in CP} \sum_{k \in ST} q_{i,j,k} + q_i^{evap} + q_i^{cu} = F_i(T_i^{in} - T_i^{out}), \quad i \in HP \quad (C-23)$$

$$\sum_{i \in HP} \sum_{k \in ST} q_{i,j,k} + q_j^{cond} + q_j^{hu} = F_j(T_j^{out} - T_j^{in}), \quad j \in CP \quad (C-24)$$

$$\sum_{j \in CP} q_{i,j,k} = F_i(t_{i,k} - t_{i,k+1}), \quad i \in HP, k \in ST \quad (C-25)$$

$$\sum_{i \in HP} q_{i,j,k} = F_j(t_{j,k} - t_{j,k+1}), \quad j \in CP, k \in ST \quad (C-26)$$

$$q_i^{cu} = F_i(t_i^{orc} - T_i^{out}), \quad i \in HP \quad (C-27)$$

$$q_j^{hu} = F_j(T_j^{out} - t_{j,1}), \quad j \in CP \quad (C-28)$$

$$q_i^{evap} = F_i(t_{i,NOK+1} - t_i^{orc}), \quad i \in HP \quad (C-29)$$

$$q_j^{cond} = F_j(t_{j,NOK+1} - T_j^{in}), \quad j \in CP \quad (C-30)$$

$$q_i^{evap} = \dot{m}_w r_{wi} \left(cp_{w(l)}(T_{evap}^{out} - T_{evap}^{in}) + \lambda_{evap} \right), \quad i \in HP \quad (C-31)$$

$$q_j^{cond} = \dot{m}_w r_{wj} \left(cp_{w(g)}(T_{cond}^{in} - T_{cond}^{out}) + \lambda_{cond} \right), \quad j \in CP \quad (C-32)$$

$$q^{acu} = \dot{m}_w \left(1 - \sum_{j \in CP} r_{wj} \right) \left(cp_{w(g)}(T_{cond}^{in} - T_{cond}^{out}) + \lambda_{cond} \right) \quad (C-33)$$

$$\sum_{i \in HP} r_{wi} = 1 \quad (C-34)$$

$$\sum_{j \in CP} r_{wj} \leq 1 \quad (C-35)$$

$$T_i^{in} = t_{i,1}, \quad i \in HP \quad (C-36)$$

$$t_{i,NOK+1} \geq t_i^{orc} \geq T_i^{out} \quad (C-37)$$

$$T_j^{out} \geq t_{j,1} \quad (C-38)$$

$$t_{j,NOK+1} \geq T_j^{in}, \quad j \in CP \quad (C-39)$$

$$t_{i,k} \geq t_{i,k+1}, \quad i \in HP, k \in ST \quad (C-40)$$

$$t_{j,k} \geq t_{j,k+1}, \quad j \in CP, k \in ST \quad (C-41)$$

$$q_{i,j,k} - \Omega z_{i,j,k} \leq 0, \quad i \in HP, j \in CP, k \in ST \quad (C-42)$$

$$q_i^{cu} - \Omega z_i^{cu} \leq 0, \quad i \in HP \quad (C-43)$$

$$q_j^{hu} - \Omega z_j^{hu} \leq 0, \quad j \in CP \quad (C-44)$$

$$q_i^{evap} - \Omega z_i^{evap} \leq 0, \quad i \in HP \quad (C-45)$$

$$q_j^{cond} - \Omega z_j^{cond} \leq 0, \quad j \in CP \quad (C-46)$$

$$q^{acu} - \Omega z^{acu} \leq 0 \quad (C-47)$$

$$\Delta T_{min} \leq dt1_{i,j,k} \leq t_{i,k} - t_{j,k} + \Gamma(1 - z_{i,j,k}), \quad i \in HP, j \in CP, k \in ST \quad (C-48)$$

$$\Delta T_{min} \leq dt2_{i,j,k} \leq t_{i,k+1} - t_{j,k+1} + \Gamma(1 - z_{i,j,k}), \quad i \in HP, j \in CP, k \in ST \quad (C-49)$$

$$\Delta T_{min} \leq dt1_i^{cu} \leq t_i^{orc} - T_{cu}^{out} + \Gamma(1 - z_i^{cu}), \quad i \in HP \quad (C-50)$$

$$\Delta T_{min} \leq dt2_i^{cu} \leq T_i^{out} - T_{cu}^{in} + \Gamma(1 - z_i^{cu}), \quad i \in HP \quad (C-51)$$

$$\Delta T_{min} \leq dt1_j^{hu} \leq T_{hu}^{in} - T_j^{out} + \Gamma(1 - z_j^{hu}), \quad j \in CP \quad (C-52)$$

$$\Delta T_{min} \leq dt2_j^{hu} \leq T_{hu}^{out} - t_{j,1} + \Gamma(1 - z_j^{hu}), \quad j \in CP \quad (C-53)$$

$$\Delta T_{min} \leq dt1_i^{evap} \leq t_{i,NOK+1} - T_{evap}^{out} + \Gamma(1 - z_i^{evap}), \quad i \in HP \quad (C-54)$$

$$\Delta T_{min} \leq dt2_i^{evap} \leq t_i^{orc} - T_{evap}^{in} + \Gamma(1 - z_i^{evap}), \quad i \in HP \quad (C-55)$$

$$\Delta T_{min} \leq dt1_j^{cond} \leq T_{cond}^{in} - t_{j,NOK+1} + \Gamma(1 - z_j^{cond}), \quad j \in CP \quad (C-56)$$

$$\Delta T_{min} \leq dt2_j^{cond} \leq T_{cond}^{out} - T_j^{in} + \Gamma(1 - z_j^{cond}), \quad j \in CP \quad (C-57)$$

$$\Delta T_{min} \leq dt1^{acu} \leq T_{cond}^{in} - T_{cu}^{out} + \Gamma(1 - z^{acu}) \quad (C-58)$$

$$\Delta T_{min} \leq dt2^{acu} \leq T_{cond}^{out} - T_{cu}^{in} + \Gamma(1 - z^{acu}) \quad (C-59)$$

$$\Delta T_{min} \leq dt3_i^{evap} \leq \left(t_i^{orc} + \frac{\dot{m}_w r_{wi} c_{p_{w(l)}} (T_{evap}^{out} - T_{evap}^{in})}{F_i} \right) - T_{evap}^{out} + \Gamma(1 - z_i^{evap}) \quad (C-60)$$

$$, \quad i \in HP$$

$$\begin{aligned} \Delta T_{min} &\leq dt 3_j^{cond} \\ &\leq T_{cond}^{out} - \left(t_{j,NOK+1} - \frac{\dot{m}_w r_{wj} cp_{w(\theta)} (T_{cond}^{in} - T_{cond}^{out})}{F_j} \right) \\ &\quad + \Gamma(1 - z_j^{cond}) \end{aligned} \quad (C-61)$$

$$, \quad j \in CP$$

$$W_{pump} = \dot{m}_w * W_{pump} \quad (C-62)$$

$$W_{turb} = \dot{m}_w * W_{turb} \quad (C-63)$$

$$\begin{aligned} &min TAC \\ &\left(\begin{aligned} &-H_y e_{price} W_{turb} + H_y e_{cost} W_{pump}) \\ &+ H_y \sum_{i \in HHP} c_{cu} q_i^{cu} + H_y \sum_{j \in CP} c_{hu} q_j^{hu} + H_y c_{cu} q^{acu} \\ &+ AF \left(c_{fix}^{HEN} \left(\sum_{i \in HHP} \sum_{j \in CP} \sum_{k \in ST} z_{i,j,k} + \sum_{i \in HHP} z_i^{cu} + \sum_{j \in CP} z_j^{hu} \right) \right. \\ &\quad \left. + \sum_{i \in HHP} z_i^{evap} + \sum_{j \in CP} z_j^{cond} + z^{acu} \right) \end{aligned} \right) \\ = &\left(\begin{aligned} &+ AF \left(c_{var}^{HEN} \left(\sum_{i \in HHP} \sum_{j \in CP} \sum_{k \in ST} \left(\frac{q_{i,j,k}}{U_{i,j,k} LMTD_{i,j,k}} \right)^\beta + \sum_{i \in HHP} \left(\frac{q_i^{cu}}{U_i^{cu} LMTD_i^{cu}} \right)^\beta \right. \right. \\ &\quad \left. \left. + \sum_{j \in CP} \left(\frac{q_j^{hu}}{U_j^{hu} LMTD_j^{hu}} \right)^\beta + \sum_{i \in HHP} \left(\frac{q_i^{evap}}{U_i^{evap} LMTD_i^{evap}} \right)^\beta \right. \right. \\ &\quad \left. \left. + \sum_{j \in CP} \left(\frac{q_j^{cond}}{U_j^{cond} LMTD_j^{cond}} \right)^\beta + \left(\frac{q^{acu}}{U^{acu} LMTD^{acu}} \right)^\beta \right) \right) \\ &+ AF (c_{fix}^{turb} + c_{fix}^{pump}) + AF (c_{var}^{turb} W_{turb}^{\beta^{turb}} + c_{var}^{pump} W_{pump}^{\beta^{pump}}) \end{aligned} \right) \end{aligned} \quad (C-64)$$

C.3 HEN-ABC

- Sets

$$HP = \{i: i \text{ is a hot process stream}\}$$

$$CP = \{j: j \text{ is a cold process stream}\}$$

$$ST = \{k: k \text{ is a stage of the superstructure, } k = 1, \dots, NOK\}$$

- Equations

$$\sum_{j \in CP} \sum_{k \in ST} q_{i,j,k} + q_i^{abcg} + q_i^{cu} + q_i^{abce} = F_i(T_i^{in} - T_i^{out}), \quad i \in HP \quad (C-65)$$

$$\sum_{i \in HP} \sum_{k \in ST} q_{i,j,k} + q_j^{hu} = F_j(T_j^{out} - T_j^{in}), \quad j \in CP \quad (C-66)$$

$$\sum_{j \in CP} q_{i,j,k} = F_i(t_{i,k} - t_{i,k+1}), \quad i \in HP, k \in ST \quad (C-67)$$

$$\sum_{i \in HP} q_{i,j,k} = F_j(t_{j,k} - t_{j,k+1}), \quad j \in CP, k \in ST \quad (C-68)$$

$$q_i^{cu} = F_i(t_i^{abcg} - t_i^{abce}), \quad i \in HP \quad (C-69)$$

$$q_j^{hu} = F_j(T_j^{out} - t_{j,1}), \quad j \in CP \quad (C-70)$$

$$q_i^{abcg} = F_i(t_{i,NOK+1} - t_i^{abcg}), \quad i \in HP \quad (C-71)$$

$$q_i^{abce} = F_i(t_i^{abce} - T_i^{out}), \quad i \in HP \quad (C-72)$$

$$T_i^{in} = t_{i,1}, \quad i \in HP \quad (C-73)$$

$$t_{i,NOK+1} \geq t_i^{abcg} \geq t_i^{abce} \geq T_i^{out}, \quad i \in HP \quad (C-74)$$

$$T_j^{out} \geq t_{j,1}, \quad j \in CP \quad (C-75)$$

$$t_{j,NOK+1} \geq T_j^{in}, \quad j \in CP \quad (C-76)$$

$$t_{i,k} \geq t_{i,k+1}, \quad i \in HP \quad (C-77)$$

$$t_{j,k} \geq t_{j,k+1}, \quad j \in CP \quad (C-78)$$

$$q_{i,j,k} - \Omega z_{i,j,k} \leq 0, \quad i \in HP, j \in CP, k \in ST \quad (C-79)$$

$$q_i^{cu} - \Omega z_i^{cu} \leq 0, \quad i \in HP \quad (C-80)$$

$$q_j^{hu} - \Omega z_j^{hu} \leq 0, \quad j \in CP \quad (C-81)$$

$$q_i^{abcg} - \Omega z_i^{abcg} \leq 0, \quad i \in HP \quad (C-82)$$

$$q_i^{abce} - \Omega z_i^{abce} \leq 0, \quad i \in HP \quad (C-83)$$

$$\Delta T_{min} \leq dt1_{i,j,k} \leq t_{i,k} - t_{j,k} + \Gamma(1 - z_{i,j,k}), \quad i \in HP, j \in CP, k \in ST \quad (C-84)$$

$$\Delta T_{min} \leq dt2_{i,j,k} \leq t_{i,k+1} - t_{j,k+1} + \Gamma(1 - z_{i,j,k}), \quad i \in HP, j \in CP, k \in ST \quad (C-85)$$

$$\Delta T_{min} \leq dt1_i^{cu} \leq t_i^{abcg} - T_{cu}^{out} + \Gamma(1 - z_i^{cu}), \quad i \in HP \quad (C-86)$$

$$\Delta T_{min} \leq dt2_i^{cu} \leq t_i^{abce} - T_{cu}^{in} + \Gamma(1 - z_i^{cu}), \quad i \in HP \quad (C-87)$$

$$\Delta T_{min} \leq dt1_j^{hu} \leq T_{hu}^{in} - T_j^{out} + \Gamma(1 - z_j^{hu}), \quad j \in CP \quad (C-88)$$

$$\Delta T_{min} \leq dt2_j^{hu} \leq T_{hu}^{out} - t_{j,1} + \Gamma(1 - z_j^{hu}), \quad j \in CP \quad (C-89)$$

$$\Delta T_{min} \leq dt1_i^{abcg} \leq t_{i,NOK+1} - t_{gen} + \Gamma(1 - z_i^{abcg}), \quad i \in HP \quad (C-90)$$

$$\Delta T_{min} \leq dt2_i^{abcg} \leq t_i^{abcg} - t_{gen}^{in} + \Gamma(1 - z_i^{abcg}), \quad i \in HP \quad (C-91)$$

$$\Delta T_{min} \leq dt1_i^{abce} \leq t_i^{abce} - T_{ref} + \Gamma(1 - z_i^{abce}), \quad i \in HP \quad (C-92)$$

$$\Delta T_{min} \leq dt2_i^{abce} \leq T_i^{out} - T_{ref} + \Gamma(1 - z_i^{abce}), \quad i \in HP \quad (C-93)$$

$$\Delta T_{min} \leq dt1^{abca} \leq t_{abs}^{in} - T_{cu}^{out} \quad (C-94)$$

$$\Delta T_{min} = dt2^{abca} \quad (C-95)$$

$$\Delta T_{min} \leq dt1^{abcc} \leq T_{gen}^{out} - T_{cu}^{out} \quad (C-96)$$

$$\Delta T_{min} = dt2^{abcc} \quad (C-97)$$

$$COP \sum_{i \in HP} q_i^{abcg} = \sum_{i \in HP} q_i^{abce} \quad (C-98)$$

$$C2G \sum_{i \in HP} q_i^{abcg} = q^{abcc} \quad (C-99)$$

$$\sum_{i \in HP} q_i^{abcg} + \sum_{i \in HP} q_i^{abce} = q^{abcc} + q^{abca} \quad (C-100)$$

$$COP = C_1 e^{C_2 t_{gen}} + C_3 e^{C_4 t_{gen}} \quad (C-101)$$

$$C2G = C_5 COP + C_6 \quad (C-102)$$

$$t_{gen}^{in} = C_7 (t_{gen})^2 + C_8 t_{gen} + C_9 \quad (C-103)$$

$$t_{abs}^{in} = C_{10} t_{gen} + C_{11} \quad (C-104)$$

$$\begin{aligned}
& \min TAC \\
& \left(\begin{aligned}
& H_y \sum_{i \in HP} c_{cu} q_i^{cu} + H_y \sum_{j \in CP} c_{hu} q_j^{hu} + H_y c_{cu} (q^{abcc} + q^{abca}) \\
& + AF \left(c_{fix}^{HEN} \left(\sum_{i \in HP} \sum_{j \in CP} \sum_{k \in ST} z_{i,j,k} + \sum_{i \in HP} z_i^{cu} + \sum_{j \in CP} z_j^{hu} \right) \right. \\
& \quad \left. + \sum_{i \in HP} z_i^{abcg} + \sum_{i \in HP} z_i^{abce} \right)
\end{aligned} \right) \\
= & \left(\begin{aligned}
& + AF \left(c_{var}^{HEN} \left(\sum_{i \in HP} \sum_{j \in CP} \sum_{k \in ST} \left(\frac{q_{i,j,k}}{U_{i,j,k} LMTD_{i,j,k}} \right)^\beta + \sum_{i \in HP} \left(\frac{q_i^{cu}}{U_i^{cu} LMTD_i^{cu}} \right)^\beta \right) \right. \\
& \quad + \sum_{j \in CP} \left(\frac{q_j^{hu}}{U_j^{hu} LMTD_j^{hu}} \right)^\beta + \sum_{i \in HP} \left(\frac{q_i^{abcg}}{U_i^{abcg} LMTD_i^{abcg}} \right)^\beta \\
& \quad + \sum_{i \in HP} \left(\frac{q_i^{abce}}{U_i^{abce} LMTD_i^{abce}} \right)^\beta + \left(\frac{q^{abcc}}{U^{abcc} LMTD^{abcc}} \right)^\beta \\
& \quad \left. + \left(\frac{q^{abca}}{U^{abca} LMTD^{abca}} \right)^\beta \right)
\end{aligned} \right) \quad (C-105)
\end{aligned}$$

C.4 HEN-WHR

- Sets

$$HP = \{i: i \text{ is a hot process stream}\}$$

$$CP = \{j: j \text{ is a cold process stream}\}$$

$$ST = \{k: k \text{ is a stage of the superstructure, } k = 1, \dots, NOK\}$$

- Equations

$$\sum_{j \in CP} \sum_{k \in ST} q_{i,j,k} + q_i^{evap} + q_i^{abcg} + q_i^{cu} + q_i^{abce} = F_i(T_i^{in} - T_i^{out}), \quad i \in HP \quad (C-106)$$

$$\sum_{i \in HP} \sum_{k \in ST} q_{i,j,k} + q_j^{cond} + q_j^{hu} = F_j(T_j^{out} - T_j^{in}), \quad j \in CP \quad (C-107)$$

$$\sum_{j \in CP} q_{i,j,k} = F_i(t_{i,k} - t_{i,k+1}), \quad i \in HP, k \in ST \quad (C-108)$$

$$\sum_{i \in HP} q_{i,j,k} = F_j(t_{j,k} - t_{j,k+1}), \quad j \in CP, k \in ST \quad (C-109)$$

$$q_i^{cu} = F_i(t_i^{abcg} - t_i^{abce}), \quad i \in HP \quad (C-110)$$

$$q_j^{hu} = F_j(T_j^{out} - t_{j,1}), \quad j \in CP \quad (C-111)$$

$$q_i^{evap} = F_i(t_{i,NOK+1} - t_i^{orc}), \quad i \in HP \quad (C-112)$$

$$q_j^{cond} = F_j(t_{j,NOK+1} - T_j^{in}), \quad j \in CP \quad (C-113)$$

$$q_i^{evap} = \dot{m}_w r_{w_i} \left(cp_{w(l)}(T_{evap}^{out} - T_{evap}^{in}) + \lambda_{evap} \right), \quad i \in HP \quad (C-114)$$

$$q_j^{cond} = \dot{m}_w r_{w_j} \left(cp_{w(g)}(T_{cond}^{in} - T_{cond}^{out}) + \lambda_{cond} \right), \quad j \in CP \quad (C-115)$$

$$q^{acu} = \dot{m}_w \left(1 - \sum_{j \in CP} r_{w_j} \right) \left(cp_{w(g)}(T_{cond}^{in} - T_{cond}^{out}) + \lambda_{cond} \right) \quad (C-116)$$

$$q_i^{abcg} = F_i(t_i^{orc} - t_i^{abcg}), \quad i \in HP \quad (C-117)$$

$$q_i^{abce} = F_i(t_i^{abce} - T_i^{out}), \quad i \in HP \quad (C-118)$$

$$\sum_{i \in HP} r_{w_i} = 1 \quad (C-119)$$

$$\sum_{j \in CP} r_{wj} \leq 1 \quad (C-120)$$

$$T_i^{in} = t_{i,1}, \quad i \in HP \quad (C-121)$$

$$t_{i,NOK+1} \geq t_i^{orc} \geq t_i^{abcg} \geq t_i^{abce} \geq T_i^{out}, \quad i \in HP \quad (C-122)$$

$$T_j^{out} \geq t_{j,1}, \quad j \in CP \quad (C-123)$$

$$t_{j,NOK+1} \geq T_j^{in}, \quad j \in CP \quad (C-124)$$

$$t_{i,k} \geq t_{i,k+1}, \quad i \in HP, k \in ST \quad (C-125)$$

$$t_{j,k} \geq t_{j,k+1}, \quad j \in CP, k \in ST \quad (C-126)$$

$$q_{i,j,k} - \Omega z_{i,j,k} \leq 0, \quad i \in HP, j \in CP, k \in ST \quad (C-127)$$

$$q_i^{cu} - \Omega z_i^{cu} \leq 0, \quad i \in HP \quad (C-128)$$

$$q_j^{hu} - \Omega z_j^{hu} \leq 0, \quad j \in CP \quad (C-129)$$

$$q_i^{evap} - \Omega z_i^{evap} \leq 0, \quad i \in HP \quad (C-130)$$

$$q_j^{cond} - \Omega z_j^{cond} \leq 0, \quad j \in CP \quad (C-131)$$

$$q^{acu} - \Omega z^{acu} \leq 0 \quad (C-132)$$

$$q_i^{abcg} - \Omega z_i^{abcg} \leq 0, \quad i \in HP \quad (C-133)$$

$$q_i^{abce} - \Omega z_i^{abce} \leq 0, \quad i \in HP \quad (C-134)$$

$$\Delta T_{min} \leq dt1_{i,j,k} \leq t_{i,k} - t_{j,k} + \Gamma(1 - z_{i,j,k}), \quad i \in HP, j \in CP, k \in ST \quad (C-135)$$

$$\Delta T_{min} \leq dt2_{i,j,k} \leq t_{i,k+1} - t_{j,k+1} + \Gamma(1 - z_{i,j,k}), \quad i \in HP, j \in CP, k \in ST \quad (C-136)$$

$$\Delta T_{min} \leq dt1_i^{cu} \leq t_i^{abcg} - T_{cu}^{out} + \Gamma(1 - z_i^{cu}), \quad i \in HP \quad (C-137)$$

$$\Delta T_{min} \leq dt2_i^{cu} \leq t_i^{abce} - T_{cu}^{in} + \Gamma(1 - z_i^{cu}), \quad i \in HP \quad (C-138)$$

$$\Delta T_{min} \leq dt1_j^{hu} \leq T_{hu}^{in} - T_j^{out} + \Gamma(1 - z_j^{hu}), \quad j \in CP \quad (C-139)$$

$$\Delta T_{min} \leq dt2_j^{hu} \leq T_{hu}^{out} - t_{j,1,p} + \Gamma(1 - z_j^{hu}), \quad j \in CP \quad (C-140)$$

$$\Delta T_{min} \leq dt1_i^{evap} \leq t_{i,NOK+1} - T_{evap}^{out} + \Gamma(1 - z_i^{evap}), \quad i \in HP \quad (C-141)$$

$$\Delta T_{min} \leq dt2_i^{evap} \leq t_i^{orc} - T_{evap}^{in} + \Gamma(1 - z_i^{evap}), \quad i \in HP \quad (C-142)$$

$$\Delta T_{min} \leq dt1_j^{cond} \leq T_{cond}^{in} - t_{j,NOK+1} + \Gamma(1 - z_j^{cond}), \quad j \in CP \quad (C-143)$$

$$\Delta T_{min} \leq dt2_j^{cond} \leq T_{cond}^{out} - T_j^{in} + \Gamma(1 - z_j^{cond}), \quad j \in CP \quad (C-144)$$

$$\Delta T_{min} \leq dt1^{acu} \leq T_{cond}^{in} - T_{cu}^{out} + \Gamma(1 - z^{acu}) \quad (C-145)$$

$$\Delta T_{min} \leq dt2^{acu} \leq T_{cond}^{out} - T_{cu}^{in} + \Gamma(1 - z^{acu}) \quad (C-146)$$

$$\Delta T_{min} \leq dt1_i^{abcg} \leq t_i^{orc} - t_{gen} + \Gamma(1 - z_i^{abcg}), \quad i \in HP \quad (C-147)$$

$$\Delta T_{min} \leq dt2_i^{abcg} \leq t_i^{abcg} - t_{gen}^{in} + \Gamma(1 - z_i^{abcg}), \quad i \in HP \quad (C-148)$$

$$\Delta T_{min} \leq dt1_i^{abce} \leq t_i^{abce} - T_{ref} + \Gamma(1 - z_i^{abce}), \quad i \in HP \quad (C-149)$$

$$\Delta T_{min} \leq dt2_i^{abce} \leq T_i^{out} - T_{ref} + \Gamma(1 - z_i^{abce}), \quad i \in HP \quad (C-150)$$

$$\Delta T_{min} \leq dt1^{abca} \leq t_{abs}^{in} - T_{cu}^{out} \quad (C-151)$$

$$\Delta T_{min} = dt2^{abca} \quad (C-152)$$

$$\Delta T_{min} \leq dt1^{abcc} \leq T_{gen}^{out} - T_{cu}^{out} \quad (C-153)$$

$$\Delta T_{min} = dt2^{abcc} \quad (C-154)$$

$$\begin{aligned} \Delta T_{min} &\leq dt3_i^{evap} \\ &\leq \left(t_i^{orc} + \frac{\dot{m}_w r_{wi} cp_{w(l)} (T_{evap}^{out} - T_{evap}^{in})}{F_i} \right) - T_{evap}^{out} \\ &\quad + \Gamma(1 - z_i^{evap}) \end{aligned} \quad (C-155)$$

, $i \in HP$

$$\begin{aligned} \Delta T_{min} &\leq dt3_j^{cond} \\ &\leq T_{cond}^{out} - \left(t_{j,NOK+1} - \frac{\dot{m}_w r_{wj} cp_{w(g)} (T_{cond}^{in} - T_{cond}^{out})}{F_j} \right) \\ &\quad + \Gamma(1 - z_j^{cond}) \end{aligned} \quad (C-156)$$

, $j \in CP$

$$W_{pump} = \dot{m}_w * w_{pump} \quad (C-157)$$

$$W_{turb} = \dot{m}_w * w_{turb} \quad (C-158)$$

$$COP \sum_{i \in HP} q_i^{abcg} = \sum_{i \in HP} q_i^{abce} \quad (C-159)$$

$$C2G \sum_{i \in HP} q_i^{abcg} = q^{abcc} \quad (C-160)$$

$$\sum_{i \in HP} q_i^{abcg} + \sum_{i \in HP} q_i^{abce} = q^{abcc} + q^{abca} \quad (C-161)$$

$$COP = C_1 e^{C_2 t_{gen}} + C_3 e^{C_4 t_{gen}} \quad (C-162)$$

$$C2G = C_5 COP + C_6 \quad (C-163)$$

$$t_{gen}^{in} = C_7 (t_{gen})^2 + C_8 t_{gen} + C_9 \quad (C-164)$$

$$t_{abs}^{in} = C_{10} t_{gen} + C_{11} \quad (C-165)$$

min TAC

$$= \left\{ \begin{array}{l} -H_y e_{price} W_{turb} + H_y e_{cost} W_{pump} \\ + H_y \sum_{i \in HHP} c_{cu} q_i^{cu} + H_y \sum_{j \in ECP} c_{hu} q_j^{hu} + H_y c_{cu} q^{acu} + H_y c_{cu} (q^{abcc} + q^{abca}) \\ + AF \left(c_{fix}^{HEN} \left(\begin{array}{l} \sum_{i \in HHP} \sum_{j \in ECP} \sum_{k \in ST} z_{i,j,k} + \sum_{i \in HHP} z_i^{cu} + \sum_{j \in ECP} z_j^{hu} \\ + \sum_{i \in HHP} z_i^{evap} + \sum_{j \in ECP} z_j^{cond} + z^{acu} \\ + \sum_{i \in HHP} z_i^{abcg} + \sum_{i \in HHP} z_i^{abce} \end{array} \right) \right) \\ + AF \left(c_{var}^{HEN} \left(\begin{array}{l} \sum_{i \in HHP} \sum_{j \in ECP} \sum_{k \in ST} \left(\frac{q_{i,j,k}}{U_{i,j,k} LMTD_{i,j,k}} \right)^\beta + \sum_{i \in HHP} \left(\frac{q_i^{cu}}{U_i^{cu} LMTD_i^{cu}} \right)^\beta \\ + \sum_{j \in ECP} \left(\frac{q_j^{hu}}{U_j^{hu} LMTD_j^{hu}} \right)^\beta + \sum_{i \in HHP} \left(\frac{q_i^{evap}}{U_i^{evap} LMTD_i^{evap}} \right)^\beta \\ + \sum_{j \in ECP} \left(\frac{q_j^{cond}}{U_j^{cond} LMTD_j^{cond}} \right)^\beta + \left(\frac{q^{acu}}{U^{acu} LMTD^{acu}} \right)^\beta \\ + \sum_{i \in HHP} \left(\frac{q_i^{abcg}}{U_i^{abcg} LMTD_i^{abcg}} \right)^\beta + \sum_{i \in HHP} \left(\frac{q_i^{abce}}{U_i^{abce} LMTD_i^{abce}} \right)^\beta \\ + \left(\frac{q^{abcc}}{U^{abcc} LMTD^{abcc}} \right)^\beta + \left(\frac{q^{abca}}{U^{abca} LMTD^{abca}} \right)^\beta \end{array} \right) \right) \\ + AF (c_{fix}^{turb} + c_{fix}^{pump}) + AF (c_{var}^{turb} W_{turb}^{\beta^{turb}} + c_{var}^{pump} W_{pump}^{\beta^{pump}}) \end{array} \right\} \quad (C-166)$$

C.5 MP-ORC

- Sets

$$HP = \{i: i \text{ is a hot process stream}\}$$

$$CP = \{j: j \text{ is a cold process stream}\}$$

$$ST = \{k: k \text{ is a stage of the superstructure, } k = 1, \dots, NOK\}$$

$$P = \{p: p \text{ is a period of operation of the system, } p = 1, \dots, NOP\}$$

- Equations

$$\sum_{j \in CP} \sum_{k \in ST} q_{i,j,k,p} + q_{i,p}^{evap} + q_{i,p}^{cu} = F_{i,p}(T_{i,p}^{in} - T_{i,p}^{out}), \quad i \in HP, p \in P \quad (C-167)$$

$$\sum_{i \in HP} \sum_{k \in ST} q_{i,j,k,p} + q_{j,p}^{cond} + q_{j,p}^{hu} = F_{j,p}(T_{j,p}^{out} - T_{j,p}^{in}), \quad j \in CP, p \in P \quad (C-168)$$

$$\sum_{j \in CP} q_{i,j,k,p} = F_{i,p}(t_{i,k,p} - t_{i,k+1,p}), \quad i \in HP, k \in ST, p \in P \quad (C-169)$$

$$\sum_{i \in HP} q_{i,j,k,p} = F_{j,p}(t_{j,k,p} - t_{j,k+1,p}), \quad j \in CP, k \in ST, p \in P \quad (C-170)$$

$$q_{i,p}^{cu} = F_{i,p}(t_{i,p}^{orc} - T_{i,p}^{out}), \quad i \in HP, p \in P \quad (C-171)$$

$$q_{j,p}^{hu} = F_{j,p}(T_{j,p}^{out} - t_{j,1}), \quad j \in CP, p \in P \quad (C-172)$$

$$q_{i,p}^{evap} = F_{i,p}(t_{i,NOK+1,p} - t_{i,p}^{orc}), \quad i \in HP, p \in P \quad (C-173)$$

$$q_{j,p}^{cond} = F_{j,p}(t_{j,NOK+1,p} - T_{j,p}^{in}), \quad j \in CP, p \in P \quad (C-174)$$

$$q_{i,p}^{evap} = \dot{m}_{w,p} r_{w,i,p} (cp_{w(l)}(T_{evap}^{out} - T_{evap}^{in}) + \lambda_{evap}), \quad i \in HP, p \in P \quad (C-175)$$

$$q_{j,p}^{cond} = \dot{m}_{w,p} r_{w,j,p} (cp_{w(g)}(T_{cond}^{in} - T_{cond}^{out}) + \lambda_{cond}), \quad j \in CP, p \in P \quad (C-176)$$

$$q_p^{acu} = \dot{m}_{w,p} \left(1 - \sum_{j \in CP} r_{w,j,p} \right) (cp_{w(g)}(T_{cond}^{in} - T_{cond}^{out}) + \lambda_{cond}), p \in P \quad (C-177)$$

$$\sum_{i \in HP} r_{w,i,p} = 1, \quad i \in HP, p \in P \quad (C-178)$$

$$\sum_{j \in CP} r_{w,j,p} \leq 1, \quad j \in CP, p \in P \quad (C-179)$$

$$T_{i,p}^{in} = t_{i,1,p}, \quad i \in HP, p \in P \quad (C-180)$$

$$t_{i,NOK+1,p} \geq t_{i,p}^{orc} \geq T_{i,p}^{out}, \quad i \in HP, p \in P \quad (C-181)$$

$$T_{j,p}^{out} \geq t_{j,1,p}, \quad j \in CP, p \in P \quad (C-182)$$

$$t_{i,k,p} \geq t_{i,k+1,p}, \quad i \in HP, k \in ST, p \in P \quad (C-183)$$

$$t_{j,k,p} \geq t_{j,k+1,p}, \quad j \in CP, k \in ST, p \in P \quad (C-184)$$

$$q_{i,j,k,p} - \Omega z_{i,j,k} \leq 0, \quad i \in HP, j \in CP, k \in ST, p \in P \quad (C-185)$$

$$q_{i,p}^{cu} - \Omega z_i^{cu} \leq 0, \quad i \in HP, p \in P \quad (C-186)$$

$$q_{j,p}^{hu} - \Omega z_j^{hu} \leq 0, \quad j \in CP, p \in P \quad (C-187)$$

$$q_{i,p}^{evap} - \Omega z_i^{evap} \leq 0, \quad i \in HP, p \in P \quad (C-188)$$

$$q_{j,p}^{cond} - \Omega z_j^{cond} \leq 0, \quad j \in CP, p \in P \quad (C-189)$$

$$q_p^{acu} - \Omega z^{acu} \leq 0, p \in P \quad (C-190)$$

$$\Delta T_{min} \leq dt1_{i,j,k,p} \leq t_{i,k,p} - t_{j,k,p} + \Gamma(1 - z_{i,j,k}), \quad i \in HP, j \in CP, k \in ST, p \in P \quad (C-191)$$

$$\Delta T_{min} \leq dt2_{i,j,k,p} \leq t_{i,k+1,p} - t_{j,k+1,p} + \Gamma(1 - z_{i,j,k}), \quad i \in HP, j \in CP, k \in ST, p \in P \quad (C-192)$$

$$\Delta T_{min} \leq dt1_{i,p}^{cu} \leq t_{i,p}^{orc} - T_{cu}^{out} + \Gamma(1 - z_i^{cu}), \quad i \in HP, p \in P \quad (C-193)$$

$$\Delta T_{min} \leq dt2_{i,p}^{cu} \leq T_{i,p}^{out} - T_{cu}^{in} + \Gamma(1 - z_i^{cu}), \quad i \in HP, p \in P \quad (C-194)$$

$$\Delta T_{min} \leq dt1_{j,p}^{hu} \leq T_{hu}^{in} - T_{j,p}^{out} + \Gamma(1 - z_j^{hu}), \quad j \in CP, p \in P \quad (C-195)$$

$$\Delta T_{min} \leq dt2_{j,p}^{hu} \leq T_{hu}^{out} - t_{j,1} + \Gamma(1 - z_j^{hu}), \quad j \in CP, p \in P \quad (C-196)$$

$$\Delta T_{min} \leq dt1_{i,p}^{evap} \leq t_{i,NOK+1,p} - T_{evap}^{out} + \Gamma(1 - z_i^{evap}), \quad i \in HP, p \in P \quad (C-197)$$

$$\Delta T_{min} \leq dt2_{i,p}^{evap} \leq t_{i,p}^{orc} - T_{evap}^{in} + \Gamma(1 - z_i^{evap}), \quad i \in HP, p \in P \quad (C-198)$$

$$\Delta T_{min} \leq dt1_{j,p}^{cond} \leq T_{cond}^{in} - t_{j,NOK+1,p} + \Gamma(1 - z_j^{cond}), \quad j \in CP, p \in P \quad (C-199)$$

$$\Delta T_{min} \leq dt2_{j,p}^{cond} \leq T_{cond}^{out} - T_{j,p}^{in} + \Gamma(1 - z_j^{cond}), \quad j \in CP, p \in P \quad (C-200)$$

$$\Delta T_{min} \leq dt1^{acu} \leq T_{cond}^{in} - T_{cu}^{out} + \Gamma(1 - z^{acu}) \quad (C-201)$$

$$\Delta T_{min} \leq dt2^{acu} \leq T_{cond}^{out} - T_{cu}^{in} + \Gamma(1 - z^{acu}) \quad (C-202)$$

$$\begin{aligned} \Delta T_{min} \leq dt3_{i,p}^{evap} & \leq \left(t_{i,p}^{orc} + \frac{\dot{m}_{wp} r_{w,i,p} c_{p,w(t)} (T_{evap}^{out} - T_{evap}^{in})}{F_{i,p}} \right) - T_{evap}^{out} \\ & + \Gamma(1 - z_i^{evap}), \quad i \in HP, p \in P \end{aligned} \quad (C-203)$$

$$\begin{aligned} \Delta T_{min} &\leq dt3_{j,p}^{cond} \\ &\leq T_{cond}^{out} - \left(t_{j,NOK+1,p} - \frac{\dot{m}_{w_p} r_{w_j,p} c_{p_{w(g)}} (T_{cond}^{in} - T_{cond}^{out})}{F_{j,p}} \right) \\ &\quad + \Gamma(1 - z_j^{cond}), \quad j \in CP, p \in P \end{aligned} \quad (C-204)$$

$$W_{pump_p} = \dot{m}_{w_p} * w_{pump}, p \in P \quad (C-205)$$

$$W_{turb_p} = \dot{m}_{w_p} * w_{turb}, p \in P \quad (C-206)$$

$$A_{i,j,k} \geq \frac{q_{i,j,k,p}}{U_{i,j,k,p} LMTD_{i,j,k,p}}, \quad i \in HP, j \in CP, k \in ST, p \in P \quad (C-207)$$

$$A_i^{cu} \geq \frac{q_{i,p}^{cu}}{U_{i,p}^{cu} LMTD_{i,p}^{cu}}, \quad i \in HP, p \in P \quad (C-208)$$

$$A_j^{hu} \geq \frac{q_{j,p}^{hu}}{U_{j,p}^{hu} LMTD_{j,p}^{hu}}, \quad j \in CP, p \in P \quad (C-209)$$

$$A_i^{evap} \geq \frac{q_{i,p}^{evap}}{U_{i,p}^{evap} LMTD_{i,p}^{evap}}, \quad i \in HP, p \in P \quad (C-210)$$

$$A_j^{cond} \geq \frac{q_{j,p}^{cond}}{U_{j,p}^{cond} LMTD_{j,p}^{cond}}, \quad j \in CP, p \in P \quad (C-211)$$

$$A^{acu} \geq \frac{q_p^{acu}}{U_p^{acu} LMTD_p^{acu}} \quad (C-212)$$

$$W_{pump}^{max} \geq W_{pump_p}, p \in P \quad (C-213)$$

$$W_{turb}^{max} \geq W_{turb_p}, p \in P \quad (C-214)$$

min TAC

$$= \left\{ \begin{aligned} &H_y \sum_{p \in P} \left(\frac{DOP_p}{\sum_{p \in P} DOP_p} \right) \left(-e_{price_p} W_{turb_p} + e_{cost_p} W_{pump_p} \right. \\ &\quad \left. + \sum_{j \in CP} c_{hu_p} q_{j,p}^{hu} + \sum_{i \in HP} c_{cu_p} q_{i,p}^{cu} + c_{cu_p} q_p^{acu} \right) \\ &+ AF c_{fix}^{HEN} \left(\sum_{i \in HP} \sum_{j \in CP} \sum_{k \in ST} z_{i,j,k} + \sum_{i \in HP} z_i^{cu} + \sum_{j \in CP} z_j^{hu} \right. \\ &\quad \left. + \sum_{i \in HP} z_i^{evap} + \sum_{j \in CP} z_j^{cond} + z^{acu} \right) \\ &+ AF c_{var}^{HEN} \left(\sum_{i \in HP} \sum_{j \in CP} \sum_{k \in ST} (A_{i,j,k})^\beta + \sum_{i \in HP} (A_i^{cu})^\beta + \sum_{j \in CP} (A_j^{hu})^\beta \right. \\ &\quad \left. + \sum_{i \in HP} (A_i^{evap})^\beta + \sum_{j \in CP} (A_j^{cond})^\beta + (A^{acu})^\beta \right) \\ &+ AF \left(c_{fix}^{pump} + c_{var}^{pump} (W_{pump}^{max})^{\beta^{pump}} \right) + AF \left(c_{fix}^{turb} + c_{var}^{turb} (W_{turb}^{max})^{\beta^{turb}} \right) \end{aligned} \right\} \quad (C-215)$$

C.6 MP-ABC

- Sets

$$HP = \{i: i \text{ is a hot process stream}\}$$

$$CP = \{j: j \text{ is a cold process stream}\}$$

$$ST = \{k: k \text{ is a stage of the superstructure, } k = 1, \dots, NOK\}$$

$$P = \{p: p \text{ is a period of operation of the system, } p = 1, \dots, NOP\}$$

- Equations

$$\sum_{j \in CP} \sum_{k \in ST} q_{i,j,k,p} + q_{i,p}^{abcg} + q_{i,p}^{cu} + q_{i,p}^{abce} = F_{i,p}(T_{i,p}^{in} - T_{i,p}^{out}), \quad i \in HP, p \in P \quad (C-216)$$

$$\sum_{i \in HP} \sum_{k \in ST} q_{i,j,k,p} + q_{j,p}^{hu} = F_{j,p}(T_{j,p}^{out} - T_{j,p}^{in}), \quad j \in CP, p \in P \quad (C-217)$$

$$\sum_{j \in CP} q_{i,j,k,p} = F_{i,p}(t_{i,k,p} - t_{i,k+1,p}), \quad i \in HP, k \in ST, p \in P \quad (C-218)$$

$$\sum_{i \in HP} q_{i,j,k,p} = F_{j,p}(t_{j,k,p} - t_{j,k+1,p}), \quad j \in CP, k \in ST, p \in P \quad (C-219)$$

$$q_{i,p}^{cu} = F_{i,p}(t_{i,p}^{abcg} - t_{i,p}^{abce}), \quad i \in HP, p \in P \quad (C-220)$$

$$q_{j,p}^{hu} = F_{j,p}(T_{j,p}^{out} - t_{j,1}), \quad j \in CP, p \in P \quad (C-221)$$

$$q_{i,p}^{abcg} = F_{i,p}(t_{i,NOK+1,p} - t_{i,p}^{abcg}), \quad i \in HP, p \in P \quad (C-222)$$

$$q_{i,p}^{abce} = F_{i,p}(t_{i,p}^{abce} - T_{i,p}^{out}), \quad i \in HP, p \in P \quad (C-223)$$

$$T_{i,p}^{in} = t_{i,1}, \quad i \in HP \quad (C-224)$$

$$t_{i,NOK+1,p} \geq t_{i,p}^{abcg} \geq t_{i,p}^{abce} \geq T_{i,p}^{out}, \quad i \in HP, p \in P \quad (C-225)$$

$$T_{j,p}^{out} \geq t_{j,1}, \quad j \in CP, p \in P \quad (C-226)$$

$$t_{j,NOK+1,p} \geq T_{j,p}^{in}, \quad j \in CP, p \in P \quad (C-227)$$

$$t_{i,k,p} \geq t_{i,k+1,p}, \quad i \in HP, p \in P \quad (C-228)$$

$$t_{j,k,p} \geq t_{j,k+1,p}, \quad j \in CP, p \in P \quad (C-229)$$

$$q_{i,j,k,p} - \Omega z_{i,j,k} \leq 0, \quad i \in HP, j \in CP, k \in ST, p \in P \quad (C-230)$$

$$q_{i,p}^{cu} - \Omega z_i^{cu} \leq 0, \quad i \in HP, p \in P \quad (C-231)$$

$$q_{j,p}^{hu} - \Omega z_j^{hu} \leq 0, \quad j \in CP, p \in P \quad (C-232)$$

$$q_{i,p}^{abcg} - \Omega z_i^{abcg} \leq 0, \quad i \in HP, p \in P \quad (C-233)$$

$$q_{i,p}^{abce} - \Omega z_i^{abce} \leq 0, \quad i \in HP, p \in P \quad (C-234)$$

$$\Delta T_{min} \leq dt1_{i,j,k,p} \leq t_{i,k,p} - t_{j,k,p} + \Gamma(1 - z_{i,j,k}), \quad i \in HP, j \in CP, k \in ST, p \in P \quad (C-235)$$

$$\Delta T_{min} \leq dt2_{i,j,k,p} \leq t_{i,k+1,p} - t_{j,k+1,p} + \Gamma(1 - z_{i,j,k}), \quad i \in HP, j \in CP, k \in ST, p \in P \quad (C-236)$$

$$\Delta T_{min} \leq dt1_{i,p}^{cu} \leq t_{i,p}^{abcg} - T_{cu}^{out} + \Gamma(1 - z_i^{cu}), \quad i \in HP, p \in P \quad (C-237)$$

$$\Delta T_{min} \leq dt2_{i,p}^{cu} \leq t_{i,p}^{abce} - T_{cu}^{in} + \Gamma(1 - z_i^{cu}), \quad i \in HP, p \in P \quad (C-238)$$

$$\Delta T_{min} \leq dt1_{j,p}^{hu} \leq T_{hu}^{in} - T_{j,p}^{out} + \Gamma(1 - z_j^{hu}), \quad j \in CP, p \in P \quad (C-239)$$

$$\Delta T_{min} \leq dt2_{j,p}^{hu} \leq T_{hu}^{out} - t_{j,1} + \Gamma(1 - z_j^{hu}), \quad j \in CP, p \in P \quad (C-240)$$

$$\Delta T_{min} \leq dt1_{i,p}^{abcg} \leq t_{i,NOK+1,p} - t_{gen} + \Gamma(1 - z_i^{abcg}), \quad i \in HP, p \in P \quad (C-241)$$

$$\Delta T_{min} \leq dt2_{i,p}^{abcg} \leq t_{i,p}^{abcg} - t_{gen}^{in} + \Gamma(1 - z_i^{abcg}), \quad i \in HP, p \in P \quad (C-242)$$

$$\Delta T_{min} \leq dt1_{i,p}^{abce} \leq t_{i,p}^{abce} - T_{ref} + \Gamma(1 - z_i^{abce}), \quad i \in HP, p \in P \quad (C-243)$$

$$\Delta T_{min} \leq dt2_{i,p}^{abce} \leq T_{i,p}^{out} - T_{ref} + \Gamma(1 - z_i^{abce}), \quad i \in HP, p \in P \quad (C-244)$$

$$\Delta T_{min} \leq dt1_p^{abca} \leq t_{abs}^{in} - T_{cu}^{out}, p \in P \quad (C-245)$$

$$\Delta T_{min} \leq dt2_p^{abca}, p \in P \quad (C-246)$$

$$\Delta T_{min} \leq dt1_p^{abcc} \leq T_{gen}^{out} - T_{cu}^{out}, p \in P \quad (C-247)$$

$$\Delta T_{min} \leq dt2_p^{abcc}, p \in P \quad (C-248)$$

$$COP \sum_{i \in HP} q_{i,p}^{abcg} = \sum_{i \in HP} q_{i,p}^{abce}, p \in P \quad (C-249)$$

$$C2G \sum_{i \in HP} q_{i,p}^{abcg} = q_p^{abcc}, p \in P \quad (C-250)$$

$$\sum_{i \in HP} q_{i,p}^{abcg} + \sum_{i \in HP} q_{i,p}^{abce} = q_p^{abcc} + q_p^{abca}, p \in P \quad (C-251)$$

$$COP = C_1 e^{C_2 t_{gen}} + C_3 e^{C_4 t_{gen}} \quad (C-252)$$

$$C2G = C_5 COP + C_6 \quad (C-253)$$

$$t_{gen}^{in} = C_7 (t_{gen})^2 + C_8 t_{gen} + C_9 \quad (C-254)$$

$$t_{abs}^{in} = C_{10} t_{gen} + C_{11} \quad (C-255)$$

$$A_{i,j,k} \geq \frac{q_{i,j,k,p}}{U_{i,j,k,p} LMTD_{i,j,k,p}}, \quad i \in HP, j \in CP, k \in ST, p \in P \quad (C-256)$$

$$A_i^{cu} \geq \frac{q_{i,p}^{cu}}{U_{i,p}^{cu} LMTD_{i,p}^{cu}}, \quad i \in HP, p \in P \quad (C-257)$$

$$A_j^{hu} \geq \frac{q_{j,p}^{hu}}{U_{j,p}^{hu} LMTD_{j,p}^{hu}}, \quad j \in CP, p \in P \quad (C-258)$$

$$A_i^{abcg} \geq \frac{q_{i,p}^{abcg}}{U_{i,p}^{abcg} LMTD_{i,p}^{abcg}}, \quad i \in HP, p \in P \quad (C-259)$$

$$A_i^{abce} \geq \frac{q_{i,p}^{abce}}{U_{i,p}^{abce} LMTD_{i,p}^{abce}}, \quad i \in HP, p \in P \quad (C-260)$$

$$A^{abca} \geq \frac{q_p^{abca}}{U_p^{abca} LMTD_p^{abca}}, \quad p \in P \quad (C-261)$$

$$A^{abcc} \geq \frac{q_p^{abcc}}{U_p^{abcc} LMTD_p^{abcc}}, \quad p \in P \quad (C-262)$$

min TAC

$$= \left\{ \begin{array}{l} H_y \sum_{p \in P} \left(\frac{DOP_p}{\sum_{p \in P} DOP_p} \right) \left(\sum_{j \in CP} c_{hu} q_{j,p}^{hu} + \sum_{i \in HP} c_{cu} q_{i,p}^{cu} \right) \\ + AF c_{fix}^{HEN} \left(\sum_{i \in HP} \sum_{j \in CP} \sum_{k \in ST} z_{i,j,k} + \sum_{i \in HP} z_i^{cu} + \sum_{j \in CP} z_j^{hu} \right) \\ \quad + \sum_{i \in HP} z_i^{abcg} + \sum_{i \in HP} z_i^{abce} \\ + AF c_{var}^{HEN} \left(\sum_{i \in HP} \sum_{j \in CP} \sum_{k \in ST} (A_{i,j,k})^\beta + \sum_{i \in HP} (A_i^{cu})^\beta + \sum_{j \in CP} (A_j^{hu})^\beta \right) \\ \quad + \sum_{i \in HP} (A_i^{abcg})^\beta + \sum_{i \in HP} (A_i^{abce})^\beta + (A^{abca})^\beta + (A^{abcc})^\beta \end{array} \right\} \quad (C-263)$$

C.7 MP-WHR

- Sets

$$HP = \{i: i \text{ is a hot process stream}\}$$

$$CP = \{j: j \text{ is a cold process stream}\}$$

$$ST = \{k: k \text{ is a stage of the superstructure, } k = 1, \dots, NOK\}$$

$$P = \{p: p \text{ is a period of operation of the system, } p = 1, \dots, NOP\}$$

- Equations

$$\sum_{j \in CP} \sum_{k \in ST} q_{i,j,k,p} + q_{i,p}^{evap} + q_{i,p}^{abcg} + q_{i,p}^{cu} + q_{i,p}^{abce} = F_{i,p}(T_{i,p}^{in} - T_{i,p}^{out}), \quad i \in HP, p \in P \quad (C-264)$$

$$\sum_{i \in HP} \sum_{k \in ST} q_{i,j,k,p} + q_{j,p}^{cond} + q_{j,p}^{hu} = F_{j,p}(T_{j,p}^{out} - T_{j,p}^{in}), \quad j \in CP, p \in P \quad (C-265)$$

$$\sum_{j \in CP} q_{i,j,k,p} = F_{i,p}(t_{i,k,p} - t_{i,k+1,p}), \quad i \in HP, k \in ST, p \in P \quad (C-266)$$

$$\sum_{i \in HP} q_{i,j,k,p} = F_{j,p}(t_{j,k,p} - t_{j,k+1,p}), \quad j \in CP, k \in ST, p \in P \quad (C-267)$$

$$q_{i,p}^{cu} = F_{i,p}(t_{i,p}^{abcg} - t_{i,p}^{abce}), \quad i \in HP, p \in P \quad (C-268)$$

$$q_{j,p}^{hu} = F_{j,p}(T_{j,p}^{out} - t_{j,1,p}), \quad j \in CP, p \in P \quad (C-269)$$

$$q_{i,p}^{evap} = F_{i,p}(t_{i,NOK+1,p} - t_{i,p}^{orc}), \quad i \in HP, p \in P \quad (C-270)$$

$$q_{j,p}^{cond} = F_{j,p}(t_{j,NOK+1,p} - T_{j,p}^{in}), \quad j \in CP, p \in P \quad (C-271)$$

$$q_{i,p}^{evap} = \dot{m}_{w,p} r_{w,i,p} (cp_{w(l)}(T_{evap}^{out} - T_{evap}^{in}) + \lambda_{evap}), \quad i \in HP, p \in P \quad (C-272)$$

$$q_{j,p}^{cond} = \dot{m}_{w,p} r_{w,j,p} (cp_{w(g)}(T_{cond}^{in} - T_{cond}^{out}) + \lambda_{cond}), \quad j \in CP, p \in P \quad (C-273)$$

$$q_p^{acu} = \dot{m}_{w,p} \left(1 - \sum_{j \in CP} r_{w,j,p}\right) (cp_{w(g)}(T_{cond}^{in} - T_{cond}^{out}) + \lambda_{cond}), p \in P \quad (C-274)$$

$$q_{i,p}^{abcg} = F_{i,p}(t_{i,NOK+1,p} - t_{i,p}^{abcg}), \quad i \in HP, p \in P \quad (C-275)$$

$$q_{i,p}^{abce} = F_{i,p}(t_{i,p}^{abce} - T_{i,p}^{out}), \quad i \in HP, p \in P \quad (C-276)$$

$$\sum_{i \in HP} r_{w,i,p} = 1, \quad i \in HP, p \in P \quad (C-277)$$

$$\sum_{j \in CP} r_{w,j,p} \leq 1, \quad j \in CP, p \in P \quad (C-278)$$

$$T_{i,p}^{in} = t_{i,1,p}, \quad i \in HP, p \in P \quad (C-279)$$

$$t_{i,NOK+1,p} \geq t_{i,p}^{orc} \geq t_{i,p}^{abcg} \geq t_{i,p}^{abce} \geq T_{i,p}^{out}, \quad i \in HP, p \in P \quad (C-280)$$

$$T_{j,p}^{out} \geq t_{j,1,p}, \quad j \in CP, p \in P \quad (C-281)$$

$$t_{i,k,p} \geq t_{i,k+1,p}, \quad i \in HP, k \in ST, p \in P \quad (C-282)$$

$$t_{j,k,p} \geq t_{j,k+1,p}, \quad j \in CP, k \in ST, p \in P \quad (C-283)$$

$$q_{i,j,k,p} - \Omega z_{i,j,k} \leq 0, \quad i \in HP, j \in CP, k \in ST, p \in P \quad (C-284)$$

$$q_{i,p}^{cu} - \Omega z_i^{cu} \leq 0, \quad i \in HP, p \in P \quad (C-285)$$

$$q_{j,p}^{hu} - \Omega z_j^{hu} \leq 0, \quad j \in CP, p \in P \quad (C-286)$$

$$q_{i,p}^{evap} - \Omega z_i^{evap} \leq 0, \quad i \in HP, p \in P \quad (C-287)$$

$$q_{j,p}^{cond} - \Omega z_j^{cond} \leq 0, \quad j \in CP, p \in P \quad (C-288)$$

$$q_p^{acu} - \Omega z^{acu} \leq 0, p \in P \quad (C-289)$$

$$q_{i,p}^{abcg} - \Omega z_i^{abcg} \leq 0, \quad i \in HP, p \in P \quad (C-290)$$

$$q_{i,p}^{abce} - \Omega z_i^{abce} \leq 0, \quad i \in HP, p \in P \quad (C-291)$$

$$\Delta T_{min} \leq dt1_{i,j,k,p} \leq t_{i,k,p} - t_{j,k,p} + \Gamma(1 - z_{i,j,k}), \quad i \in HP, j \in CP, k \in ST, p \in P \quad (C-292)$$

$$\Delta T_{min} \leq dt2_{i,j,k,p} \leq t_{i,k+1,p} - t_{j,k+1,p} + \Gamma(1 - z_{i,j,k}), \quad i \in HP, j \in CP, k \in ST, p \in P \quad (C-293)$$

$$\Delta T_{min} \leq dt1_{i,p}^{cu} \leq t_{i,p}^{abcg} - T_{cu}^{out} + \Gamma(1 - z_i^{cu}), \quad i \in HP, p \in P \quad (C-294)$$

$$\Delta T_{min} \leq dt2_{i,p}^{cu} \leq t_{i,p}^{abce} - T_{cu}^{in} + \Gamma(1 - z_i^{cu}), \quad i \in HP, p \in P \quad (C-295)$$

$$\Delta T_{min} \leq dt1_{j,p}^{hu} \leq T_{hu}^{in} - T_{j,p}^{out} + \Gamma(1 - z_j^{hu}), \quad j \in CP, p \in P \quad (C-296)$$

$$\Delta T_{min} \leq dt2_{j,p}^{hu} \leq T_{hu}^{out} - t_{j,1,p} + \Gamma(1 - z_j^{hu}), \quad j \in CP, p \in P \quad (C-297)$$

$$\Delta T_{min} \leq dt1_{i,p}^{evap} \leq t_{i,NOK+1,p} - T_{evap}^{out} + \Gamma(1 - z_i^{evap}), \quad i \in HP, p \in P \quad (C-298)$$

$$\Delta T_{min} \leq dt2_{i,p}^{evap} \leq t_{i,p}^{orc} - T_{evap}^{in} + \Gamma(1 - z_i^{evap}), \quad i \in HP, p \in P \quad (C-299)$$

$$\Delta T_{min} \leq dt1_{j,p}^{cond} \leq T_{cond}^{in} - t_{j,NOK+1,p} + \Gamma(1 - z_j^{cond}), \quad j \in CP, p \in P \quad (C-300)$$

$$\Delta T_{min} \leq dt2_{j,p}^{cond} \leq T_{cond}^{out} - T_{j,p}^{in} + \Gamma(1 - z_j^{cond}), \quad j \in CP, p \in P \quad (C-301)$$

$$\Delta T_{min} \leq dt1_{acu} \leq T_{cond}^{in} - T_{cu}^{out} + \Gamma(1 - z^{acu}) \quad (C-302)$$

$$\Delta T_{min} \leq dt2^{acu} \leq T_{cond}^{out} - T_{cu}^{in} + \Gamma(1 - z^{acu}) \quad (C-303)$$

$$\Delta T_{min} \leq dt1_{i,p}^{abcg} \leq t_{i,p}^{orc} - t_{gen} + \Gamma(1 - z_i^{abcg}), \quad i \in HP, p \in P \quad (C-304)$$

$$\Delta T_{min} \leq dt2_{i,p}^{abcg} \leq t_{i,p}^{abcg} - t_{gen}^{in} + \Gamma(1 - z_i^{abcg}), \quad i \in HP, p \in P \quad (C-305)$$

$$\Delta T_{min} \leq dt1_{i,p}^{abce} \leq t_{i,p}^{abce} - T_{ref} + \Gamma(1 - z_i^{abce}), \quad i \in HP, p \in P \quad (C-306)$$

$$\Delta T_{min} \leq dt2_{i,p}^{abce} \leq T_{i,p}^{out} - T_{ref} + \Gamma(1 - z_i^{abce}), \quad i \in HP, p \in P \quad (C-307)$$

$$\Delta T_{min} \leq dt1_p^{abca} \leq t_{abs}^{in} - T_{cu}^{out}, p \in P \quad (C-308)$$

$$\Delta T_{min} \leq dt2_p^{abca}, p \in P \quad (C-309)$$

$$\Delta T_{min} \leq dt1_p^{abcc} \leq T_{gen}^{out} - T_{cu}^{out}, p \in P \quad (C-310)$$

$$\Delta T_{min} \leq dt2_p^{abcc}, p \in P \quad (C-311)$$

$$\begin{aligned} \Delta T_{min} &\leq dt3_{i,p}^{evap} \\ &\leq \left(t_{i,p}^{orc} + \frac{\dot{m}_{wp} r_{w,i,p} cp_{w(l)} (T_{evap}^{out} - T_{evap}^{in})}{F_{i,p}} \right) - T_{evap}^{out} \\ &\quad + \Gamma(1 - z_i^{evap}), \quad i \in HP, p \in P \end{aligned} \quad (C-312)$$

$$\begin{aligned} \Delta T_{min} &\leq dt3_{j,p}^{cond} \\ &\leq T_{cond}^{out} - \left(t_{j,NOK+1,p} - \frac{\dot{m}_{wp} r_{w,j,p} cp_{w(g)} (T_{cond}^{in} - T_{cond}^{out})}{F_{j,p}} \right) \\ &\quad + \Gamma(1 - z_j^{cond}), \quad j \in CP, p \in P \end{aligned} \quad (C-313)$$

$$W_{pump_p} = \dot{m}_{wp} * w_{pump}, p \in P \quad (C-314)$$

$$W_{turb_p} = \dot{m}_{wp} * w_{turb}, p \in P \quad (C-315)$$

$$COP \sum_{i \in HP} q_{i,p}^{abcg} = \sum_{i \in HP} q_{i,p}^{abce}, p \in P \quad (C-316)$$

$$C2G \sum_{i \in HP} q_{i,p}^{abcg} = q_p^{abcc}, p \in P \quad (C-317)$$

$$\sum_{i \in HP} q_{i,p}^{abcg} + \sum_{i \in HP} q_{i,p}^{abce} = q_p^{abcc} + q_p^{abca}, p \in P \quad (C-318)$$

$$COP = C_1 e^{C_2 t_{gen}} + C_3 e^{C_4 t_{gen}} \quad (C-319)$$

$$C2G = C_5 COP + C_6 \quad (C-320)$$

$$t_{gen}^{in} = C_7 (t_{gen})^2 + C_8 t_{gen} + C_9 \quad (C-321)$$

$$t_{abs}^{in} = C_{10} t_{gen} + C_{11} \quad (C-322)$$

$$A_{i,j,k} \geq \frac{q_{i,j,k,p}}{U_{i,j,k,p} LMTD_{i,j,k,p}}, \quad i \in HP, j \in CP, k \in ST, p \in P \quad (C-323)$$

$$A_i^{cu} \geq \frac{q_{i,p}^{cu}}{U_{i,p}^{cu} LMTD_{i,p}^{cu}}, \quad i \in HP, p \in P \quad (C-324)$$

$$A_j^{hu} \geq \frac{q_{j,p}^{hu}}{U_{j,p}^{hu} LMTD_{j,p}^{hu}}, \quad j \in CP, p \in P \quad (C-325)$$

$$A_i^{evap} \geq \frac{q_{i,p}^{evap}}{U_{i,p}^{evap} LMTD_{i,p}^{evap}}, \quad i \in HP, p \in P \quad (C-326)$$

$$A_j^{cond} \geq \frac{q_{j,p}^{cond}}{U_{j,p}^{cond} LMTD_{j,p}^{cond}}, \quad j \in CP, p \in P \quad (C-327)$$

$$A^{acu} \geq \frac{q_p^{acu}}{U_p^{acu} LMTD_p^{acu}} \quad (C-328)$$

$$A_i^{abcg} \geq \frac{q_{i,p}^{abcg}}{U_{i,p}^{abcg} LMTD_{i,p}^{abcg}}, \quad i \in HP, p \in P \quad (C-329)$$

$$A_i^{abce} \geq \frac{q_{i,p}^{abce}}{U_{i,p}^{abce} LMTD_{i,p}^{abce}}, \quad i \in HP, p \in P \quad (C-330)$$

$$A^{abca} \geq \frac{q_p^{abca}}{U_p^{abca} LMTD_p^{abca}}, \quad p \in P \quad (C-331)$$

$$A^{abcc} \geq \frac{q_p^{abcc}}{U_p^{abcc} LMTD_p^{abcc}}, \quad p \in P \quad (C-332)$$

$$W_{pump}^{max} \geq W_{pump,p}, p \in P \quad (C-333)$$

$$W_{turb}^{max} \geq W_{turb,p}, p \in P \quad (C-334)$$

min TAC

$$\begin{aligned}
& H_y \sum_{p \in P} \left(\frac{DOP_p}{\sum_{p \in P} DOP_p} \right) \left(+ \sum_{j \in CP} c_{hu} q_{j,p}^{hu} + \sum_{i \in HP} c_{cu} q_{i,p}^{cu} + c_{cu} q_p^{acu} \right) \\
& + AF c_{fix}^{HEN} \left(\sum_{i \in HP} \sum_{j \in CP} \sum_{k \in ST} z_{i,j,k} + \sum_{i \in HP} z_i^{cu} + \sum_{j \in CP} z_j^{hu} \right) \\
& \quad + \sum_{i \in HP} z_i^{evap} + \sum_{j \in CP} z_j^{cond} + z^{acu} \\
& \quad + \sum_{i \in HP} z_i^{abcg} + \sum_{i \in HP} z_i^{abce} \\
& + AF c_{var}^{HEN} \left(\sum_{i \in HP} \sum_{j \in CP} \sum_{k \in ST} (A_{i,j,k})^\beta + \sum_{i \in HP} (A_i^{cu})^\beta + \sum_{j \in CP} (A_j^{hu})^\beta \right) \\
& \quad + \sum_{i \in HP} (A_i^{evap})^\beta + \sum_{j \in CP} (A_j^{cond})^\beta + (A^{acu})^\beta \\
& \quad + \sum_{i \in HP} (A_i^{abcg})^\beta + \sum_{i \in HP} (A_i^{abce})^\beta + (A^{abca})^\beta + (A^{abcc})^\beta \\
& + AF \left(c_{fix}^{pump} + c_{var}^{pump} (W_{pump}^{max})^{\beta^{pump}} \right) + AF \left(c_{fix}^{pump} + c_{var}^{turb} (W_{turb}^{max})^{\beta^{turb}} \right)
\end{aligned} \tag{C-335}$$

C.8 MP-ST-ORC

- Sets

$$HP = \{i: i \text{ is a hot process stream}\}$$

$$CP = \{j: j \text{ is a cold process stream}\}$$

$$ST = \{k: k \text{ is a stage of the superstructure, } k = 1, \dots, NOK\}$$

$$P = \{p: p \text{ is a period of operation of the system, } p = 1, \dots, NOP\}$$

$$LV = \{lv: lv \text{ is a storage level, } lv = 1, \dots, NOLV\}$$

- Equations

$$\sum_{j \in CP} \sum_{k \in ST} q_{i,j,k,p} + \sum_{k \in ST} \sum_{lv \in LV} q_{i,k,p,lv}^{stoc} + q_{i,p}^{evap} + q_{i,p}^{cu} = F_{i,p} (T_{i,p}^{in} - T_{i,p}^{out}), \quad i \in HP, p \in P \quad (C-336)$$

$$\sum_{i \in HP} \sum_{k \in ST} q_{i,j,k,p} + \sum_{k \in ST} \sum_{lv \in LV} q_{j,k,p,lv}^{stoh} + q_{j,p}^{cond} + q_{j,p}^{hu} = F_{j,p} (T_{j,p}^{out} - T_{j,p}^{in}), \quad j \in CP, p \in P \quad (C-337)$$

$$\sum_{j \in CP} q_{i,j,k,p} + \sum_{lv \in LV} q_{i,k,p,lv}^{stoc} = F_{i,p} (t_{i,k,p} - t_{i,k+1,p}), \quad i \in HP, k \in ST, p \in P \quad (C-338)$$

$$\sum_{i \in HP} q_{i,j,k,p} + \sum_{lv \in LV} q_{j,k,p,lv}^{stoh} = F_{j,p} (t_{j,k,p} - t_{j,k+1,p}), \quad j \in CP, k \in ST, p \in P \quad (C-339)$$

$$q_{i,p}^{cu} = F_{i,p} (t_{i,p}^{orc} - T_{i,p}^{out}), \quad i \in HP, p \in P \quad (C-340)$$

$$q_{j,p}^{hu} = F_{j,p} (T_{j,p}^{out} - t_{j,1}), \quad j \in CP, p \in P \quad (C-341)$$

$$q_{i,p}^{evap} = F_{i,p} (t_{i,NOK+1,p} - t_{i,p}^{orc}), \quad i \in HP, p \in P \quad (C-342)$$

$$q_{j,p}^{cond} = F_{j,p} (t_{j,NOK+1,p} - T_{j,p}^{in}), \quad j \in CP, p \in P \quad (C-343)$$

$$q_{i,p}^{evap} = \dot{m}_{w,p} r_{w,i,p} (cp_{w(l)} (T_{evap}^{out} - T_{evap}^{in}) + \lambda_{evap}), \quad i \in HP, p \in P \quad (C-344)$$

$$q_{j,p}^{cond} = \dot{m}_{w,p} r_{w,j,p} (cp_{w(g)} (T_{cond}^{in} - T_{cond}^{out}) + \lambda_{cond}), \quad j \in CP, p \in P \quad (C-345)$$

$$q_p^{acu} = \dot{m}_{w,p} \left(1 - \sum_{j \in CP} r_{w,j,p} \right) (cp_{w(g)} (T_{cond}^{in} - T_{cond}^{out}) + \lambda_{cond}), p \in P \quad (C-346)$$

$$\sum_{i \in HP} r_{w,i,p} = 1, \quad i \in HP, p \in P \quad (C-347)$$

$$\sum_{j \in CP} r_{w,j,p} \leq 1, \quad j \in CP, p \in P \quad (C-348)$$

$$T_{i,p}^{in} = t_{i,1,p}, \quad i \in HP, p \in P \quad (C-349)$$

$$t_{i,NOK+1,p} \geq t_{i,p}^{orc} \geq T_{i,p}^{out}, \quad i \in HP, p \in P \quad (C-350)$$

$$T_{j,p}^{out} \geq t_{j,1,p}, \quad j \in CP, p \in P \quad (C-351)$$

$$t_{i,k,p} \geq t_{i,k+1,p}, \quad i \in HP, k \in ST, p \in P \quad (C-352)$$

$$t_{j,k,p} \geq t_{j,k+1,p}, \quad j \in CP, k \in ST, p \in P \quad (C-353)$$

$$q_{i,j,k,p} - \Omega z_{i,j,k} \leq 0, \quad i \in HP, j \in CP, k \in ST, p \in P \quad (C-354)$$

$$q_{i,p}^{cu} - \Omega z_i^{cu} \leq 0, \quad i \in HP, p \in P \quad (C-355)$$

$$q_{j,p}^{hu} - \Omega z_j^{hu} \leq 0, \quad j \in CP, p \in P \quad (C-356)$$

$$q_{i,p}^{evap} - \Omega z_i^{evap} \leq 0, \quad i \in HP, p \in P \quad (C-357)$$

$$q_{j,p}^{cond} - \Omega z_j^{cond} \leq 0, \quad j \in CP, p \in P \quad (C-358)$$

$$q_p^{acu} - \Omega z^{acu} \leq 0, p \in P \quad (C-359)$$

$$\Delta T_{min} \leq dt1_{i,j,k,p} \leq t_{i,k,p} - t_{j,k,p} + \Gamma(1 - z_{i,j,k}), \quad i \in HP, j \in CP, k \in ST, p \in P \quad (C-360)$$

$$\Delta T_{min} \leq dt2_{i,j,k,p} \leq t_{i,k+1,p} - t_{j,k+1,p} + \Gamma(1 - z_{i,j,k}), \quad i \in HP, j \in CP, k \in ST, p \in P \quad (C-361)$$

$$\Delta T_{min} \leq dt1_{i,p}^{cu} \leq t_{i,p}^{orc} - T_{cu}^{out} + \Gamma(1 - z_i^{cu}), \quad i \in HP, p \in P \quad (C-362)$$

$$\Delta T_{min} \leq dt2_{i,p}^{cu} \leq T_{cu}^{out} - T_{cu}^{in} + \Gamma(1 - z_i^{cu}), \quad i \in HP, p \in P \quad (C-363)$$

$$\Delta T_{min} \leq dt1_{j,p}^{hu} \leq T_{hu}^{in} - T_{j,p}^{out} + \Gamma(1 - z_j^{hu}), \quad j \in CP, p \in P \quad (C-364)$$

$$\Delta T_{min} \leq dt2_{j,p}^{hu} \leq T_{hu}^{out} - t_{j,1} + \Gamma(1 - z_j^{hu}), \quad j \in CP, p \in P \quad (C-365)$$

$$\Delta T_{min} \leq dt1_{i,p}^{evap} \leq t_{i,NOK+1,p} - T_{evap}^{out} + \Gamma(1 - z_i^{evap}), \quad i \in HP, p \in P \quad (C-366)$$

$$\Delta T_{min} \leq dt2_{i,p}^{evap} \leq t_{i,p}^{orc} - T_{evap}^{in} + \Gamma(1 - z_i^{evap}), \quad i \in HP, p \in P \quad (C-367)$$

$$\Delta T_{min} \leq dt1_{j,p}^{cond} \leq T_{cond}^{in} - t_{j,NOK+1,p} + \Gamma(1 - z_j^{cond}), \quad j \in CP, p \in P \quad (C-368)$$

$$\Delta T_{min} \leq dt2_{j,p}^{cond} \leq T_{cond}^{out} - T_{j,p}^{in} + \Gamma(1 - z_j^{cond}), \quad j \in CP, p \in P \quad (C-369)$$

$$\Delta T_{min} \leq dt1^{acu} \leq T_{cond}^{in} - T_{cu}^{out} + \Gamma(1 - z^{acu}) \quad (C-370)$$

$$\Delta T_{min} \leq dt2^{acu} \leq T_{cond}^{out} - T_{cu}^{in} + \Gamma(1 - z^{acu}) \quad (C-371)$$

$$\begin{aligned} \Delta T_{min} &\leq dt3_{i,p}^{evap} \\ &\leq \left(t_{i,p}^{orc} + \frac{\dot{m}_{w_p} r_{w_{i,p}} cp_{w_{(l)}} (T_{evap}^{out} - T_{evap}^{in})}{F_{i,p}} \right) - T_{evap}^{out} \\ &\quad + \Gamma(1 - z_i^{evap}), \quad i \in HP, p \in P \end{aligned} \quad (C-372)$$

$$\begin{aligned} \Delta T_{min} &\leq dt3_{j,p}^{cond} \\ &\leq T_{cond}^{out} - \left(t_{j,NOK+1,p} - \frac{\dot{m}_{w_p} r_{w_{j,p}} cp_{w_{(g)}} (T_{cond}^{in} - T_{cond}^{out})}{F_{j,p}} \right) \\ &\quad + \Gamma(1 - z_j^{cond}), \quad j \in CP, p \in P \end{aligned} \quad (C-373)$$

$$W_{pump_p} = \dot{m}_{w_p} * w_{pump}, p \in P \quad (C-374)$$

$$W_{turb_p} = \dot{m}_{w_p} * w_{turb}, p \in P \quad (C-375)$$

$$A_{i,j,k} \geq \frac{q_{i,j,k,p}}{U_{i,j,k,p} LMTD_{i,j,k,p}}, \quad i \in HP, j \in CP, k \in ST, p \in P \quad (C-376)$$

$$A_i^{cu} \geq \frac{q_{i,p}^{cu}}{U_{i,p}^{cu} LMTD_{i,p}^{cu}}, \quad i \in HP, p \in P \quad (C-377)$$

$$A_j^{hu} \geq \frac{q_{j,p}^{hu}}{U_{j,p}^{hu} LMTD_{j,p}^{hu}}, \quad j \in CP, p \in P \quad (C-378)$$

$$A_i^{evap} \geq \frac{q_{i,p}^{evap}}{U_{i,p}^{evap} LMTD_{i,p}^{evap}}, \quad i \in HP, p \in P \quad (C-379)$$

$$A_j^{cond} \geq \frac{q_{j,p}^{cond}}{U_{j,p}^{cond} LMTD_{j,p}^{cond}}, \quad j \in CP, p \in P \quad (C-380)$$

$$A^{acu} \geq \frac{q_p^{acu}}{U_p^{acu} LMTD_p^{acu}} \quad (C-381)$$

$$W_{pump}^{max} \geq W_{pump_p}, p \in P \quad (C-382)$$

$$W_{turb}^{max} \geq W_{turb_p}, p \in P \quad (C-383)$$

$$q_{p,lv}^{charh} = q_{p,lv}^{discharc} = \sum_{i \in HP} \sum_{k \in ST} q_{i,k,p,lv}^{stoc}, \quad i \in HP, k \in ST, p \in P, lv \in LV \quad (C-384)$$

$$q_{p,lv}^{charc} = q_{p,lv}^{discharh} = \sum_{j \in CP} \sum_{k \in ST} q_{j,k,p,lv}^{stoh}, \quad j \in CP, k \in ST, p \in P, lv \in LV \quad (C-385)$$

$$Q_{p,lv}^h = Q_{lv,start}^h + \sum_{p=1}^p q_{p,lv}^{charh} DOP_p - \sum_{p=1}^p q_{p,lv}^{discharh} DOP_p, p \in P, lv \in LV \quad (C-386)$$

$$Q_{p,lv}^c = Q_{lv,start}^c + \sum_{p=1}^p q_{p,lv}^{charc} DOP_p - \sum_{p=1}^p q_{p,lv}^{discharc} DOP_p, p \in P, lv \in LV \quad (C-387)$$

$$\max\{Q_{p,lv}^h\} - \min\{Q_{p,lv}^h\} = (t_{lv}^{sth} - t_{lv}^{stc}) cp_{st} M_{lv}^{sth}, p \in P, lv \in LV \quad (C-388)$$

$$\max\{Q_{p,lv}^c\} - \min\{Q_{p,lv}^c\} = (t_{lv}^{sth} - t_{lv}^{stc}) cp_{st} M_{lv}^{stc}, p \in P, lv \in LV \quad (C-389)$$

$$\frac{M_{lv}^{sth}}{\rho_{st}} = V_{lv}^{sth}, lv \in LV \quad (C-390)$$

$$\frac{M_{lv}^{stc}}{\rho_{st}} = V_{lv}^{stc}, lv \in LV \quad (C-391)$$

$$t_{1,lv}^{stoc} = t_{1,lv}^{stoh} = t_{lv}^{sth}, lv \in LV \quad (C-392)$$

$$t_{NOK+1,lv}^{stoc} = t_{NOK+1,lv}^{stoh} = t_{lv}^{stc}, lv \in LV \quad (C-393)$$

$$t_{k,lv}^{stoc} \geq t_{k+1,lv}^{stoc}, k \in ST, lv \in LV \quad (C-394)$$

$$t_{k,lv}^{stoh} \geq t_{k+1,lv}^{stoh}, k \in ST, lv \in LV \quad (C-395)$$

$$Q_{NOP,lv}^h = Q_{lv_{start}}^h, lv \in LV \quad (C-396)$$

$$Q_{NOP,lv}^c = Q_{lv_{start}}^c, lv \in LV \quad (C-397)$$

$$Q_{p,lv}^c = Q_{p,lv+1}^h, \forall lv < NOLV \quad (C-398)$$

$$M_{lv}^{stc} = M_{lv+1}^{sth}, \forall lv < NOLV \quad (C-399)$$

$$t_{lv}^{stc} = t_{lv+1}^{sth}, \forall lv < NOLV \quad (C-400)$$

$$q_{p,lv}^{charh} \leq \Psi y_{lv}^{charge}, p \in P, lv \in LV \quad (C-401)$$

$$q_{p,lv}^{charc} \leq \Psi (1 - y_{lv}^{charge}), p \in P, lv \in LV \quad (C-402)$$

$$q_{i,k,p,lv}^{stoc} - \Omega z_{i,k,lv}^{stoc} \leq 0, \quad i \in HP, k \in ST, p \in P, lv \in LV \quad (C-403)$$

$$q_{j,k,p,lv}^{stoh} - \Omega z_{j,k,lv}^{stoh} \leq 0, \quad j \in CP, k \in ST, p \in P, lv \in LV \quad (C-404)$$

$$\Delta T_{min} \leq dt1_{i,k,p}^{stoc} \leq t_{i,k,p} - t_{k,p,lv}^{stoc} + \Gamma(1 - z_{i,k,lv}^{stoc}), \quad i \in HP, k \in ST, p \in P, lv \in LV \quad (C-405)$$

$$\Delta T_{min} \leq dt2_{i,k,p}^{stoc} \leq t_{i,k+1,p} - t_{k+1,p,lv}^{stoc} + \Gamma(1 - z_{i,k,lv}^{stoc}), \quad i \in HP, k \in ST, p \in P, lv \in LV \quad (C-406)$$

$$\Delta T_{min} \leq dt1_{j,k,p}^{stoh} \leq t_{j,k,p} - t_{k,p,lv}^{stoh} + \Gamma(1 - z_{j,k,lv}^{stoh}), \quad j \in CP, k \in ST, p \in P, lv \in LV \quad (C-407)$$

$$\Delta T_{min} \leq dt2_{j,k,p}^{stoh} \leq t_{j,k+1,p} - t_{k+1,p,lv}^{stoh} + \Gamma(1 - z_{j,k,lv}^{stoh}), \quad j \in CP, k \in ST, p \in P, lv \in LV \quad (C-408)$$

$$A_{i,k,lv}^{stoc} \geq \frac{q_{i,k,p,lv}^{stoc}}{U_{i,k,p}^{stoc} LMTD_{i,k,p}^{stoc}}, \quad i \in HP, k \in ST, p \in P, lv \in LV \quad (C-409)$$

$$A_{j,k,lv}^{stoh} \geq \frac{q_{j,k,p,lv}^{stoh}}{U_{j,k,p}^{stoh} LMTD_{ijk,p}^{stoh}}, \quad j \in CP, k \in ST, p \in P, lv \in LV \quad (C-410)$$

min TAC

$$= \left\{ \begin{aligned} & H_y \sum_{p \in P} \left(\frac{DOP_p}{\sum_{p \in P} DOP_p} \right) \left(-e_{price_p} W_{turb_p} + e_{cost_p} W_{pump_p} \right. \\ & \quad \left. + \sum_{j \in CP} c_{hu_p} q_{j,p}^{hu} + \sum_{i \in HP} c_{cu_p} q_{i,p}^{cu} + c_{cu_p} q_p^{acu} \right) \\ & \quad + AF c_{fix}^{HEN} \left(\sum_{i \in HP} \sum_{j \in CP} \sum_{k \in ST} z_{i,j,k} + \sum_{i \in HP} z_i^{cu} + \sum_{j \in CP} z_j^{hu} \right) \\ & \quad \quad + \sum_{i \in HP} z_i^{evap} + \sum_{j \in CP} z_j^{cond} + z^{acu} \\ & \quad \quad \left(\sum_{i \in HP} \sum_{k \in ST} \sum_{lv \in LV} z_{i,k,lv}^{stoc} + \sum_{j \in CP} \sum_{k \in ST} \sum_{lv \in LV} z_{j,k,lv}^{stoh} \right) \\ & \quad + AF c_{var}^{HEN} \left(\sum_{i \in HP} \sum_{j \in CP} \sum_{k \in ST} (A_{i,j,k})^\beta + \sum_{i \in HP} (A_i^{cu})^\beta + \sum_{j \in CP} (A_j^{hu})^\beta \right) \\ & \quad \quad + \sum_{i \in HP} (A_i^{evap})^\beta + \sum_{j \in CP} (A_j^{cond})^\beta + (A^{acu})^\beta \\ & \quad \quad \left(\sum_{i \in HP} \sum_{k \in ST} \sum_{lv \in LV} (A_{i,k,lv}^{stoc})^\beta + \sum_{j \in CP} \sum_{k \in ST} \sum_{lv \in LV} (A_{j,k,lv}^{stoh})^\beta \right) \\ & \quad + AF \left(c_{fix}^{pump} + c_{var}^{pump} (W_{pump}^{max})^{\beta^{pump}} \right) + AF \left(c_{fix}^{turb} + c_{var}^{turb} (W_{turb}^{max})^{\beta^{turb}} \right) \\ & \quad + AF \left(\sum_{lv \in LV} c_{fix}^{sto} + c_{var}^{sto} \sum_{lv \in LV} (V_{lv}^{sth})^{\beta^{sto}} \right) + AF \left(c_{fix}^{sto} + c_{var}^{sto} (V_{NOLV}^{stc})^{\beta^{sto}} \right) \end{aligned} \right\} \quad (C-411)$$

C.9 MP-ST-ABC

- Sets

$$HP = \{i: i \text{ is a hot process stream}\}$$

$$CP = \{j: j \text{ is a cold process stream}\}$$

$$ST = \{k: k \text{ is a stage of the superstructure, } k = 1, \dots, NOK\}$$

$$P = \{p: p \text{ is a period of operation of the system, } p = 1, \dots, NOP\}$$

$$LV = \{lv: lv \text{ is a storage level, } lv = 1, \dots, NOLV\}$$

- Equations

$$\sum_{j \in CP} \sum_{k \in ST} q_{i,j,k,p} + \sum_{k \in ST} \sum_{lv \in LV} q_{i,k,p,lv}^{stoc} + q_{i,p}^{abce} + q_{i,p}^{cu} + q_{i,p}^{abcc} = F_{i,p}(T_{i,p}^{in} - T_{i,p}^{out}), \quad i \in HP, p \in P \quad (C-412)$$

$$\sum_{i \in HP} \sum_{k \in ST} q_{i,j,k,p} + \sum_{k \in ST} \sum_{lv \in LV} q_{j,k,p,lv}^{stoh} + q_{j,p}^{hu} = F_{j,p}(T_{j,p}^{out} - T_{j,p}^{in}), \quad j \in CP, p \in P \quad (C-413)$$

$$\sum_{j \in CP} q_{i,j,k,p} + \sum_{lv \in LV} q_{i,k,p,lv}^{stoc} = F_{i,p}(t_{i,k,p} - t_{i,k+1,p}), \quad i \in HP, k \in ST, p \in P \quad (C-414)$$

$$\sum_{i \in HP} q_{i,j,k,p} + \sum_{lv \in LV} q_{j,k,p,lv}^{stoh} = F_{j,p}(t_{j,k,p} - t_{j,k+1,p}), \quad j \in CP, k \in ST, p \in P \quad (C-415)$$

$$q_{i,p}^{cu} = F_{i,p}(t_{i,p}^{abcg} - t_{i,p}^{abce}), \quad i \in HP, p \in P \quad (C-416)$$

$$q_{j,p}^{hu} = F_{j,p}(T_{j,p}^{out} - t_{j,1}), \quad j \in CP, p \in P \quad (C-417)$$

$$q_{i,p}^{abcg} = F_{i,p}(t_{i,NOK+1,p} - t_{i,p}^{abcg}), \quad i \in HP, p \in P \quad (C-418)$$

$$q_{i,p}^{abce} = F_{i,p}(t_{i,p}^{abce} - T_{i,p}^{out}), \quad i \in HP, p \in P \quad (C-419)$$

$$T_{i,p}^{in} = t_{i,1}, \quad i \in HP \quad (C-420)$$

$$t_{i,NOK+1,p} \geq t_{i,p}^{abcg} \geq t_{i,p}^{abce} \geq T_{i,p}^{out}, \quad i \in HP, p \in P \quad (C-421)$$

$$T_{j,p}^{out} \geq t_{j,1}, \quad j \in CP, p \in P \quad (C-422)$$

$$t_{j,NOK+1,p} \geq T_{j,p}^{in}, \quad j \in CP, p \in P \quad (C-423)$$

$$t_{i,k,p} \geq t_{i,k+1,p}, \quad i \in HP, p \in P \quad (C-424)$$

$$t_{j,k,p} \geq t_{j,k+1,p}, \quad j \in CP, p \in P \quad (C-425)$$

$$q_{i,j,k,p} - \Omega z_{i,j,k} \leq 0, \quad i \in HP, j \in CP, k \in ST, p \in P \quad (C-426)$$

$$q_{i,p}^{cu} - \Omega z_i^{cu} \leq 0, \quad i \in HP, p \in P \quad (C-427)$$

$$q_{j,p}^{hu} - \Omega z_j^{hu} \leq 0, \quad j \in CP, p \in P \quad (C-428)$$

$$q_{i,p}^{abcg} - \Omega z_i^{abcg} \leq 0, \quad i \in HP, p \in P \quad (C-429)$$

$$q_{i,p}^{abce} - \Omega z_i^{abce} \leq 0, \quad i \in HP, p \in P \quad (C-430)$$

$$\Delta T_{min} \leq dt1_{i,j,k,p} \leq t_{i,k,p} - t_{j,k,p} + \Gamma(1 - z_{i,j,k}), \quad i \in HP, j \in CP, k \in ST, p \in P \quad (C-431)$$

$$\Delta T_{min} \leq dt2_{i,j,k,p} \leq t_{i,k+1,p} - t_{j,k+1,p} + \Gamma(1 - z_{i,j,k}), \quad i \in HP, j \in CP, k \in ST, p \in P \quad (C-432)$$

$$\Delta T_{min} \leq dt1_{i,p}^{cu} \leq t_{i,p}^{abcg} - T_{cu}^{out} + \Gamma(1 - z_i^{cu}), \quad i \in HP, p \in P \quad (C-433)$$

$$\Delta T_{min} \leq dt2_{i,p}^{cu} \leq t_{i,p}^{abce} - T_{cu}^{in} + \Gamma(1 - z_i^{cu}), \quad i \in HP, p \in P \quad (C-434)$$

$$\Delta T_{min} \leq dt1_{j,p}^{hu} \leq T_{hu}^{in} - T_{j,p}^{out} + \Gamma(1 - z_j^{hu}), \quad j \in CP, p \in P \quad (C-435)$$

$$\Delta T_{min} \leq dt2_{j,p}^{hu} \leq T_{hu}^{out} - t_{j,1} + \Gamma(1 - z_j^{hu}), \quad j \in CP, p \in P \quad (C-436)$$

$$\Delta T_{min} \leq dt1_{i,p}^{abcg} \leq t_{i,NOK+1,p} - t_{gen} + \Gamma(1 - z_i^{abcg}), \quad i \in HP, p \in P \quad (C-437)$$

$$\Delta T_{min} \leq dt2_{i,p}^{abcg} \leq t_{i,p}^{abcg} - t_{gen}^{in} + \Gamma(1 - z_i^{abcg}), \quad i \in HP, p \in P \quad (C-438)$$

$$\Delta T_{min} \leq dt1_{i,p}^{abce} \leq t_{i,p}^{abce} - T_{ref} + \Gamma(1 - z_i^{abce}), \quad i \in HP, p \in P \quad (C-439)$$

$$\Delta T_{min} \leq dt2_{i,p}^{abce} \leq T_{i,p}^{out} - T_{ref} + \Gamma(1 - z_i^{abce}), \quad i \in HP, p \in P \quad (C-440)$$

$$\Delta T_{min} \leq dt1_p^{abca} \leq t_{abs}^{in} - T_{cu}^{out}, p \in P \quad (C-441)$$

$$\Delta T_{min} \leq dt2_p^{abca}, p \in P \quad (C-442)$$

$$\Delta T_{min} \leq dt1_p^{abcc} \leq T_{gen}^{out} - T_{cu}^{out}, p \in P \quad (C-443)$$

$$\Delta T_{min} \leq dt2_p^{abcc}, p \in P \quad (C-444)$$

$$COP \sum_{i \in HP} q_{i,p}^{abcg} = \sum_{i \in HP} q_{i,p}^{abce}, p \in P \quad (C-445)$$

$$C2G \sum_{i \in HP} q_{i,p}^{abcg} = q_p^{abcc}, p \in P \quad (C-446)$$

$$\sum_{i \in HP} q_{i,p}^{abcg} + \sum_{i \in HP} q_{i,p}^{abce} = q_p^{abcc} + q_p^{abca}, p \in P \quad (C-447)$$

$$COP = C_1 e^{C_2 t_{gen}} + C_3 e^{C_4 t_{gen}} \quad (C-448)$$

$$C2G = C_5 COP + C_6 \quad (C-449)$$

$$t_{gen}^{in} = C_7(t_{gen})^2 + C_8 t_{gen} + C_9 \quad (C-450)$$

$$t_{abs}^{in} = C_{10} t_{gen} + C_{11} \quad (C-451)$$

$$A_{i,j,k} \geq \frac{q_{i,j,k,p}}{U_{i,j,k,p} LMTD_{i,j,k,p}}, \quad i \in HP, j \in CP, k \in ST, p \in P \quad (C-452)$$

$$A_i^{cu} \geq \frac{q_{i,p}^{cu}}{U_{i,p}^{cu} LMTD_{i,p}^{cu}}, \quad i \in HP, p \in P \quad (C-453)$$

$$A_j^{hu} \geq \frac{q_{j,p}^{hu}}{U_{j,p}^{hu} LMTD_{j,p}^{hu}}, \quad j \in CP, p \in P \quad (C-454)$$

$$A_i^{abcg} \geq \frac{q_{i,p}^{abcg}}{U_{i,p}^{abcg} LMTD_{i,p}^{abcg}}, \quad i \in HP, p \in P \quad (C-455)$$

$$A_i^{abce} \geq \frac{q_{i,p}^{abce}}{U_{i,p}^{abce} LMTD_{i,p}^{abce}}, \quad i \in HP, p \in P \quad (C-456)$$

$$A^{abca} \geq \frac{q_p^{abca}}{U_p^{abca} LMTD_p^{abca}}, \quad p \in P \quad (C-457)$$

$$A^{abcc} \geq \frac{q_p^{abcc}}{U_p^{abcc} LMTD_p^{abcc}}, \quad p \in P \quad (C-458)$$

$$q_{p,lv}^{charh} = q_{p,lv}^{discharc} = \sum_{i \in HP} \sum_{k \in ST} q_{i,k,p,lv}^{stoc}, \quad i \in HP, k \in ST, p \in P, lv \in LV \quad (C-459)$$

$$q_{p,lv}^{charc} = q_{p,lv}^{discharh} = \sum_{j \in CP} \sum_{k \in ST} q_{j,k,p,lv}^{stoh}, \quad j \in CP, k \in ST, p \in P, lv \in LV \quad (C-460)$$

$$Q_{p,lv}^h = Q_{lv,start}^h + \sum_{p=1}^p q_{p,lv}^{charh} DOP_p - \sum_{p=1}^p q_{p,lv}^{discharh} DOP_p, \quad p \in P, lv \in LV \quad (C-461)$$

$$Q_{p,lv}^c = Q_{lv,start}^c + \sum_{p=1}^p q_{p,lv}^{charc} DOP_p - \sum_{p=1}^p q_{p,lv}^{discharc} DOP_p, \quad p \in P, lv \in LV \quad (C-462)$$

$$\max\{Q_{p,lv}^h\} - \min\{Q_{p,lv}^h\} = (t_{lv}^{sth} - t_{lv}^{stc}) cp_{st} M_{lv}^{sth}, \quad p \in P, lv \in LV \quad (C-463)$$

$$\max\{Q_{p,lv}^c\} - \min\{Q_{p,lv}^c\} = (t_{lv}^{sth} - t_{lv}^{stc}) cp_{st} M_{lv}^{stc}, \quad p \in P, lv \in LV \quad (C-464)$$

$$\frac{M_{lv}^{sth}}{\rho_{st}} = V_{lv}^{sth}, \quad lv \in LV \quad (C-465)$$

$$\frac{M_{lv}^{stc}}{\rho_{st}} = V_{lv}^{stc}, \quad lv \in LV \quad (C-466)$$

$$t_{1,lv}^{stoc} = t_{1,lv}^{stoh} = t_{lv}^{sth}, lv \in LV \quad (C-467)$$

$$t_{NOK+1,lv}^{stoc} = t_{NOK+1,lv}^{stoh} = t_{lv}^{stc}, lv \in LV \quad (C-468)$$

$$t_{k,lv}^{stoc} \geq t_{k+1,lv}^{stoc}, k \in ST, lv \in LV \quad (C-469)$$

$$t_{k,lv}^{stoh} \geq t_{k+1,lv}^{stoh}, k \in ST, lv \in LV \quad (C-470)$$

$$Q_{NOP,lv}^h = Q_{lv_{start}}^h, lv \in LV \quad (C-471)$$

$$Q_{NOP,lv}^c = Q_{lv_{start}}^c, lv \in LV \quad (C-472)$$

$$Q_{p,lv}^c = Q_{p,lv+1}^h, \forall lv < NOLV \quad (C-473)$$

$$M_{lv}^{stc} = M_{lv+1}^{sth}, \forall lv < NOLV \quad (C-474)$$

$$t_{lv}^{stc} = t_{lv+1}^{sth}, \forall lv < NOLV \quad (C-475)$$

$$q_{p,lv}^{charh} \leq \Psi y_{lv}^{charge}, p \in P, lv \in LV \quad (C-476)$$

$$q_{p,lv}^{charc} \leq \Psi (1 - y_{lv}^{charge}), p \in P, lv \in LV \quad (C-477)$$

$$q_{i,k,p,lv}^{stoc} - \Omega z_{i,k,lv}^{stoc} \leq 0, \quad i \in HP, k \in ST, p \in P, lv \in LV \quad (C-478)$$

$$q_{j,k,p,lv}^{stoh} - \Omega z_{j,k,lv}^{stoh} \leq 0, \quad j \in CP, k \in ST, p \in P, lv \in LV \quad (C-479)$$

$$\Delta T_{min} \leq dt1_{i,k,p}^{stoc} \leq t_{i,k,p} - t_{k,p,lv}^{stoc} + \Gamma(1 - z_{i,k,lv}^{stoc}), \quad i \in HP, k \in ST, p \in P, lv \in LV \quad (C-480)$$

$$\Delta T_{min} \leq dt2_{i,k,p}^{stoc} \leq t_{i,k+1,p} - t_{k+1,p,lv}^{stoc} + \Gamma(1 - z_{i,k,lv}^{stoc}), \quad i \in HP, k \in ST, p \in P, lv \in LV \quad (C-481)$$

$$\Delta T_{min} \leq dt1_{j,k,p}^{stoh} \leq t_{j,k,p} - t_{k,p,lv}^{stoh} + \Gamma(1 - z_{j,k,lv}^{stoh}), \quad j \in CP, k \in ST, p \in P, lv \in LV \quad (C-482)$$

$$\Delta T_{min} \leq dt2_{j,k,p}^{stoh} \leq t_{j,k+1,p} - t_{k+1,p,lv}^{stoh} + \Gamma(1 - z_{j,k,lv}^{stoh}), \quad j \in CP, k \in ST, p \in P, lv \in LV \quad (C-483)$$

$$A_{i,k,lv}^{stoc} \geq \frac{q_{i,k,p,lv}^{stoc}}{U_{i,k,p}^{stoc} LMTD_{i,k,p}^{stoc}}, \quad i \in HP, k \in ST, p \in P, lv \in LV \quad (C-484)$$

$$A_{j,k,lv}^{stoh} \geq \frac{q_{j,k,p,lv}^{stoh}}{U_{j,k,p}^{stoh} LMTD_{ijk,p}^{stoh}}, \quad j \in CP, k \in ST, p \in P, lv \in LV \quad (C-485)$$

min TAC

$$\begin{aligned}
& \left. \begin{aligned}
& H_y \sum_{p \in P} \left(\frac{DOP_p}{\sum_{p \in P} DOP_p} \right) \left(\sum_{j \in CP} c_{hu} q_{j,p}^{hu} + \sum_{i \in HP} c_{cu} q_{i,p}^{cu} \right) \\
& + AF c_{fix}^{HEN} \left(\begin{aligned}
& \sum_{i \in HP} \sum_{j \in CP} \sum_{k \in ST} z_{i,j,k} + \sum_{i \in HP} z_i^{cu} + \sum_{j \in CP} z_j^{hu} \\
& + \sum_{i \in HP} z_i^{abcg} + \sum_{i \in HP} z_i^{abce} \\
& \sum_{i \in HP} \sum_{k \in ST} \sum_{lv \in LV} z_{i,k,lv}^{stoc} + \sum_{j \in CP} \sum_{k \in ST} \sum_{lv \in LV} z_{j,k,lv}^{stoh}
\end{aligned} \right) \\
& + AF c_{var}^{HEN} \left(\begin{aligned}
& \sum_{i \in HP} \sum_{j \in CP} \sum_{k \in ST} (A_{i,j,k})^\beta + \sum_{i \in HP} (A_i^{cu})^\beta + \sum_{j \in CP} (A_j^{hu})^\beta \\
& + \sum_{i \in HP} (A_i^{abcg})^\beta + \sum_{i \in HP} (A_i^{abce})^\beta + (A^{abca})^\beta + (A^{abcc})^\beta \\
& \sum_{i \in HP} \sum_{k \in ST} \sum_{lv \in LV} (A_{i,k,lv}^{stoc})^\beta + \sum_{j \in CP} \sum_{k \in ST} \sum_{lv \in LV} (A_{j,k,lv}^{stoh})^\beta
\end{aligned} \right) \\
& + AF \left(\sum_{lv \in LV} c_{fix}^{sto} + c_{var}^{sto} \sum_{lv \in LV} (V_{lv}^{sth})^{\beta^{sto}} \right) + AF (c_{fix}^{sto} + c_{var}^{sto} (V_{NOLV}^{stc})^{\beta^{sto}})
\end{aligned} \right\} \quad (C-486)
\end{aligned}$$

C.10 MP-ST-WHR

- Sets

$$HP = \{i: i \text{ is a hot process stream}\}$$

$$CP = \{j: j \text{ is a cold process stream}\}$$

$$ST = \{k: k \text{ is a stage of the superstructure, } k = 1, \dots, NOK\}$$

$$P = \{p: p \text{ is a period of operation of the system, } p = 1, \dots, NOP\}$$

$$LV = \{lv: lv \text{ is a storage level, } lv = 1, \dots, NOLV\}$$

- Equations

$$\sum_{j \in CP} \sum_{k \in ST} q_{i,j,k,p} + q_{i,p}^{evap} + q_{i,p}^{abcg} + q_{i,p}^{cu} + q_{i,p}^{abce} = F_{i,p}(T_{i,p}^{in} - T_{i,p}^{out}), \quad i \in HP, p \in P \quad (C-487)$$

$$\sum_{i \in HP} \sum_{k \in ST} q_{i,j,k,p} + q_{j,p}^{cond} + q_{j,p}^{hu} = F_{j,p}(T_{j,p}^{out} - T_{j,p}^{in}), \quad j \in CP, p \in P \quad (C-488)$$

$$\sum_{j \in CP} q_{i,j,k,p} = F_{i,p}(t_{i,k,p} - t_{i,k+1,p}), \quad i \in HP, k \in ST, p \in P \quad (C-489)$$

$$\sum_{i \in HP} q_{i,j,k,p} = F_{j,p}(t_{j,k,p} - t_{j,k+1,p}), \quad j \in CP, k \in ST, p \in P \quad (C-490)$$

$$q_{i,p}^{cu} = F_{i,p}(t_{i,p}^{abcg} - t_{i,p}^{abce}), \quad i \in HP, p \in P \quad (C-491)$$

$$q_{j,p}^{hu} = F_{j,p}(T_{j,p}^{out} - t_{j,1,p}), \quad j \in CP, p \in P \quad (C-492)$$

$$q_{i,p}^{evap} = F_{i,p}(t_{i,NOK+1,p} - t_{i,p}^{orc}), \quad i \in HP, p \in P \quad (C-493)$$

$$q_{j,p}^{cond} = F_{j,p}(t_{j,NOK+1,p} - T_{j,p}^{in}), \quad j \in CP, p \in P \quad (C-494)$$

$$q_{i,p}^{evap} = \dot{m}_{w,p} r_{w,i,p} (cp_{w(l)}(T_{evap}^{out} - T_{evap}^{in}) + \lambda_{evap}), \quad i \in HP, p \in P \quad (C-495)$$

$$q_{j,p}^{cond} = \dot{m}_{w,p} r_{w,j,p} (cp_{w(g)}(T_{cond}^{in} - T_{cond}^{out}) + \lambda_{cond}), \quad j \in CP, p \in P \quad (C-496)$$

$$q_p^{acu} = \dot{m}_{w,p} \left(1 - \sum_{j \in CP} r_{w,j,p} \right) (cp_{w(g)}(T_{cond}^{in} - T_{cond}^{out}) + \lambda_{cond}), \quad p \in P \quad (C-497)$$

$$q_{i,p}^{abcg} = F_{i,p}(t_{i,NOK+1,p} - t_{i,p}^{abcg}), \quad i \in HP, p \in P \quad (C-498)$$

$$q_{i,p}^{abce} = F_{i,p}(t_{i,p}^{abce} - T_{i,p}^{out}), \quad i \in HP, p \in P \quad (C-499)$$

$$\sum_{i \in HP} r_{wi,p} = 1, \quad i \in HP, p \in P \quad (C-500)$$

$$\sum_{j \in CP} r_{wj,p} \leq 1, \quad j \in CP, p \in P \quad (C-501)$$

$$T_{i,p}^{in} = t_{i,1,p}, \quad i \in HP, p \in P \quad (C-502)$$

$$t_{i,NOK+1,p} \geq t_{i,p}^{orc} \geq t_{i,p}^{abcg} \geq t_{i,p}^{abce} \geq T_{i,p}^{out}, \quad i \in HP, p \in P \quad (C-503)$$

$$T_{j,p}^{out} \geq t_{j,1,p}, \quad j \in CP, p \in P \quad (C-504)$$

$$t_{i,k,p} \geq t_{i,k+1,p}, \quad i \in HP, k \in ST, p \in P \quad (C-505)$$

$$t_{j,k,p} \geq t_{j,k+1,p}, \quad j \in CP, k \in ST, p \in P \quad (C-506)$$

$$q_{i,j,k,p} - \Omega z_{i,j,k} \leq 0, \quad i \in HP, j \in CP, k \in ST, p \in P \quad (C-507)$$

$$q_{i,p}^{cu} - \Omega z_i^{cu} \leq 0, \quad i \in HP, p \in P \quad (C-508)$$

$$q_{j,p}^{hu} - \Omega z_j^{hu} \leq 0, \quad j \in CP, p \in P \quad (C-509)$$

$$q_{i,p}^{evap} - \Omega z_i^{evap} \leq 0, \quad i \in HP, p \in P \quad (C-510)$$

$$q_{j,p}^{cond} - \Omega z_j^{cond} \leq 0, \quad j \in CP, p \in P \quad (C-511)$$

$$q_p^{acu} - \Omega z^{acu} \leq 0, p \in P \quad (C-512)$$

$$q_{i,p}^{abcg} - \Omega z_i^{abcg} \leq 0, \quad i \in HP, p \in P \quad (C-513)$$

$$q_{i,p}^{abce} - \Omega z_i^{abce} \leq 0, \quad i \in HP, p \in P \quad (C-514)$$

$$\Delta T_{min} \leq dt1_{i,j,k,p} \leq t_{i,k,p} - t_{j,k,p} + \Gamma(1 - z_{i,j,k}), \quad i \in HP, j \in CP, k \in ST, p \in P \quad (C-515)$$

$$\Delta T_{min} \leq dt2_{i,j,k,p} \leq t_{i,k+1,p} - t_{j,k+1,p} + \Gamma(1 - z_{i,j,k}), \quad i \in HP, j \in CP, k \in ST, p \in P \quad (C-516)$$

$$\Delta T_{min} \leq dt1_{i,p}^{cu} \leq t_{i,p}^{abcg} - T_{cu}^{out} + \Gamma(1 - z_i^{cu}), \quad i \in HP, p \in P \quad (C-517)$$

$$\Delta T_{min} \leq dt2_{i,p}^{cu} \leq t_{i,p}^{abce} - T_{cu}^{in} + \Gamma(1 - z_i^{cu}), \quad i \in HP, p \in P \quad (C-518)$$

$$\Delta T_{min} \leq dt1_{j,p}^{hu} \leq T_{hu}^{in} - T_{j,p}^{out} + \Gamma(1 - z_j^{hu}), \quad j \in CP, p \in P \quad (C-519)$$

$$\Delta T_{min} \leq dt2_{j,p}^{hu} \leq T_{hu}^{out} - t_{j,1,p} + \Gamma(1 - z_j^{hu}), \quad j \in CP, p \in P \quad (C-520)$$

$$\Delta T_{min} \leq dt1_{i,p}^{evap} \leq t_{i,NOK+1,p} - T_{evap}^{out} + \Gamma(1 - z_i^{evap}), \quad i \in HP, p \in P \quad (C-521)$$

$$\Delta T_{min} \leq dt2_{i,p}^{evap} \leq t_{i,p}^{orc} - T_{evap}^{in} + \Gamma(1 - z_i^{evap}), \quad i \in HP, p \in P \quad (C-522)$$

$$\Delta T_{min} \leq dt1_{j,p}^{cond} \leq T_{cond}^{in} - t_{j,NOK+1,p} + \Gamma(1 - z_j^{cond}), \quad j \in CP, p \in P \quad (C-523)$$

$$\Delta T_{min} \leq dt2_{j,p}^{cond} \leq T_{cond}^{out} - T_{j,p}^{in} + \Gamma(1 - z_j^{cond}), \quad j \in CP, p \in P \quad (C-524)$$

$$\Delta T_{min} \leq dt1^{acu} \leq T_{cond}^{in} - T_{cu}^{out} + \Gamma(1 - z^{acu}) \quad (C-525)$$

$$\Delta T_{min} \leq dt2^{acu} \leq T_{cond}^{out} - T_{cu}^{in} + \Gamma(1 - z^{acu}) \quad (C-526)$$

$$\Delta T_{min} \leq dt1_{i,p}^{abcg} \leq t_{i,p}^{orc} - t_{gen} + \Gamma(1 - z_i^{abcg}), \quad i \in HP, p \in P \quad (C-527)$$

$$\Delta T_{min} \leq dt2_{i,p}^{abcg} \leq t_{i,p}^{abcg} - t_{gen}^{in} + \Gamma(1 - z_i^{abcg}), \quad i \in HP, p \in P \quad (C-528)$$

$$\Delta T_{min} \leq dt1_{i,p}^{abce} \leq t_{i,p}^{abce} - T_{ref} + \Gamma(1 - z_i^{abce}), \quad i \in HP, p \in P \quad (C-529)$$

$$\Delta T_{min} \leq dt2_{i,p}^{abce} \leq T_{i,p}^{out} - T_{ref} + \Gamma(1 - z_i^{abce}), \quad i \in HP, p \in P \quad (C-530)$$

$$\Delta T_{min} \leq dt1_p^{abca} \leq t_{abs}^{in} - T_{cu}^{out}, p \in P \quad (C-531)$$

$$\Delta T_{min} \leq dt2_p^{abca}, p \in P \quad (C-532)$$

$$\Delta T_{min} \leq dt1_p^{abcc} \leq T_{gen}^{out} - T_{cu}^{out}, p \in P \quad (C-533)$$

$$\Delta T_{min} \leq dt2_p^{abcc}, p \in P \quad (C-534)$$

$$\begin{aligned} \Delta T_{min} &\leq dt3_{i,p}^{evap} \\ &\leq \left(t_{i,p}^{orc} + \frac{\dot{m}_{wp} r_{w,i,p} cp_{w(l)} (T_{evap}^{out} - T_{evap}^{in})}{F_{i,p}} \right) - T_{evap}^{out} \\ &\quad + \Gamma(1 - z_i^{evap}), \quad i \in HP, p \in P \end{aligned} \quad (C-535)$$

$$\begin{aligned} \Delta T_{min} &\leq dt3_{j,p}^{cond} \\ &\leq T_{cond}^{out} - \left(t_{j,NOK+1,p} - \frac{\dot{m}_{wp} r_{w,j,p} cp_{w(g)} (T_{cond}^{in} - T_{cond}^{out})}{F_{j,p}} \right) \\ &\quad + \Gamma(1 - z_j^{cond}), \quad j \in CP, p \in P \end{aligned} \quad (C-536)$$

$$W_{pump_p} = \dot{m}_{wp} * w_{pump}, p \in P \quad (C-537)$$

$$W_{turb_p} = \dot{m}_{wp} * w_{turb}, p \in P \quad (C-538)$$

$$COP \sum_{i \in HP} q_{i,p}^{abcg} = \sum_{i \in HP} q_{i,p}^{abce}, p \in P \quad (C-539)$$

$$C2G \sum_{i \in HP} q_{i,p}^{abcg} = q_p^{abcc}, p \in P \quad (C-540)$$

$$\sum_{i \in HP} q_{i,p}^{abcg} + \sum_{i \in HP} q_{i,p}^{abce} = q_p^{abcc} + q_p^{abca}, p \in P \quad (C-541)$$

$$COP = C_1 e^{C_2 t_{gen}} + C_3 e^{C_4 t_{gen}} \quad (C-542)$$

$$C2G = C_5 COP + C_6 \quad (C-543)$$

$$t_{gen}^{in} = C_7 (t_{gen})^2 + C_8 t_{gen} + C_9 \quad (C-544)$$

$$t_{abs}^{in} = C_{10} t_{gen} + C_{11} \quad (C-545)$$

$$A_{i,j,k} \geq \frac{q_{i,j,k,p}}{U_{i,j,k,p} LMTD_{i,j,k,p}}, \quad i \in HP, j \in CP, k \in ST, p \in P \quad (C-546)$$

$$A_i^{cu} \geq \frac{q_{i,p}^{cu}}{U_{i,p}^{cu} LMTD_{i,p}^{cu}}, \quad i \in HP, p \in P \quad (C-547)$$

$$A_j^{hu} \geq \frac{q_{j,p}^{hu}}{U_{j,p}^{hu} LMTD_{j,p}^{hu}}, \quad j \in CP, p \in P \quad (C-548)$$

$$A_i^{evap} \geq \frac{q_{i,p}^{evap}}{U_{i,p}^{evap} LMTD_{i,p}^{evap}}, \quad i \in HP, p \in P \quad (C-549)$$

$$A_j^{cond} \geq \frac{q_{j,p}^{cond}}{U_{j,p}^{cond} LMTD_{j,p}^{cond}}, \quad j \in CP, p \in P \quad (C-550)$$

$$A^{acu} \geq \frac{q_p^{acu}}{U_p^{acu} LMTD_p^{acu}} \quad (C-551)$$

$$A_i^{abcg} \geq \frac{q_{i,p}^{abcg}}{U_{i,p}^{abcg} LMTD_{i,p}^{abcg}}, \quad i \in HP, p \in P \quad (C-552)$$

$$A_i^{abce} \geq \frac{q_{i,p}^{abce}}{U_{i,p}^{abce} LMTD_{i,p}^{abce}}, \quad i \in HP, p \in P \quad (C-553)$$

$$A^{abca} \geq \frac{q_p^{abca}}{U_p^{abca} LMTD_p^{abca}}, \quad p \in P \quad (C-554)$$

$$A^{abcc} \geq \frac{q_p^{abcc}}{U_p^{abcc} LMTD_p^{abcc}}, \quad p \in P \quad (C-555)$$

$$W_{pump}^{max} \geq W_{pump,p}, p \in P \quad (C-556)$$

$$W_{turb}^{max} \geq W_{turb,p}, p \in P \quad (C-557)$$

$$q_{p,lv}^{charh} = q_{p,lv}^{discharc} = \sum_{i \in HP} \sum_{k \in ST} q_{i,k,p,lv}^{stoc}, \quad i \in HP, k \in ST, p \in P, lv \in LV \quad (C-558)$$

$$q_{p,lv}^{charc} = q_{p,lv}^{discharh} = \sum_{j \in CP} \sum_{k \in ST} q_{j,k,p,lv}^{stoh}, \quad j \in CP, k \in ST, p \in P, lv \in LV \quad (C-559)$$

$$Q_{p,lv}^h = Q_{lv,start}^h + \sum_{p=1}^p q_{p,lv}^{charh} DOP_p - \sum_{p=1}^p q_{p,lv}^{discharh} DOP_p, p \in P, lv \in LV \quad (C-560)$$

$$Q_{p,lv}^c = Q_{lv,start}^c + \sum_{p=1}^p q_{p,lv}^{charc} DOP_p - \sum_{p=1}^p q_{p,lv}^{discharc} DOP_p, p \in P, lv \in LV \quad (C-561)$$

$$\max\{Q_{p,lv}^h\} - \min\{Q_{p,lv}^h\} = (t_{lv}^{sth} - t_{lv}^{stc}) cp_{st} M_{lv}^{sth}, p \in P, lv \in LV \quad (C-562)$$

$$\max\{Q_{p,lv}^c\} - \min\{Q_{p,lv}^c\} = (t_{lv}^{sth} - t_{lv}^{stc}) cp_{st} M_{lv}^{stc}, p \in P, lv \in LV \quad (C-563)$$

$$\frac{M_{lv}^{sth}}{\rho_{st}} = V_{lv}^{sth}, lv \in LV \quad (C-564)$$

$$\frac{M_{lv}^{stc}}{\rho_{st}} = V_{lv}^{stc}, lv \in LV \quad (C-565)$$

$$t_{1,lv}^{stoc} = t_{1,lv}^{stoh} = t_{lv}^{sth}, lv \in LV \quad (C-566)$$

$$t_{NOK+1,lv}^{stoc} = t_{NOK+1,lv}^{stoh} = t_{lv}^{stc}, lv \in LV \quad (C-567)$$

$$t_{k,lv}^{stoc} \geq t_{k+1,lv}^{stoc}, k \in ST, lv \in LV \quad (C-568)$$

$$t_{k,lv}^{stoh} \geq t_{k+1,lv}^{stoh}, k \in ST, lv \in LV \quad (C-569)$$

$$Q_{NOP,lv}^h = Q_{lv_{start}}^h, lv \in LV \quad (C-570)$$

$$Q_{NOP,lv}^c = Q_{lv_{start}}^c, lv \in LV \quad (C-571)$$

$$Q_{p,lv}^c = Q_{p,lv+1}^h, \forall lv < NOLV \quad (C-572)$$

$$M_{lv}^{stc} = M_{lv+1}^{sth}, \forall lv < NOLV \quad (C-573)$$

$$t_{lv}^{stc} = t_{lv+1}^{sth}, \forall lv < NOLV \quad (C-574)$$

$$q_{p,lv}^{charh} \leq \Psi y_{lv}^{charge}, p \in P, lv \in LV \quad (C-575)$$

$$q_{p,lv}^{charc} \leq \Psi (1 - y_{lv}^{charge}), p \in P, lv \in LV \quad (C-576)$$

$$q_{i,k,p,lv}^{stoc} - \Omega z_{i,k,lv}^{stoc} \leq 0, \quad i \in HP, k \in ST, p \in P, lv \in LV \quad (C-577)$$

$$q_{j,k,p,lv}^{stoh} - \Omega z_{j,k,lv}^{stoh} \leq 0, \quad j \in CP, k \in ST, p \in P, lv \in LV \quad (C-578)$$

$$\Delta T_{min} \leq dt1_{i,k,p}^{stoc} \leq t_{i,k,p} - t_{k,p,lv}^{stoc} + \Gamma(1 - z_{i,k,lv}^{stoc}), \quad i \in HP, k \in ST, p \in P, lv \in LV \quad (C-579)$$

$$\Delta T_{min} \leq dt2_{i,k,p}^{stoc} \leq t_{i,k+1,p} - t_{k+1,p,lv}^{stoc} + \Gamma(1 - z_{i,k,lv}^{stoc}), \quad i \in HP, k \in ST, p \in P, lv \in LV \quad (C-580)$$

$$\Delta T_{min} \leq dt1_{j,k,p}^{stoh} \leq t_{j,k,p} - t_{k,p,lv}^{stoh} + \Gamma(1 - z_{j,k,lv}^{stoh}), \quad j \in CP, k \in ST, p \in P, lv \in LV \quad (C-581)$$

$$\Delta T_{min} \leq dt2_{j,k,p}^{stoh} \leq t_{j,k+1,p} - t_{k+1,p,lv}^{stoh} + \Gamma(1 - z_{j,k,lv}^{stoh}), \quad j \in CP, k \in ST, p \in P, lv \in LV \quad (C-582)$$

$$A_{i,k,lv}^{stoc} \geq \frac{q_{i,k,p,lv}^{stoc}}{U_{i,k,p}^{stoc} LMTD_{i,k,p}^{stoc}}, \quad i \in HP, k \in ST, p \in P, lv \in LV \quad (C-583)$$

$$A_{j,k,lv}^{stoh} \geq \frac{q_{j,k,p,lv}^{stoh}}{U_{j,k,p}^{stoh} LMTD_{ijk,p}^{stoh}}, \quad j \in CP, k \in ST, p \in P, lv \in LV \quad (C-584)$$

min TAC

$$= \left\{ \begin{aligned} & H_y \sum_{p \in P} \left(\frac{DOP_p}{\sum_{p \in P} DOP_p} \right) \left(+ \sum_{j \in CP} c_{hu} q_{j,p}^{hu} + \sum_{i \in HHP} c_{cu} q_{i,p}^{cu} + c_{cu} q_p^{acu} \right) \\ & + AF c_{fix}^{HEN} \left(\begin{aligned} & \sum_{i \in HHP} \sum_{j \in CP} \sum_{k \in ST} z_{i,j,k} + \sum_{i \in HHP} z_i^{cu} + \sum_{j \in CP} z_j^{hu} \\ & + \sum_{i \in HHP} z_i^{evap} + \sum_{j \in CP} z_j^{cond} + z^{acu} \\ & + \sum_{i \in HHP} z_i^{abcg} + \sum_{i \in HHP} z_i^{abce} \\ & \sum_{i \in HHP} \sum_{k \in ST} \sum_{lv \in LV} z_{i,k,lv}^{stoc} + \sum_{j \in CP} \sum_{k \in ST} \sum_{lv \in LV} z_{j,k,lv}^{stoh} \end{aligned} \right) \\ & + AF c_{var}^{HEN} \left(\begin{aligned} & \sum_{i \in HHP} \sum_{j \in CP} \sum_{k \in ST} (A_{i,j,k})^\beta + \sum_{i \in HHP} (A_i^{cu})^\beta + \sum_{j \in CP} (A_j^{hu})^\beta \\ & + \sum_{i \in HHP} (A_i^{evap})^\beta + \sum_{j \in CP} (A_j^{cond})^\beta + (A^{acu})^\beta \\ & + \sum_{i \in HHP} (A_i^{abcg})^\beta + \sum_{i \in HHP} (A_i^{abce})^\beta + (A^{abca})^\beta + (A^{abcc})^\beta \\ & \sum_{i \in HHP} \sum_{k \in ST} \sum_{lv \in LV} (A_{i,k,lv}^{stoc})^\beta + \sum_{j \in CP} \sum_{k \in ST} \sum_{lv \in LV} (A_{j,k,lv}^{stoh})^\beta \end{aligned} \right) \\ & + AF \left(c_{fix}^{pump} + c_{var}^{pump} (W_{pump}^{max})^{\beta^{pump}} \right) + AF \left(c_{fix}^{pump} + c_{var}^{turb} (W_{turb}^{max})^{\beta^{turb}} \right) \\ & + AF \left(\sum_{lv \in LV} c_{fix}^{sto} + c_{var}^{sto} \sum_{lv \in LV} (V_{lv}^{sth})^{\beta^{sto}} \right) + AF \left(c_{fix}^{sto} + c_{var}^{sto} (V_{NOLV}^{stc})^{\beta^{sto}} \right) \end{aligned} \right\} \quad (C-585)$$

Appendix D Additional results from Case Studies

D.1 HEN1

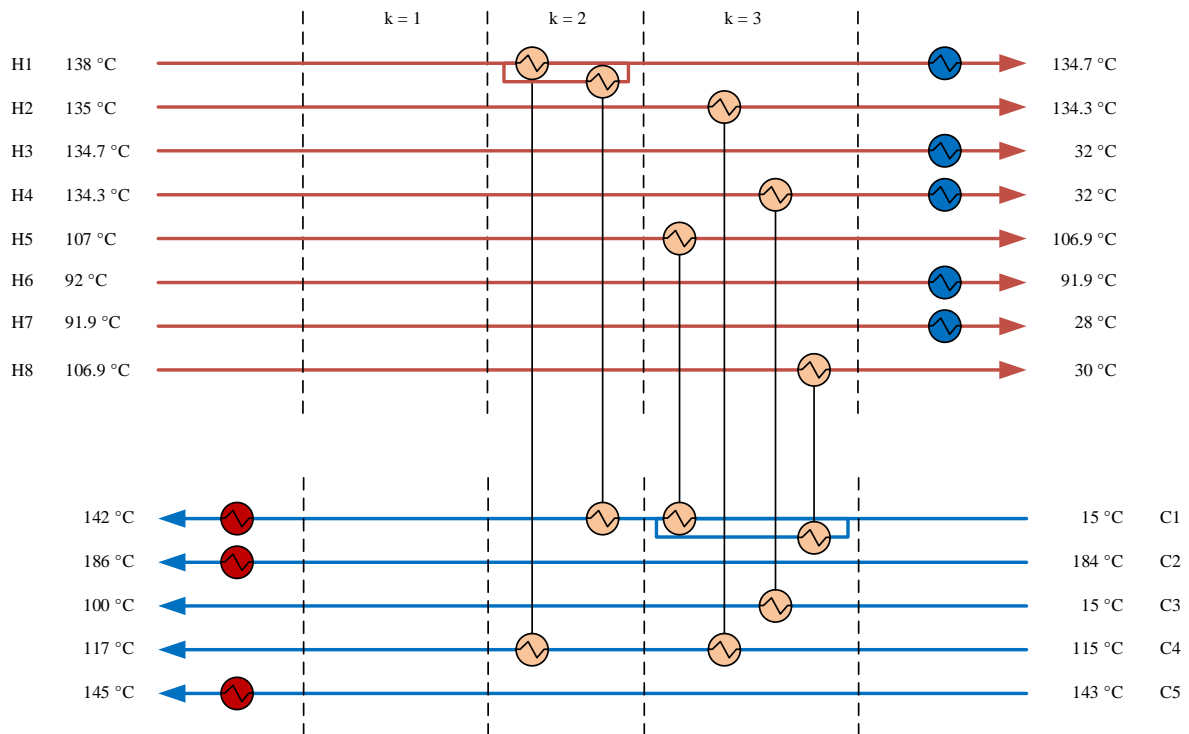


Figure D-1. Grid diagram HEN1 for Case Study 1

Source: Own diagram

Table D-1. Heat exchanger information for HEN1 in Case Study 1

Type of Heat Exchanger	Match	Area (m ²)	Heat Exchanger Duty (kW)
Intra-Process (i,j,k)	1,1,2	29.1	417.8
	1,4,2	102.8	1049.0
	2,4,3	176.4	1678.0
	4,3,3	59.1	884.0
	5,1,3	22.0	516.0
	8,1,3	36.8	319.0
	Hot Utility (j)	1	3.6
2		114.3	3999.0
5		59.5	3302.0
Cold Utility (i)	1	17.0	1066.2
	3	50.1	1468.0
	4	6.5	85.0
	6	40.4	1655.0
	7	39.9	835.0

Source: Own table

D.2 HEN2

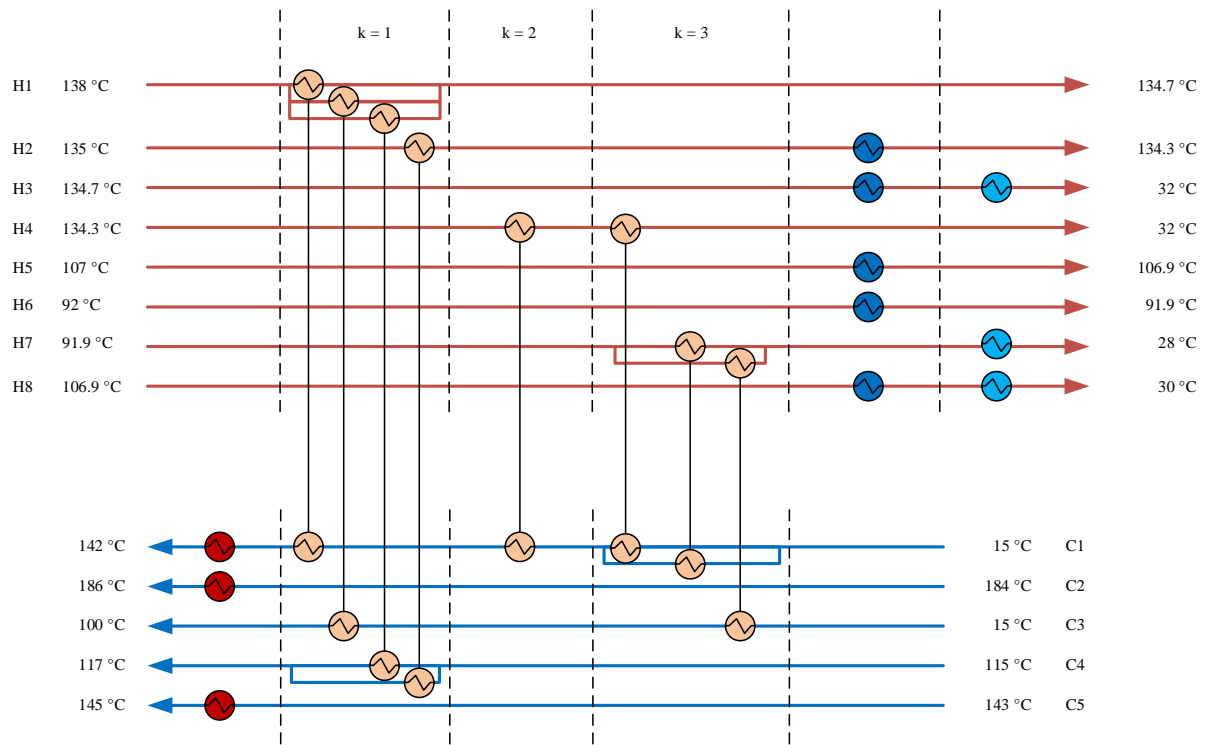


Figure D-2. Grid diagram HEN2 for Case Study 1 Source: Own diagram

Table D-2. Heat exchanger information for HEN2 in Case Study 1

Type of Heat Exchanger	Match	Area (m ²)	Heat Exchanger Duty (kW)
Intra-Process (i,j,k)	1,1,1	14.2	133.1
	1,3,1	10.2	240.2
	1,4,1	212.4	2159.6
	2,4,1	60.2	567.4
	4,1,2	43.2	401.6
	4,1,3	71.0	567.4
	7,1,3	19.4	150.7
	7,3,3	82.8	643.8
Hot Utility (j)	1	3.6	220.4
	2	114.3	3999.0
	5	59.5	3302.0
Cold Utility (i)	2	21.3	1110.6
	3	108.7	1282.2
	5	13.4	516.0
	6	53.5	1655.0
VCR (i)	8	21.8	256.8
	3	-	185.8
	7	-	40.6
	8	-	62.2

Source: Own table

D.3 HEN-ORC

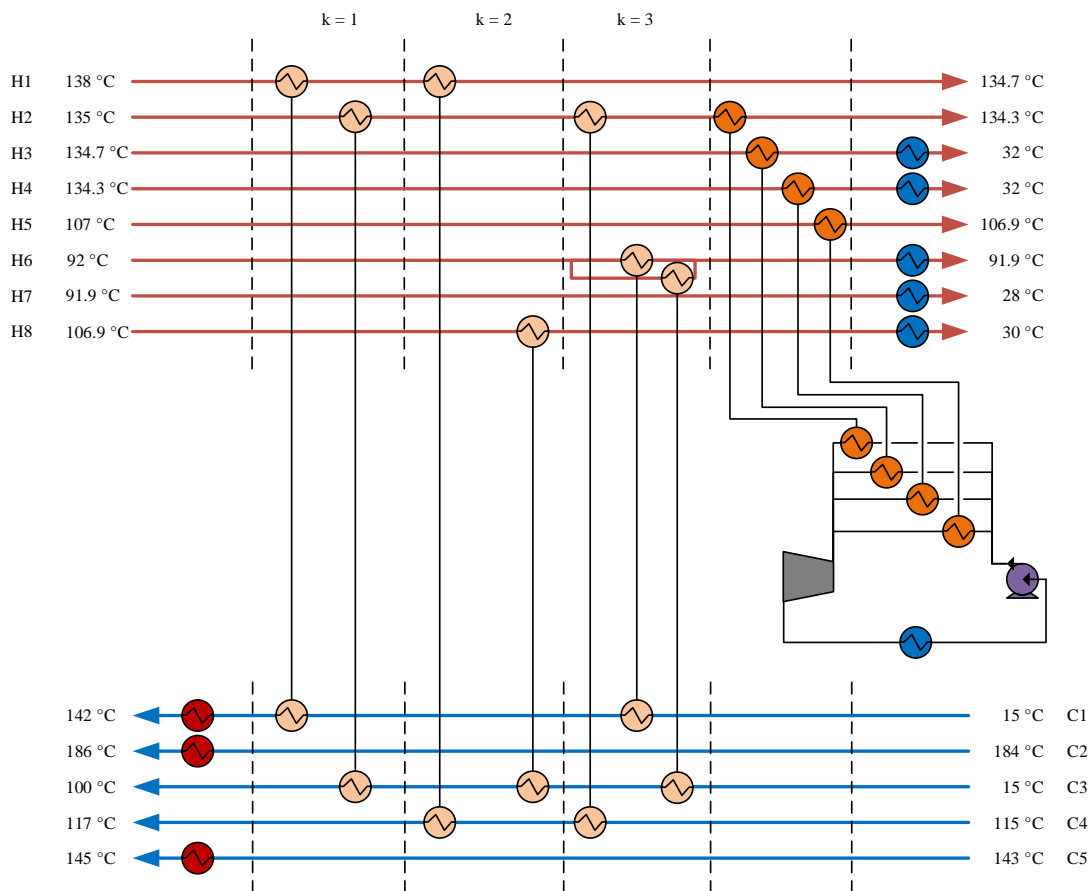


Figure D-3. Grid diagram HEN-ORC for Case Study 1

Source: Own diagram

Table D-3. Heat exchanger information for HEN-ORC in Case Study 1

Type of Heat Exchanger	Match	Area (m ²)	Heat Exchanger Duty (kW)
Intra-Process (i,j,k)	1,1,1	32.9	533.6
	2,3,1	8.3	177.4
	1,4,2	202.7	1999.4
	8,3,2	6.5	61.8
	2,4,3	74.6	727.6
	6,1,3	38.3	719
	6,3,3	34.3	644.8
	Hot Utility (j)	1	3.6
	2	114.3	3999
	5	59.5	3302
Cold Utility (i)	3	35.2	759.1
	4	23.4	504.8
	6	7.1	291
	7	39.8	835
	8	11.8	257.2

Table D-3.(Continued) Heat exchanger information for HEN-ORC in Case Study 1

Type of Heat Exchanger	Match	Area (m ²)	Heat Exchanger Duty (kW)
ORC Evaporator (i)	2	20.6	733
	3	26.1	708.9
	4	17.2	464.2
	5	23.1	516
ORC Cold Utility		221.7	2177.2

Source: Own table

D.4 HEN-ABC

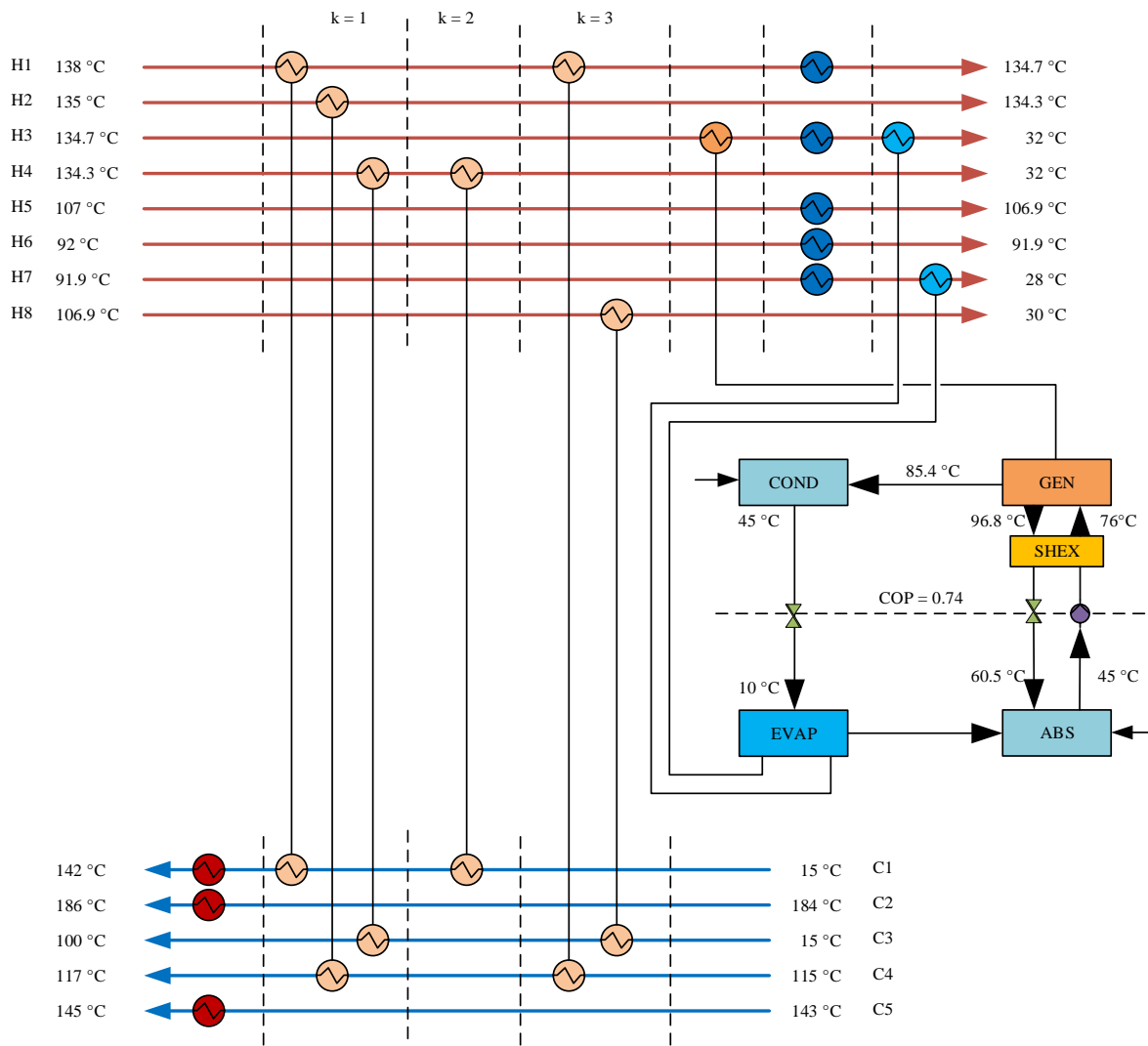


Figure D-4. Grid diagram HEN-ABC for Case Study 1

Source: Own diagram

Table D-4. Heat exchanger information for HEN-ABC in Case Study 1

Type of Heat Exchanger	Match	Area (m ²)	Heat Exchanger Duty (kW)	
Intra-Process (i,j,k)	1,1,1	41.9	848.0	
	2,4,1	183.8	1678.0	
	4,3,1	35.8	565.0	
	4,1,2	39.1	404.0	
	1,4,3	100.7	1049.0	
	8,3,3	19.5	139.0	
	Hot Utility (j)	1	3.6	220.4
	2	114.3	3999.0	
	5	59.5	3302.0	
Cold Utility (i)	1	12.1	635.2	
	3	42.6	730.6	
	5	13.4	516.0	
	6	53.4	1655.0	
	7	37.2	612.9	
	ABC- Generator (i)	3	39.3	551.6
	ABC-Evaporator (i)	3	13.3	185.8
	7	17.4	222.1	
ABC-Condenser		28.1	432.7	
ABC-Absorber		48.2	526.9	

Source: Own table

D.5 MP-HEN1

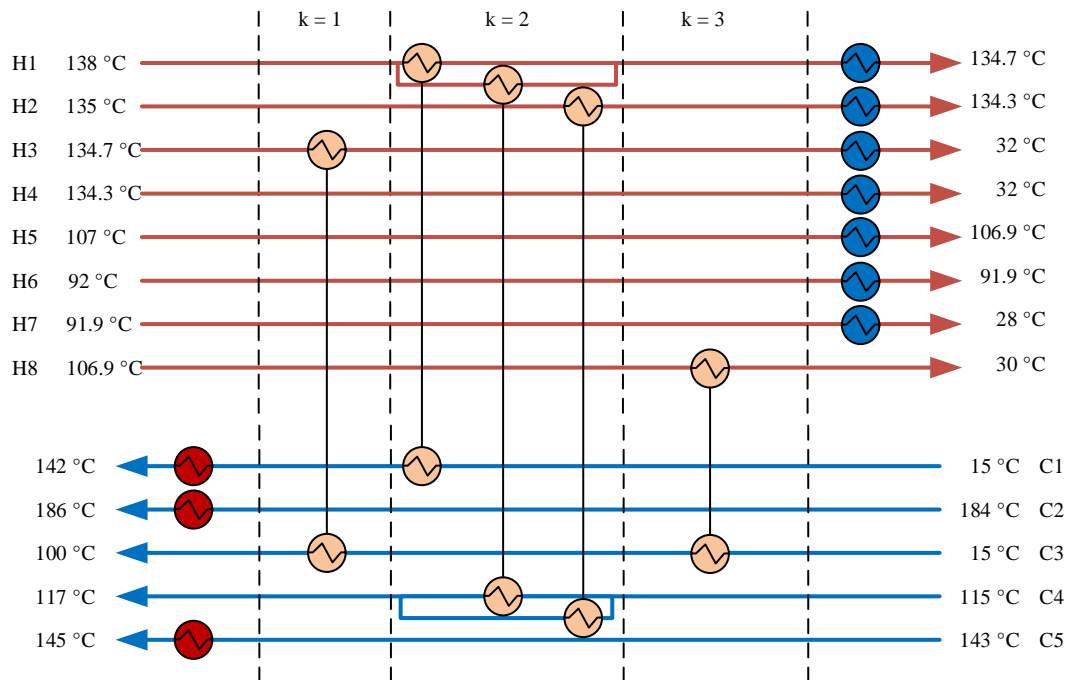


Figure D-5. Grid diagram HEN1 for Case Study 2

Source: Own diagram

Table D-5. Heat exchanger information for HEN1 in Case Study 2

Type of Heat Exchanger	Match	Maximum Area (m ²)	Heat Exchanger Duty (kW)		
			Period 1	Period 2	Period 3
Intra-Process (i,j,k)	3,3,1	27.1	0	565.0	0
	1,1,2	50.6	1252.8	1252.8	1252.8
	1,4,2	105.0	0	1075.6	0
	2,4,2	177.0	0	1651.4	0
	8,3,3	19.5	0	319.0	0
Hot Utility (j)	1	3.6	220.4	220.4	220.4
	2	114.2	3999	3999	3999
	5	59.5	0	3302	0
Cold Utility (i)	1	19.6	1280.2	204.6	1280.2
	2	25.9	1678.0	26.6	1678.0
	3	45.2	1468.0	903.0	1468.0
	4	29.9	969.0	969.0	969.0
	5	10.1	0	516.0	0
	6	38.1	0	1655.0	0
	7	34.9	0	835.0	0

Source: Own table

D.6 MP-HEN2

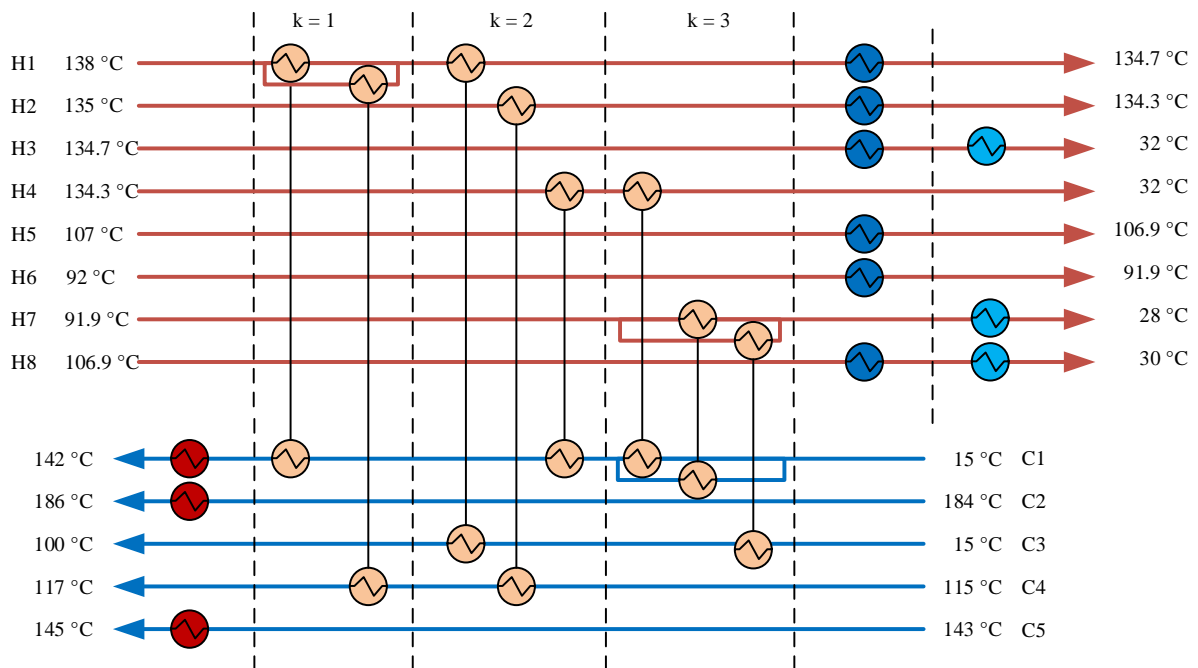


Figure D-6. Grid diagram HEN2 for Case Study 2

Source: Own diagram

Table D-6. Heat exchanger information for HEN2 in Case Study 2

Type of Heat Exchanger	Match	Maximum Area (m ²)	Heat Exchanger Duty (kW)		
			Period 1	Period 2	Period 3
Intra-Process (i,j,k)	1,1,1	22.6	283.8	133.1	283.0
	1,4,1	212.8	0	2159.6	0
	1,3,2	10.6	0	240.4	0
	2,4,2	57.7	0	567.4	0
	4,1,2	43.1	436.4	401.6	323.6
	4,1,3	71.0	532.6	567.4	645.4
	7,1,3	19.4	0	150.7	0
	7,3,3	82.8	0	643.8	0
Hot Utility (j)	1	3.6	220.4	220.4	220.4
	2	114.2	3999	3999	3999
	5	59.5	0	3302	0
Cold Utility (i)	1	42.4	2249.2	0	2249.2
	2	32.1	1678.0	1110.6	1678.0
	3	56.4	1282.2	1282.2	1282.2
	5	13.4	0	516.0	0
	6	53.4	0	1655.0	0
	8	13.7	0	256.8	0
VCR(i)	3	-	185.8	185.8	185.8
	7	-	0	40.6	0
	8	-	0	62.2	0

Source: Own table

D.7 MP-ORC

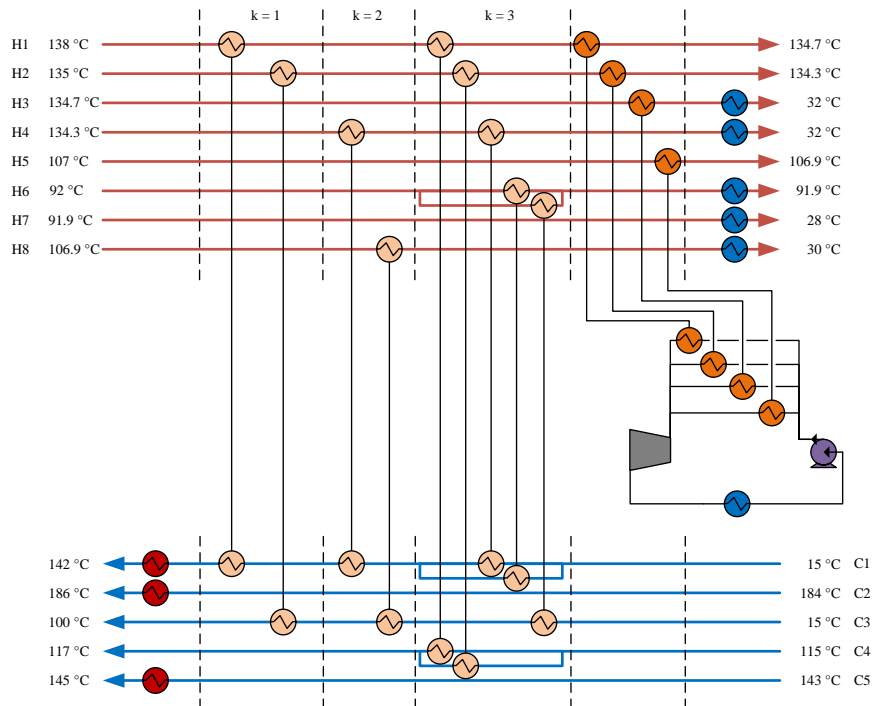


Figure D-7. Grid diagram MP-ORC for Case Study 2

Source: Own diagram

Table D-7. Heat exchanger information for MP-ORC in Case Study 2

Type of Heat Exchanger	Match	Maximum Area (m ²)	Heat Exchanger Duty (kW)		
			Period 1	Period 2	Period 3
Intra-Process (i,j,k)	1,1,1	22.59	283.8	132.93	283.8
	2,3,1	8.26		177.39	
	4,1,2	43.06	629.64	400.67	629.64
	8,3,2	6.46	0	61.81	0
	1,4,3	236.96	0	2400.07	0
	2,4,3	34.7	0	326.93	0
	4,1,3	33.76	339.36	398	339.36
	6,1,3	17.1	0	321.2	0
	6,3,3	34.32	0	644.8	0
Hot Utility (j)	1	3.61	220.4	220.4	220.4
	2	114.27	3999	3999	3999
	5	59.5	0	3302	0
Cold Utility (i)	3	37.77	858.49	858.49	858.49
	4	11.32	0	170.33	0
	6	16.82	0	389	0
	7	39.85	0	835	0
	8	11.76	0	257.19	0
ORC Evaporator (i)	1	61.54	2249.2	0	2249.2
	2	47.19	1678	1173.68	1678
	3	22.57	609.52	609.52	609.52
	5	26.25	0	516	0
ORC Cold Utility		336.97	3978.66	2016.38	3978.66

Source: Own table

Table D-8. Turbine and pump information for MP-ORC in Case Study 2

Type of Component	Maximum Duty (kW)	Duty (kW)		
		Period 1	Period 2	Period 3
Turbine	570.41	570.41	289.02	570.41
Pump	12.26	12.26	6.21	12.26

Source: Own table

D.8 MP-ABC

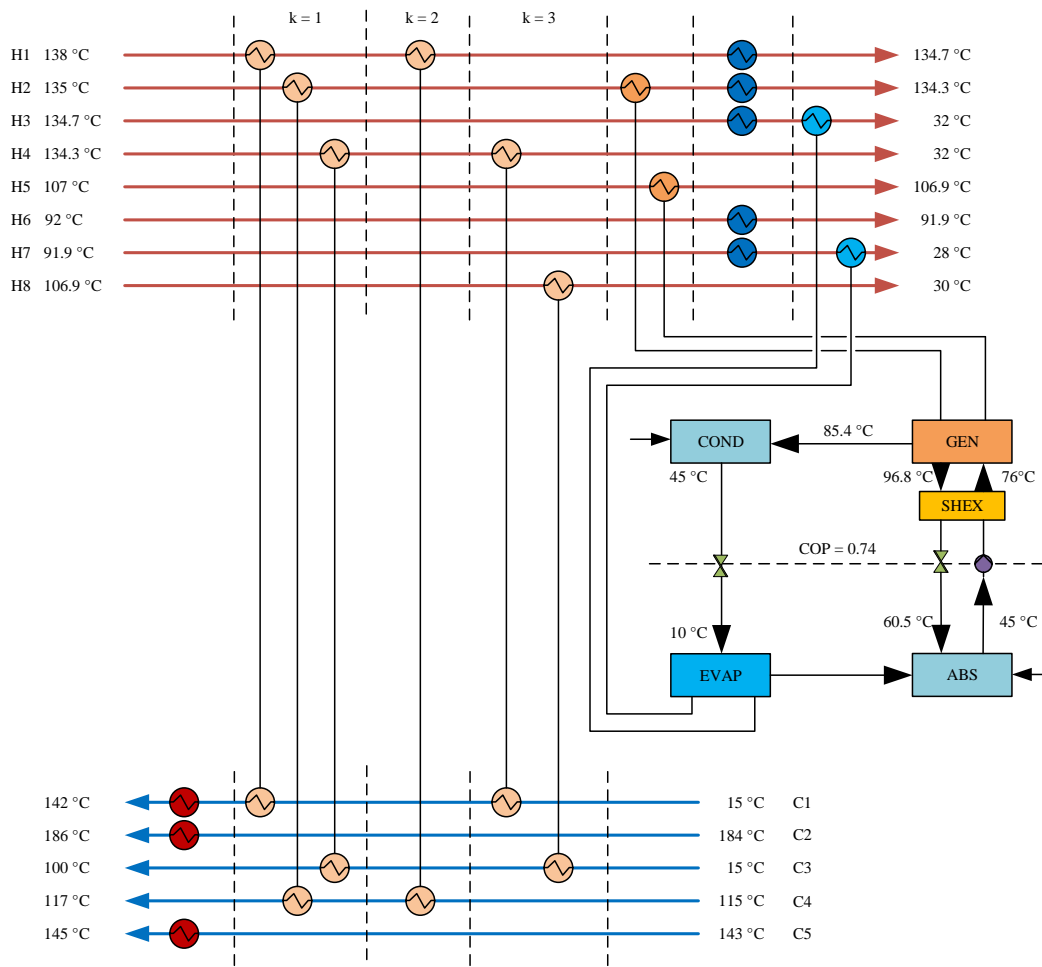


Figure D-8. Grid diagram MP-ABC for Case Study 2

Source: Own diagram

Table D-9. Heat exchanger information for MP-ABC in Case Study 2

Type of Heat Exchanger	Match	Maximum Area (m ²)	Heat Exchanger Duty (kW)		
			Period 1	Period 2	Period 3
Intra-Process (i,j,k)	1,1,1	22.59	283.8	283.8	283.8
	2,4,1	176.37	0	1609.59	0
	3,3,1	27.12	0	565	0
	1,4,2	103.99	0	1117.41	0
	4,1,3	76.85	969	969	969
	8,3,3	19.5	0	319	0
	Hot Utility (j)	1	3.61	220.4	220.4
2		114.27	3999	3999	3999
5		59.5	0	3302	0
Cold Utility (i)	1	42.38	2249.2	1131.79	2249.2
	2	27	1411.81	0	1411.81
	3	56.4	1282.18	717.18	1282.18
	6	53.43	0	1655	0
	7	47.27	0	612.87	0

Table D-9. (Continued) Heat exchanger information for MP-ABC in Case Study 2

Type of Heat Exchanger	Match	Maximum Area (m ²)	Heat Exchanger Duty (kW)		
			Period 1	Period 2	Period 3
ABC- Generator (i)	2	10.44	266.19	68.41	266.19
	5	46.08	0	516	0
ABC-Evaporator (i)	3	13.28	185.82	185.82	185.82
	7	17.38	0	222.14	0
ACB-Condenser		28.09	197.08	432.68	197.08
ABC-Absorber		52.62	254.93	559.7	254.93

Source: Own table

D.9 MP-ST-HEN1

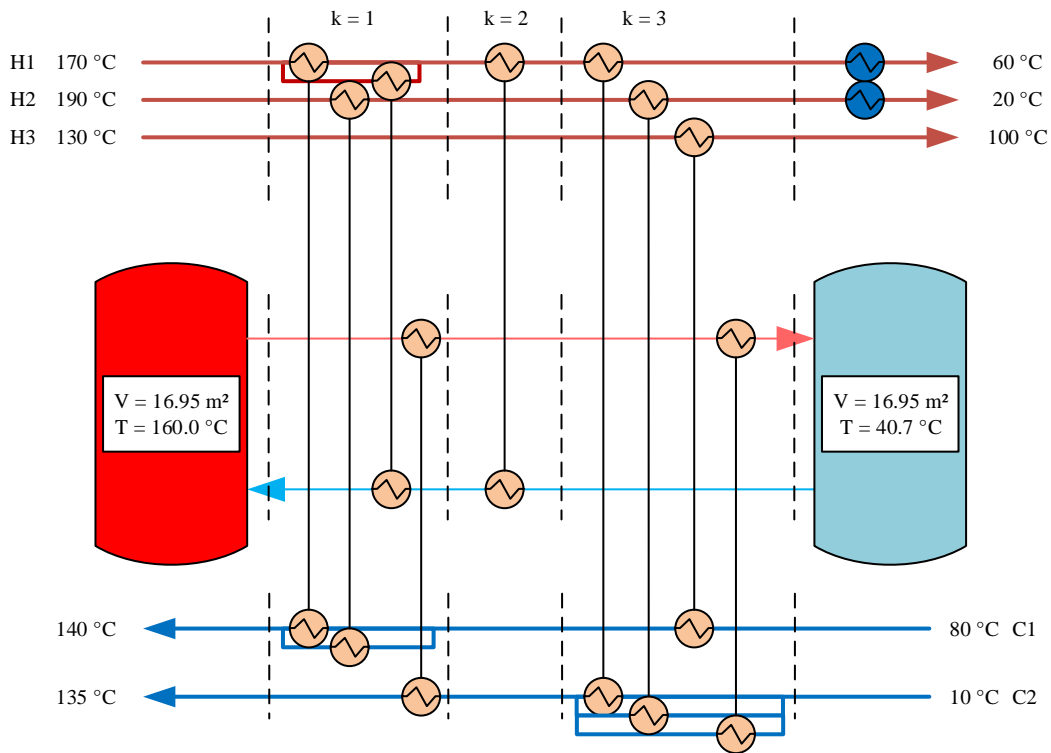


Figure D-9. Grid diagram HEN1 for Case Study 3

Source: Own diagram

Table D-10. Heat exchanger information for HEN1 in Case Study 3

Type of Heat Exchanger	Match	Maximum Area (m ²)	Heat Exchanger Duty (kW)			
			Period 1	Period 2	Period 3	Period 4
Intra-Process (i,j,k)	1,1,1	19.8	180.0	240.0	148.7	0.0
	2,1,1	24.3	300.0	240.0	281.2	0.0
	1,2,3	16.2	0.0	200.0	0.0	0.0
	2,2,3	24.5	0.0	215.0	0.0	0.0
	3,1,3	3.3	0.0	0.0	50.1	0.0
Cold Utility (i)	1	1.8	51.3	0.0	54.7	12.1

Table D-10.(Continued) Heat exchanger information for HEN1 in Case Study 3

Type of Heat Exchanger	Match	Maximum Area (m ²)	Heat Exchanger Duty (kW)			
			Period 1	Period 2	Period 3	Period 4
	2	11.0	210.0	55.0	228.8	0.0
Hot Streams to Cold Storage (i,k,l _v)	1,1,1	45.4	140.0	0.0	146.3	320.0
	1,2,1	10.4	68.7	0.0	90.3	107.9
Cold Streams to Hot Storage (j,k,l _v)	2,1,1	42.8	0.0	350.0	0.0	0.0
	2,3,1	52.6	0.0	485.0	0.0	0.0

Source: Own table

D.10 MP-ST-HEN2

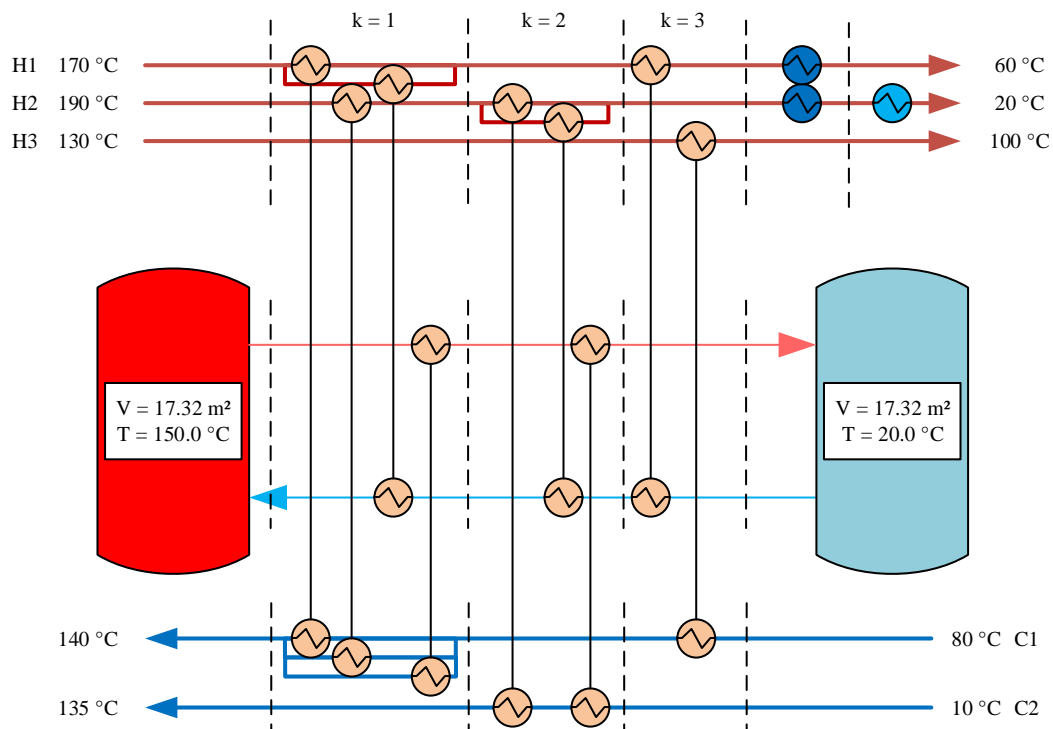


Figure D-10. Grid diagram HEN2 for Case Study 3

Source: Own diagram

Table D-11. Heat exchanger information for HEN2 in Case Study 3

Type of Heat Exchanger	Match	Maximum Area (m ²)	Heat Exchanger Duty (kW)			
			Period 1	Period 2	Period 3	Period 4
Intra-Process (i,j,k)	1,1,1	35.2	180.0	320.0	278.6	0.0
	2,1,1	24.3	300.0	135.0	151.3	0.0
	2,2,2	47.8	0.0	345.0	0.0	0.0
	3,1,3	5.0	0.0	0.0	50.1	0.0
Cold Utility (i)	1	6.0	0.0	120.0	26.3	0.0
	2	13.5	180.0	0.0	198.8	0.0
Hot Streams to Cold Storage (i,k,l _v)	1,1,1	32.4	140.0	0.0	0.0	320.0

Table D-11.(Continued). Heat exchanger information for HEN2 in Case Study 3

	1,3,1	27.0	120.0	0.0	135.1	120.0
	2,1,1	18.0	0.0	0.0	129.9	0.0
Cold Streams to Hot Storage (j,k,lv)	1,1,1	1.9	0.0	25.0	0.0	0.0
	2,2,1	168.6	0.0	905.0	0.0	0.0
VCR(i)	2	-	30.0	30.0	30.0	0.0

Source: Own table

D.11 MP-ST-ORC

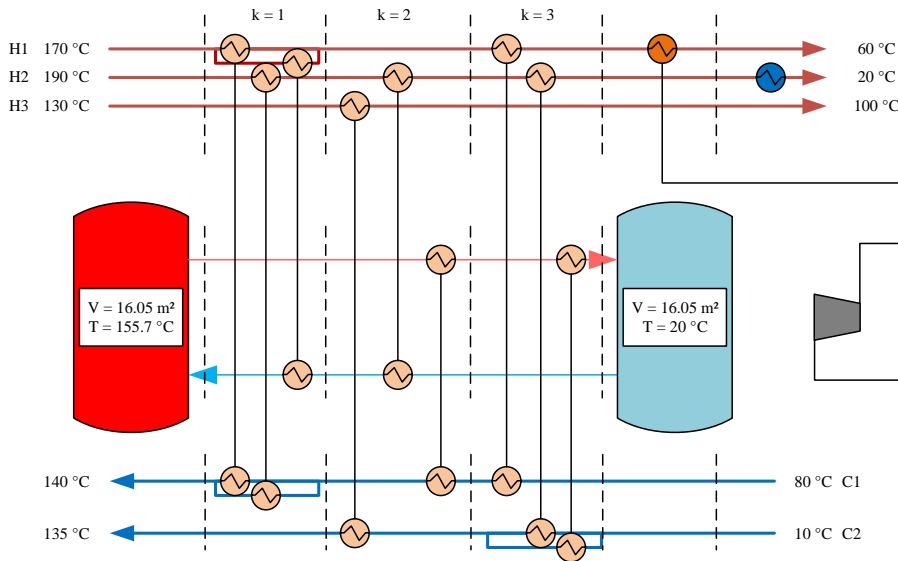


Figure D-11. Grid diagram MP-ST-ORC for Case Study 3

Source: Own diagram

Table D-12. Heat exchanger information for MP-ST-ORC in Case Study 3

Type of Heat Exchanger	Match	Maximum Area (m²)	Heat Exchanger Duty (kW)			
			Period 1	Period 2	Period 3	Period 4
Intra-Process (i,j,k)	1,1,1	19.8	180.0	100.0	117.4	0.0
	2,1,1	24.3	300.0	122.0	262.4	0.0
	3,1,2	4.2	0.0	0.0	50.1	0.0
	1,1,3	21.2	0.0	220.0	50.1	0.0
	2,2,3	64.5	0.0	399.0	0.0	0.0
Cold Utility (i)	1	0.5	13.3	13.3	13.3	13.3
	2	7.0	99.1	0.0	72.5	0.0
Hot Streams to Cold Storage (i,k,lv)	1,1,1	25.4	140.0	0.0	152.5	320.0
	2,2,1	21.8	110.9	0.0	175.0	0.0
Cold Streams to Hot Storage (j,k,lv)	1,2,1	1.8	0.0	38.0	0.0	0.0
	2,3,1	139.9	0.0	862.0	0.0	0.0
ORC-Evaporator (i)	1	5.9	106.7	106.7	106.7	106.7
ORC-Cold Utility		9.5	97.8	97.8	97.8	97.8

Source: Own table

Table D-13. Turbine and pump information for MP-ST-ORC in Case Study 3

Type of Component	Maximum Duty (kW)	Duty (kW)			
		Period 1	Period 2	Period 3	Period 4
Turbine	9.23	9.23	9.23	9.23	9.23
Pump	0.28	0.28	0.28	0.28	0.28

Source: Own table

D.12 MP-ST-ABC

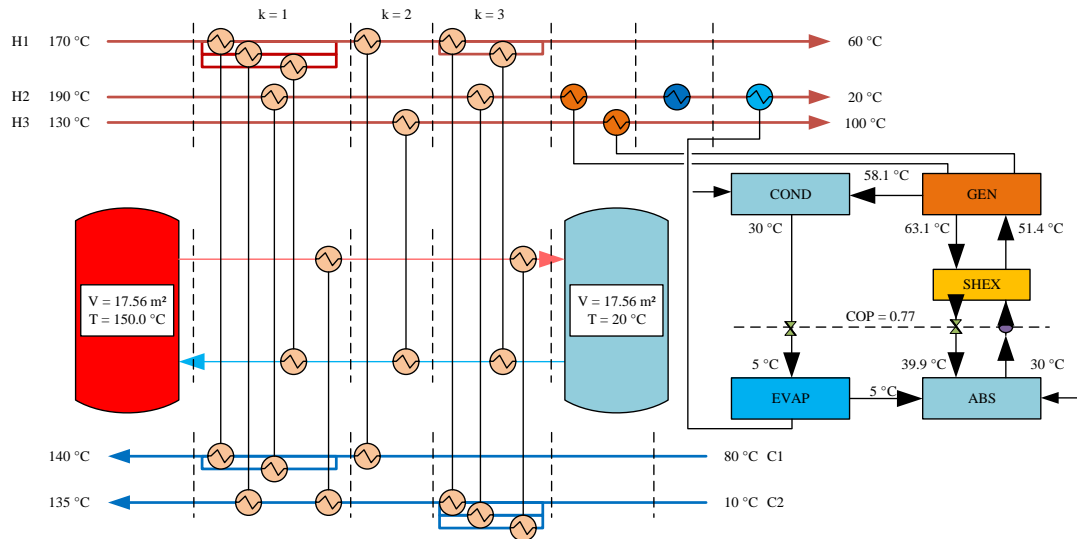


Figure D-12. Grid diagram MP-ST-ABC for Case Study 3

Source: Own diagram

Table D-14. Heat exchanger information for MP-ST-ABC in Case Study 3

Type of Heat Exchanger	Match	Maximum Area (m ²)	Heat Exchanger Duty (kW)			
			Period 1	Period 2	Period 3	Period 4
Intra-Process (i,j,k)	1,1,1	19.8	180.0	180.0	145.7	0.0
	1,2,1	14.1	0.0	140.0	0.0	0.0
	2,1,1	24.3	300.0	300.0	279.5	0.0
	1,1,2	8.4	0.0	0.0	54.8	0.0
	1,2,3	9.7	0.0	120.0	0.0	0.0
	2,2,3	3.3	0.0	47.0	0.0	0.0
Cold Utility (i)	2	11.7	141.2	94.1	175.4	0.0
Hot Streams to Cold Storage (i,k,lv)	1,1,1	19.4	140.0	0.0	119.5	243.3
	1,3,1	11.1	120.0	0.0	120.0	196.7
	3,2,1	2.2	0.0	0.0	36.4	0.0
Cold Streams to Hot Storage (j,k,lv)	2,1,1	57.7	0.0	410.0	0.0	0.0
	2,3,1	91.5	0.0	533.0	0.0	0.0
ABC-Generator (i)	2	7.3	38.8	38.8	25.1	0.0
	3	0.6	0.0	0.0	13.7	0.0
ABC-Evaporator (i)	2	3.1	30.0	30.0	30.0	0.0
ABC-Condenser		3.0	31.3	31.3	31.3	0.0
ABC-Absorber		5.2	37.6	37.6	37.6	0.0

Source: Own table

Appendix E Extended State-of-the-Art

Table E-1. Extended State-of-the-Art for the Process Integration of Organic Rankine Cycles and Absorption Chillers into Heat Exchanger Networks

	Waste Heat Recovery Technology		Approach		Type of Process		Working Fluid/Pair Properties	Main Contribution	
	ORC	ABC	PA	MP		Cont.			Discont.
				SQ	SM				
Chamorro-Romero (2023) *	x	x		x	x	x	x	Integration of HEN, ORC and ABC considering working fluid/pair properties. First formulation including discontinuous processes (Multi-period with and without FTVM Heat Storage). Multiple storage levels (more than 2 storage tanks) possible and size and temperatures are part of the optimization variables.	
Elsido et al. (2021)	x			x		x	x	Extension of Elsidido et al. (2017) and Elsidido et al. (2019) for multi-period processes. Includes two-tank storage systems (FTVM storages) with know temperatures. First formulation for the integration of ORCs into multi-period HENs.	
Chamorro-Romero and Radgen (2020)	x			x	x		x	Extension of Chen, et-al (2014) to include indirect integration between ORC and Process Streams using intermediate HTFs in HRLs.	
Huang et al. (2020)	x			x	x		x	Similar to Dong et al. (2020) but includes also Steam Rankine Cycles and Cooling Tower into the formulation.	
Dong et al. (2020)	x			x	x		x	Extension of Chen, et-al (2014) integrating working fluid properties into the optimization.	
Xu et al. (2020)	x			x	x		x	Extension of Chen, et-al (2014) for multi-objective optimization. Working fluid temperature as variables.	
Sun, et-al (2020b)		x		x	x		x	Different arrangement for ABC and VCR than in Sun, et-al (2020a).	
Sun, et-al (2020a)		x		x	x		x	Consideration of hybrid system combining ABCs and VCRs.	
Sun, et-al (2019)		x		x	x		x	Consideration of the working pair properties and temperatures inside of the ABCs.	
Elsido et al. (2019)	x			x	x		x	Extension of Elsidido et al. (2017) for better computatioanal performance. Bilevel decompostion of MINLP. Master problem (upper level) optimizes HEN structure (binary variables) using a linearized objective function. Continuous variables are then re-optimized solving a NLP (lower level).	

Kermani et al. (2018)	x		x	x	x	General superstructure including most of the possible ORC configurations (multiple pressure levels, regeneration, superheating, transcritical, etc.)
Elsido, et-al (2017)	x		x	x	x	Consideration of multiple pressure levels for ORC expansion and use of metaheuristics for the MINLP. Extension of Chen, et-al (2014).
Yu et al. (2017b)	x		x	x	x	MP formulation considering intermediate HTF (Water) for the connection between ORC and Process Streams.
Yu et al. (2017a)	x		x	x	x	MP formulation including working fluid properties and temperatures into the optimization problem.
Yu et al. (2016)	x	x		x	x	Case Study Refinery for the integration of ORC in HEN using Intermediate HTF (Water). Method based on PA.
Chen, et-al (2015)	x		x	x	x	Extension of Chen, et-al (2014) for Transcritical Cycles.
Chen, et-al (2014)	x		x	x	x	Consideration of Latent Heat of Evaporation and thermophysical properties of the working fluids. Calculated independently of the optimization model.
Lira-Barragan, et-al (2014b)		x		x	x	Extension of Lira-Barragan, et-al (2013) to include Heat Storage design for the Solar Energy.
Hipolito-Valencia, et-al (2014a)	x	x		x	x	Extension of Lira-Barragan, et-al (2014a, 2014c) for interplant integration.
Hipolito-Valencia, et-al (2014c)	x			x	x	Case Study Bioethanol Separation Plant using Hipolito-Valencia, et-al (2013)
Hipolito-Valencia, et-al (2014b)	x			x	x	Interplant integration of ORCs into HENs. Extension of Hipolito-Valencia, et-al (2013)
Lira-Barragan, et-al (2014a,2014c)	x	x		x	x	First MP model for the simultaneous integration of ORCs and ABCs into HENs. Combination of Hipolito-Valencia, et-al (2013) and Lira-Barragan, et-al (2013).
Hipolito-Valencia, et-al (2013)	x			x	x	First MP formulation for the integration of ORCs into HENs. Extension of SYNHEAT (Yee and Grossmann, 1990).
Lira-Barragan, et-al (2013)		x		x	x	First MP formulation for the integration of ABC into HENs. ABC could be driven by Process Streams or Hot Utility (including solar energy).
Ponce-Ortega et al., 2011		x	(x)		x	Extension of Tora and El-Halwagi (2010) for multi-objective optimization (NLP). No HEN synthesis.
Tora and El-Halwagi (2010)		x	(x)		x	First dedicated study on the integration of ABCs into Industrial Processes using PA. HEN was not generated.
Desai and Bandyopadhyay (2009)	x		x		x	First dedicated study on the integration of ORCs into HEN using PA.

Townsend and Linnhoff (1983b)	x	(x)	x	x	x	Consideration of technical limitations and shapes of heat profiles of working fluids in Steam, ORC and Bryton cycles.
Townsend and Linnhoff (1983a)	x	(x)	x	x		Pinch rules for the integration of Heat Engines and Heat Pumps into Industrial Processes.

¹⁾ Absorption chillers were not mentioned but general pinch rules for the integration of Heat Pumps were provided.

²⁾ No HEN synthesis considered. Pinch rules for the integration of ABCs into HEN explicitly presented.

ORC: Organic Rankine Cycle; ABC: Absorption Refrigeration/Chiller; PA: Pinch Analysis; MP: Mathematical Programming; SQ: Sequential Method; SM: Simultaneous Method

Source: *Own table*

Appendix F Estimations of theoretical industrial waste heat potentials (Ext.)

Table F-1. Estimations of theoretical industrial waste heat potentials (Extended)

Source	Area	Approach	Temperature Level	Estimation (PJ/a)	Type of Potential	Ref. Year	Comments
Papapetrou et al. (2018)	EU	Top-Down	< 100°C	4.5	Theoretical	2015	1. Based on waste heat fractions per industry, country and temperature level.
			100-200°C	360.0			2. Waste heat fractions per industry and temperature level taken from UK study by Hammond (2014) with reference years 2000-2003.
			200-500°C	280.8			3. Data adjusted for country using energy intensities for country and industrial sector and for energy efficiency improvements between 2000-2003 and 2015.
			>500°C	446.4			
Brücker et al. (2017)	Germany	Bottom-Up	>35°C	223.0	Theoretical	2008	1. Based on German emission report data 2. Data set of 81000 emitters (127 PJ) 3. Value for the whole industrial sector was extrapolated.
Forman et al. (2015)	World	Top-Down	<100°C	13399.0	Theoretical	2012	1. Based on world energy balance from the IEA and assumed efficiencies for typical devices, processes and energy sources in the different sectors.
			100-299°C	6380.0			2. Includes other sectors (transport, commercial, residential, etc.)
			>=300°C	12123.0			3. Data presented is only for the industrial waste heat.
Persson et al. (2014)	EU	Top-Down	N.A	2924.0	Theoretical	2010	1. Based on CO2 emissions of industrial sites from European Pollutant Release and Transfer Register (E-PRTR). 2. CO2 to Energy Consumption using characteristic carbon dioxide emission factors reflecting average national fuel mixes per main activity sector. 3. Energy to waste heat using recovery efficiencies per Industrial Sector.
Pehnt et al. (2010)	Germany	Top-Down	60-140°C	160.0	Theoretical	2007	1. Multiple Sources /AG Energiebilanzen 2007 and efficiencies and energy intensities taken from studies in US (US Department of Energy 2004) and Norway (Enova 2009)
			>140°C	316.0			

Source: Own table

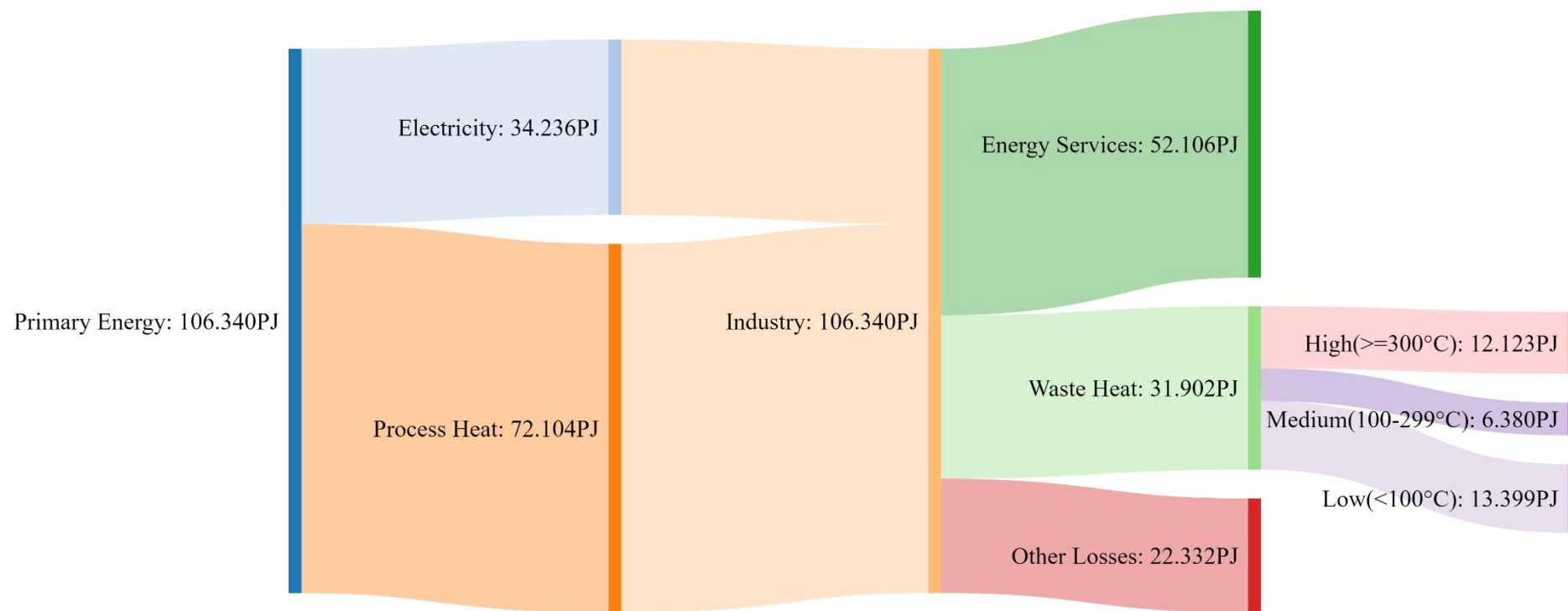


Figure F-1. Sankey diagram for the estimated energy flows and waste heat potential in the industrial sector worldwide for 2012.

Source: Own diagram based on Forman et al. (2016)

Forschungsberichte des Instituts für Energiewirtschaft und Rationelle Energieanwendung

Bezugsadresse: Universität Stuttgart
Institut für Energiewirtschaft und Rationelle Energieanwendung
- Bibliothek –
Tel.: 0711 / 685 87861
Fax: 0711 / 685 87873
E-Mail: bib@ier.uni-stuttgart.de

Bestellungen sind auch über Internet möglich:

<https://www.ier.uni-stuttgart.de>

- Band 153 L. C. Chamorro Romero
On the Process Integration of Organic Rankine Cycles and Absorption Chillers into Heat Exchanger Networks
2023, 266 Seiten
- Band 152 H. Scheben
Analysis of Electricity Prices in Power Systems with High Shares of Renewables and Storage through Electricity Market Modelling
2022, 105 Seiten
- Band 151 H. Godin
A model-based framework for the assessment of energy-efficiency and CO₂-mitigation measures in multi-cylinder paper drying
2022, 129 Seiten
- Band 150 A. Dobbins
System analysis of the significance of energy poverty on household energy use and emissions in Germany
2022, 222 Seiten

- Band 149 D. Chudinzow
Modelling the energy yield of bifacial photovoltaic plants and their integration into European power supply systems
2022, 92 Seiten
- Band 146 N. Seckinger
Methodische Weiterentwicklung dynamischer, prospektiver Treibhausgasemissionsfaktoren zur Analyse von Technologien der Sektorkopplung
2022, 242 Seiten
- Band 145 M. Unger
Systematische Analyse von Druckluftleckagen
August 2021, 186 Seiten
- Band 144 N. Li, G. Huang, R. Friedrich, U. Vogt, S. Schürmann, D. Straub
Messung und Bewertung der Schadstoffemissionen von Holzfeuerungen in Innenräumen
Juli 2019, 44 Seiten
- Band 143 N. Li
Long-term Exposure of European Population Subgroups to PM2.5 and NO2
August 2020, 152 Seiten
- Band 142 M. Miller
Wege zur Ermittlung von Energieeffizienzpotenzialen von Informations- und Kommunikationstechnologien
Februar 2020, 391 Seiten
- Band 141 R. Flatau
Integrierte Bewertung interdependenter Energieeffizienzmaßnahmen – Eine modellgestützte Analyse am Beispiel von Querschnittstechnologien
Juli 2019, 216 Seiten

- Band 140 B. Fleischer
- Systemeffekte von Bioenergie in der Elektrizitäts- und Fernwärmewirtschaft – Eine modellgestützte Analyse langfristiger Energiewendeszenarien für Deutschland**
- April 2019, 190 Seiten
-
- Band 139 B. Mousavi
- Analysis of the relative roles of supply-side and demand-side measures in tackling global climate change – Application of a hybrid energy system model**
- Januar 2019, 167 Seiten
-
- Band 138 S. Bothor
- Prognose von Netzverlusten**
- August 2019, 152 Seiten
-
- Band 137 C. Schieberle
- Development of a stochastic optimization approach to determine costefficient environmental protection strategies: Case study of policies for the future European passenger transport sector with a focus on railbound and on-road activities**
- Mai 2019, 218 Seiten
-
- Band 136 J. Welsch
- Modellierung von Energiespeichern und Power-to-X im deutschen und europäischen Energiesystem**
- Dezember 2018, 158 Seiten
-
- Band 135 M. Stenull
- Stand und Entwicklungspotenziale der landwirtschaftlichen Biogasnutzung in Baden-Württemberg – ein regionalspezifischer Vergleich**
- Juni 2017, 171 Seiten
-
- Band 134 J. Brunke
- Energieeinsparpotenziale von energieintensiven Produktionsprozessen in Deutschland: Eine Analyse mit Hilfe von Energieeinsparkostenkurven**

August 2017, 353 Seiten

- Band 133 S. Wolf
Integration von Wärmepumpen in industrielle Produktionssysteme – Potenziale und Instrumente zur Potenzialerschließung
Juli 2017, 177 Seiten
- Band 132 S. Marathe
Recognising the Change in Land Use Patterns and its Impacts on Energy Demand and Emissions in Gauteng, South Africa
April 2017, 202 Seiten
- Band 131 T. Haasz
Entwicklung von Methoden zur Abbildung von Demand Side Management in einem optimierenden Energiesystemmodell – Fallbeispiele für Deutschland in den Sektoren Industrie, Gewerbe, Handel, Dienstleistungen und Haushalte
April 2017, 177 Seiten
- Band 130 M. Steurer
Analyse von Demand Side Integration im Hinblick auf eine effiziente und umweltfreundliche Energieversorgung
April 2017, 230 Seiten
- Band 129 S. Bubeck
Potenziale elektrischer Energieanwendungstechniken zur rationellen Energieanwendung
Januar 2017, 255 Seiten
- Band 128 R. Beestermöller
Die Energienachfrage privater Haushalte und ihre Bedeutung für den Klimaschutz – Volkswirtschaftliche Analysen zur deutschen und europäischen Klimapolitik mit einem technologiefundierten Allgemeinen Gleichgewichtsmodell
Januar 2017, 211 Seiten
- Band 127 M. Ohl
Analyse der Einsatzpotenziale von Wärmeerzeugungstechniken in industriellen Anwendungen

August 2016, 202 Seiten

- Band 126 W. Genius
Grüne Bilanzierung - Internalisierung von Umwelt- und Gesundheitsschäden im Rahmen der Input-Output-Rechnung
April 2015, 243 Seiten
- Band 125 E. Heyden
Kostenoptimale Abwärmerückgewinnung durch integriert-iteratives Systemdesign (KOARiS) - Ein Verfahren zur energetisch-ökonomischen Bewertung industrieller Abwärmepotenziale
2016, 121 Seiten
- Band 124 K. Ohlau
Strategien zur wirksamen Minderung von Fluglärm in Deutschland - Minderungsmaßnahmen und langfristige Perspektiven
2015, 192 Seiten
- Band 123 T. Telsnig
Standortabhängige Analyse und Bewertung solarthermischer Kraftwerke am Beispiel Südafrikas
September 2015, 285 Seiten
- Band 122 M. Henßler
Ganzheitliche Analyse thermochemischer Verfahren bei der Nutzung fester Biomasse zur Kraftstoffproduktion in Deutschland
April 2015, 243 Seiten
- Band 121 B. Fais
Modelling policy instruments in energy system models - the example of renewable electricity generation in Germany
Januar 2015, 194 Seiten
- Band 120 M. Blesl
Kraft-Wärme-Kopplung im Wärmemarkt Deutschlands und Europas – eine Energiesystem- und Technikanalyse

August 2014, 204 Seiten

- Band 119 S. Kempe
Räumlich detaillierte Potenzialanalyse der Fernwärmeversorgung in Deutschland mit einem hoch aufgelösten Energiesystemmodell
Juli 2014, 204 Seiten
- Band 118 B. Thiruchittampalam
Entwicklung und Anwendung von Methoden und Modellen zur Berechnung von räumlich und zeitlich hochaufgelösten Emissionen in Europa

April 2014, 238 Seiten
- Band 117 T. Kober
Energiewirtschaftliche Anforderungen an neue fossil befeuerte Kraftwerke mit CO₂-Abscheidung im liberalisierten europäischen Elektrizitätsmarkt
März 2014, 158 Seiten
- Band 116 S. Wissel
Ganzheitlich-integrierte Betrachtung der Kernenergie im Hinblick auf eine nachhaltige Energieversorgung
Februar 2014, 230 Seiten
- Band 115 R. Kuder
Energieeffizienz in der Industrie – Modellgestützte Analyse des effizienten Energieeinsatzes in der EU-27 mit Fokus auf den Industriesektor
Februar 2014, 286 Seiten
- Band 114 J. Tomaschek
Long-term optimization of the transport sector to address greenhouse gas reduction targets under rapid growth – Application of an energy system model for Gauteng province, South Africa
Dezember 2013, 263 Seiten
- Band 113 B. Rühle
Kosten regionaler Energie- und Klimapolitik - Szenarioanalysen mit einem Energiesystemmodell auf Bundesländerebene

November 2013, 196 Seiten

- Band 112 N. Sun
Modellgestützte Untersuchung des Elektrizitätsmarktes - Kraftwerkseinsatzplanung und -investitionen
August 2013, 173 Seiten
- Band 111 J. Lambauer
Auswirkungen von Basisinnovationen auf die Energiewirtschaft und die Energienachfrage in Deutschland - Am Beispiel der Nano und Biotechnologie
März 2013, 303 Seiten
- Band 110 R. Barth
Ökonomische und technisch-betriebliche Auswirkungen verteilter Elektrizitätserzeugung in Verteilungsnetzen - eine modellgestützte Analyse am Beispiel eines Mittelspannungsnetzes
März 2013, 234 Seiten
- Band 109 D. Bruchof
Energiewirtschaftliche Verkehrsstrategie - Möglichkeiten und Grenzen alternativer Kraftstoffe und Antriebe in Deutschland und der EU-27
März 2012, 226 Seiten
- Band 108 E. D. Özdemir
The Future Role of Alternative Powertrains and Fuels in the German Transport Sector - A model based scenario analysis with respect to technical, economic and environmental aspects with a focus on road transport
Januar 2012, 194 Seiten
- Band 107 U. Kugler
Straßenverkehrsemissionen in Europa - Emissionsberechnung und Bewertung von Minderungsmaßnahmen
Januar 2012, 236 Seiten
- Band 106 M. Blesl, D. Bruchof, U. Fahl, T. Kober, R. Kuder, B. Götz, A. Voß

Integrierte Szenarioanalysen zu Energie- und Klimaschutzstrategien in Deutschland in einem Post-Kyoto-Regime

Februar 2011, 200 Seiten

Band 105 O. Mayer-Spohn

Parametrised Life Cycle Assessment of Electricity Generation in Hard-Coal-Fuelled Power Plants with Carbon Capture and Storage

Dezember 2009, 210 Seiten

Band 104 A. König

Ganzheitliche Analyse und Bewertung konkurrierender energetischer Nutzungspfade für Biomasse im Energiesystem Deutschland bis zum Jahr 2030

Juli 2009, 194 Seiten

Band 103 C. Kruck

Integration einer Stromerzeugung aus Windenergie und Speicher-systemen unter besonderer Berücksichtigung von Druckluft-Speicherkraftwerken

Mai 2008, 162 Seiten

Band 102 U. Fahl, B. Rühle, M. Blesl, I. Ellersdorfer, L. Eltrop, D.-C. Harlinghausen, R. Küster, T. Rehrl, U. Remme, A. Voß

Energieprognose Bayern 2030

Oktober 2007, 296 Seiten

Band 101 U. Remme, M. Blesl, U. Fahl

Global resources and energy trade: An overview for coal, natural gas, oil and uranium

Juli 2007, 108 Seiten

Band 100 S. Eckardt

Energie- und Umweltmanagement in Hotels und Gaststätten: Entwicklung eines Softwaretools zur systematischen Prozessanalyse und Management-unterstützung

Mai 2007, 152 Seiten

- Band 99 U. Remme
Zukünftige Rolle erneuerbarer Energien in Deutschland: Sensitivitätsanalysen mit einem linearen Optimierungsmodell
August 2006, 336 Seiten
- Band 98 L. Eltrop, J. Moerschner, M. Härdtlein, A. König
Bilanz und Perspektiven der Holzenergienutzung in Baden-Württemberg
Mai 2006, 102 Seiten
- Band 97 B. Frey
Modellierung systemübergreifender Energie- und Kohlenstoffbilanzen in Entwicklungsländern
Mai 2006, 148 Seiten
- Band 96 K. Sander
Potenziale und Perspektiven stationärer Brennstoffzellen
Juni 2004, 256 Seiten
- Band 95 M. A. dos Santos Bernardes
Technische, ökonomische und ökologische Analyse von Aufwindkraftwerken
März 2004, 228 Seiten
- Band 94 J. Bagemihl
Optimierung eines Portfolios mit hydro-thermischem Kraftwerkspark im börslichen Strom- und Gasterminmarkt
Februar 2003, 138 Seiten
- Band 93 A. Stuble
Ein Verfahren zur graphentheoretischen Dekomposition und algebraischen Reduktion von komplexen Energiesystemmodellen
November 2002, 156 Seiten
- Band 92 M. Blesl

Räumlich hoch aufgelöste Modellierung leitungsgebundener Energieversorgungs-systeme zur Deckung des Niedertemperaturwärmebedarfs

August 2002, 282 Seiten

Band 91 S. Briem, M. Blesl, M. A. dos Santos Bernardes, U. Fahl, W. Krewitt, M. Nill, S. Rath-Nagel, A. Voß

Grundlagen zur Beurteilung der Nachhaltigkeit von Energiesystemen in Baden-Württemberg

August 2002, 138 Seiten

Band 90 B. Frey, M. Neubauer

Energy Supply for Three Cities in Southern Africa

Juli 2002, 96 Seiten

Band 89 A. Heinz, R. Hartmann, G. Hitzler, G. Baumbach

Wissenschaftliche Begleitung der Betriebsphase der mit Rapsölmethylester befeuerten Energieversorgungsanlage des Deutschen Bundestages in Berlin

Juli 2002, 212 Seiten

Band 88 M. Sawillion

Aufbereitung der Energiebedarfsdaten und Einsatzanalysen zur Auslegung von Blockheizkraftwerken

Juli 2002, 136 Seiten

Band 87 T. Marheineke

Lebenszyklusanalyse fossiler, nuklearer und regenerativer Stromerzeugungstechniken

Juli 2002, 222 Seiten

Band 86 B. Leven, C. Hoeck, C. Schaefer, C. Weber, A. Voß

Innovationen und Energiebedarf - Analyse ausgewählter Technologien und Branchen mit dem Schwerpunkt Stromnachfrage

Juni 2002, 224 Seiten

Band 85 E. Laege

Entwicklung des Energiesektors im Spannungsfeld von Klimaschutz und

Februar 2001, 248 Seiten

Band 77

W. Rüffler

Integrierte Ressourcenplanung für Baden-Württemberg

Januar 2001, 284 Seiten

Band 76

S. Rivas

Ein agro-ökologisches regionalisiertes Modell zur Analyse des Brennholz-versorgungssystems in Entwicklungsländern

Januar 2001, 200 Seiten

Band 75

M. Härdtlein

Ansatz zur Operationalisierung ökologischer Aspekte von "Nachhaltigkeit" am Beispiel der Produktion und Nutzung von Triticale (*×Triticosecale* Wittmack)-Ganzpflanzen unter besonderer Berücksichtigung der luftgetragenen N-Freisetzungen

September 2000, 168 Seiten

Band 74

T. Marheineke, W. Krewitt, J. Neubarth, R. Friedrich, A. Voß

Ganzheitliche Bilanzierung der Energie- und Stoffströme von Energie-versorgungstechniken

August 2000, 118 Seiten

Band 73

J. Sontow

Energiewirtschaftliche Analyse einer großtechnischen Windstrom-erzeugung

Juli 2000, 242 Seiten

Band 72

H. Hermes

Analysen zur Umsetzung rationeller Energieanwendung in kleinen und mittleren Unternehmen des Kleinverbrauchersektors

Juli 2000, 188 Seiten

Band 71

C. Schaefer, C. Weber, H. Voss-Uhlenbrock, A. Schuler, F. Oosterhuis, E.

Nieuwlaar, R. Angioletti, E. Kjellsson, S. Leth-Petersen, M. Togeby, J. Munksgaard

Effective Policy Instruments for Energy Efficiency in Residential Space Heating - an International Empirical Analysis (EPISODE)

Juni 2000, 146 Seiten

Band 70 U. Fahl, J. Baur, I. Ellersdorfer, D. Herrmann, C. Hoeck, U. Remme, H. Specht, T. Steidle, A. Stuibler, A. Voß

Energieverbrauchsprognose für Bayern

Mai 2000, 240 Seiten

Band 69 J. Baur

Verfahren zur Bestimmung optimaler Versorgungsstrukturen für die Elektrifizierung ländlicher Gebiete in Entwicklungsländern

Mai 2000, 154 Seiten

Band 68 G. Weinrebe

Technische, ökologische und ökonomische Analyse von solarthermischen Turmkraftwerken

April 2000, 212 Seiten

Band 67 C.-O. Wene, A. Voß, T. Fried (eds.)

Experience Curves for Policy Making - The Case of Energy Technologies

April 2000, 282 Seiten

Band 66 A. Schuler

Entwicklung eines Modells zur Analyse des Endenergieeinsatzes in Baden-Württemberg

März 2000, 236 Seiten

Band 65 A. Schäfer

Reduction of CO₂-Emissions in the Global Transportation Sector

März 2000, 290 Seiten

Band 64 A. Freibauer, M. Kaltschmitt (eds.)

Biogenic Emissions of Greenhouse Gases Caused by Arable and Animal Agriculture - Processes, Inventories, Mitigation

März 2000, 148 Seiten

- Band 63 A. Heinz, R. Stülpnagel, M. Kaltschmitt, K. Scheffer, D. Jeziarska
Feucht- und Trockengutlinien zur Energiegewinnung aus biogenen Festbrennstoffen. Vergleich anhand von Energie- und Emissionsbilanzen sowie anhand der Kosten
Dezember 1999, 308 Seiten
- Band 62 U. Fahl, M. Blesl, D. Herrmann, C. Kemfert, U. Remme, H. Specht, A. Voß
Bedeutung der Kernenergie für die Energiewirtschaft in Baden-Württemberg - Auswirkungen eines Kernenergieausstiegs
November 1999, 146 Seiten
- Band 61 A. Greßmann, M. Sawillion, W. Krewitt, R. Friedrich
Vergleich der externen Effekte von KWK-Anlagen mit Anlagen zur getrennten Erzeugung von Strom und Wärme
September 1999, 138 Seiten
- Band 60 R. Lux
Auswirkungen fluktuierender Einspeisung auf die Stromerzeugung konventioneller Kraftwerkssysteme
September 1999, 162 Seiten
- Band 59 M. Kayser
Energetische Nutzung hydrothermalen Erdwärmevorkommen in Deutschland - Eine energiewirtschaftliche Analyse -
Juli 1999, 184 Seiten
- Band 58 C. John

Emissionen von Luftverunreinigungen aus dem Straßenverkehr in hoher räumlicher und zeitlicher Auflösung - Untersuchung von Emissions-szenarien am Beispiel Baden-Württembergs

Juni 1999, 214 Seiten

Band 57 T. Stelzer

Biokraftstoffe im Vergleich zu konventionellen Kraftstoffen - Lebensweganalysen von Umweltwirkungen

Mai 1999, 212 Seiten

Band 56 R. Lux, J. Sontow, A. Voß

Systemtechnische Analyse der Auswirkungen einer windtechnischen Stromerzeugung auf den konventionellen Kraftwerkspark

Mai 1999, 322 Seiten

Band 55 B. Biffar

Messung und Synthese von Wärmelastgängen in der Energieanalyse

Mai 1999, 236 Seiten

Band 54 E. Fleißner

Statistische Methoden der Energiebedarfsanalyse im Kleinverbraucher-sektor

Januar 1999, 306 Seiten

Band 53 A. Freibauer, M. Kaltschmitt (Hrsg.)

Approaches to Greenhouse Gas Inventories of Biogenic Sources in Agriculture

Januar 1999, 252 Seiten

Band 52 J. Haug, B. Gebhardt, C. Weber, M. van Wees, U. Fahl, J. Adnot, L. Cauret, A. Pierru, F. Lantz, J.-W. Bode, J. Vis, A. van Wijk, D. Staniaszek, Z. Zavody

Evaluation and Comparison of Utility's and Governmental DSM-Programmes for the Promotion of Condensing Boilers

Oktober 1998, 156 Seiten

- Band 51 M. Blesl, A. Schweiker, C. Schlenzig
Erweiterung der Analysemöglichkeiten von *NetWork* - Der Netzwerkeditor
September 1998, 112 Seiten
- Band 50 S. Becher
Biogene Festbrennstoffe als Substitut für fossile Brennstoffe - Energie- und Emissionsbilanzen
Juli 1998, 200 Seiten
- Band 49 P. Schaumann, M. Blesl, C. Böhringer, U. Fahl, R. Kühner, E. Läge, S. Molt, C. Schlenzig, A. Stuible, A. Voß
Einbindung des ECOLOG-Modells '*E³Net*' und Integration neuer methodischer Ansätze in das IKARUS-Instrumentarium (*ECOLOG II*)
Juli 1998, 110 Seiten
- Band 48 G. Poltermann, S. Berret
ISO 14000ff und Öko-Audit - Methodik und Umsetzung
März 1998, 184 Seiten
- Band 47 C. Schlenzig
PlaNet: Ein entscheidungsunterstützendes System für die Energie- und Umweltplanung
Januar 1998, 230 Seiten
- Band 46 R. Friedrich, P. Bickel, W. Krewitt (Hrsg.)
External Costs of Transport
April 1998, 144 Seiten
- Band 45 H.-D. Hermes, E. Thöne, A. Voß, H. Desprez, G. Weimann, G. Kamelander, C. Ureta
Tools for the Dissemination and Realization of Rational Use of Energy in Small and Medium Enterprises

Januar 1998, 352 Seiten

- Band 44 C. Weber, A. Schuler, B. Gebhardt, H.-D. Hermes, U. Fahl, A. Voß
Grundlagenuntersuchungen zum Energiebedarf und seinen Bestimmungsfaktoren
Dezember 1997, 186 Seiten
- Band 43 J. Albiger
Integrierte Ressourcenplanung in der Energiewirtschaft mit Ansätzen aus der Kraftwerkseinsatzplanung
November 1997, 168 Seiten
- Band 42 P. Berner
Maßnahmen zur Minderung der Emissionen flüchtiger organischer Verbindungen aus der Lackanwendung - Vergleich zwischen Abluftreinigung und primären Maßnahmen am Beispiel Baden-Württembergs
November 1997, 238 Seiten
- Band 41 J. Haug, M. Sawillion, U. Fahl, A. Voß, R. Werner, K. Weiß, J. Rösch, W. Wölfle
Analysis of Impediments to the Rational Use of Energy in the Public Sector and Implementation of Third Party Financing Strategies to improve Energy Efficiency
August 1997, 122 Seiten
- Band 40 U. Fahl, R. Krüger, E. Läge, W. Ruffler, P. Schaumann, A. Voß
Kostenvergleich verschiedener CO₂-Minderungsmaßnahmen in der Bundesrepublik Deutschland
August 1997, 156 Seiten
- Band 39 M. Sawillion, B. Biffar, K. Hufendiek, R. Lux, E. Thöne
MOSAİK - Ein EDV-Instrument zur Energieberatung von Gewerbe und mittelständischer Industrie
Juli 1997, 172 Seiten
- Band 38 M. Kaltschmitt

Systemtechnische und energiewirtschaftliche Analyse der Nutzung erneuerbarer Energien in Deutschland

April 1997, 108 Seiten

- Band 37 C. Böhringer, T. Rutherford, A. Pahlke, U. Fahl, A. Voß
Volkswirtschaftliche Effekte einer Umstrukturierung des deutschen Steuersystems unter besonderer Berücksichtigung von Umweltsteuern
März 1997, 82 Seiten
- Band 36 P. Schaumann
Klimaverträgliche Wege der Entwicklung der deutschen Strom- und Fernwärmeversorgung - Systemanalyse mit einem regionalisierten Energiemodell
Januar 1997, 282 Seiten
- Band 35 R. Kühner
Ein verallgemeinertes Schema zur Bildung mathematischer Modelle energiewirtschaftlicher Systeme
Dezember 1996, 262 Seiten
- Band 34 U. Fahl, P. Schaumann
Energie und Klima als Optimierungsproblem am Beispiel Niedersachsen
November 1996, 124 Seiten
- Band 33 W. Krewitt
Quantifizierung und Vergleich der Gesundheitsrisiken verschiedener Stromerzeugungssysteme
November 1996, 196 Seiten
- Band 32 C. Weber, B. Gebhardt, A. Schuler, T. Schulze, U. Fahl, A. Voß, A. Perrels, W. van Arkel, W. Pellekaan, M. O'Connor, E. Schenk, G. Ryan
Consumers' Lifestyles and Pollutant Emissions
September 1996, 118 Seiten
- Band 31 W. Röffler, A. Schuler, U. Fahl, H.W. Balandynowicz, A. Voß

Szenariorechnungen für das Projekt *Klimaverträgliche Energieversorgung in Baden-Württemberg*

Juli 1996, 140 Seiten

Band 30 C. Weber, B. Gebhardt, A. Schuler, U. Fahl, A. Voß

Energy Consumption and Air-Borne Emissions in a Consumer Perspective

September 1996, 264 Seiten

Band 29 M. Hanselmann

Entwicklung eines Programmsystems zur Optimierung der Fahrweise von Kraft-Wärme-Kopplungsanlagen

August 1996, 138 Seiten

Band 28 G. Schmid

Die technisch-ökonomische Bewertung von Emissionsminderungsstrategien mit Hilfe von Energiemodellen

August 1996, 184 Seiten

Band 27 A. Obermeier, J. Seier, C. John, P. Berner, R. Friedrich

TRACT: Erstellung einer Emissionsdatenbasis für TRACT

August 1996, 172 Seiten

Band 26 T. Hellwig

OMNIUM - Ein Verfahren zur Optimierung der Abwärmenutzung in Industriebetrieben

Mai 1998, 118 Seiten

Band 25 R. Laing

CAREAIR - ein EDV-gestütztes Instrumentarium zur Untersuchung von Emissionsminderungsstrategien für Dritte-Welt-Länder dargestellt am Beispiel Nigerias

Februar 1996, 221 Seiten

Band 24 P. Mayerhofer, W. Krewitt, A. Trukenmüller, A. Greßmann, P. Bickel, R. Friedrich

Externe Kosten der Energieversorgung

März 1996, Kurzfassung, 40 Seiten

- Band 23 M. Blesl, C. Schlenzig, T. Steidle, A. Voß
Entwicklung eines Energieinformationssystems
März 1996, 76 Seiten
- Band 22 M. Kaltschmitt, A. Voß
Integration einer Stromerzeugung aus Windkraft und Solarstrahlung in den konventionellen Kraftwerksverbund
Juni 1995, Kurzfassung, 51 Seiten
- Band 21 U. Fahl, E. Läge, W. Ruffler, P. Schaumann, C. Böhringer, R. Krüger, A. Voß
Emissionsminderung von energiebedingten klimarelevanten Spurengasen in der Bundesrepublik Deutschland und in Baden-Württemberg
September 1995, 454 Seiten
- Band 20 M. Fishedick
Erneuerbare Energien und Blockheizkraftwerke im Kraftwerksverbund - Technische Effekte, Kosten, Emissionen
Dezember 1995, 196 Seiten
- Band 19 A. Obermeier
Ermittlung und Analyse von Emissionen flüchtiger organischer Verbindungen in Baden-Württemberg
Mai 1995, 208 Seiten
- Band 18 N. Kalume
Strukturmodule - Ein methodischer Ansatz zur Analyse von Energiesystemen in Entwicklungsländern
Dezember 1994, 113 Seiten
- Band 17 Th. Müller
Ermittlung der SO₂- und NO_x-Emissionen aus stationären Feuerungsanlagen in Baden-Württemberg in hoher räumlicher und zeitlicher Auflösung
November 1994, 142 Seiten

- Band 16 A. Wiese
Simulation und Analyse einer Stromerzeugung aus erneuerbaren Energien in Deutschland
Juni 1994, 223 Seiten
- Band 15 M. Sawillion, T. Hellwig, B. Biffar, R. Schelle, E. Thöne
Optimierung der Energieversorgung eines Industrieunternehmens unter Umweltschutz- und Wirtschaftlichkeitsaspekten - Wertanalyse-Projekt
Januar 1994, 154 Seiten
- Band 14 M. Heymann, A. Trukenmüller, R. Friedrich
Development prospects for emission inventories and atmospheric transport and chemistry models
November 1993, 105 Seiten
- Band 13 R. Friedrich
Ansatz zur Ermittlung optimaler Strategien zur Minderung von Luftschadstoffemissionen aus Energieumwandlungsprozessen
Juli 1992, 292 Seiten
- Band 12 U. Fahl, M. Fishedick, M. Hanselmann, M. Kaltschmitt, A. Voß
Abschätzung der technischen und wirtschaftlichen Minderungspotentiale energiebedingter CO₂-Emissionen durch einen verstärkten Erdgaseinsatz in der Elektrizitätsversorgung Baden-Württembergs unter besonderer Berücksichtigung konkurrierender Nutzungsmöglichkeiten
August 1992, 471 Seiten
- Band 11 M. Kaltschmitt, A. Wiese
Potentiale und Kosten regenerativer Energieträger in Baden-Württemberg
April 1992, 320 Seiten
- Band 10 A. Reuter

Entwicklung und Anwendung eines mikrocomputergestützte Energieplanungsinstrumentariums für den Einsatz in Entwicklungsländern

November 1991, 170 Seiten

Band 9 T. Kohler

Einsatzmöglichkeiten für Heizreaktoren im Energiesystem der Bundesrepublik Deutschland

Juli 1991, 162 Seiten

Band 8 M. Mattis

Kosten und Auswirkungen von Maßnahmen zur Minderung der SO₂- und NO_x-Emissionen aus Feuerungsanlagen in Baden-Württemberg

Juni 1991, 188 Seiten

Band 7 M. Kaltschmitt

Möglichkeiten und Grenzen einer Stromerzeugung aus Windkraft und Solarstrahlung am Beispiel Baden-Württembergs

Dezember 1990, 178 Seiten

Band 6 G. Schmid, A. Voß, H.W. Balandynowicz, J. Cofala, Z. Parczewski

Air Pollution Control Strategies - A Comparative Analysis for Poland and the Federal Republic of Germany

Juli 1990, 92 Seiten

Band 5 Th. Müller, B. Boysen, U. Fahl, R. Friedrich, M. Kaltschmitt, R. Laing, A. Voß, J. Giesecke, K. Jorde, C. Voigt

Regionale Energie- und Umweltanalyse für die Region Neckar-Alb

Juli 1990, 484 Seiten

Band 4 Th. Müller, B. Boysen, U. Fahl, R. Friedrich, M. Kaltschmitt, R. Laing, A. Voß, J. Giesecke, K. Jorde, C. Voigt

Regionale Energie- und Umweltanalyse für die Region Hochrhein-Bodensee

Juni 1990, 498 Seiten

Band 3 D. Kluck

Einsatzoptimierung von Kraftwerkssystemen mit Kraft-Wärme-Kopplung

Mai 1990, 155 Seiten

Band 2 M. Fleischhauer, R. Friedrich, S. Häring, A. Haugg, J. Müller, A. Reuter,
A. Voß, H.-G. Wystrcil

**Grundlagen zur Abschätzung und Bewertung der von Kohlekraftwerken
ausgehenden Umweltbelastungen in Entwicklungsländern**

Mai 1990, 316 Seiten

Band 1 U. Fahl

**KDS - Ein System zur Entscheidungsunterstützung in Energiewirtschaft und
Energiepolitik**

März 1990, 265 Seiten

Inhalt

The industrial sector accounts for almost a third of the global GHG emissions, from which around 80% correspond to energy-related emissions. The decrease of energy consumption in the industrial sectors has therefore a direct impact in the reduction of the global GHG emission as required by the Paris Agreement, in order to limit the increase of the global average temperature below 2°C above pre-industrial levels. Around 30% of the energy input into the industrial sector worldwide is released unused to the environment as waste heat. The internal and external recovery of waste heat represents in consequence, an attractive strategy for the reduction of the industrial energy consumption. Typically, the internal waste heat recovery and the external waste heat recovery are treated as separated problems in the hierarchical sequential approach for the design of industrial processes. Although a practical and successful design strategy, this sequential approach neglects possible synergies generated by considering simultaneously the internal and external waste heat recovery options during the process design.

In this work, a mathematical framework considering simultaneously internal (represented by the synthesis of the heat exchanger network for the system) and external (represented by the use of waste heat transformation technologies) waste heat recovery options is presented. The mathematical framework focuses on two of the most mature waste heat transformation technologies, Organic Rankine Cycles (ORCs) and Absorption Chillers (ABCs), and integrates them into Heat Exchanger Networks (HENs) in continuous and multi-period process with and without Fixed Temperature Variable Mass (FTVM) heat storage. The generated system designs have the potential to be economically, technically and environmentally more attractive than systems solely factoring heat exchanger networks.

The main conclusion from this dissertation is, that combined design methodologies, considering the process integration of ORCs, ABCs or both, into HENs in continuous and multi-period processes with and without FTVM heat storage, can generate economically, technically or environmentally attractive system designs.